Université de Toulouse

THÈSE

En vue de l'obtention du

DOCTORAT DE L'UNIVERSITÉ DE TOULOUSE

Délivré par :
Université Toulouse III Paul Sabatier (UT3 Paul Sabatier)

Discipline ou spécialité :

Pharmacologie

Présentée et soutenue par :
Pierre-Marie Badin

le : 12 Juillet 2013

Titre :

Étude du rôle des lipases musculaires dans la régulation du métabolisme des lipides et de la sensibilité à l'insuline

---

Ecole doctorale :
Biologie, Santé, Biotechnologies (BSB)

Unité de recherche :
INSERM, U1048, Institut des maladies métaboliques et cardiovasculaires

Directeur(s) de Thèse :
Dr Cédric Moro
Pr Dominique Langin

Rapporteurs :

Dr Jean-François Tanti
Dr Jennifer Rieusset

Membre(s) du jury :
Pr Isabelle Castan-Laurell (Président)
Dr Jean-François Tanti
Dr Jennifer Rieusset
Dr Francesca Amati
Dr Cédric Moro

Voilà déjà plusieurs semaines que la soutenance de thèse est finie. Il est maintenant temps de s'occuper de l'impression ! A cette occasion, je voudrais utiliser les premières lignes de ce manuscrit pour remercier un certain nombre de personnes qui sont associées de près ou de loin à ces travaux de thèse.

Tout d'abord je souhaiterais remercier les membres de mon jury de thèse. En premier lieu les Dr **Jennifer Rieusset** et **Jean-François Tanti** qui ont accepté d'évaluer mon manuscrit de thèse malgré le temps restreint mis à leur disposition. Je les remercie d'autant plus qu'ils ont tout deux été associés à cette thèse depuis le départ. Le Dr Jennifer Rieusset collaborant depuis plusieurs années avec le laboratoire et le Dr Jean-François Tanti ayant été le premier évaluateur de mes travaux de recherche lors de la présentation d'un poster durant le congrès de l'AFERO de 2010. Je remercie également le **Dr Francesca Amati** que j'ai eu le plaisir de rencontrer lors de ma soutenance et qui a accepté de participer à sa première thèse Française. Enfin merci au **Pr Isabelle Castan-Laurell** qui a bien voulu être présidente de jury à deux reprises lors de la même semaine. C'est de plus un clin d'œil à nos activités d'enseignement puisque j'aurais réalisé l'ensemble de mes TD avec toi !

Ensuite je voudrais remercier un grand nombre de personnes du laboratoire, et en premier lieu **Cédric Moro**. Tout d'abord merci de m'avoir fait confiance. J'ai passé 4 supers années à tes côtés. Merci pour nos interminables discussions scientifiques et sportives. Merci de m'avoir permis de ne pas toujours être d'accord avec toi (comment peut-on par exemple soutenir le PSG ?). Merci de ton encadrement sans faille et de m'avoir toujours guidé, des premières manips (premières cultures de myocytes) à la recherche d'un postdoc en passant par l'écriture de nos articles et par les congrès. Merci aussi pour l'apprentissage de techniques permettant de ne pas assister aux mariages ennuyeux (et oui je la refais). Je ne te remercierai jamais assez d'avoir été un chef couillu (au CV impressionnant) mais aussi un mentor et un ami. J'espère sincèrement que nous pourrons trouver les moyens de continuer à travailler ensemble dans le futur ici là-bas ou ailleurs.

Merci à **Dominique Langin** de m'avoir accueilli dans son équipe, et pour son travail intense permettant à toute l'équipe d'avoir des moyens matériels jalousés par beaucoup. Je te remercie également pour le travail intellectuel fourni sur l'ensemble de nos publications communes. Je te remercie surtout pour une chose, malgré pas mal de déboires lors de tes premiers recrutements qui nous ont tous deux affectés, je te suis reconnaissant d'avoir persévéré jusqu'au recrutement d'Isabelle…

Par la suite je voudrais remercier les gens du groupe muscle : en premier lieu **Katie** qui est arrivée au laboratoire seulement quelques mois après moi. Merci à toi d'avoir été là durant ces 4 années pour m'aider dans toutes mes manips, pour passer toutes mes commandes et pour conserver le sourire (même si parfois c'est difficile). Mais surtout merci à toi pour tes fesses fermes et tes lapsus mythiques (à signaler par exemple : les fameux *« signal inmenuménique »* et *« baisons futé »*…). **Virg'** merci de m'avoir écouté en M1, de toujours être accessible pour discuter. Merci aussi de m'avoir donné les TP respi en première année mais surtout de ne pas me les avoir donné les années suivantes. Merci de m'avoir fait connaitre la purée de panais et un nouveau type de collection, celui des sacs plastiques. Merci aux deux nouvelles, **Marine** (miss BNP**)** et **Claire** (miss lipases) qui vont avoir la lourde tâche de me remplacer… Il faut bien deux femmes pour faire un homme.

Je remercie aussi toutes les autres personnes du labo. En premier lieu GT et Aline toutes deux très investies dans nos travaux. **GT** encore une fois merci d'avoir géré pendant ces 4 années nos lignées de souris merci d'être toujours dispo et merci pour ta gentillesse. **Aline** merci pour tes phrases mythiques et tes petits mots mais surtout merci de nous avoir aidé sur de nombreuses mises au point et manips, « Allez tchao ». Merci à **Camille** et **Marteen**, tous deux passés sous la tutelle de Cédric durant leur M2, pour leur collaboration prolifique et leur bonne humeur. A **Marie** pour dégainer les kits ELISA plus vite que son ombre et pour ces santiagues croco qu'Isabelle jalouse (on attend toujours de voir les bleus). A **François C** pour la relecture de ce manuscrit et de bien d'autres et pour nous avoir appris à taper les sms discrètement en réunion. A **Corinne** pour ses crêpes et ses griottes (comme dirait Katie) et pour son éternuement discret. A **Nat'** toujours très disponible pour mes répétitions d'oraux ou pour dicussion. A **Dominique L** pour me tenir informé régulièrement des résultats du CAPES. **A Sylvie** pour ta sympathie. A **Etienne** pour nous débarrasser de toute nourriture trainant dans le bureau. A **Marianne** pour m'avoir appris deux trois bricoles au poker. A **Valentin** pour m'avoir donné l'adresse de son coiffeur. A **Emilie** qui finit sa thèse en compagnie de ses miRNA. A **Lucile** pour son soutien-gorge sans bretelle et son T-shirt wingsuit. A **Laurent** pour son aide sur le phénotypage. A **Marion** pour ne parler que de vins et de fromages. Et à **Diane** qui assure la relève côté gras.

Merci aussi aux collègues de l'institut et de la fac : Merci à **Mano** pour m'avoir épaulé dans tous mes TP, pour ta gentillesse et ta disponibilité. Je finis l'enseignement avec toi et j'en suis très content j'aurais été nostalgique de trouver quelqu'un à ta place. **Claude** avec qui on a plus souvent parlé heure de l'apéro que science merci pour organiser le foot avec succès depuis de nombreuses années. Merci à **Anne** pour faire foirer mes WB avec du Cornoy et pour concurrencer Isabelle niveau classe. Merci également à **Matteo**, **Chantal**, **Mylène**, **Chloé**, **Thibaud**, et autres.

Merci aux plateformes et à leur personnel notamment la plateforme **Get-TQ**, **l'animalerie** et la plateforme **lipidomique**.

Merci à nos collaborateurs notamment le **Pr Arild Rustan**, et le **Pr Steve Smith,** respectivement pour nous avoir fourni en cellules et en souris.

Merci enfin au personnel administratif et technique.

Si je suis arrivé jusqu'à la thèse c'est surtout grâce à vous, **Maman, papa**. Merci de m'avoir toujours aidé, d'avoir fait des centaines d'aller-retour la maison/chasse s/Rhone (merci d'ailleurs à **Linda**), puis la maison/Le péage de Roussillon. Merci pour m'avoir aidé à travailler au début puis forcé à travailler par la suite (je me rappellerai longtemps des lignes de syllabes). Surtout merci de m'avoir toujours soutenu aussi bien dans mes choix scolaires qu'extra scolaire. Maman, merci d'avoir cru en moi lorsque j'ai passé le Bac. Merci papa d'avoir gardé l'Alpine contre vents et marrées. **Gab' et Mel'** merci d'avoir été toujours si brillants (j'avais la pression). Gab' merci surtout d'avoir grandi je me rappelle sans nostalgie toutes les fois où tu m'as fait tourné chèvre avant que j'abandonne le foyer familial (c'est peut être pas pour rien que tu as choisi Camille !). Mel', merci à toi d'avoir toujours tout fait pour qu'on reste proches même si mon caractère ne s'y prête pas toujours. Je suis fier de vous deux. Petit coucou à **Camille** la nouvelle bijoutière de la famille qui accepte toujours

de jouer à la belotte parfois contre sa volonté. Merci aussi à **Gilou** (mon BE préféré devenu bof) notamment pour m'avoir hébergé de nombreuses fois. Et bien sur une petite dédicace à mon premier neveu **Louis**.

François, Linda, merci à vous pour m'avoir accueilli lors de mon arrivée à Toulouse. Merci pour nos nombreux repas du dimanche. François, merci à toi pour avoir participé activement à ma réorientation et pour les séances de rattrapage de BM et autre. **Mami, papi**, merci pour les milliers de fois où vous nous avez gardé. Certains de mes meilleurs souvenirs d'enfance seront toujours à Saint Just, à l'atelier ou à la cantine entre sardines au beurre et sciure de bois. **Mémé** merci pour tes innombrables pulls et écharpes. Merci également d'être venu en Juillet ça nous a fait très plaisir. Merci à la belle famille, notamment **José et Christian** pour leurs gentillesse leur accueil chaleureux et pour m'avoir fait découvrir les escargots à la catalane, le mel i meto et leurs patés. Merci aussi pour les cours de Catalan gratuit et pour m'avoir révélé les coins à oronges et morilles, promis je saurai garder ma langue.

C'est aussi le moment de remercier tous les amis qui m'ont accompagné depuis le Lycée. **« Mouloude »** rappelle toi nos promesses et commence à chercher une bonne maison de retraite. **Nathan** mon colloque d'alors retrouvé à Toulouse et les autres Diois. Merci aussi aux Valentinois en premier lieu **Juju**. Merci à **Nico** mon coéquipier de toujours, pour les week-ends « clé en main » et les trois magnifiques médailles. Et enfin merci aux Toulousains notamment **Roustan**, **Gigi** et **Baki**, merci pour les poulets les frites et les Palas. Un clin d'œil à **Rom'**, le stéphanois de service et bravo pour ton premier papier. Merci aussi à mes collègues de bureau préférés **Aurélien** pour sa légèreté légendaire et sa façon d'aborder les filles chez tonton. **Naurel** pour ses connaissances intarissables et les après-midi rugby/Borderland.

Le meilleur pour la fin : **Isabelle**, merci pour les après midi Kaamelott sans DVD et pour m'avoir appris quelques techniques de dragues sympas à base de bâtons de bois. Merci aussi pour me soutenir au quotidien aussi bien au laboratoire qu'à la maison. Merci surtout de me supporter 24h sur 24 puisque je suis aussi pénible éveillé qu'en dormant à ce qu'on dit. T'estimo meu doudette.

SOMMAIRE

LISTE DES ILLUSTRATIONS

GLOSSAIRE

Acyl-CoA	Acyl-coenzyme A
ACoA-LC	Acyl CoA à longue chaine
AG	Acides gras
Akt	V-akt murine thymoma viral oncogene homolog 1
AMPK	5’-AMP protéine kinase
ATGL	Adipose triglyceride lipase
CerK	Céramide kinase
CD36	Cluster of differentiation 36
CGI-58	Comparative gene identification 58
DAG	Diacylglycérol
DAGH	Diacylglycérol hydrolase
DAGK	Diacylgycérol kinase
DGAT	Diacylglycérol O-acyltransférase
FATP	Fatty acid transport protein
G0S2	G0/G1 switch gene 2
G3P	Glucose 3 phosphate
G6P	Glucose 6 phosphate
GAT	Glycérol acyltransférase
GLUT4	Glucose transporter 4
GM3	Ganglioside monosialo 3
GPAT	Glycérol-3-phosphate acyltransferase

HK	Hexokinase
IMC	Indice de masse corporelle
IR	Récepteur à l'insuline
IRS1	Insulin receptor substrat 1
LHS	Lipase hormone-sensible
LPA	Acide lysophosphatidique
LPAAT	LPA acyltransférase
MAG	Monoacylglycérols
MCK	Muscle creatine kinase
MGAT	MAG acyltransférase
MGL	MAG lipase
PAP1	Phosphatidic acid phosphatase 1
PDK4	Pyruvate dehydrogenase kinase isozyme 4
PGC1α	PPARγ coactivator 1 α
PI3K	PIP 3 kinases
PIP	Phosphatidyl-inositol
PIP2	PIP-diphosphate
PIP3	PIP-triphosphate
PKA	Protéine Kinase A
PKC	Protéine Kinase C
PLC	Phospholipase C
PLIN	Périlipine
PP2A	Protéine Phosphatase 2A

PPAR	Peroxisome proliferator-activated receptor
S1P	Sphingosine 1 phosphate
Ser	Sérine
SMase	Sphingomyélinase
SMsynthase	Sphingomyéline synthase
SPT	Sérine palmitoyltransférase
TAG	Triacylglycérol
TAGH	Triacylglycérol hydrolase
TGIM	TAG intra-myocellulaire
Tyr	Tyrosine

1 CONTEXTE

L'obésité est en constante augmentation en France et dans le monde depuis plus de 30 ans. Cette prise de poids excessive est dans une grande partie des cas associée à de nombreuses pathologies cardiovasculaires et métaboliques. Une des principales pathologies liées à l'obésité est le diabète de type 2 dit non insulino-dépendant. Cette pathologie qui touche environ 4% des personnes en France est attribuée à une perte de sensibilité progressive des tissus à l'insuline notamment le foie et le muscle squelettique, on parle d'insulino-résistance.

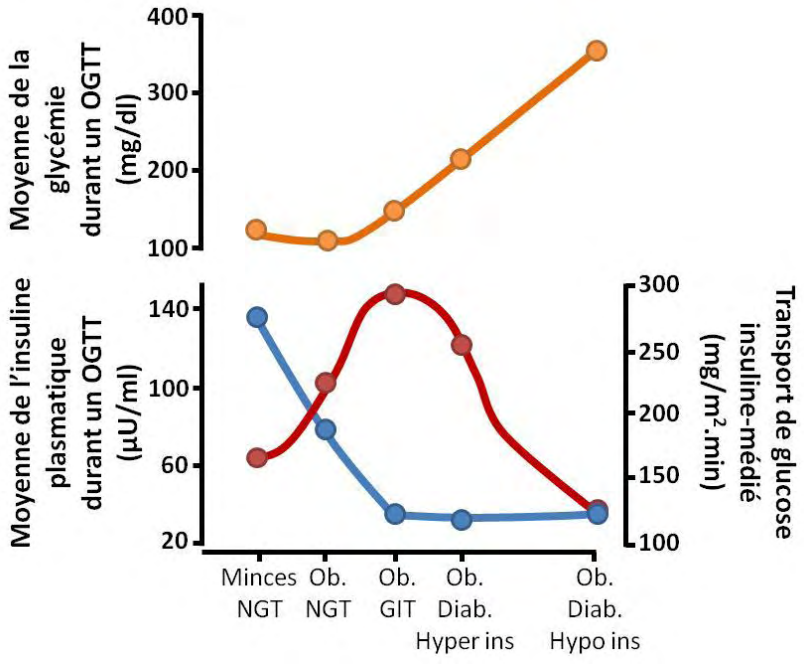

Figure 1. Dégradation de la gluco-tolérance et de la sensibilité à l'insuline à différents stades de développement du diabète

Au cours de l'évolution de la l'obésité (Ob.), on note une perte de la gluco-tolérance (mesurée après une prise orale de glucose (OGTT)). Les patients sont de moins en moins aptes à normaliser leur glycémie après une prise de glucose (courbe jaune), ils passent donc du statut de normo-gluco-tolérance (NGT) à celui de gluco-intolérance (GIT) ces étapes précèdent le développement du diabète (Diab.). Cette intolérance au glucose, s'explique par une perte progressive de la sensibilité à l'insuline (courbe bleue) (mesurée par clamp hyperinsulinémique-euglycémique). Durant les premiers stades de la pathologie, cette perte de sensibilité est compensée par une augmentation de la sécrétion d'insuline (Hyper ins) (courbe rouge). Dans les phases terminales la production d'insuline diminue progressivement (Hypo ins) en raison d'une disparition progressive des cellules β pancréatiques. *D'après DeFronzo RA (DeFronzo, 1988).*

Il est maintenant établi que le développement du diabète de type 2 passe par trois étapes (DeFronzo, 1988) (figure 1) :

- Dans un premier temps les tissus cibles de l'insuline perdent leur sensibilité à l'hormone. Il y a alors hypersécrétion d'insuline par les cellules β des îlots de Langerhans du pancréas afin de compenser la perte de sensibilité à l'insuline des tissus périphériques. Les patients demeurent ainsi normoglycémiques mais sont hyperinsulinémiques à jeun.

- Dans un deuxième temps le pancréas n'est plus capable de compenser la forte diminution de la sensibilité à l'insuline. Durant cette étape les patients sont hyperglycémiques et hyperinsulinémiques à jeun.

- L'hyperproduction d'insuline entraîne la mort des cellules β des îlots de Langherans. La maladie entre alors dans sa phase terminale. Les patients deviennent alors hyperglycémiques et hypoinsulinémiques à jeun.

L'action hypoglycémiante de l'insuline passe en premier lieu par deux mécanismes distincts :

- Une augmentation de l'entrée de glucose (transport) dans la cellule musculaire et adipocytaire. Le glucose est stocké, au sein des myocytes, sous forme de glycogène (synthèse de glycogène).

- Une inhibition du déstockage du glycogène hépatique (glycogénolyse) et de la néoglucogenèse.

En plus du pancréas, le muscle et le foie apparaissent donc comme centraux dans la régulation de la glycémie. De manière intéressante, il a été montré que l'indice de masse corporelle (IMC en kg/m2) (qui est un index d'adiposité) et/ou le pourcentage de masse grasse sont inversement corrélés à la sensibilité à l'insuline (Moro et al., 2008). Les lipides ont alors été considérés comme pouvant être une cause de l'insulino-résistance. L'étude de certains organes (foie, muscle) impliqués dans la régulation de la glycémie a permis de montrer une forte augmentation de leur contenu en lipides associée à la prise de poids (Samuel and Shulman, 2012). De nombreuses études ont alors établi un lien entre accumulation de lipides ectopiques

et insulino-résistance. Ainsi s'est progressivement développé le concept de « lipotoxicité ».

En période post-prandiale le muscle est un des premiers sites d'entrée de glucose qu'il peut oxyder ou stocker sous forme de glycogène. Ainsi lors d'un clamp hyperinsulinique-euglycémique le muscle est responsable d'environ 80% du captage du glucose sanguin (DeFronzo and Tripathy, 2009; Thiebaud et al., 1982). Ces constats ont très tôt poussé la communauté scientifique à considérer le muscle squelettique comme un élément clé dans le développement de la résistance à l'insuline et du diabète (DeFronzo and Tripathy, 2009). C'est pourquoi, une des thématiques de travail de l'équipe est de comprendre comment se développe l'insulino-résistance musculaire liée à l'obésité.

2 LIPIDES ET INSULINO-RESISTANCE MUSCULAIRE

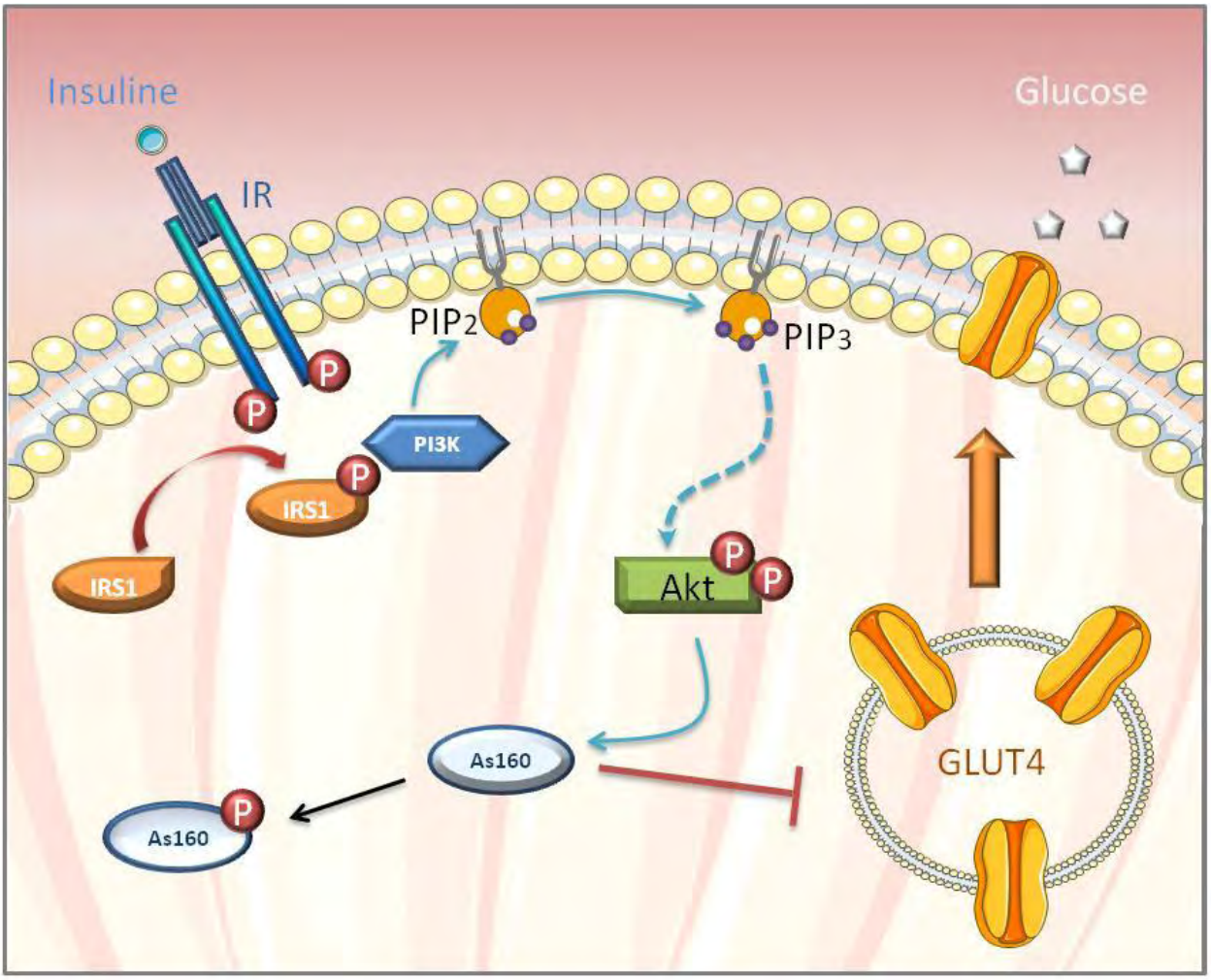

Figure 2: Signalisation de l'insuline

Lors de sa fixation, l'insuline conduit à la phosphorylation des résidus tyrosine (tyr) de son récepteur (IR). Ceci induit le recrutement et l'activation d'IRS1 par phosphorylation sur son résidu tyr612. L'IRS1 active ensuite la PI3K qui phosphoryle le phosphatidyl-inositol (PIP) diphosphate (PIP2) en PIP-triphosphate (PIP3). Ceci permet de recruter Akt à la membrane plasmique, elle est alors activée par phosphorylation notamment sur son site ser473. Lorsqu'Akt est active, elle phosphoryle As160 libérant ainsi les vésicules de *glucose transporter 4* (GLUT4) qui transloquent à la membrane.

2.1 TAG INTRA-MYOCELLULAIRES ET INSULINO-RESISTANCE

Les triacylglycérols (TAGs) représentent la source lipidique principale du muscle squelettique. Historiquement il s'agit de la première espèce lipidique incriminée dans la lipotoxicité musculaire. En effet plusieurs travaux réalisés dans des populations sédentaires ont montré une corrélation négative entre le contenu en TAGs intra-myocellulaires (TGIM) et la sensibilité à l'insuline (Goodpaster et al., 1997; Jacob et al., 1999; Krssak et al., 1999; Pan et al., 1997). Cependant l'analyse du contenu en TGIM chez des athlètes entraînés en endurance a révélé qu'ils disposent à la fois d'une sensibilité à l'insuline accrue et d'un contenu en TGIM bien supérieur à des sujets sains non entraînés. Ce paradoxe est depuis connu sous le nom de « paradoxe des athlètes » (Goodpaster et al., 2001; Moro et al., 2008). De plus des études d'entrainement en endurance de plusieurs semaines améliorent la sensibilité à l'insuline de patients normo-pondérés comme de patients obèses et augmentent parallèlement le contenu en TGIM des patients (Dubé et al., 2008, 2011; Schrauwen-Hinderling et al., 2003; Shepherd et al., 2013). Ces résultats démontrent qu'il existe en réponse à l'entraînement un découplage entre le contenu en TGIM et l'insulino-résistance. Ce constat suggère que les TAGs musculaires ne sont probablement pas responsables *per se* de l'insulino-résistance musculaire.

2.2 ROLE DES LIPIDES INTERMEDIAIRES DANS L'INSULINO-RESISTANCE MUSCULAIRE

S'il est établi que les TGIM ne sont pas impliqués dans le développement de l'insulino-résistance musculaire, d'autre espèces lipidiques tel que les acyl-coenzyme A (acyl-CoA) à longues chaines (ACoA-LC), les diacylglycérols (DAGs) et les céramides ont été associés au developpement de l'obésité et de l'insulino-résistance.

2.2.1 ACIDES GRAS A LONGUES CHAINES

Les ACoA-LC musculaires ont été trouvés comme étant augmentés dans plusieurs cohortes de rongeurs soumis à des régimes riches en lipides (Chen et al., 1992; Ellis et al., 2000). Parallèlement des résultats similaires ont été observés chez des sujets obèses comparés à des sujets de poids normal (Ellis et al., 2000). Cette accumulation d'ACoA-LC a été envisagée pour expliquer la dégradation de l'insulino-sensibilité chez l'obèse.

Afin d'étudier l'effet d'une élévation des taux plasmatiques d'AGs sur l'insulino-résistance, des études d'infusion de lipides chez le rongeur ont été réalisées. Celles-ci conduisent à une augmentation du contenu musculaire en lipides ainsi qu' à une insulino-résistance musculaire et hépatique. Dans le muscle, le dosage des ACoA-LC post-infusion a permis de confirmer une association entre l'accumulation de cette espèce lipidique et l'insulino-résistance (Chalkley et al., 1998). Des études réalisées sur cultures cellulaires montrent que les ACoA-LC sont capables d'inhiber l'*hexokinase* (HK) musculaire (Thompson and Cooney, 2000) ainsi que la *glucokinase* hépatique (Tippett and Neet, 1982). Ces enzymes phosphorylent le glucose en glucose 6 phosphate (G6P), elles sont par conséquence limitantes dans le transport de glucose (Fueger et al., 2005). La diminution de leur expression due aux ACoA-LC pourrait ainsi expliquer la baisse du transport de glucose. Cette voie pourrait participer de manière transitoire à bloquer l'entrée du glucose dans la cellule sans doute afin de prévilégier l'oxydation des lipides et éviter leur accumulation. Cependant cet effet sur le transport ne consiste qu'en une compétition de substrat transitoire et il est peu probable qu'elle soit suffisante pour promouvoir durablement

l'insulino-résistance. En revanche les ACoA-LC pourraient entrer dans la synthèse musculaire d'autres espèces lipotoxiques comme les DAGs et les céramides (figure 3).

2.2.2 CÉRAMIDES

Des études tranversales ont montré que les concentrations de céramides musculaires étaient significativement plus élevées dans le muscle de patients obèses ou insulino-résistants par rapport à des patients sains (Adams et al., 2004; Amati et al., 2011; Galgani et al., 2013; Moro et al., 2009; Straczkowski et al., 2007). De plus un régime riche en lipides saturés chez le rongeur tout comme une infusion d'acides gras (AGs) chez l'homme dégradent la sensibilité à l'insuline et induisent parallèlement une augmentation des concentrations musculaires en céramides (Blachnio-Zabielska et al., 2010; Frangioudakis et al., 2010; Straczkowski et al., 2004). Il est également intéressant de noter que des études d'interventions (entraînement en endurance) montrent une association entre diminution du contenu musculaire en céramides et amélioration de la sensibilité à l'insuline aussi bien chez l'homme que chez le rat (Dobrzyń et al., 2004; Dubé et al., 2008). Plusieurs études menées sur cellules musculaires démontrent qu'un traitement au palmitate induit une augmentation de céramides associée à une baisse de la synthèse de glycogène (marqueur de la sensibilité à l'insuline) et à une altération du signal insulinique. De façon intéressante, il n'y a pas de perte de sensibilité à l'insuline au sein des myocytes traités au palmitate lorsque la synthèse de céramides est bloquée (Chavez et al., 2003; Pickersgill et al., 2007). Ces résultats montrent qu'il existe un lien causal entre synthèse de céramides et développement de l'insulino-résistance au sein de myocytes.

De nombreux travaux menés sur cultures cellulaires ont permis d'identifier les mécanismes par lesquels les céramides induisent l'insulino-résistance. Deux mecanismes indépendants semblent se dégager :

- Premièrement, la *Protéine Kinase C* (PKC) ξ est activée par les céramides et phosphoryle la protéine *v-akt murine thymoma viral oncogene homolog 1* (Akt) sur un résidu sérine (ser) situé dans son domaine pleckstrin homology (Powell et al., 2003).

Ceci bloque l'action d'Akt en empêchant sa translocation à la membrane plasmique et par conséquence son activation (figure 2) (Fox et al., 2007).

- Deuxièmement, les céramides sont également capables d'activer la *protéine phosphatase 2A* (PP2A) connue pour déphosphoryler Akt sur son résidu activateur ser473 (figure 2) (Teruel et al., 2001). Cette voie, lorsqu'elle est activée dans des cellules musculaires, semble grandement participer à l'insulino-résistance induite par les céramides (Chavez et al., 2003).

Ces travaux cliniques et cellulaires montrent le rôle clé de la voie céramides/PP2A musculaire dans le développement de l'insulino-résistance liée à l'obésité (figure 3).

2.2.3 DIACYLGLYCEROLS ET PROTEINE KINASE C

Plusieurs études d'infusion de lipides menées à la fois chez l'homme et le rat montrent que la dégradation de la sensibilité à l'insuline observée est associée à une élévation des concentrations intramusculaires de DAGs. Cette hausse de DAGs est associée à une diminution de l'activité de l'*insulin receptor substrate 1* (IRS1) conduisant à l'inhibition de la *PIP 3 kinases* (PI3K) et de l'ensemble de la voie de signalisation de l'insuline (Griffin et al., 1999; Schmitz-Peiffer and Biden, 2008; Yu et al., 2002). De plus, des travaux cliniques rapportent que les concentrations de DAGs sont plus élevées dans des biopsies de muscles de personnes obèses et/ou insulino-résistantes comparées à des personnes en bonne santé (Moro et al., 2009; Straczkowski et al., 2007). Une élévation des DAGs a également été décrite dans le muscle de rongeurs soumis à un régime riche en lipides (Chibalin et al., 2008; Timmers et al., 2011). De façon intéressante, l'association entre le contenu en DAGs intramusculaires et la sensibilité à l'insuline est conservée dans des études interventionnelles par l'exercice ou par la restriction calorique visant à améliorer l'insulino-sensibilité (Bruce et al., 2006; Dubé et al., 2008; Lessard et al., 2007).

Les DAGs sont connus pour activer de façon allostérique les PKCs conventionelles (α, βI, βII, γ) et les PKC nouvelles (δ, ε, η, θ). En revanche les PKCs dites atypiques ne comprennent pas de site de liaison C1 et sont par conséquence non répondantes aux DAGs (Nishizuka, 1995). Les PKCs sont notamment capables d'inhiber l'activité

d'IRS1 par phosphorylation sur des résidus sérine (ser1101 et ser307). Ceci se traduit par une diminution de l'activité de la voie insulinique (figure 2) (Li et al., 2004; Ravichandran et al., 2001; Schmitz-Peiffer and Biden, 2008). De façon intéressante plusieurs études montrent une augmentation de la translocation de certaines PKCs à la membrane plasmique associée à l'insulino-résistance (Griffin et al., 1999; Itani et al., 2000, 2001, 2002; Yu et al., 2002). Il semble unanimement admis que la PKCθ est impliquée dans l'action délétère des DAGs au niveau musculaire (Erion and Shulman, 2010; Kim et al., 2004a). Cependant la participation d'autre isoformes, tel que la PKCε grandement impliquée dans l'insulino-résistance hépatique, a déjà largement été suggérée et semble pleinement probable (Itani et al., 2000, 2002).

En conclusion, il y a beaucoup d'évidences montrant que les DAGs, *via* l'action de certaines PKCs, sont capables d'entraîner une inhibition du signal insulinique musculaire chez l'homme (figure 3).

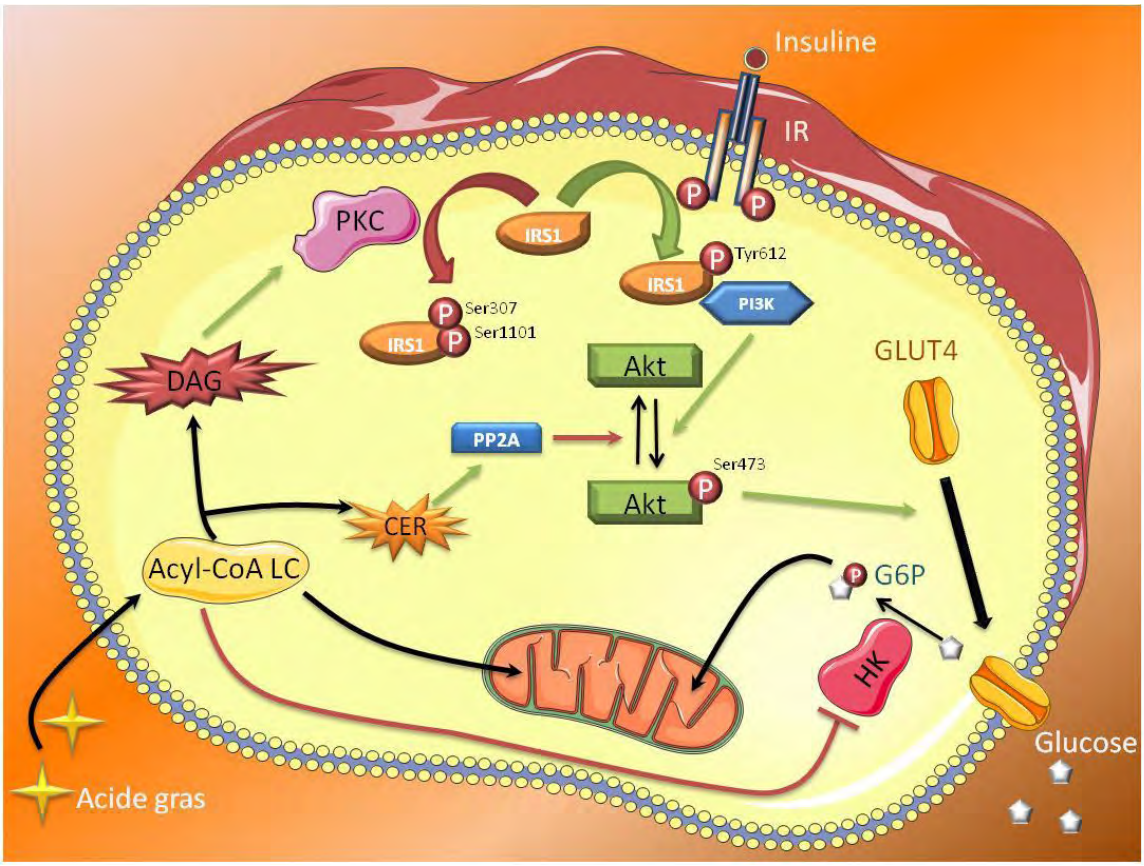

Figure 3. Lipides intermédiaires et insulino-résistance musculaire

L'augmentation des AcoA-LC, des DAGs et des céramides a été décrite pour inhiber la voie de signalisation de l'insuline durant l'obésité. Ceci passerait principalement par la synthèse des DAGs et des céramides à partir d'ACoA-LC. Les DAGs sont connus pour activer certaines PKCs qui sont elles capables d'inhiber par phosphorylation IRS1 sur des résidus sérines. Les céramides sont connus pour activer la phosphatase PP2A capable dans le muscle de déphosphoryler Akt sur son résidu activateur ser473.

2.2.4 LES LIPIDES INTERMEDIAIRES SONT-ILS TOUS TOXIQUES ?

Il semble clair que l'augmentation des concentrations en céramides et en DAGs, notamment due à une hausse des concentrations en ACoA-LC, peut être impliquée dans l'insulino-résistance liée au surpoids. Cependant beaucoup de réponses demeurent encore en suspens. En effet beaucoup d'études présentées ci-dessus ne montrent l'accumulation que de l'une ou de l'autre de ces espèces lipidiques dans des cohortes de patients obèses ou durant une infusion de lipides (Amati et al., 2011; Coen et al., 2010; Itani et al., 2002; Jocken et al., 2010; Skovbro et al., 2008; Yu et

al., 2002). Ceci s'explique en partie par le choix des cohortes et des protocoles expérimentaux qui influencent grandement les résultats obtenus. Lors de la mesure de sensibilité à l'insuline menée durant une infusion de lipides, il est important de regarder le niveau de saturation des triglycérides utilisés. En effet l'ensemble des études ne montrant pas d'augmentation des céramides intramusculaires ont notamment été réalisés avec des espèces lipidiques insaturées incapables d'initier la synthèse de céramides (Itani et al., 2002; Yu et al., 2002). Certaines études de cohorte présentent également des résultats contradictoires, ceci peut s'expliquer par des variations dans les critères de recrutement de chaque étude, notamment du sexe, de l'âge, de la sensibilité à l'insuline ou de la masse grasse. En plus des modalités expérimentales il semblerait que la localisation ainsi que les types d'AGs, composant les DAGs et les céramides, influencent grandement leurs effets lipotoxiques. De nombreuses données sur ces questions sont notamment disponibles pour les DAGs. Il est par exemple établi que les DAGs insaturés sont plus aptes à l'activation des PKCs que les DAGs composés d'AGs saturés (Schmitz-Peiffer and Biden, 2008). De plus, de façon intéressante Bergman *et al* ont récemment montré, dans le muscle squelettique, que les DAGs membranaires sont de meilleurs prédicteurs de l'insulino-résistance que les DAGs totaux (Bergman et al., 2012). A l'inverse, peu d'informations sont disponibles sur le niveau de toxicité des différents types de céramides et sur l'impact de leur localisation intra-myoellulaire dans l'insulino-résistance. Plusieurs travaux ont récemment étudié les types d'AGs composant les DAGs et les céramides dans diverses cohortes de patients (Amati et al., 2011; Bergman et al., 2010, 2012; Skovbro et al., 2008; Straczkowski et al., 2007). Pour l'heure, il semble cependant compliqué d'incriminer spécifiquement certaines sous espèces musculaire de DAGs et céramides dans l'insulino-résistance.

3 VOIES D'ACCUMULATION DES DIACYLGLYCEROLS ET DES CERAMIDES

3.1 VOIES ENTRAINANT L'ACCUMULATION D'ACIDES GRAS INTRA-MYOCELLULAIRES

3.1.1 ENTREE DES ACIDES GRAS ET INSULINO-RESISTANCE

Chez l'homme et le rongeur obèse plusieurs études ont montré une hausse de l'entrée des AGs dans le muscle squelettique. Ceci pourrait participer à l'augmentation des concentrations intra-myocellulaires de lipides toxiques. Deux hypothèses semblent pouvoir expliquer ce phénomène (Bonen et al., 2004; Luiken et al., 2001)

3.1.1.1 ELEVATION DES NIVEAUX D'ACIDES GRAS CIRCULANTS

Comme le montrent les études d'infusion de lipides, une élévation des taux circulants d'AGs est suffisante pour conduire à une augmentation des DAGs et céramides musculaires et induire l'insulino-résistance (Griffin et al., 1999; Straczkowski et al., 2004; Yu et al., 2002). De façon intéressante de nombreux travaux ont trouvé une élévation des taux circulants d'AGs chez des patients diabétiques ou obèses à jeûn (Golay et al., 1986; Gordon, 1960; Jensen et al., 1989; Reaven et al., 1988). Pourtant plus récemment des études de cohortes menées sur plus d'un millier de sujets n'ont étonnamment pas retrouvé d'association entre l'IMC et l'élévation des taux plasmatiques d'AGs à jeûn (Karpe et al., 2011). Il existe donc un fort débat sur la relation entre les taux plasmatiques d'AGs à jeûn et l'IMC. Pourtant tout le monde s'accorde sur le fait que les organes insulino-sensibles des patients obèses et diabétiques sont plus exposés aux AGs (figure 4). Ceci pourrait notamment s'expliquer par une augmentation du flux d'AGs plasmatiques chez l'obèse et le

diabétique sans que cela ne se traduise nécessairement par une augmentation de leur concentration plasmatique (Fabbrini et al., 2008; Jensen et al., 1989; Mittendorfer et al., 2009). De plus il semblerait que le métabolisme adipocytaire des personnes obèses et insulino-résistantes puisse favoriser l'exposition du muscle squelettique aux AGs. Ceci est médiée par plusieurs phénomènes distincts : les adipocytes présentent une diminution de l'activation par l'insuline de la *lipoprotéine lipase* en période post-prandiale (lipase impliquée dans l'hydrolyse des TAGs des lipoprotéines pour permettre l'entrée des AGs dans les tissus) (Fried et al., 1993; Ong and Kern, 1989) ce qui se traduit par une diminution du captage adipocytaire des AGs issus des lipoprotéines formées en période post-prandiale, les chylomicrons (McQuaid et al., 2011). De plus l'insuline est connue pour avoir une action antilipolitique sur l'adipocyte (Jensen et al., 1987). Après la mise en place de l'insulino-résistance, il pourrait donc y avoir diminution de l'inhibition de la lipolyse par l'insuline (Bush et al., 2012). Ceci aurait pour conséquence une baisse moins importante de la libération d'AGs par les adipocytes en période post-prandiale. Ces mécanismes peuvent expliquer la diminution minorée des concentrations plasmatiques d'AGs observées chez l'obèse et le diabétique en période post-prandiale (McQuaid et al., 2011; Roust and Jensen, 1993). Cependant la mise en place de ces dérégulations pourrait être dépendante du développement de l'insulino-résistance adipocytaire. Ceci peut expliquer pourquoi certaines études ne trouvent pas de différence dans la baisse des concentration d'AGs plasmatiques observées après un repas, chez le jeune obèse (Heptulla et al., 2001).

3.1.1.2 ROLE DES TRANSPORTEURS AUX ACIDES GRAS MUSCULAIRES

Enfin et bien que les AGs puissent pénétrer les cellules par diffusion passive, les transporteurs d'AGs pourraient jouer un rôle dans l'entrée de ces derniers au sein des myocytes. C'est ce que laissent envisager les modèles murins invalidés pour deux d'entre eux, le *cluster of differentiation 36* (CD36) et le *fatty acid transport protein 1* (FATP1). Parallèlement à la baisse de l'entrée des lipides dans le muscle, ces mutations limitent également l'accumulation de lipides ectopiques ainsi que le développement de l'insulino-résistance musculaire (Bonen et al., 2007; Goudriaan et al., 2003; Kim et al., 2004b).

Des études menées chez des rats Zucker prédisposés à l'obésité ont montré une augmentation de l'entrée des AGs au sein du muscle squelettique. L'augmentation du flux et/ou des concentrations d'AGs circulant pourrait suffire à expliquer cela, cependant les auteurs ont voulu savoir s'il existait un lien avec une dérégulation de l'expression et de la localisation des transporteurs d'AGs musculaires. Si la mesure de l'expression protéique de CD36, FATP1 et FATP4 n'a révélé aucune modification entre les rats Zucker et leur contrôles, une augmentation du nombre de CD36 à la membrane a été observée chez les rats obèses (Holloway et al., 2009). Cette plus forte présence de transporteurs d'AGs à la membrane plasmique du muscle squelettique pourrait participer à l'augmentation de l'entrée d'AGs musculaire chez le rat obèse. Chez l'homme très peu d'études se sont intéressées à l'association entre les transporteurs aux AGs et l'insulino-résistance. Cependant il semblerait que comme chez le rongeur, le nombre de transporteurs CD36 localisés à la membrane plasmique soit fortement augmenté chez des personnes obèses et diabétiques, alors que son expression protéique n'est pas modifiée (Aguer et al., 2010; Bonen et al., 2004). La présence de ce transporteur à la membrane est fortement corrélée à l'entrée d'AGs dans le muscle squelettique et au contenu en TGIM. De façon intéressante cette étude montre chez l'homme que l'expression et le contenu membranaire d'autres transporteurs d'AGs ne sont eux pas modifiés (Bonen et al., 2004).

L'ensemble de ces études menées à la fois chez le rongeur et chez l'homme montre clairement que la localisation du récepteur CD36 est fortement modifiée durant l'obésité et l'insulino-résistance. Chez l'obèse, il semble, qu'associée à l'augmentation du flux/concentration d'AGs circulant, une augmentation des transporteurs présents à la membrane plasmique des myocytes pourrait participer à l'augmentation de l'entrée d'AGs au sein du muscle squelettique et au développement de l'insulino-résistance (figure 4). Cependant d'autres études chez l'homme doivent être réalisées pour démontrer le lien de causalité entre l'excès de CD36 à la membrane et l'insulino-résistance.

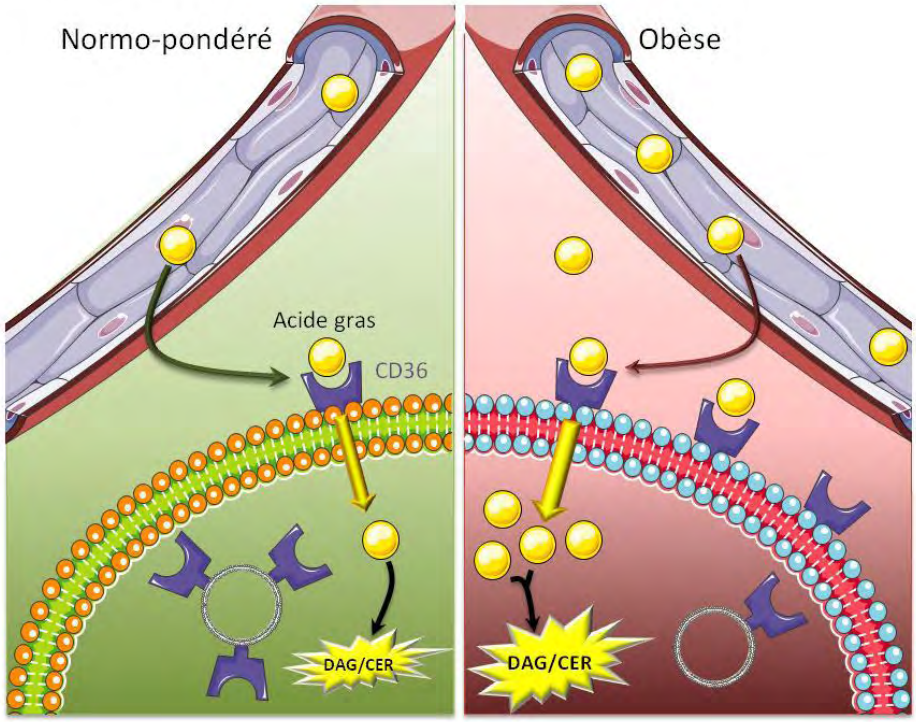

Figure 1. Exposition du muscle aux acides gras en contexte physiologique et physiopathologique

Le muscle squelettique des sujets obèses est confronté à une augmentation du flux/concentration d'AGs circulants. De plus des dérégulations internes aux myocytes conduisent à une augmentation du nombre de CD36 à la membrane plasmique. Ensemble ces phénomènes pourraient participer à l'augmentation de la synthèse de DAGs et céramides musculaires.

3.1.2 MITOCHONDRIES ET INSULINO-RESISTANCE

Une fois que les AGs ont pénétré dans la cellule musculaire, ils peuvent soit être oxydés soit participer à la formation de TAGs, de phospholipides ou former des lipides intermédiaires lipotoxiques. Il a donc été envisagé que l'oxydation des AGs par la mitochondrie puisse être un moyen important de lutter contre l'accumulation de lipides intermédiaires. A l'inverse des défauts d'oxydation des AGs pourraient privilégier l'accumulation de lipides toxiques et l'insulino-résistance (Lowell and Shulman, 2005). Cette hypothèse a été étayée par de nombreux travaux notamment du groupe de J.A. Simoneau et D.E. Kelley montrant une diminution de l'activité d'enzymes impliquées dans l'oxydation des lipides (*3 hydroxyacyl-CoA déshydrogénase*, *citrate synthase*, *succinate déshydrogénase*, *cytochrome C oxydase*) en contexte d'obésité et d'insulino-résistance (Blaak et al., 2000; Colberg et al., 1995; He et al., 2001; Simoneau and Kelley, 1997; Simoneau et al., 1995, 1999). Ces dérégulations de l'oxydation ont largement été imputées à la diminution du nombre et de la taille des mitochondries (Kelley et al., 2002; Morino et al., 2005) ainsi qu'à une diminution consécutive de leur activité (Bajpeyi et al., 2011; Petersen et al., 2004, 2005). Ceci est principalement expliqué par une diminution de l'expression de plusieurs gènes régulant la biogenèse mitochondriale comme le *peroxisome proliferator-activated receptors* (PPAR) α, *PPARγ coactivator 1 α* (PGC1*α)* (Mootha et al., 2003) et le *nuclear respiratory factor 1* (Patti et al., 2003).

Ces résultats associatifs placent les dysfonctions mitochondriales comme une cause possible de l'accumulation des lipides intermédiaires et de l'insulino-résistance. Pourtant de nombreuses données vont à l'encontre de cette hypothèse. Premièrement la création de deux modèles transgéniques murins ayant des déficiences mitochondriales n'a pas permis de confirmer l'existance du lien causal entre dysfonction de la mitochondrie et insulino-résistance. En effet l'invalidation muscle spécifique de la protéine PGC1α, ainsi que de *l'apoptosis-inducing factor*, ont respectivement entraîné une diminution du nombre de mitochondries et une altération de leurs fonctions (Finck and Kelly, 2006; Joza et al., 2005). Dans ces deux cas, de façon surprenante, les souris sont protégées contre la prise de poids et présentent même une meilleure sensibilité musculaire à l'insuline (Handschin et al., 2007; Pospisilik et al., 2007). Deuxièmement, les personnes obèses diabétiques, lors

de l'exercise, ont une capacité mitochondriale suffisante pour accroitre leur oxydation de substrats d'environ quarante fois (Holloszy, 2013). Il semble donc difficilement envisageable que la capacité mitochondriale de repos de ces individus soit insuffisante et conditionne l'accumulation de lipides. Malgré une capacité mitochondriale suffisante il a été montré, chez l'obèse diabétique, une baisse de l'oxydation des lipides en faveur de celle du glucose (Goodpaster, 2013; Kelley et al., 1999). Cependant, beaucoup d'autres études ont montré une plus forte oxydation des lipides chez l'obèse, au repos comme à l'exercice (Golay et al., 1986; Holloszy, 2013). C'est pourquoi, l'implication des défauts mitochondriaux dans l'accumulation de lipides musculaires toxiques fait encore l'objet de nombreux débats (Goodpaster, 2013; Holloszy, 2013). L'ensemble de ces données ne remet pas en cause l'existence de dommages mitochondriaux associés à l'obésité et au diabète. En revanche elles permettent de penser que les défauts mitochondriaux ne sont pas primaires à l'accumulation de lipides musculaires. Cependant, iindépendamment de l'accumulation d'espèces lipidiques toxiques, il pourrait tout de même exister un lien entre la mitochondrie et l'insulino-résistance. Ceci passerait durant l'obésité par une surcharge en substrats de ces organelles. Cette surcharge favoriserait alors la synthèse d'acylcarnitines (dérivés de l'oxydation incomplète des AGs) et/ou d'espèces réactives de l'oxygène ayant des actions néfastes sur le signal insulinique (Koves et al., 2008).

De plus il semblerait probable que la perte de sensibilité à l'insuline participe à la détérioration du contenu et/ou de la fonction mitochondriale du muscle squelettique. Ceci pourrait être liée à plusieurs facteurs, comme l'augmentation de la production d'espèces réactives de l'oxygène (comme le peroxyde d'hydrogène) par la mitochondrie (Bonnard et al., 2008), la perte de sensibilité à l'insuline elle-même (Asmann et al., 2006) ou simplement dû à un faible niveau d'activité physique des individus (Holloszy, 2013).

3.2 MECANISMES INTRAMUSCULAIRES D'ACCUMULATION DES CERAMIDES

3.2.1 ANABOLISME DES CERAMIDES ET INSULINO-RESISTANCE

La production des céramides comprend plusieurs voies, dont la majoritaire est la synthèse *de novo* (figure 5) (Merrill, 2002). L'enzyme *sérine palmitoyltransférase* (SPT) est responsables de la première étape de synthèse *de novo* des céramides en permettant d'associer la sérine au palmitoyl-CoA pour donner du 3-oxosphinganine. Plusieurs études menées sur des modèles murins ont montré le rôle clé que pouvait avoir cette voie de synthèse des céramides dans le développement de l'insulino-résistance. En effet un traitement avec un inhibiteur de SPT permet de protéger des rongeurs comme des cellules musculaires du développement de l'insulino-résistance observée suite à un régime gras ou suite à un traitement au palmitate, ceci en limitant l'accumulation de céramides musculaires (Chavez et al., 2003; Holland et al., 2007; Hu et al., 2011; Pickersgill et al., 2007; Straczkowski et al., 2007; Watson et al., 2009). L'inhibition de l'activité *dihydrocéramide synthase* ainsi que la diminution d'expression de la *dihydroceramide désaturase*, autres enzymes impliquées dans la voie de synthèse *de novo* de céramides, protègent également de l'accumulation de céramides et de l'insulino-résistance musculaire chez la souris (Chavez and Summers, 2012; Chavez et al., 2003; Holland et al., 2007). S'il semble clair que l'inhibition de la synthèse de céramides, notamment au niveau musculaire, protège du développement de l'insulino-résistance, très peu de données, sont pour l'instant, disponibles quant à la dérégulation musculaire de ces enzymes dans des contextes d'obésité et d'insulino-résistance. Si certaines études chez le rat montrent une augmentation de l'expression d'une sous unité de SPT, la SPT1 et de la *dyhydrocéramide synthase 1* en régime hyperlipidique (Blachnio-Zabielska et al., 2010; Frangioudakis et al., 2010), chez l'homme il ne semble pas y avoir de différence d'expression de ces enzymes entre normo-pondérés et obèses ou entre sensibles et insensibles à l'insuline (Coen et al., 2010; Thrush et al., 2009).

Les céramides peuvent aussi être synthétisés à partir de sphingomyéline et minoritairement par d'autres espèces comme la sphingosine (Lipina and Hundal,

2011). Dans des cellules musculaires, l'inhibition de la *sphingomyélinase* (SMase) qui synthétise des céramides à partir de sphingomyéline entraîne une diminution du contenu en céramides (Ferreira et al., 2010). De plus son inhibition protège contre le développement de l'insulino-résistance médiée par un régime riche en lipides mais les effets musculaires ne sont pour l'heure pas caractérisés (Boini et al., 2010; Deevska et al., 2009). Cependant, tout comme les enzymes impliquées dans la synthèse *de novo* de céramides, l'expression des SMases n'est pas modifiée chez des personnes obèses par rapport à des personnes normo-pondérés (Thrush et al., 2009).

Ces résultats tendent à montrer que cibler la synthèse de céramide pourrait être efficace pour améliorer l'insulino-sensibilité. Cependant, les principales enzymes impliquées dans la synthèse de céramides n'ont pas été montrées comme étant dérégulées chez l'obèse. Par conséquence ces modifications ne peuvent pas, pour l'instant, expliquer le développement de l'insulino-résistance dans cette pathologie.

3.2.2 CATABOLISME DES CERAMIDES ET INSULINO-RESISTANCE

Un ralentissement du catabolisme des céramides pourrait également participer à leur accumulation chez l'obèse. La voie amenant à la formation de sphingosine 1 phosphate (S1P) à partir de céramides semble être une voie privilégiée dans le catabolisme de cette espèce toxique. En effet le S1P une fois produit peut être recyclé et ainsi sortir du cycle des sphingolipides (Hannun and Obeid, 2008). Deux enzymes sont impliquées, la *céramidase* qui permet la formation de sphingosine à partir des céramides ainsi que la *sphingosine kinase* qui phosphoryle ce dernier en S1P. De façon intéressante, plusieurs études ont montré qu'une augmentation de l'activation musculaire de la *céramidase* et de la *sphingosine kinase* améliorait la sensibilité à l'insuline de myocytes comme de modèle murin (Bruce et al., 2012; Chavez et al., 2005). Des études ont été menées sur une autre voie de catabolisme des céramides amenant à la production de glycosphingolipides. De façon interéssante, l'inhibition pharmacologique ou l'extinction d'enzymes impliquées dans la synthèse de ces dérivés à partir de céramides (*Glucosylceramide synthase*, *Ganglioside monosialo 3 (GM3) synthase*) améliore la sensibilité à l'insuline des

souris notamment au niveau du muscle squelettique (Aerts et al., 2007; Yamashita et al., 2003). Ces effets surprenants sont liés à la diminution de la synthèse de GM3 qui est depuis peu connu pour inhiber l'action de l'insuline dans le tissu adipeux, le muscle et le foie (Aerts et al., 2007; Tagami et al., 2002). D'autres études ont été menées sur d'autres voies de catabolisme des céramides comme la voie de synthèse des sphingomyélines et des céramides 1 phosphate. Cependant les modèles murins créés par invalidation de la *céramide kinase* (CerK) comme de la *sphingomyeline synthase* (SMsynthase) sont protégés contre la prise de poids induite par un régime hyperlipidique, les résultats sur la sensibilité à l'insuline sont par conséquence difficiles à interpréter en tenant uniquement compte des variations de la concentration en sphingolipide (Li et al., 2011b; Mitsutake et al., 2012).

En conclusion, il semble que l'activation de la voie du S1P soit une stratégie intéressante pour diminuer le contenu en céramides musculaires et améliorer la sensibilité à l'insuline. Il ne semble pas y avoir, chez l'homme, de diminution d'expression de la *céramidase* avec l'obésité (Thrush et al., 2009). Finalement des études complémentaires devront mesurer l'expression des autres enzymes impliquées dans le catabolisme des céramides afin d'établir un lien potentiel avec l'insulino-résistance musculaire.

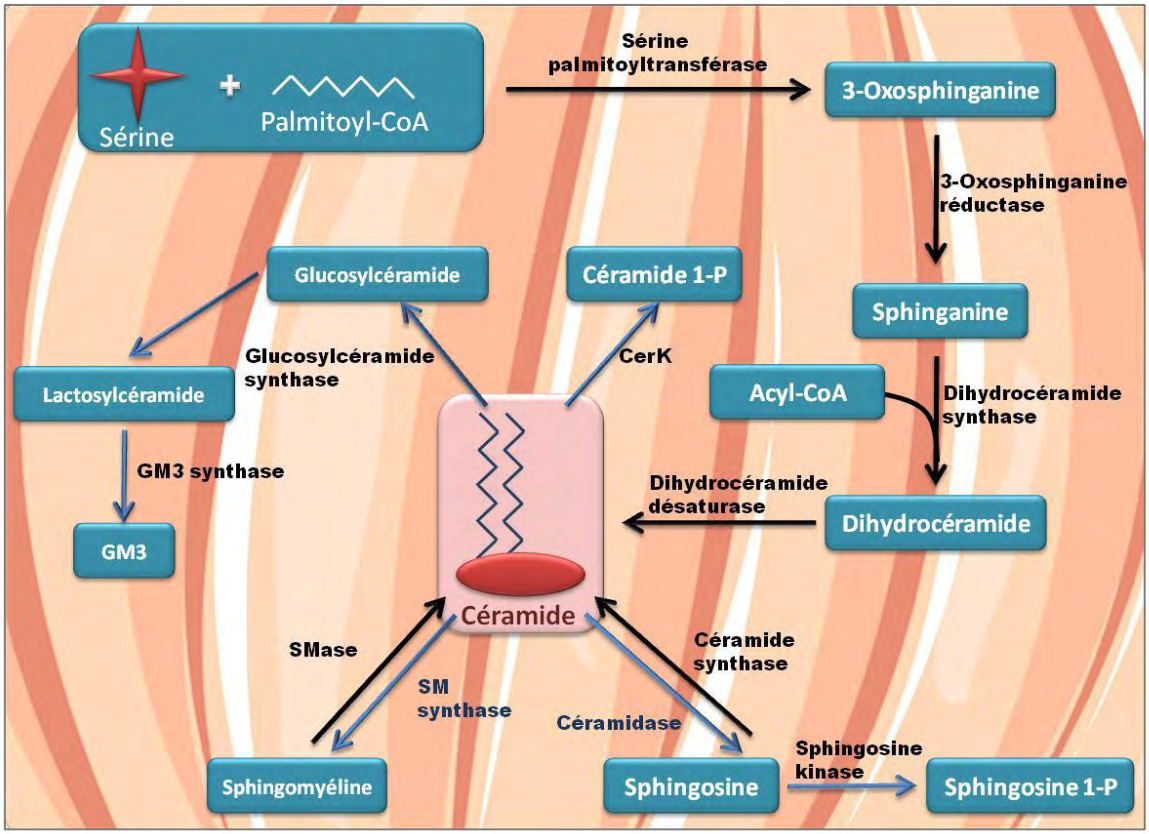

Figure 5. Voie anabolique et catabolique des céramides

D'après Lipina C et Hundal HS (Lipina and Hundal, 2011).

3.3 MECANISMES INTRAMUSCULAIRES D'ACCUMULATION DES DAG

3.3.1 ANABOLISME DES DAG ET INSULINO-RESISTANCE

La synthèse des DAGs peut se faire *via* certains phospholipides comme les PIP2 sous l'action de la *phospholipase C* (PLC), cependant la voie de synthèse de novo des DAGs semble être la voie d'accumulation privilégiée (figure 6). La synthèse *de novo* peut s'opérer par deux voies distinctes :

La première voie appelée voie de synthèse des glycérophospholipides se déroule en trois étapes. Elle commence par l'acylation du glycerol-3-phosphate (G3P) par la *glycerol-3-phosphate acyltransférase* (GPAT) produisant ainsi de l'acide lysophosphatidique (LPA). Il existe plusieurs GPATs, deux sont situées à la membrane mitochondriale (mtGPAT) et une au niveau du reticulum endoplasmique (msGPAT). Sous l'action d'une *LPA acyltransférase* (LPAAT1-6), un deuzième acyl-CoA est greffé à la molécule de LPA tout juste formée pour donner du PA. Enfin l'action de la *phosphatidic acid phosphatase 1* (PAP1) entraîne la déphosphorylation de l'acide phosphatidique en DAG (Coleman and Lee, 2004). Cette voie de synthèse a été très étudiée et semble être pour la communauté scientifique la voie canonique de formation des DAGs dans bon nombre de tissus et notamment dans le muscle squelettique. De façon intéressante plusieurs études montrent qu'une extinction de l'expression de la mtGPAT1 entraîne une diminution de la concentration de DAGs hépatiques et par conséquence une meilleure sensibilité hépatique à l'insuline (Neschen et al., 2005). Cette délétion n'entraîne aucun effet au niveau du muscle squelettique, ceci s'explique en partie car la mtGPAT1 est surtout active dans le foie et le tissu adipeux en condition basale (Coleman et al., 2000; Lewin et al., 2001). A l'inverse une surexpression de GPAT1 spécifiquement au niveau hépatique et induit une insulino-résistance (Nagle et al., 2007). Cependant il n'y a pas à notre connaissance d'études menées dans le muscle squelettique sur le lien entre cette voie de synthèse des DAGs et l'insulino-résistance. Ceci s'explique, sans doute, par le fait qu'il ne semble pas y avoir, chez des patients obèses insulino-résistants, d'augmentation de l'expression ou de l'activité des GPATs et de PAP1 pouvant

expliquer une hausse de la synthèse de DAGs (Bergman et al., 2012; Li et al., 2011a; Thrush et al., 2009).

L'autre voie de synthèse *de novo* des DAGs semble notamment très importante dans la production des TAGs intestinaux indispensables à l'absorption des lipides (Coleman and Lee, 2004). Cette voie permet la formation de monoacylglycérols (MAG) à partir d'un glycérol et d'un acyl-CoA sous l'action d'une *acyl CoA : glycérol acyltransférase* (GAT) (Lee et al., 2001). Un DAG peut alors être formé en associant à un MAG un nouvel acyl-CoA grâce à la *MAG acyltransférase* (MGAT) (Lehner and Kuksis, 1995). La relevance physiologique de cette voie de synthèse des DAGs a très peu été étudiée dans le muscle squelettique, cependant quelques articles montrent que son existence est probable, puisque le muscle squelettique possède une activité GAT (Lee et al., 2001) et une activité MGAT (Yen et al., 2002). Ces résultats sont confirmés par des données non publiées de notre laboratoire qui montre que la MGAT est exprimée dans des myocytes primaires en culture et est surexprimée par un traitement pharmacologique mimant l'exercice et augmentant le contenu en TAGs (Sparks et al., 2011). Cependant des études complémentaires sont nécessaires pour mieux décrire cette voie au niveau musculaire et évaluer son importance relative dans la production de TGIM par rapport à la voie des glycérophospholipides. Il serait également intéressant d'identifier sa possible implication dans le développement de l'insulino-résistance.

3.3.2 CATABOLISME DES DAG ET INSULINO-RESISTANCE

Les DAGs peuvent être utilisés afin de produire plusieurs autres espèces lipidiques. Ils peuvent notamment être retransformés en acide phosphatidique et en MAGs sous l'action respective de *DAG kinases* (DAGK) (Topham and Epand, 2009) et de la *lipase hormono-sensible* (LHS) (Lafontan and Langin, 2009) (évoquée dans la partie lipolyse). Grâce à l'action de *DAG acyltransférase* (DGAT) (Yen et al., 2008), les DAGs peuvent également être estérifiés pour former des TAGs considérés comme la forme de stockage principale des AGs. Des dérégulations de ces voies cataboliques des DAGs dans le muscle squelettique pourraient contribuer à une modification du contenu en DAGs et par conséquence jouer sur la sensibilité à l'insuline. C'est ce

que montre notamment une étude de surexpression de la DGAT1 dans le muscle squelettique (muscle creatine kinase (MCK)-DGAT1) dans laquelle la sensibilité à l'insuline des souris transgéniques est améliorée en régime hyperlipidique (Liu et al., 2007). En revanche le modèle de surexpression muscle-spécifique de la DGAT2 présente des résultats contradictoires sur la sensibilité à l'insuline, comparés au modèle MCK-DGAT1. Ceci pourrait être dû à des actions légèrement différentes de ces deux enzymes entraînant une accumulation d'espèces de lipides intermédiaires différente (Levin et al., 2007; Shi and Cheng, 2009). Ces deux enzymes n'ont d'ailleurs aucune homologie de séquence ce qui pourrait argumenter en faveur d'actions légèrement différentes. De manière interéssante une augmentation musculaire de l'expression de la DGAT1 associée à une augmentation des TAGs et une diminution des DAGs et des céramides est retrouvée en post-exercice et expliquerait l'amélioration de la sensibilité à l'insuline alors observée après un exercice aïgu (Schenk and Horowitz, 2007). Chez l'obèse et le diabétique l'expression de la DGAT1 ne semble cependant pas être significativement modifiée (Amati et al., 2011; Li et al., 2011a).

Plusieurs DAGKs sont exprimées dans le muscle squelettique, notamment les DAGKs α, δ, ξ, ε, et η (van Blitterswijk and Houssa, 2000; Miele et al., 2007). L'action des DAGKs musculaires sur la sensibilité à l'insuline a aussi été étudiée. En culture la DAGKδ permettrait notamment de diminuer les DAGs intra-myocellulaires et, par conséquence, de lever l'action inhibitrice des PKCs sur la voie de signalisation à l'insuline (Miele et al., 2007). De plus Chibalin *et al* ont créé un modèle murin hétérozygote pour la DAGKδ majoritairement exprimée dans le muscle squelettique. Leurs résultats montrent que la diminution d'expression de la DAGKδ altère la sensibilité à l'insuline et la tolérance au glucose ainsi que le signal insulinique musculaire. Ces observations sont corrélées à une forte augmentation des DAGs musculaires chez les souris mutantes (Chibalin et al., 2008). De façon intéressante cette même étude montre que l'expression protéique de DAGKδ est diminuée chez des patients diabétiques ainsi que chez des rats Goto-Kakizaki prompts à développer un diabète de type 2. L'ensemble de ces données montre clairement que l'expression de la DAGKδ musculaire régule la sensibilité à l'insuline *via* son action sur la concentration en DAGs.

Ensemble les données accumulées sur la fonction des DGATs et des DAGKs musculaires montrent qu'elles pourraient activement participer à l'accumulation de DAGs et par conséquence à l'activation de PKCs néfastes à l'action musculaire de l'insuline. Cependant seule la DAGKδ, semble pouvoir participer à la perte de sensibilité à l'insuline liée à l'obésité, l'expression de la DGAT1 n'étant pas modifiée avec le statut métabolique des sujets étudiés.

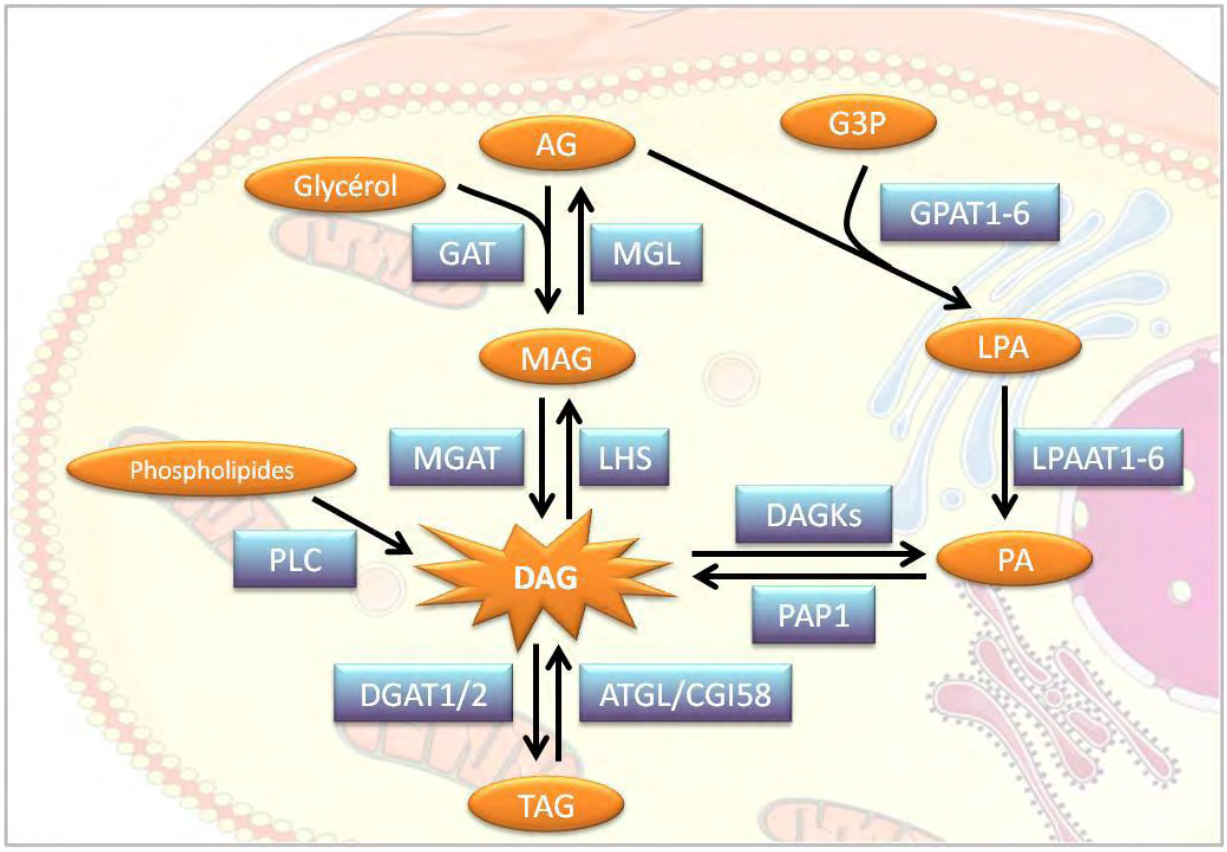

Figure 6. Voie anabolique et catabolique des DAGs

4 LIPOLYSE MUSCULAIRE ET INSULINO-RESISTANCE

4.1 LES ENZYMES LIPOLYTIQUES

La lipolyse permet la libération d'AGs à partir des TAGs stockés au niveau de la gouttelette lipidique. Les lipases sont des enzymes impliquées dans l'hydrolyse des TAGs. Leur rôle dans le métabolisme lipidique du muscle squelettique à l'exercice et durant l'obésité semble crucial. Pourtant elles ont surtout été étudiées dans le tissu adipeux. Jusqu'à peu la lipolyse était décrite comme étant régulée par deux lipases, la LHS capable d'hydrolyser les TAGs et les DAGs (Belfrage et al., 1977; Fredrikson et al., 1981) et la *MAG lipase* (MGL) connue pour hydrolyser les MAGs (Fredrikson et al., 1986), ces lipases étant notamment exprimées dans le tissu adipeux et le muscle (Karlsson et al., 1997; Langfort et al., 1999; Langin et al., 2005; Watt et al., 2006). Cependant la création de modèles murins invalidés pour la LHS a permis de montrer qu'une autre enzyme était capable d'hydrolyser les TAGs et ce pour plusieurs raisons : certains modèles invalidés pour la LHS sont résistants à la prise de poids induite par un régime riche en lipides (Girousse and Langin, 2012; Harada et al., 2003; Sekiya et al., 2004), ce qui paraissait illogique par rapport à la fonction connue de la LHS et qui laissait envisager de possibles compensations par d'autres lipases inconnues. De plus certaines études ont montré que l'extinction de l'enzyme n'éliminait que partiellement la lipolyse des TAGs dans le tissu adipeux (Okazaki et al., 2002) et conduisait à une accumulation de DAGs et non de TAGs dans le muscle squelettique (Haemmerle et al., 2002). Ces résultats ont abouti à la découverte en 2004 par trois groupes indépendants d'une lipase alors inconnue possédant une forte activité d'hydrolyse des TAGs, l'*adipose triglycéride lipase* (ATGL) (aussi appelé *Patatin-like phospholipase domain containing 2* ou *Desnutrine*) (Jenkins et al., 2004; Villena et al., 2004; Zimmermann et al., 2004). A l'origine décrite dans le tissu adipeux, l'expression de l'ATGL a depuis été identifiée dans de nombreux tissus dont le muscle squelettique humain (Jocken et al., 2008, 2010). Son extinction dans un modèle de cellule adipocytaire humaine a pour effet de grandement diminuer la lipolyse basale et stimulée (Bezaire et al., 2009). Chez la souris son invalidation conduit à une augmentation de la prise de poids ainsi qu'à une forte accumulation de

TAGs dans le tissu adipeux, le muscle squelettique ainsi que le cœur (Haemmerle et al., 2006). De façon intéressante, il semblerait que la perte d'expression de l'ATGL s'associe chez la souris à une moins bonne capacité d'endurance à l'exercice et une plus forte utilisation de glucides représentée par la hausse du quotient respiratoire ainsi qu'une diminution des stocks hépatiques et musculaires de glycogène (Huijsman et al., 2009; Schoiswohl et al., 2010). Ces résultats peuvent notamment s'expliquer par l'incapacité des souris à utiliser leurs réserves lipidiques et montre que l'ATGL est essentielle dans la mobilisation des TAGs.

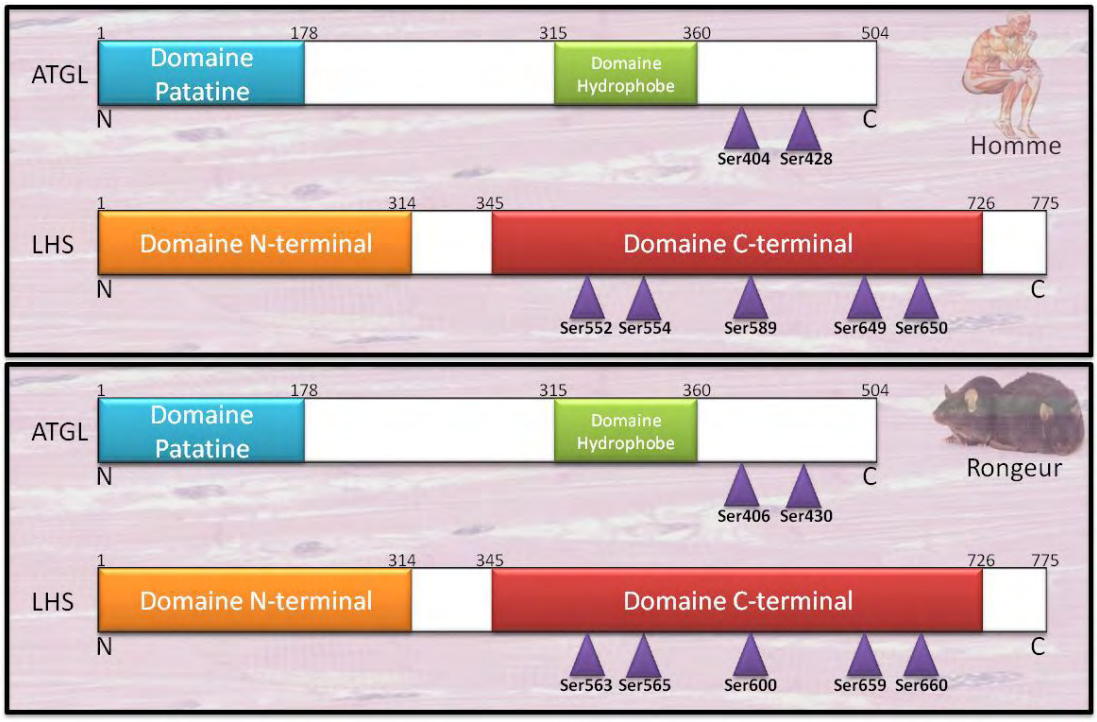

Figure 7. Sites de phosphorylation connus de la LHS et de l'ATGL chez l'homme et la souris

D'après Watt MJ et Spriet LL (Watt and Spriet, 2010).

4.2 REGULATION DE LA LIPOLYSE MUSCULAIRE

4.2.1 REGULATION DE L'ACTIVITE DE LA LHS

La LHS est phosphorylable sur cinq résidus sérine, ser552, ser554, ser589, ser649 et ser650, chez l'homme et ser563, ser565, ser600, ser659, ser660 chez le rat (Figure 7) (par souci de simplicité seule la nomenclature humaine sera utilisée dans ce paragraphe). Certains résidus sérines ont été décrits comme pouvant réguler l' activité enzymatique de la LHS dans le muscle squelettique (Figure 8) (Donsmark et al., 2003; Greenberg et al., 2001; Roepstorff et al., 2004, 2006). Prats *et al* ont observé que la LHS est transloquée au niveau des gouttelettes lipidiques dans des fibres musculaires durant la contraction ou lors d'un traitement avec de l'épinéphrine (Prats et al., 2006). Parallèlement des études menées sur des soléaires de rats ont permis de montrer que l'activité de la LHS était fortement induite suite à la contraction musculaire ou suite à un traitement par l'épinéphrine (Langfort et al., 1999, 2000). L'épinéphrine par l'activation du récepteur β2-adrénergique stimule la *protéine kinase AMPc-dépendante* (PKA), cette dernière étant capable de phosphoryler la LHS sur ses résidus ser552, ser649 et ser650. Cependant chez l'homme l'activation de la LHS semble principalement due aux résidus ser649 et ser650 (Krintel et al., 2008; Talanian et al., 2006). De plus des études, menées chez des patients adrénalectomisés, ont permis de montrer que l'épinéphrine joue un rôle important dans l'augmentation de l'activité de la LHS induite par l'exercice (Kjaer et al., 2000). La contraction musculaire serait également capable d'activer la LHS, de façon épinéphrine indépendante, de par l'activation calcium-dépendante de PKCs ainsi que par l'activation de proteines *extracellular signal-regulated kinases* (Donsmark et al., 2003; Watt et al., 2003). La LHS possède également un site de phosphorylation inhibiteur en ser554, dans le tissu adipeux il est bien décrit que ce site est ciblé par la *5'-AMP protéine kinase* (AMPK), cependant l'effet inhibiteur de l'AMPK dans le muscle squelettique est toujours débattu et ne semble pas si clair (Kiens, 2006; Muoio et al., 1999; Roepstorff et al., 2004).

4.2.2 REGULATION DE L'ACTIVITE DE L'ATGL

Comme la LHS, l'ATGL possède des sites de phosphorylation. Pour l'instant deux sites sont décrits, chez l'homme ils se situent en ser404 et ser428 (ser406 et ser430 chez la souris, par souci de simplicité, les résidus humains seront utilisés comme référence) (Figure 7). Il a été montré que l'AMPK était capable de phosphoryler le résidu ser404 entraînant une augmentation de l'activité d'hydrolyse des TAGs dans des adipocytes murins (Ahmadian et al., 2011). La PKA pourrait aussi, dans l'adipocyte humain, phosphoryler ce résidu ser404 (Pagnon et al., 2012). Ceci n'a pas été retrouvé par Zimmerman *et al* dans des cellules hépatiques HepG2 (Zimmermann et al., 2004). Cependant les travaux de Mason *et al* tendent à relativiser l'importance de ce résidu sur l'activité musculaire de l'ATGL. En effet il montrent *in vitro* et *in vivo*, que l'augmentation de l'activité de l'ATGL musculaire à l'exercice est indépendant d'une augmentation de phosphorylation en ser404 (Mason et al., 2012). Il est maintenant important d'identifier la fonction et les kinases phosphorylant le résidu ser428 afin d'établir s'il peut participer au contrôle de la lipolyse du muscle squelettique.

En plus du rôle potentiel des phosphorylations, l'activité de l'ATGL est finement régulée par son co-activateur, le *comparative gene identification 58* (CGI-58) (Figure 8). Sa fonction a été rapporté en 2006 par Lass *et al* qui ont montré qu'une mutation de ce gène était responsable du syndrome de Chanarin Dorfman connu pour entraîner une forte accumulation de lipides dans divers tissus (Lass et al., 2006). CGI-58 a été décrit comme étant un puissant activateur de l'activité de l'ATGL dans différents types cellulaires notamment l'adipocyte (Lass et al., 2006; Yamaguchi et al., 2007). A l'inverse l'activité de l'ATGL est également régulée négativement par une autre protéine, la *G0/G1 switch gene 2* (G0S2) dont l'effet sur l'ATGL vient d'être rapporté récemment dans des adipocytes murins et humains. (Cornaciu et al., 2011; Schweiger et al., 2012; Yang et al., 2010). Si l'expression de CGI-58 (Lass et al., 2006; Subramanian et al., 2004) et de G0S2 a été identifiée dans le muscle squelettique (Welch et al., 2009; Zandbergen et al., 2005), des études complémentaires sont nécessaires pour évaluer la fonction de ces protéines dans ce tissu.

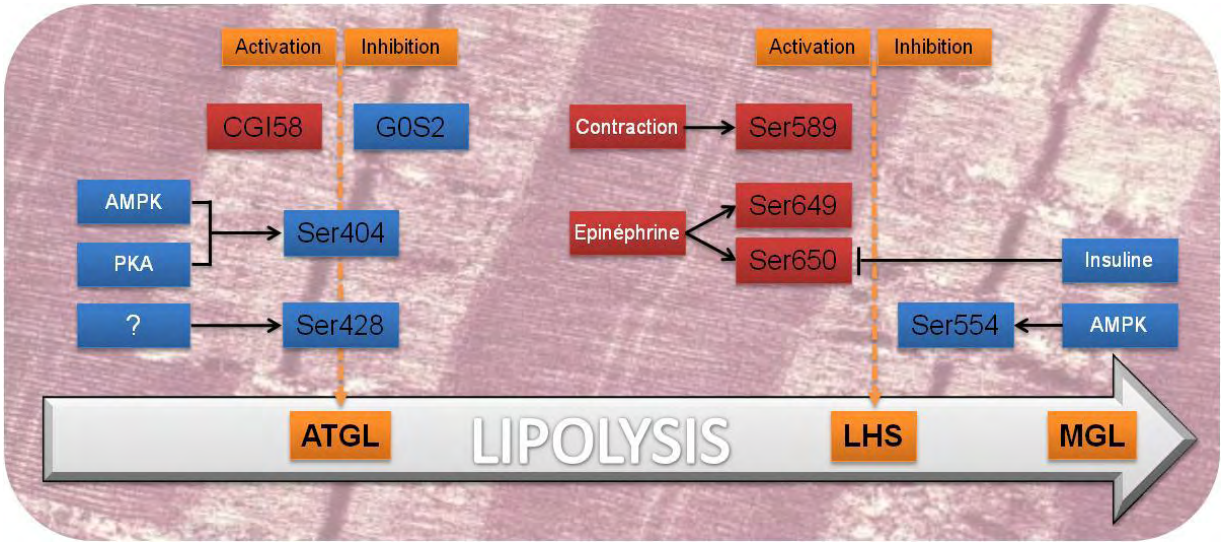

Figure 8. Régulateurs connus de l'ATGL et de la LHS dans le muscle squelettique

Les cadres rouges correspondent aux régulations ayant déjà été décrites dans le muscle squelettique. Les cadres bleus correspondent aux régulations ayant été décrites dans d'autres organes et pouvant exister dans le muscle squelettique. Les inscriptions en noirs représentent les sites de phosphorylation ou les protéines connues pour réguler l'activité des lipases. Les inscriptions blanches représentent les facteurs pouvant faire varier le niveau de phosphorylation des lipases.

4.2.3 PÉRILIPINES ET LIPOLYSE

Les protéines de la famille des *périlipines* (PLIN) sont les principales protéines associées à la gouttelette lipidique. A l'heure actuelle, cinq PLINs sont connues et semblent toutes avoir un rôle dans le développement et la dynamique des gouttelettes lipidiques. Leur expression a été décrite dans de nombreux types cellulaires et a notamment été étudiée dans l'adipocyte, le cœur, le muscle squelettique et le foie. De façon intéressante leur niveau d'expression varie beaucoup d'un tissu à l'autre, PLIN1 est par exemple très exprimée dans le tissu adipeux et n'est pas présente dans le muscle squelettique. A l'inverse PLIN5 est surtout exprimée dans les tissus très oxydatifs comme le muscle squelettique et le cœur (Dalen et al., 2007; Wolins et al., 2006; Yamaguchi et al., 2006). PLIN1 est la périlipine la plus étudiée à l'heure actuelle et elle semble être au cœur de la régulation de la lipolyse adipocytaire en contrôlant l'accès des lipases à la gouttelette lipidique (Granneman et al., 2007, 2009; Miyoshi et al., 2006, 2007; Moore et al., 2005; Subramanian et al., 2004). D'autres travaux ont également été menés sur les

protéines PLIN2 et PLIN5 plus exprimées dans les tissus oxydatifs. Les études menées sur ces protéines l'ont souvent été sur des modèles cellulaires par des approches de surexpression. Elles ont permis de montrer que la surexpression de l'une ou l'autre de ces PLINs dans différents modèles de culture notamment des myocytes et des adipocytes favorisait l'accumulation de TAGs (Bosma et al., 2012; Imamura et al., 2002; Larigauderie et al., 2004; Li et al., 2012; Listenberger et al., 2007; Wang et al., 2011a). De plus, très récemment, plusieurs études *in vivo* ont permis de confirmer qu'une surexpression par électroporation ou une surexpression par transgénèse additive de PLIN5 et PLIN2, dans le muscle squelettique ou le cœur spécifiquement, avait également pour conséquence d'augmenter le contenu en TGIM (Bosma et al., 2012, 2013; Pollak et al., 2013; Wang et al., 2013). L'influence de ces deux périlipines sur le contenu en TAGs s'explique en partie par leur rôle démontré sur la lipolyse. L'augmentation de l'expression de ces protéines est en effet associée à une diminution des capacités lipolytiques (Dalen et al., 2007; Listenberger et al., 2007; Pollak et al., 2013; Wang et al., 2011a, 2011b). Les travaux menés par Wang et Granneman sur la colocalisation probable de PLIN5 avec l'ATGL ainsi que le récent article de MacPherson montrant une diminution de l'interaction de PLIN2 avec l'ATGL durant la contraction, permettent de penser que PLIN2 et PLIN5 pourraient participer à la régulation de la lipolyse musculaire en conditionnant l'accès des lipases à la gouttelette, tout comme PLIN1 dans le tissu adipeux (Figure 9) (Granneman et al., 2011; Macpherson et al., 2013; Wang et al., 2011b). Ces résultats montrent l'importance des PLINs 2 et 5 dans la régulation de la lipolyse et la régulation du métabolisme lipidique des tissus oxydatifs. De futures études devront confirmer le rôle de ces protéines dans le muscle squelettique et s'attacher à comprendre les mécanismes précis mis en œuvre.

Si d'autres PLINs (PLIN3 et 4 notamment) sont exprimées dans le muscle squelettique humain et murin (Wolins et al., 2006), leur importance possible dans la régulation de la lipolyse n'est pour l'heure pas établie.

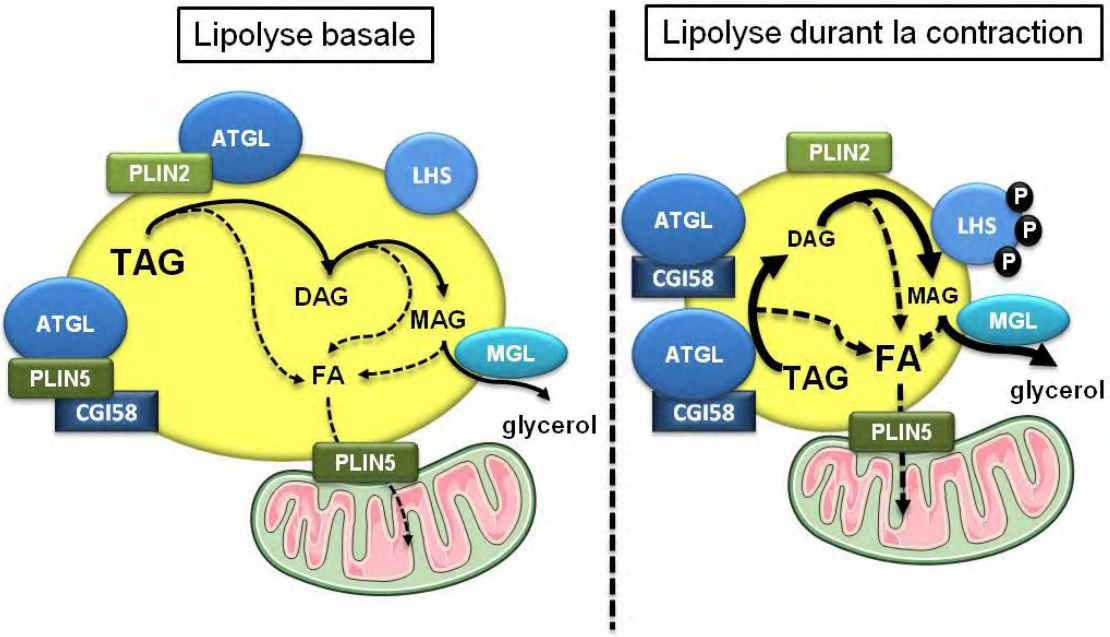

Figure 9. La lipolyse musculaire au repos et à l'exercice

Peu d'éléments sont connus à propos du contrôle de la lipolyse musculaire au repos et à l'exercice. Au repos, on sait que l'ATGL est liée à PLIN2 et PLIN5 tandis que CGI-58 est seulement liée à PLIN5. A l'exercice les PLINs pourraient libérer l'ATGL et CGI-58 afin de faciliter leur interaction et donc la lipolyse.

4.3 LIPOLYSE MUSCULAIRE ET LIPIDES INTERMEDIAIRES

4.3.1 LIPASES ET INSULINO-RESISTANCE : MECANISMES MOLECULAIRES

De part leur fonction, des dérégulations des lipases musculaires pourraient conduire à une accumulation d'espèces lipidiques lipotoxiques. En effet une augmentation du flux lipolytique pourrait contribuer à l'augmentation du contenu en AGs intramusculaires et ainsi augmenter le contenu en céramides. De plus au vu des substrats préférentiels de l'ATGL et de la LHS, le déséquilibre d'expression ou d'activité des lipases pourraient également participer à une augmentation du contenu en DAGs. Le lien causal pouvant exister entre la dérégulation des lipases musculaires et l'accumulation de lipidiques cytotoxiques a pu être vérifié dans plusieurs modèles murins transgéniques. Ainsi l'extinction globale de la LHS entraîne une forte augmentation du contenu musculaire en DAGs et une légère diminution de la sensibilité à l'insuline (Haemmerle et al., 2002; Mulder et al., 2003; Park et al., 2005). Les faibles variations de la sensibilité à l'insuline musculaire dans ce modèle peuvent en partie s'expliquer par l'effet bénéfique d'une diminution de la lipolyse adipocytaire sur la sensibilité à l'insuline. Ces effets passeraient par une diminution du flux d'AGs circulants (Girousse and Langin, 2012; Girousse et al., 2013). A l'inverse les souris invalidées pour l'ATGL demeurent aussi sensibles à l'insuline et gluco-tolérantes que leurs contrôles malgré une prise de poids plus importante et une forte accumulation de TAGs musculaires en régime standard (Haemmerle et al., 2006).

4.3.2 DEREGULATION DE L'EQUILIBRE LIPOLYTIQUE MUSCULAIRE ET INSULINO-RESISTANCE CHEZ L'HOMME

Des études de cohortes conduites par notre équipe se sont intéressées chez l'homme au lien potentiel existant entre dérégulation de l'expression/activité des lipases musculaires et insulino-résistance. Ainsi des dérégulations de l'expression de la LHS et de l'ATGL ont été rapportées chez des individus obèses comparés à des individus de poids normal. En effet l'expression de la LHS est diminuée alors que

celle de l'ATGL est augmentée. Ces observations sont corroborées par la mesure des activités TAG hydrolase (TAGH) et DAG hydrolase (DAGH) montrant une diminution de l'activité DAGH chez l'obèse ainsi qu'une diminution du ratio DAGH/TAGH. Ceci reflète une lipolyse incomplète chez l'obèse (Jocken et al., 2008, 2010; Moro et al., 2009). Il est intéressant de noter que le ratio DAGH sur TAGH explique respectivement 54% et 38% de la variance des DAGs et des céramides intra-myocellulaires.

L'ensemble des résultats obtenus grâces aux études cliniques et grâce aux modèles murins transgéniques pour l'une ou l'autre des lipases montrent clairement qu'une dérégulation musculaire de l'équilibre de la balance entre l'ATGL et la LHS pourrait activement participer à l'insulino-résistance chez l'homme (Figure 10).

5 OBJECTIFS DE THESE

A partir de l'ensemble de ces données préliminaires, le but de ma thèse a été de contribuer à :

-L'amélioration de la compréhension du rôle de la dérégulation des lipases musculaires dans le développement de l'insulino-résistance liée à la prise de poids. Ceci est notamment passé par l'étude des dérégulations des lipases musculaires chez l'homme et la souris en contexte d'obésité et d'insulino-résistance. Dans ce but, nous avons également étudié de manière causale l'effet d'une dérégulation provoquée de l'expression/activité des lipases musculaires sur l'accumulation d'espèces lipotoxiques et la sensibilité à l'insuline. Ces travaux ont été menés sur myocytes primaires humains.

-L'amélioration des connaissances portant sur le contrôle de la lipolyse musculaire, notamment par l'étude du co-activateur de l'ATGL, CGI-58.

6 RESULTATS

6.1 PUBLICATION 1 : L'ALTERATION DE L'EXPRESSION ET DE L'ACTIVITE DES LIPASES MUSCULAIRES CONTRIBUE A L'INSULINO-RESISTANCE CHEZ L'HOMME

6.1.1 ARTICLE 1

Publication 1: Altered skeletal muscle lipases expression and activity contributes to insulin resistance in humans

Badin PM, Louche K, Mairal A, Liebisch G, Schmitz G, Rustan AC, Smith SR, Langin D, and Moro C. *(2011) Diabetes. 60(6):1734-42.*

ORIGINAL ARTICLE

Altered Skeletal Muscle Lipase Expression and Activity Contribute to Insulin Resistance in Humans

Pierre-Marie Badin,[1,2] Katie Louche,[1,2] Aline Mairal,[1,2] Gerhard Liebisch,[3] Gerd Schmitz,[3] Arild C. Rustan,[4] Steven R. Smith,[5] Dominique Langin,[1,2,6] and Cedric Moro[1,2]

OBJECTIVE—Insulin resistance is associated with elevated content of skeletal muscle lipids, including triacylglycerols (TAGs) and diacylglycerols (DAGs). DAGs are by-products of lipolysis consecutive to TAG hydrolysis by adipose triglyceride lipase (ATGL) and are subsequently hydrolyzed by hormone-sensitive lipase (HSL). We hypothesized that an imbalance of ATGL relative to HSL (expression or activity) may contribute to DAG accumulation and insulin resistance.

RESEARCH DESIGN AND METHODS—We first measured lipase expression in vastus lateralis biopsies of young lean ($n = 9$), young obese ($n = 9$), and obese-matched type 2 diabetic ($n = 8$) subjects. We next investigated in vitro in human primary myotubes the impact of altered lipase expression/activity on lipid content and insulin signaling.

RESULTS—Muscle ATGL protein was negatively associated with whole-body insulin sensitivity in our population ($r = -0.55$, $P = 0.005$), whereas muscle HSL protein was reduced in obese subjects. We next showed that adenovirus-mediated ATGL overexpression in human primary myotubes induced DAG and ceramide accumulation. ATGL overexpression reduced insulin-stimulated glycogen synthesis (-30%, $P < 0.05$) and disrupted insulin signaling at Ser1101 of the insulin receptor substrate-1 and downstream Akt activation at Ser473. These defects were fully rescued by nonselective protein kinase C inhibition or concomitant HSL overexpression to restore a proper lipolytic balance. We show that selective HSL inhibition induces DAG accumulation and insulin resistance.

CONCLUSIONS—Altogether, the data indicate that altered ATGL and HSL expression in skeletal muscle could promote DAG accumulation and disrupt insulin signaling and action. Targeting skeletal muscle lipases may constitute an interesting strategy to improve insulin sensitivity in obesity and type 2 diabetes. ***Diabetes*** **60:1734–1742, 2011**

From [1]INSERM, U1048, Obesity Research Laboratory, Institute of Metabolic and Cardiovascular Diseases (I2MC), Toulouse, France; the [2]Paul Sabatier University, University of Toulouse, Toulouse, France; the [3]Institute of Clinical Chemistry, University of Regensburg, Regensburg, Germany; the [4]Department of Pharmaceutical Biosciences, School of Pharmacy, University of Oslo, Oslo, Norway; the [5]Translational Research Institute for Metabolism and Diabetes and the Burnham Institute, Florida Hospital, Winter Park, Florida; and the [6]Centre Hospitalier Universitaire de Toulouse, Biochemistry Laboratory, Biology Institute of Purpan, Toulouse, France.
Corresponding author: Cedric Moro, cedric.moro@inserm.fr.
Received 24 September 2010 and accepted 3 March 2011.
DOI: 10.2337/db10-1364
This article contains Supplementary Data online at http://diabetes.diabetesjournals.org/lookup/suppl/doi:10.2337/db10-1364/-/DC1.

Skeletal muscle insulin resistance is a strong risk factor of type 2 diabetes and cardiovascular diseases (1,2). Dysfunctional adipose tissue can lead to lipid oversupply and increased flux of free fatty acids (FFAs) into skeletal muscle and is associated with the accumulation of intramyocellular triacylglycerols (IMTGs) (3–5). This chronic lipid overload in tissues can evolve to a state of lipotoxicity leading to cell dysfunction (6). The term "lipotoxicity" defines more generally in skeletal muscle a state of lipid overload (increased concentrations of long-chain acyl-CoA, diacylglycerols [DAGs], and ceramide) causing insulin resistance (7–12). DAGs have been shown to activate novel protein kinase C (PKC) isoforms, such as the novel PKCθ leading to insulin receptor substrate-1 (IRS-1) serine phosphorylation and impaired downstream insulin signaling (10–13). DAGs can be formed through multiple pathways but are also formed as intermediates during triacylglycerol (TAG) synthesis and hydrolysis (14). The control of lipolysis in skeletal muscle has mainly been attributed to hormone-sensitive lipase (HSL), which exhibits a 10-fold higher specific activity for DAG than TAG (15). HSL null mice display normal TAG hydrolase activity after an overnight fast and accumulate large amounts of DAG (16). Recently it was shown that adipose triglyceride lipase (ATGL) plays a major role in the regulation of cellular TAG stores in various tissues of the body, including heart and skeletal muscle (17,18). ATGL specifically drives the hydrolysis of TAG into DAG (18). ATGL-deficient mice are more insulin sensitive and glucose tolerant despite a threefold increase in TAG content in their skeletal muscle (17). The molecular mechanism underlying this phenotype remains unclear. In the current study, we hypothesized that an imbalance of ATGL relative to HSL could increase intracellular DAG concentrations and promote insulin resistance. To test this hypothesis, we first examined the relationship between muscle ATGL expression and whole-body insulin sensitivity in a wide range of subjects. We next manipulated the expression/activity of ATGL and HSL in vitro in cultured human primary skeletal muscle cells and evaluated its impact on lipid pools and insulin signaling.

RESEARCH DESIGN AND METHODS

Skeletal muscle cell culture. Satellite cells from vastus lateralis or rectus abdominis biopsies of lean, healthy, insulin-sensitive subjects were isolated by trypsin digestion, preplated on an uncoated petri dish for 1 h to remove fibroblasts, and subsequently transferred to T-25 collagen-coated flasks in Dulbecco's modified Eagle's medium (DMEM) low glucose (1 g/L) supplemented with 10% FBS and growth factors (human epidermal growth factor, BSA, dexamethasone, gentamicin, amphotericin B [Fungizone, Invitrogen, Grand Island, NY], and fetuin) as previously described (19). Cells from several donors were pooled and grown at 37°C in a humidified atmosphere of 5% CO_2. Differentiation of myoblasts into myotubes was initiated at approximately 90% confluence by switching to α-minimum essential medium with antibiotics,

2% FBS, and fetuin. The medium was changed every other day, and cells were grown up to 5–6 days.

Overexpression of lipases. Human ATGL and HSL cDNAs were cloned into the pcDNA3 vector (Invitrogen Corp., Carlsbad, CA). DNA sequencing was performed to check correct insertion of the cDNA using an ABI3100 automatic sequencer (Applied Biosystems, Courtaboeuf, France). Adenoviruses expressing in tandem green fluorescent protein (GFP) and ATGL or HSL were constructed, purified, and titrated (Vector Biolabs, Philadelphia, PA). An adenovirus containing the *GFP* gene only was used as a control. Myotubes were infected with the control (GFP), ATGL, and HSL adenoviruses at day 4 of differentiation and remained exposed to the virus for 24 h in serum-free DMEM containing 150 μmol/L of oleate complexed to BSA (ratio 4:1). Oleate was preferred to palmitate for lipid loading of the cells to favor TAG synthesis and to avoid the intrinsic lipotoxic effect of palmitate (20,21). No adenovirus-induced cellular toxicity was observed as determined by chemiluminescent quantification of adenylate kinase activity (ToxiLight, Lonza Group Ltd., Basel, Switzerland). For insulin signaling experiments, infected myotubes were incubated for 20 min in DMEM low glucose with or without 100 nmol/L of insulin (Sigma-Aldrich, Lyon, France).

Determination of glycogen synthesis. Cells were preincubated with a glucose- and serum-free α-minimum essential medium for 90 min and then exposed to DMEM supplemented with D[U-^{14}C]glucose (1 μCi/mL; PerkinElmer, Boston, MA) in the presence or absence of 100 nmol/L insulin for 3 h. After incubation, glycogen synthesis was determined as described previously (22).

Pulse-chase studies of lipid metabolism. Cells were pulsed overnight (18 h) with a combination of [1-^{14}C]oleate (1 μCi/mL; PerkinElmer) and unlabeled oleate (100 μmol/L final concentration) to prelabel the endogenous TAG pool. After incubation, myotubes were chased for 3 h in nutrient-deficient DMEM containing 0.1 mmol/L glucose and 0.5% FFA-free BSA. At the end of incubation, total lipids were extracted in chloroform/methanol (2v/1v) and separated by thin-layer chromatography as previously described (23). Incorporation rates were normalized to total protein content measured in each well.

Western blot analysis. Muscle tissues and cell extracts were homogenized in a buffer containing 50 mmol/L HEPES, pH 7.4, 2 mmol/L EDTA, 150 mmol/L NaCl, 30 mmol/L $NaPO_4$, 10 mmol/L NaF, 1% Triton X-100, 10 μL/mL protease inhibitor (Sigma-Aldrich), 10 μL/mL phosphatase I inhibitor (Sigma-Aldrich), 10 μL/mL phosphatase II inhibitor (Sigma-Aldrich), and 1.5 mg/mL benzamidine HCl. Tissue homogenates were centrifuged for 25 min at 15,000*g*, and supernatants were stored at −80°C. Solubilized proteins from muscle tissue and myotubes were run on a 4–12% SDS-PAGE (Bio-Rad, Hercules, CA), transferred onto nitrocellulose membrane (Hybond ECL, GE Healthcare, Buckingamshire, U.K.), and incubated with the primary antibodies (ATGL, Cell Signaling Technology Inc., Beverly, MA; Perilipin-A, Abcam Inc., Cambridge, MA). The HSL antibody was as previously described (24). Antibodies for insulin signaling *p*-Ser473–Akt, Akt, *p*-Ser1101–IRS-1, *p*-Tyr612–IRS-1, IRS-1, and *p*-Ser660–HSL were all from Cell Signaling Technology Inc. Subsequently, immunoreactive proteins were determined by enhanced chemiluminescence reagent (GE Healthcare, Waukesha, WI) and visualized by exposure to Hyperfilm ECL (GE Healthcare). Glyceraldehyde-3-phosphate dehydrogenase (GAPDH) (Cell Signaling Technology Inc.) served as an internal control.

Subjects. Nine young lean, nine young obese, and eight obese subjects with type 2 diabetes were recruited in the study (Table 1). The subjects with type 2 diabetes were diet-controlled or were taking metformin (n = 6) and insulin (n = 2), and were otherwise healthy with an average HbA_{1c} of 7.0 ± 0.78%. None of them were taking thiazolidinediones. The protocol was approved by the institutional review board of the Pennington Biomedical Research Center, and all volunteers gave written informed consent. After participants completed the screening visit, fat mass was measured on a Hologic Dual Energy X-Ray Absorptiometer (QDR 2000, Hologic Inc., Bedford, MA). The participants were asked to refrain from vigorous physical activity for 48 h before presenting to the Pennington inpatient clinic and ate a weight-maintaining diet consisting of 35% fat, 16% protein, and 49% carbohydrate 2 days before the clamp and the muscle biopsy. Samples of vastus lateralis weighing 60–100 mg were obtained by muscle biopsy using the Bergstrom technique, blotted, cleaned, and snap-frozen in liquid nitrogen (25).

TABLE 1
Clinical characteristics of the subjects

	Lean (9)	Obese (9)	Type 2 diabetes (8)
Sex (male/female)	6/3	5/4	6/2
Age (years)	23.8 ± 0.8	23.7 ± 0.8	53.8 ± 3.8[b,e]
Body weight (kg)	66.4 ± 3.6	94.5 ± 3.4[c]	102.4 ± 4.2[c]
BMI (kg/m^2)	22.5 ± 0.5	32.9 ± 0.5[c]	35.4 ± 1.7[c]
Body fat (%)	20.4 ± 2.8	31.1 ± 1.6[a]	37.5 ± 2.9[b]
GDR (mg/min/kg FFM)	9.3 ± 0.8	7.0 ± 0.6[a]	5.3 ± 0.6[c]
Fasting glucose (mmol/L)	4.67 ± 0.12	4.81 ± 0.13[a]	7.51 ± 0.76[b,d]
Fasting insulin (mU/L)	8.4 ± 1.2	13.2 ± 1.1[a]	13.7 ± 2.9[a]

Data are mean ± SEM. FFM, fat-free mass; GDR, glucose disposal rate. [a]$P < 0.05$, [b]$P < 0.01$, [c]$P < 0.001$ vs. lean; [d]$P < 0.01$, [e]$P < 0.001$ vs. obese.

Hyperinsulinemic euglycemic clamp. Insulin sensitivity was measured by clamp (26). After an overnight fast, insulin (80 mU · m^{-2} · min^{-1}) and 20% glucose (to maintain plasma glucose at 90 mg/dL) were administered for 2 h. Glucose and insulin were measured in three independent blood plasma samples 5 min apart at baseline and again at steady-state after approximately 2 h. Glucose disposal rate was adjusted for kilograms of fat-free mass.

Lipase activity assays. TAG hydrolase (TAGH) and DAG hydrolase (DAGH) activities were measured on cell extracts as previously described (24,27). Briefly, 1(3)-mono[^{3}H]oleyl-2-*O*-mono-oleylglycerol (MOME) and [9, 10-^{3}H(N)]triolein were emulsified with phospholipids by sonication. MOME is a DAG analog that allows for the measurement of DAGH activity because it is not a substrate for monoacylglycerol lipase. [9, 10-^{3}H(N)]triolein was used to determine specifically TAGH activity, and [^{3}H]MOME was used to determine specifically DAGH activity.

TAG and DAG determination by gas chromatography-mass spectrometry. Total lipids were extracted from frozen muscle tissue samples and from myotubes harvested in water containing 0.25 mL 0.1% SDS. Lipids were extracted using the method of Folch et al. (28). The extracts were filtered, and lipids were recovered in the chloroform phase. TAG and DAG were isolated using thin-layer chromatography on Silica Gel 60 A plates developed in petroleum ether, ethyl ether, and acetic acid (80:20:1), and visualized by rhodamine 6G. The TAG and DAG band was scraped from the plate and methylated using BF_3/methanol as described by Morrison and Smith (29). The methylated FFAs were extracted with hexane and analyzed by gas chromatography using an HP 5890 gas chromatograph equipped with flame ionization detectors, an HP 3365 Chemstation, and a capillary column (SP2380, 0.25 mm × 30 m, 0.25 μm film; Supelco, Bellefonte, PA). Helium was used as a carrier gas. The oven temperature was programmed from 160 to 230°C at 4°C/min. FFA methyl esters were identified by comparing the retention times with those of known standards. Inclusion of the internal standards, 20:1 (trieicosenoin) and 17:0 (diheptadecanoin), permits quantitation of the amount of TAG and DAG in the sample.

Ceramide determination by electrospray ionization tandem mass spectrometry. Ceramide was quantified by electrospray ionization tandem mass spectrometry as previously described (30). Briefly, lipid extracts were prepared by the method of Bligh and Dyer (31) in the presence of nonnaturally occurring Cer 14:0, Cer 17:0. Samples were analyzed by direct flow injection on a Quattro Ultima triple-quadrupole mass spectrometer (Micromass, Manchester, U.K.) using an HTS PAL autosampler (CTC Analytics AG, Zwingen, Switzerland) and an Agilent 1100 binary pump (Agilent Technologies GmbH, Waldbronn, Germany) with a solvent mixture of methanol containing 10 mmol/L ammonium acetate and chloroform (3:1, v/v). A flow gradient was performed starting with a flow of 55 μL/min for 6 s followed by 30 μL/min for 1.0 min and an increase to 250 μL/min for another 12 s. Ceramide was analyzed using a fragment of *m/z* 264 with *N*-heptadecanoyl-sphingosine as internal standard. Both ions $[M+H]^+$ and $[M+H-H_2O]^+$ were used, and quantification was achieved by calibration lines generated by addition of Cer 16:0, 18:0, 20:0, 24:1, 24:0 to tissue and cell samples, respectively. Correction of isotopic overlap of ceramide species and data analysis were performed by self-programmed Excel (Microsoft Corp., Redmond, WA) macros according to the principles described previously (32).

Statistical analyses. All statistical analyses were performed using GraphPad Prism 5.0 for Windows (GraphPad Software Inc., San Diego, CA). One-way ANOVA followed by Bonferroni post hoc tests and paired, two-tailed Student t tests were performed to determine differences between groups and treatments. Two-way ANOVA and Bonferroni post hoc tests were used when appropriate. Normal distribution of the data was tested using the Shapiro-Wilk normality test. The relationships between muscle ATGL protein and clinical variables were analyzed using Spearman rank correlations. All values in Figs. 1 to 7 and Table 1 are presented as mean ± SEM. Statistical significance was set at $P < 0.05$.

RESULTS

Relationship between muscle ATGL and insulin sensitivity. We first investigated the relationship between skeletal muscle ATGL protein content and insulin sensitivity

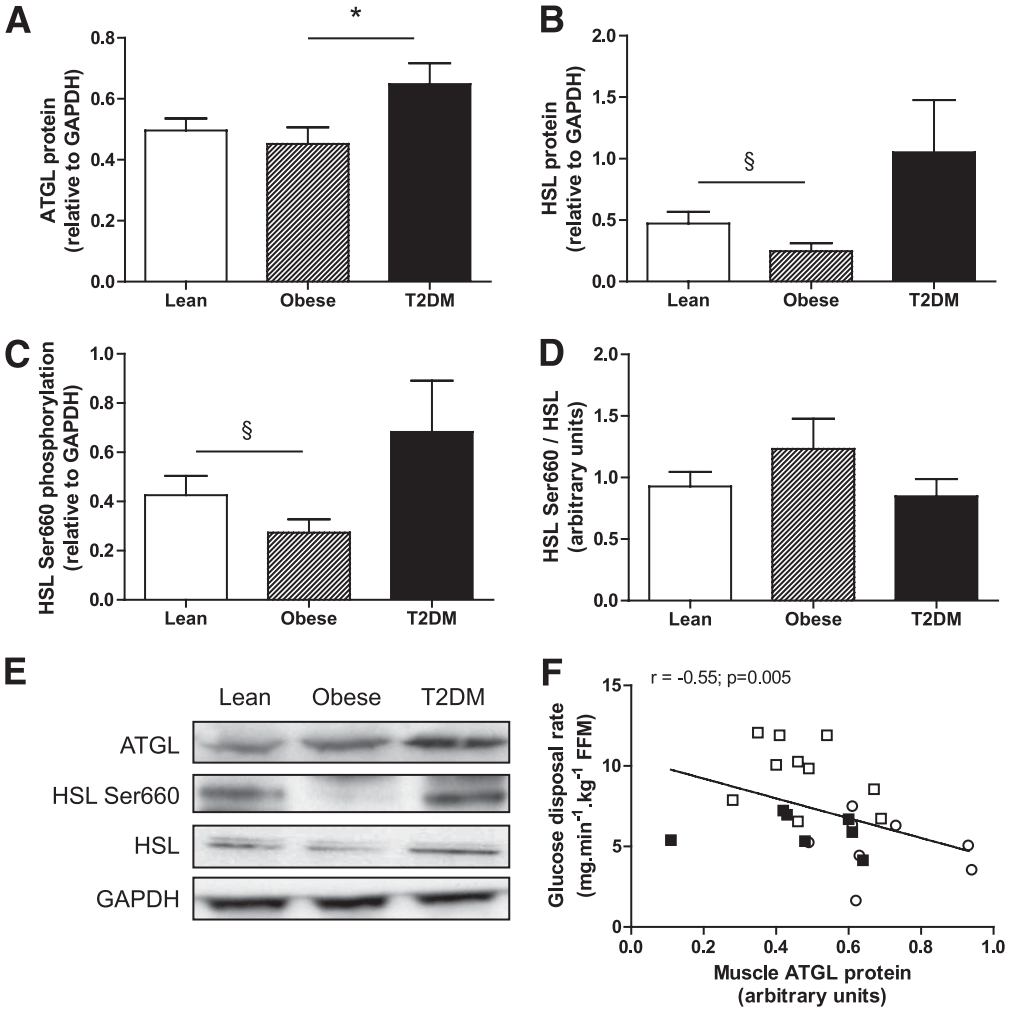

FIG. 1. Skeletal muscle lipase protein expression in lean, obese, and type 2 diabetic subjects. Quantitative bar graph of ATGL protein (*A*), HSL protein (*B*), HSL Ser660 phosphorylation (*C*), and the ratio HSL Ser660 phosphorylation to total HSL (*D*) in vastus lateralis samples of lean, obese, and type 2 diabetic subjects. *E*: Representative blots of lipases and the loading control GAPDH. *F*: Relationship between vastus lateralis ATGL protein expression and glucose disposal rate measured by euglycemic hyperinsulinemic clamp across individuals. White square, lean; black square, obese; open circle, type 2 diabetes. **P* < 0.05 compared with obese; §*P* = 0.08 compared with lean.

in human vastus lateralis samples of young lean, young obese, and type 2 diabetic subjects. The characteristics of the subjects are described in Table 1. As expected, obese and type 2 diabetic subjects had lower insulin sensitivity and higher body fat, fasting glucose, and fasting insulin compared with lean subjects. Muscle ATGL protein content was significantly elevated in type 2 diabetic subjects when compared with lean and obese subjects (0.50 ± 0.04, 0.45 ± 0.05, and 0.65 ± 0.07 arbitrary units [AU] for lean, obese, and type 2 diabetic subjects, respectively) (Fig. 1*A* and *E*). We also confirm a reduced HSL Ser660 phosphorylation (0.43 ± 0.08 vs. 0.27 ± 0.05 AU, −36%) (Fig. 1*C* and *E*) and HSL protein content (0.47 ± 0.09 vs. 0.25 ± 0.07 AU, −48%) (Fig. 1*B* and *E*) in skeletal muscle of obese compared with lean subjects. HSL Ser660 phosphorylation (0.68 ± 0.21 vs. 0.43 ± 0.08 AU) and total HSL (1.05 ± 0.43 vs. 0.47 ± 0.09 AU) tended to increase in type 2 diabetic subjects compared with lean subjects. The ratio of phosphorylated HSL Ser660 to total HSL was not significantly changed between groups (Fig. 1*D*). We noted a significant inverse relationship between muscle ATGL protein content and whole-body insulin sensitivity measured by euglycemic hyperinsulinemic clamp across individuals (Fig. 1*F*). Similarly, muscle ATGL protein was positively correlated with fasting glucose levels ($r = 0.56$, $P < 0.005$). Perilipin-A protein was not detectable in any of the muscle samples excluding significant contamination by infiltrated adipocytes (data not shown).

Adenovirus-mediated ATGL overexpression. We used an adenovirus gene delivery method to overexpress ATGL in our cell culture model. ATGL protein expression was induced by ~3.4 ± 0.2-fold (Fig. 2*A*). ATGL overexpression increased TAGH activity twofold (Fig. 2*B*), but did not change DAGH activity as expected (Fig. 2*C*). We checked that the ATGL enzyme was operative in intact cells by directly measuring the rate of incorporation of radiolabeled oleate into different lipid pools. We could show that ATGL overexpression reduced the rate of incorporation of [1-^{14}C] oleate into TAG (Fig. 2*D*), whereas the rate of incorporation was increased into DAG (Fig. 2*E*) and intracellular FFA (Fig. 2*F*).

Elevated ATGL expression promotes DAG and ceramide accumulation. We found that total TAG content was reduced in myotubes overexpressing ATGL (0.60 ± 0.07-fold, $P < 0.01$) (Fig. 3*A*). Conversely, consistent with an

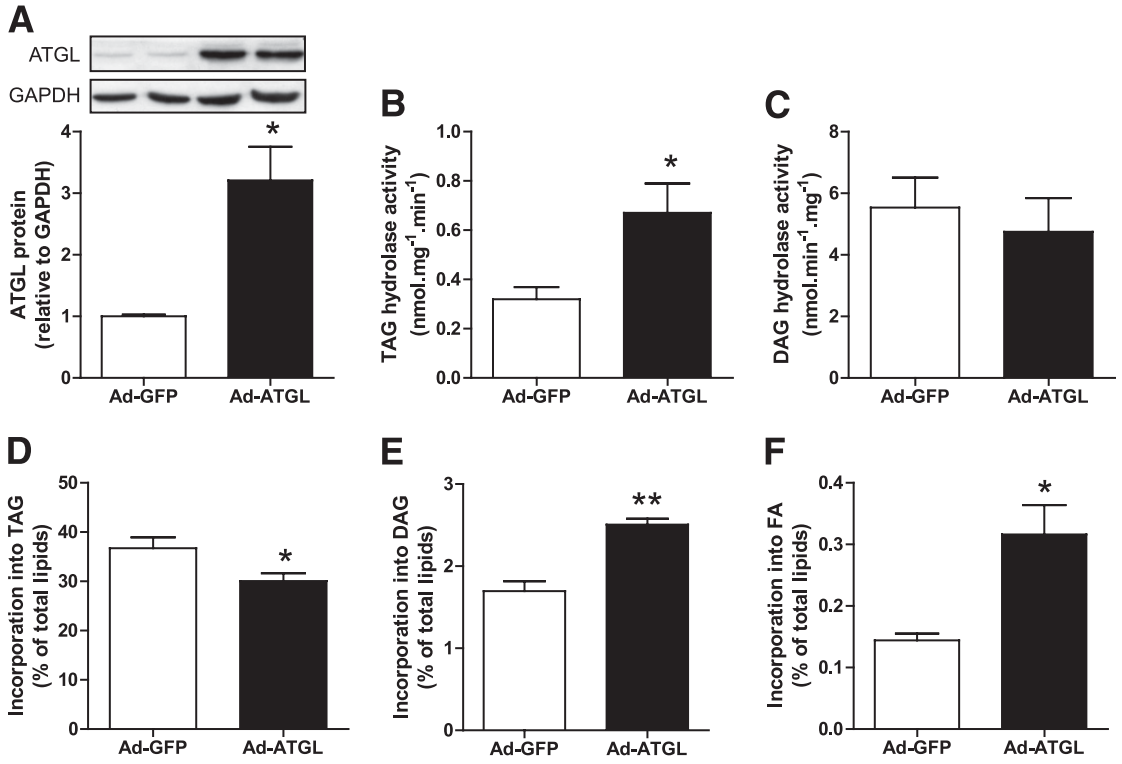

FIG. 2. ATGL overexpression increases TAG hydrolysis in myotubes. *A*: Quantitative bar graph of ATGL protein during adenovirus-mediated ATGL overexpression vs. GFP control (n = 4). *Insets* are showing representative blots of two independent experiments. TAG hydrolase activity (*B*) and DAG hydrolase activity (*C*) were measured in control myotubes (GFP) and myotubes overexpressing ATGL (n = 4). Pulse-chase studies using [1-^{14}C]oleate were performed to determine the kinetics of the different lipid pools in response to ATGL overexpression. The rate of incorporation of radiolabeled oleate into (*D*) TAG, (*E*) DAG, and (*F*) FFA was determined in control myotubes (GFP) and myotubes overexpressing ATGL. *P < 0.05; **P < 0.01 vs. GFP (n = 4).

imbalance of ATGL relative to HSL, total DAG content increased in myotubes overexpressing ATGL (1.5 ± 0.1-fold) (Fig. 3*B*). Ceramide content was also increased in myotubes overexpressing ATGL (2.9 ± 0.7-fold), possibly as a consequence of increased intracellular FFA flux and de novo ceramide synthesis (Fig. 3*C*).

Elevated ATGL expression impairs insulin signaling and action. We first showed that glycogen synthesis under insulin stimulation was impaired by 30% ($P < 0.05$) in myotubes overexpressing ATGL (Fig. 4*A*). Insulin-stimulated glycogen synthesis was significantly reduced in myotubes overexpressing ATGL (0.72 ± 0.07-fold, $P = 0.01$). We further showed that ATGL overexpression increased Ser1101–IRS-1 phosphorylation by twofold at baseline and under insulin stimulation ($P < 0.001$) (Fig. 4*B* and *D*). IRS-1 phosphorylation at Ser1101 inhibits IRS-1 tyrosine phosphorylation and function and is a primary target for PKC (13), suggesting a possible link between ATGL and PKC activation. Downstream insulin activation of Akt on the residue Ser473 was also impaired (change insulin minus baseline −31%, $P < 0.05$) during ATGL overexpression. Ser473 Akt phosphorylation was increased at baseline ($P < 0.05$) and reduced under insulin stimulation in ATGL-overexpressing myotubes, whereas total Akt protein content was not different across treatments (Fig. 4*C* and *D*).

ATGL-mediated insulin resistance involves DAG and PKC activation. Because several isoforms of novel PKC have been linked to insulin resistance (33), we used a broad range nonselective PKC inhibitor in our experiments. Calphostin C treatment greatly enhanced insulin-stimulated Akt activation in ATGL overexpressing myotubes (+163%, $P < 0.01$ compared with GFP with calphostin C)

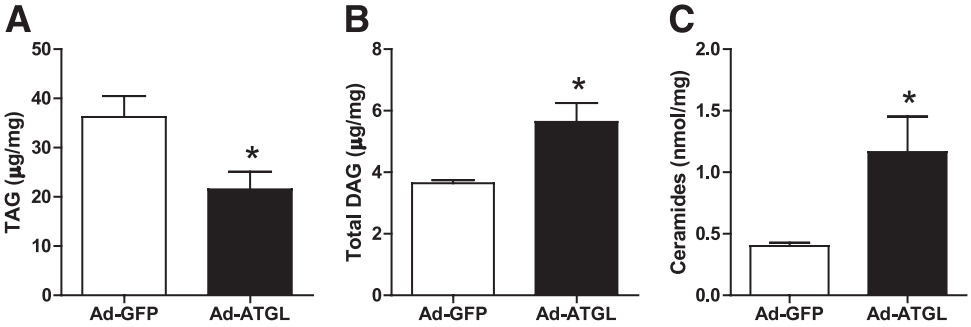

FIG. 3. Elevated ATGL expression promotes DAG and ceramide accumulation. Determination of (*A*) TAG, (*B*) DAG, and (*C*) ceramide content in control myotubes (GFP) and myotubes overexpressing ATGL. *P < 0.05 (n = 5).

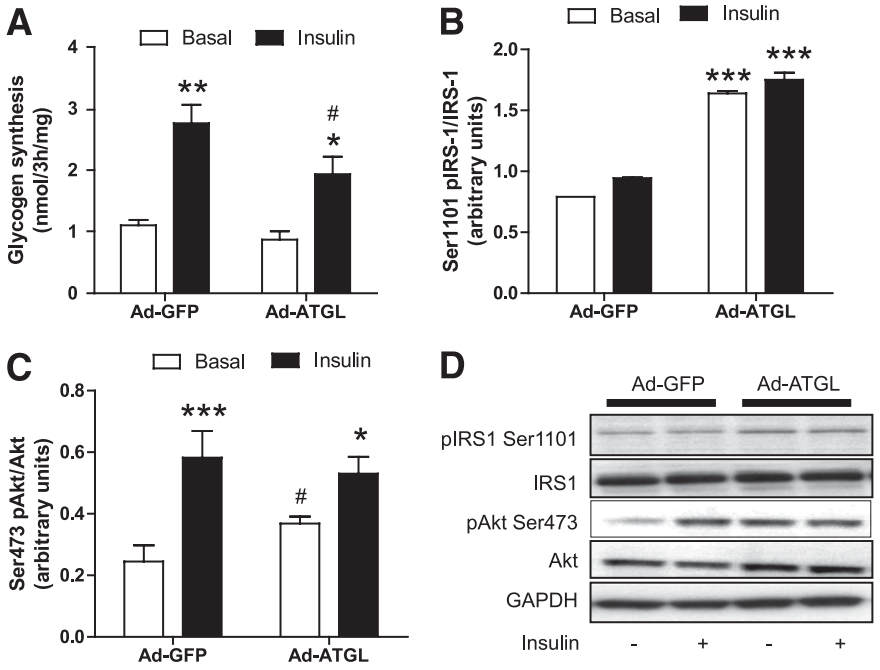

FIG. 4. Elevated ATGL expression disrupts insulin signaling and action. *A*: Glycogen synthesis was measured in the absence (open bars) or presence (black bars) of 100 nmol/L insulin in control myotubes (GFP) and myotubes overexpressing ATGL. *$P < 0.05$, **$P < 0.01$ vs. basal; #$P < 0.05$ vs. GFP insulin ($n = 8$ per group). *B*: Quantitative bar graph of basal Ser1101 IRS-1 phosphorylation ($n = 4$). ***$P < 0.001$ vs. GFP. *C*: Quantitative bar graph of Ser473 Akt phosphorylation ($n = 11$). *$P < 0.05$, ***$P < 0.001$ vs. basal; #$P < 0.05$ vs. Ad-GFP. *D*: Representative blots of Ser1101 pIRS-1, total IRS-1, Ser473 pAkt, total Akt, and the loading control GAPDH in the presence (+) or absence (−) of 100 nmol/L of insulin in control myotubes (GFP) and myotubes overexpressing ATGL.

(Fig. 5*A* and *B*). Similarly, nonselective PKC inhibition fully rescued insulin-stimulated glycogen synthesis to control GFP levels in myotubes overexpressing ATGL (Fig. 5*C*). PKC inhibition by the nonselective inhibitor calphostin C (1 μmol/L) was sufficient to fully rescue ATGL-mediated insulin resistance. ATGL-mediated inhibition of glycogen synthesis and Akt phosphorylation was not prevented by the de novo ceramide synthesis inhibitor myriocin (10 μmol/L) (Supplementary Fig. 1).

HSL overexpression is sufficient to rescue ATGL-mediated insulin resistance. We tested the hypothesis that restoring a proper cellular lipolytic balance could reverse ATGL-mediated insulin resistance. To do so, we concomitantly overexpressed ATGL and HSL in differentiated myotubes and examined insulin signaling and action. HSL overexpression by itself did not produce lipotoxicity and insulin resistance (Supplementary Fig. 2). The concomitant overexpression of HSL and ATGL increased both HSL (3.4 ± 0.8-fold, $P < 0.05$) and ATGL (3.2 ± 0.6-fold, $P < 0.05$) protein content, TAGH activity (4.4 ± 2.0-fold, $P < 0.01$), and DAGH activity (5.1 ± 1.8-fold, $P < 0.01$). When coexpressed with ATGL, HSL was sufficient to completely rescue ATGL-mediated insulin resistance. This was evidenced by a full restoration of insulin-mediated Akt activation (Fig. 6*A* and *B*) and glycogen synthesis (Fig. 6*C*) to GFP control levels in myotubes coexpressing ATGL and HSL compared with ATGL alone.

Selective HSL inhibition impairs insulin signaling. We next examined the effect of HSL-selective inhibition by the BAY compound on DAG levels and insulin action. BAY has been shown to be a highly selective HSL inhibitor in previous studies (24). We observed a moderate increase in total DAG levels (+29%, $P = 0.068$) in myotubes treated for 24 h with 1 μmol/L of BAY (Fig. 7*A*). BAY treatment did not increase ceramide content (0.57 ± 0.07 vs. 0.57 ± 0.06 nmol/mg for control and BAY, respectively). In the same treatment condition, BAY reduced Tyr612–IRS-1 phosphorylation on insulin treatment (−30%, $P < 0.05$) (Fig. 7*B* and *C*) and insulin-mediated Akt phosphorylation (−28%, $P = 0.03$) (Fig. 7*B* and *D*). We did not observe additive effects of ATGL overexpression combined with HSL inhibition compared with ATGL overexpression alone on insulin-stimulated Akt Ser473 phosphorylation (Supplementary Fig. 3).

DISCUSSION

Ectopic fat deposition in non-adipose tissues such as skeletal muscle is a common feature of insulin resistance in obesity and type 2 diabetes (3–5). The mechanisms underlying IMTG accumulation and elevated lipotoxicity in insulin-resistant states are not yet fully understood. We show for the first time a novel mechanism by which an altered lipolytic balance in skeletal muscle might contribute to lipotoxicity and insulin resistance in humans. An imbalance of ATGL relative to HSL promotes DAG accumulation and induces insulin resistance at least in part through a DAG/PKC pathway.

We first showed that ATGL protein expression in vastus lateralis samples obtained from a wide range of subjects was negatively associated with whole-body insulin sensitivity measured by euglycemic hyperinsulinemic clamp. It is interesting to note that the glucose disposal rate during this clamp is mostly accounted by skeletal muscle and thus mostly reflects skeletal muscle insulin sensitivity in lean subjects. Higher doses of insulin are required to fully suppress hepatic glucose production in obese and type 2 diabetic subjects as previously shown (34). Thus, the relationship between muscle ATGL and insulin sensitivity is stronger in lean subjects than in obese and type 2 diabetic

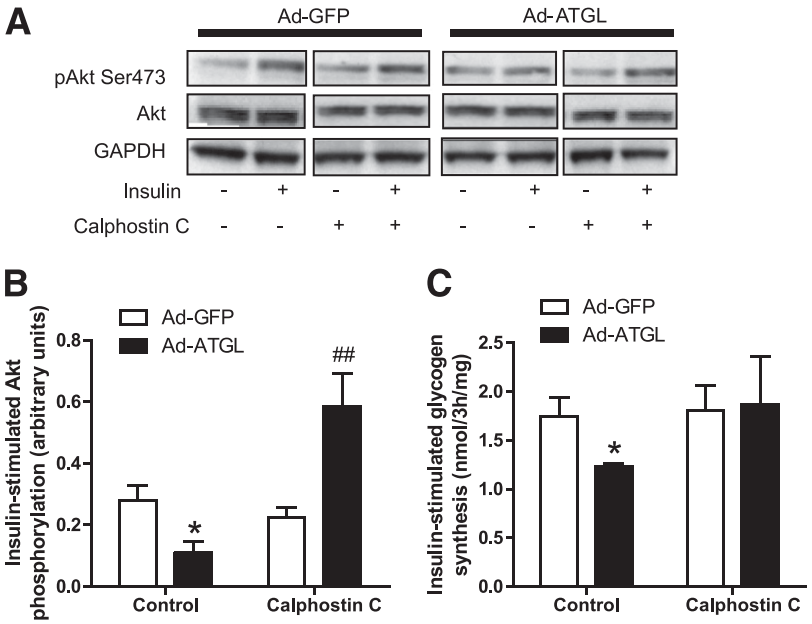

FIG. 5. ATGL-mediated insulin resistance involves PKC activation. *A*: Representative blots of Ser473 pAkt, total Akt, and GAPDH in the presence (+) or absence (−) of insulin and the nonselective PKC inhibitor calphostin C (1 μmol/L) in control myotubes (GFP) and myotubes overexpressing ATGL. *B*: Quantitative bar graph of insulin-stimulated Ser473 Akt phosphorylation (n = 3); insulin-stimulated Akt phosphorylation was calculated as the Δ between basal and insulin stimulation in each condition. *P < 0.05 vs. GFP; ##P < 0.01 vs. GFP calphostin C. *C*: Insulin-stimulated glycogen synthesis in myotubes expressing GFP and ATGL in the absence (control) or presence of calphostin C. Glycogen synthesis was expressed as the Δ change between glycogen synthesis under insulin stimulation and glycogen synthesis at baseline. *P < 0.05 vs. GFP (n = 4).

subjects. When the data were examined by group, only obese type 2 diabetic subjects displayed increased muscle ATGL protein content. This finding is slightly in contrast with recent data showing an increased skeletal muscle ATGL protein expression in nondiabetic obese versus age-matched lean individuals (35). The discrepancy could be explained by an effect of aging because the type 2 diabetic subjects were older than the lean and obese subjects in our study. Thus, age-related changes in skeletal muscle lipases with respect to insulin sensitivity should be further explored. Elevated muscle ATGL protein in obese type 2 diabetic subjects is in agreement with a higher muscle DAG

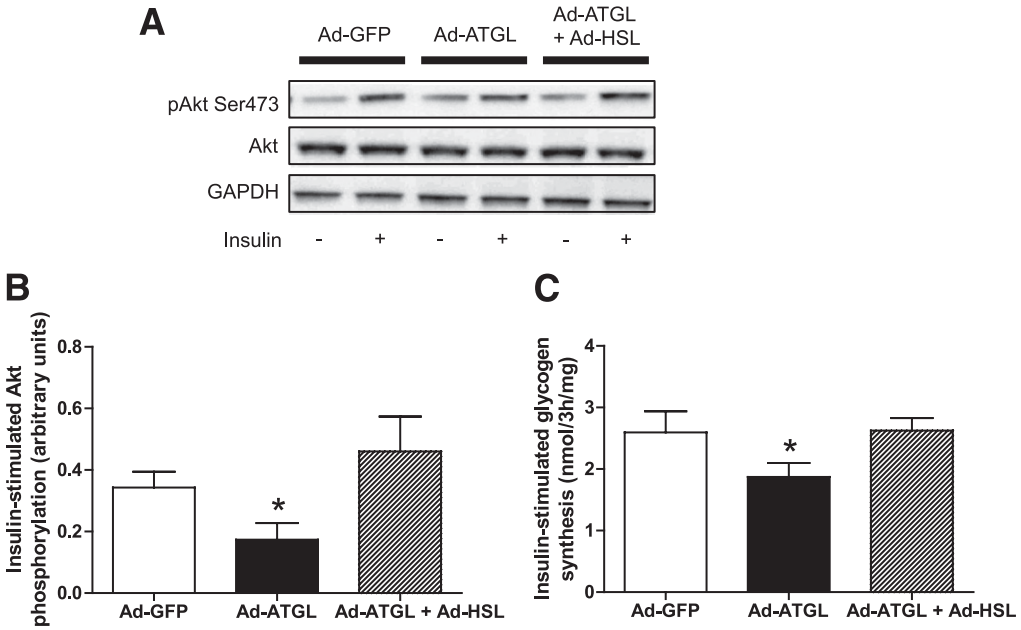

FIG. 6. Rescue of ATGL-mediated insulin resistance by HSL. *A*: Representative blots of Ser473 pAkt, total Akt, and GAPDH in the presence (+) or absence (−) of insulin in control myotubes (GFP) and myotubes overexpressing ATGL alone (Ad-ATGL) or in combination with HSL (Ad-ATGL+ Ad-HSL). *B*: Quantitative bar graph of insulin-stimulated Ser473 Akt phosphorylation (n = 4); insulin-stimulated Akt phosphorylation was calculated as the Δ between basal and insulin stimulation in each condition. *P < 0.05 vs. GFP. *C*: Insulin-stimulated glycogen synthesis was measured in control myotubes (GFP) and myotubes overexpressing ATGL alone (Ad-ATGL) or in combination with HSL (Ad-ATGL+Ad-HSL). *P < 0.05 vs. GFP (n = 6).

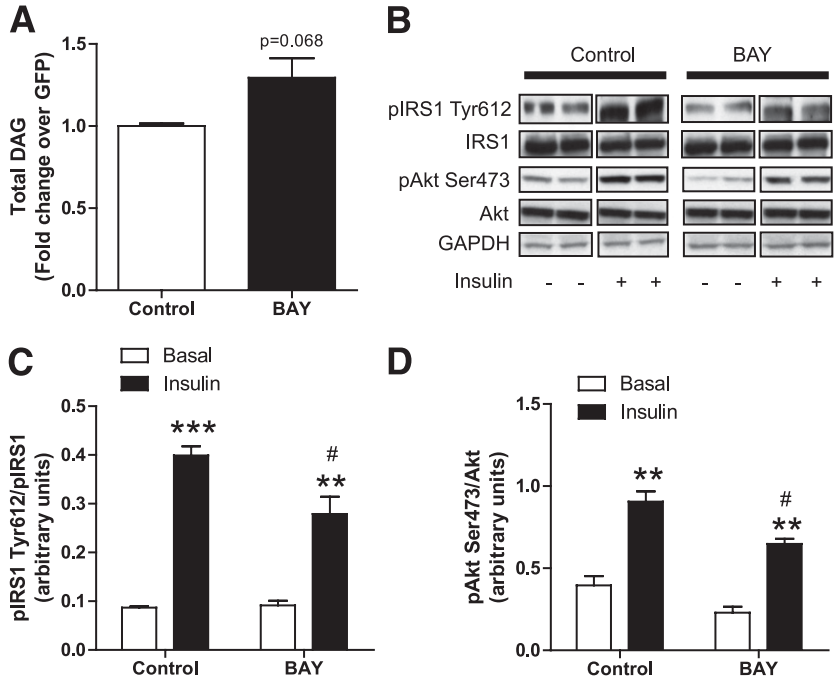

FIG. 7. Selective HSL inhibition disrupts insulin signaling. *A*: Total DAGs were measured in control myotubes and myotubes treated for 24 h with 1 μmol/L of the selective HSL inhibitor BAY ($n = 6$). *B*: Representative blots of Tyr1162 pIR, total IRalpha, Ser473 pAkt, total Akt, and GAPDH in the presence (+) or absence (−) of insulin in control myotubes and myotubes treated with BAY. Quantitative bar graphs of (*C*) Tyr612-IRS-1 phosphorylation ($n = 4$) and (*D*) Ser473 Akt phosphorylation ($n = 4$) in control myotubes and myotubes treated with the BAY compound. **$P < 0.01$; ***$P < 0.001$ vs. basal; #$P < 0.05$ vs. control insulin.

content previously reported in these subjects (36). We next evaluated the causal relationship between elevated ATGL expression and insulin resistance in primary culture of skeletal muscle cells.

We overexpressed ATGL in human primary myotubes using an adenovirus and assessed the consequences on lipids and insulin action. Elevated expression of ATGL reduced TAG content and simultaneously increased DAG and ceramide content. Ceramides are potentially produced de novo through the action of serine palmitoyl-transferase I as previously shown (8). ATGL-mediated lipotoxicity was paralleled by impairment in insulin-stimulated glycogen synthesis and insulin signaling possibly due to PKC-mediated Ser1101-IRS-1 phosphorylation and downstream inhibition of Akt Ser473 phosphorylation. Of note, increased ATGL expression induced baseline Akt Ser473 phosphorylation independently of insulin. This suggests that ATGL may activate potential regulators of Ser473 Akt, such as mTORC2, by yet unknown mechanisms (37). Future studies will be required to dissect the precise mechanism by which ATGL elicits baseline Akt activation. IRS-1 phosphorylation at Ser1101 is primarily mediated by PKCθ and induces general inhibition of IRS-1 function (13). Together, our data show that ATGL mediates insulin resistance at least in part through DAG and PKC activation. Itani et al. (38,39) have previously shown that membrane-associated PKCβ and θ protein content and activity increased the skeletal muscle of obese versus lean and obese diabetic versus nondiabetic matched control subjects, respectively. Even if the exact nature of DAG stereoisomers produced by the action of ATGL is currently unknown, the data support an important role for DAG in mediating skeletal muscle insulin resistance in this model. This observation is consistent with other studies showing a critical role of DAG in mediating insulin resistance in liver (40) and skeletal muscle (10–12) in response to high-fat diets and lipid infusions. Our results are also consistent with a study by Bell et al. (41) suggesting that AML12 liver cells lacking the lipid coat protein adipophilin and tail-interacting protein of 47 kDa develop insulin resistance with increased recruitment of ATGL to lipid droplets.

Of interest, ATGL-mediated insulin resistance was fully rescued by HSL after restoring a proper cellular lipolytic balance. Overexpression of HSL by itself did not cause lipotoxicity and insulin resistance contrary to ATGL. HSL displays a high DAG substrate specificity and is considered the major DAG hydrolase in several tissues (42). This supports the concept that the functional balance between ATGL and HSL may influence intracellular DAG concentrations and insulin action in skeletal muscle. Altogether, these data highlight a potential protective role of DAG hydrolases against intramyocellular lipotoxicity by their ability to rapidly hydrolyze DAG. The importance of DAG turnover in insulin resistance is also illustrated by the protective role of DGAT1 against intramyocellular lipotoxicity and fat-induced insulin resistance by increasing lipid partitioning into IMTG (43,44). Along these lines, reduced DAG kinase-δ activity, which converts DAG into phosphatidic acid, might also contribute to skeletal muscle insulin resistance by increasing total DAG level (45).

Consistent with recent studies that reported a robust reduction in skeletal muscle HSL protein expression in insulin-resistant obese subjects (35,46), our study confirmed that both HSL Ser660 phosphorylation and HSL protein content were reduced in skeletal muscle of obese compared with lean subjects. The trend for increased HSL protein content in skeletal muscle of patients with type 2 diabetes could be explained by the hyperglycemic milieu because glucose was shown to induce HSL transcription in adipocytes (47). To study the impact of reduced HSL

expression/activity in skeletal muscle, we next evaluated the consequences of inhibiting HSL activity on lipid pools and insulin sensitivity in myotubes. HSL activity is regulated by phosphorylation on serine residues in response to muscle contraction and catecholamines in vivo (48). Jocken et al. (46) found that reduced HSL phosphorylation at Ser563, Ser565, and Ser659 was entirely due to lower HSL protein content and associated with reduced resting glycerol release from the forearm muscle of obese subjects. We report that selective inhibition of HSL increases specifically total DAG levels and consequently disrupts insulin receptor signaling and action. This observation is somehow consistent with data on HSL knockout mice that are insulin-resistant at the level of the skeletal and cardiac muscles when fed a chow diet (49,50) and accumulate DAG in their muscles (16). Further studies will be required to unravel the precise mechanism by which reduced HSL expression/activity induces insulin resistance in skeletal muscle.

In conclusion, the current study highlights a new mechanism by which an altered lipolytic balance between ATGL and HSL induces DAG and insulin resistance in skeletal muscle. The molecular mechanism involves at least in part DAG-mediated PKC activation. Future studies should explore the cause-effect relationship between altered lipase expression and insulin resistance in vivo in animal models with targeted modulations of lipase expression in skeletal muscle. Targeting skeletal muscle lipases might be of potential therapeutic interest for improving insulin resistance in obesity and type 2 diabetes.

ACKNOWLEDGMENTS

This work was supported by grants from the National Research Agency (ANR-09-JCJC-0019-01) and the European Foundation for the Study of Diabetes/Novo Nordisk (to C.M.); the Commission of the European Communities (Integrated Project HEPADIP; http://www.hepadip.org/), Contract No. LSHM-CT-2005-018734 (to D.L.); and National Institutes of Health grants US-1P30-DK-072476 (Pennington Biomedical Research Center/Nutrition Obesity Research Center) and R01-AG-030226 (to S.R.S.). The Hormone Assay and Analytical Services Core, Vanderbilt Diabetes Research and Training Center, supported by National Institutes of Health Grant DK-20593, performed TAG and DAG analyses.

No potential conflicts of interest relevant to this article were reported.

P.-M.B., K.L., A.M., G.L., and G.S. researched data and reviewed and edited the article. A.C.R. reviewed and edited the article. S.R.S. and D.L. contributed to discussion and reviewed and edited the article. C.M. researched data and wrote the article.

The authors thank Diana Albarado (Pennington Biomedical Research Center, Baton Rouge, LA), Shantele Thomas (Burnham Institute, Winter Park, FL), and Maarten Coonen (Maastricht University, the Netherlands) for excellent technical assistance.

REFERENCES

1. DeFronzo RA. Pathogenesis of type 2 diabetes mellitus. Med Clin North Am 2004;88:787–835, ix
2. McGarry JD. Banting lecture 2001: dysregulation of fatty acid metabolism in the etiology of type 2 diabetes. Diabetes 2002;51:7–18
3. Krssak M, Falk Petersen K, Dresner A, et al. Intramyocellular lipid concentrations are correlated with insulin sensitivity in humans: a ^{1}H NMR spectroscopy study. Diabetologia 1999;42:113–116
4. Pan DA, Lillioja S, Kriketos AD, et al. Skeletal muscle triglyceride levels are inversely related to insulin action. Diabetes 1997;46:983–988
5. Perseghin G, Scifo P, De Cobelli F, et al. Intramyocellular triglyceride content is a determinant of in vivo insulin resistance in humans: a ^{1}H-^{13}C nuclear magnetic resonance spectroscopy assessment in offspring of type 2 diabetic parents. Diabetes 1999;48:1600–1606
6. Unger RH. Minireview: weapons of lean body mass destruction: the role of ectopic lipids in the metabolic syndrome. Endocrinology 2003;144:5159–5165
7. Adams JM 2nd, Pratipanawatr T, Berria R, et al. Ceramide content is increased in skeletal muscle from obese insulin-resistant humans. Diabetes 2004;53:25–31
8. Chavez JA, Knotts TA, Wang LP, et al. A role for ceramide, but not diacylglycerol, in the antagonism of insulin signal transduction by saturated fatty acids. J Biol Chem 2003;278:10297–10303
9. Holland WL, Brozinick JT, Wang LP, et al. Inhibition of ceramide synthesis ameliorates glucocorticoid-, saturated-fat-, and obesity-induced insulin resistance. Cell Metab 2007;5:167–179
10. Dresner A, Laurent D, Marcucci M, et al. Effects of free fatty acids on glucose transport and IRS-1-associated phosphatidylinositol 3-kinase activity. J Clin Invest 1999;103:253–259
11. Griffin ME, Marcucci MJ, Cline GW, et al. Free fatty acid-induced insulin resistance is associated with activation of protein kinase C theta and alterations in the insulin signaling cascade. Diabetes 1999;48:1270–1274
12. Itani SI, Ruderman NB, Schmieder F, Boden G. Lipid-induced insulin resistance in human muscle is associated with changes in diacylglycerol, protein kinase C, and IkappaB-alpha. Diabetes 2002;51:2005–2011
13. Li Y, Soos TJ, Li X, et al. Protein kinase C Theta inhibits insulin signaling by phosphorylating IRS1 at Ser(1101). J Biol Chem 2004;279:45304–45307
14. Timmers S, Schrauwen P, de Vogel J. Muscular diacylglycerol metabolism and insulin resistance. Physiol Behav 2008;94:242–251
15. Langfort J, Ploug T, Ihlemann J, Saldo M, Holm C, Galbo H. Expression of hormone-sensitive lipase and its regulation by adrenaline in skeletal muscle. Biochem J 1999;340:459–465
16. Haemmerle G, Zimmermann R, Hayn M, et al. Hormone-sensitive lipase deficiency in mice causes diglyceride accumulation in adipose tissue, muscle, and testis. J Biol Chem 2002;277:4806–4815
17. Haemmerle G, Lass A, Zimmermann R, et al. Defective lipolysis and altered energy metabolism in mice lacking adipose triglyceride lipase. Science 2006;312:734–737
18. Zimmermann R, Strauss JG, Haemmerle G, et al. Fat mobilization in adipose tissue is promoted by adipose triglyceride lipase. Science 2004;306:1383–1386
19. Ukropcova B, McNeil M, Sereda O, et al. Dynamic changes in fat oxidation in human primary myocytes mirror metabolic characteristics of the donor. J Clin Invest 2005;115:1934–1941
20. Listenberger LL, Han X, Lewis SE, et al. Triglyceride accumulation protects against fatty acid-induced lipotoxicity. Proc Natl Acad Sci U S A 2003;100:3077–3082
21. Turpin SM, Lancaster GI, Darby I, Febbraio MA, Watt MJ. Apoptosis in skeletal muscle myotubes is induced by ceramides and is positively related to insulin resistance. Am J Physiol Endocrinol Metab 2006;291:E1341–E1350
22. Pickersgill L, Litherland GJ, Greenberg AS, Walker M, Yeaman SJ. Key role for ceramides in mediating insulin resistance in human muscle cells. J Biol Chem 2007;282:12583–12589
23. Hessvik NP, Bakke SS, Fredriksson K, et al. Metabolic switching of human myotubes is improved by n-3 fatty acids. J Lipid Res 2010;51:2090–2104
24. Langin D, Dicker A, Tavernier G, et al. Adipocyte lipases and defect of lipolysis in human obesity. Diabetes 2005;54:3190–3197
25. Bergstrom J. Percutaneous needle biopsy of skeletal muscle in physiological and clinical research. Scand J Clin Lab Invest 1975;35:609–616
26. DeFronzo RA, Tobin JD, Andres R. Glucose clamp technique: a method for quantifying insulin secretion and resistance. Am J Physiol 1979;237:E214–E223
27. Mairal A, Langin D, Arner P, Hoffstedt J. Human adipose triglyceride lipase (PNPLA2) is not regulated by obesity and exhibits low in vitro triglyceride hydrolase activity. Diabetologia 2006;49:1629–1636
28. Folch J, Lees M, Sloane Stanley GH. A simple method for the isolation and purification of total lipides from animal tissues. J Biol Chem 1957;226:497–509
29. Morrison WR, Smith LM. Preparation of fatty acid methyl esters and dimethylacetals from lipids with boron fluoride–methanol. J Lipid Res 1964;5:600–608
30. Liebisch G, Drobnik W, Reil M, et al. Quantitative measurement of different ceramide species from crude cellular extracts by electrospray

ionization tandem mass spectrometry (ESI-MS/MS). J Lipid Res 1999;40:1539–1546
31. Bligh EG, Dyer WJ. A rapid method of total lipid extraction and purification. Can J Biochem Physiol 1959;37:911–917
32. Liebisch G, Lieser B, Rathenberg J, Drobnik W, Schmitz G. High-throughput quantification of phosphatidylcholine and sphingomyelin by electrospray ionization tandem mass spectrometry coupled with isotope correction algorithm. Biochim Biophys Acta 2004;1686:108–117
33. Schmitz-Peiffer C, Biden TJ. Protein kinase C function in muscle, liver, and beta-cells and its therapeutic implications for type 2 diabetes. Diabetes 2008;57:1774–1783
34. Bonadonna RC, Groop L, Kraemer N, Ferrannini E, Del Prato S, DeFronzo RA. Obesity and insulin resistance in humans: a dose-response study. Metabolism 1990;39:452–459
35. Jocken JW, Moro C, Goossens GH, et al. Skeletal muscle lipase content and activity in obesity and type 2 diabetes. J Clin Endocrinol Metab 2010;95:5449–5453
36. Moro C, Galgani JE, Luu L, et al. Influence of gender, obesity, and muscle lipase activity on intramyocellular lipids in sedentary individuals. J Clin Endocrinol Metab 2009;94:3440–3447
37. Huang J, Manning BD. A complex interplay between Akt, TSC2 and the two mTOR complexes. Biochem Soc Trans 2009;37:217–222
38. Itani SI, Pories WJ, Macdonald KG, Dohm GL. Increased protein kinase C theta in skeletal muscle of diabetic patients. Metabolism 2001;50:553–557
39. Itani SI, Zhou Q, Pories WJ, MacDonald KG, Dohm GL. Involvement of protein kinase C in human skeletal muscle insulin resistance and obesity. Diabetes 2000;49:1353–1358
40. Neschen S, Morino K, Dong J, et al. n-3 Fatty acids preserve insulin sensitivity in vivo in a peroxisome proliferator-activated receptor-alpha-dependent manner. Diabetes 2007;56:1034–1041
41. Bell M, Wang H, Chen H, et al. Consequences of lipid droplet coat protein downregulation in liver cells: abnormal lipid droplet metabolism and induction of insulin resistance. Diabetes 2008;57:2037–2045
42. Holm C. Molecular mechanisms regulating hormone-sensitive lipase and lipolysis. Biochem Soc Trans 2003;31:1120–1124
43. Liu L, Zhang Y, Chen N, Shi X, Tsang B, Yu YH. Upregulation of myocellular DGAT1 augments triglyceride synthesis in skeletal muscle and protects against fat-induced insulin resistance. J Clin Invest 2007;117:1679–1689
44. Schenk S, Horowitz JF. Acute exercise increases triglyceride synthesis in skeletal muscle and prevents fatty acid-induced insulin resistance. J Clin Invest 2007;117:1690–1698
45. Chibalin AV, Leng Y, Vieira E, et al. Downregulation of diacylglycerol kinase delta contributes to hyperglycemia-induced insulin resistance. Cell 2008;132:375–386
46. Jocken JW, Roepstorff C, Goossens GH, et al. Hormone-sensitive lipase serine phosphorylation and glycerol exchange across skeletal muscle in lean and obese subjects: effect of beta-adrenergic stimulation. Diabetes 2008;57:1834–1841
47. Smih F, Rouet P, Lucas S, et al. Transcriptional regulation of adipocyte hormone-sensitive lipase by glucose. Diabetes 2002;51:293–300
48. Jocken JW, Blaak EE. Catecholamine-induced lipolysis in adipose tissue and skeletal muscle in obesity. Physiol Behav 2008;94:219–230
49. Park SY, Kim HJ, Wang S, et al. Hormone-sensitive lipase knockout mice have increased hepatic insulin sensitivity and are protected from short-term diet-induced insulin resistance in skeletal muscle and heart. Am J Physiol Endocrinol Metab 2005;289:E30–E39
50. Mulder H, Sörhede-Winzell M, Contreras JA, et al. Hormone-sensitive lipase null mice exhibit signs of impaired insulin sensitivity whereas insulin secretion is intact. J Biol Chem 2003;278:36380–36388

SUPPLEMENTARY DATA

Supplementary Figure 1. Insulin-stimulated glycogen synthesis in myotubes expressing GFP or ATGL in absence (-) or presence (+) of 10 μM myriocin (serine palmitoyl-CoA transferase I inhibitor). Glycogen synthesis was expressed as the delta change between glycogen synthesis under insulin stimulation and glycogen synthesis at baseline. $^{**}p<0.01$ versus GFP (n=4).

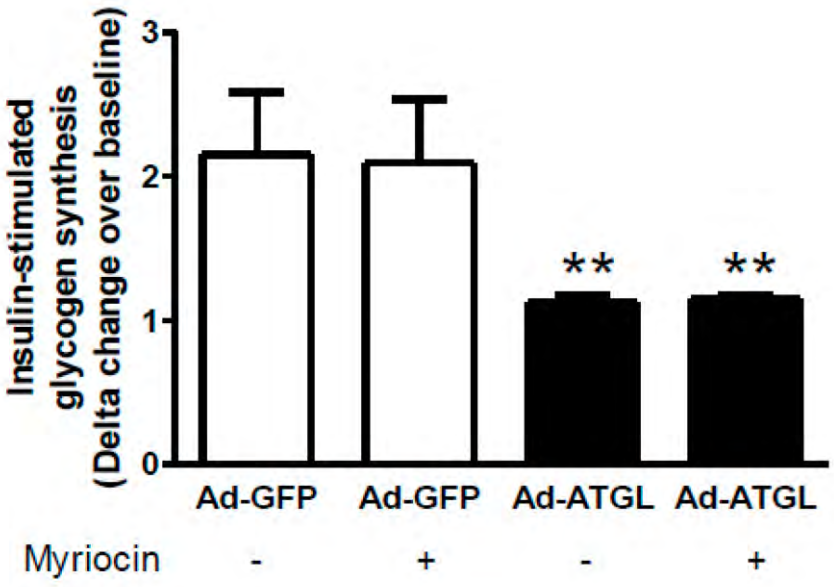

SUPPLEMENTARY DATA

Supplementary Figure 2. (A) Inset is showing a representative blot of HSL and the loading control GAPDH in control myotubes (GFP) and myotubes overexpressing HSL; Determination of (B) DAG, and (C) ceramide content in control myotubes (GFP) and myotubes overexpressing HSL (n=6). (D) Insulin-stimulated glycogen synthesis in myotubes expressing GFP and HSL (n=4). Glycogen synthesis was expressed as the delta change between glycogen synthesis under insulin stimulation and glycogen synthesis at baseline.

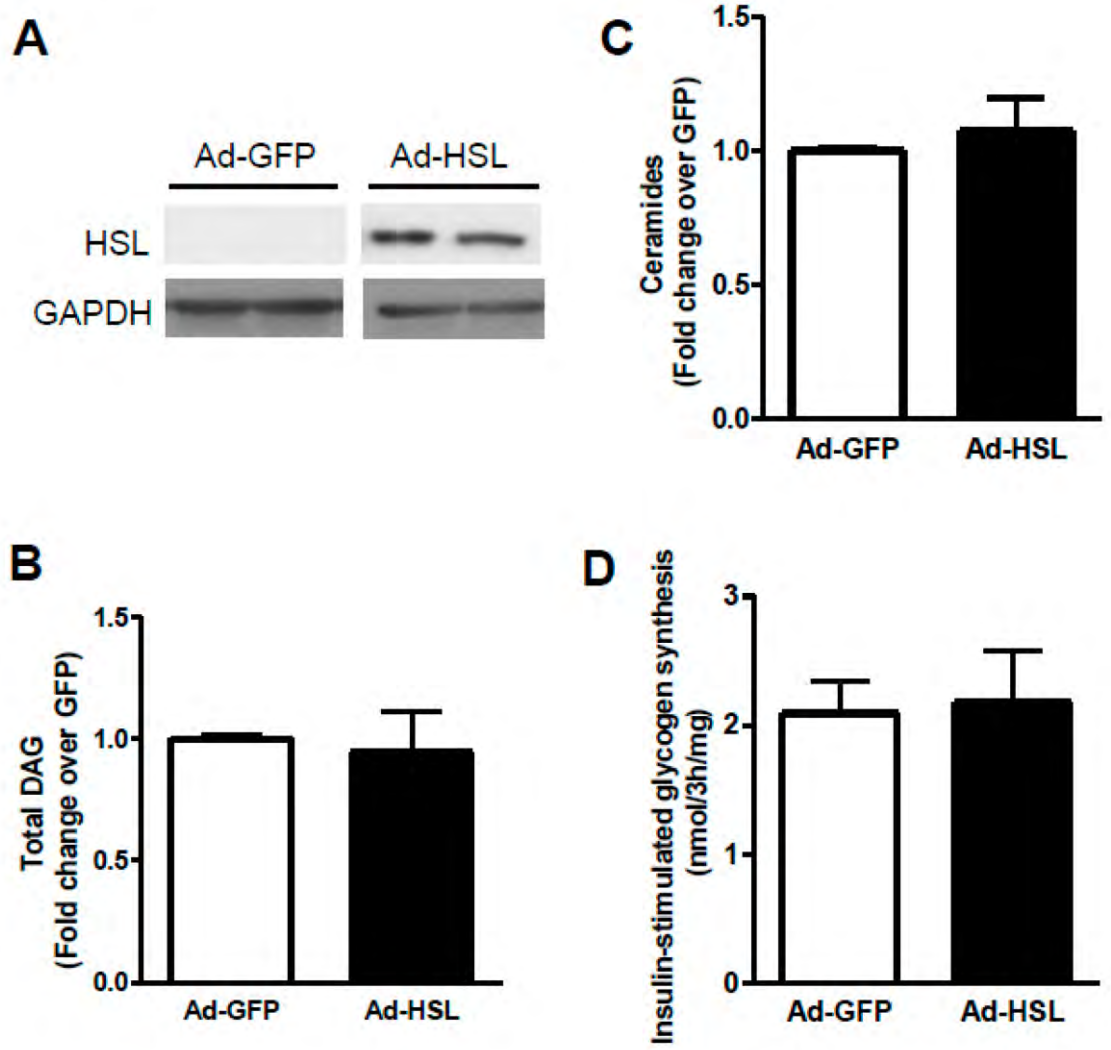

SUPPLEMENTARY DATA

Supplementary Figure 3. Quantitative bar graph of insulin-stimulated Ser473 Akt phosphorylation in myotubes overexpressing ATGL alone or in combination with BAY 1 M treatment (n=3); insulin-stimulated Akt phosphorylation was calculated as the delta change between basal and insulin stimulation for each condition; $^{*}p<0.05$, $^{**}p<0.01$ versus GFP.

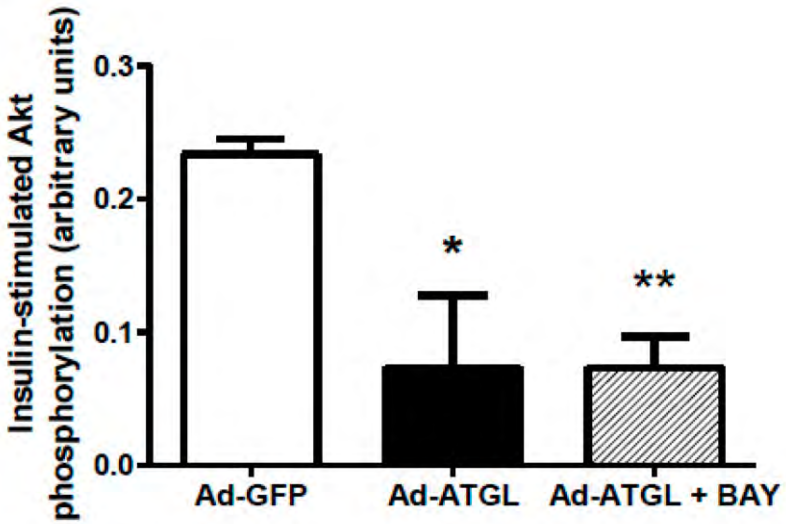

6.1.2 DISCUSSION

Dans un premier temps, nous avons montré dans ce travail que l'expression de l'ATGL était inversement corrélée à la sensibilité à l'insuline dans une cohorte de sujets regroupant des personnes de poids normal, obèses, et/ou diabétiques. Ces résultats confirment l'association forte existant entre l'élévation de l'expression de l'ATGL et l'insulino-résistance (Jocken et al., 2010).

Dans un deuxième temps, nous avons voulu voir si l'élévation de l'expression de l'ATGL, qui corrèle négativement avec la sensibilité à l'insuline mesuré par clamp hyperinsulinémique-euglycémique, peut expliquer à elle seule une dégradation du métabolisme glucidique des myocytes. Pour cela nous avons étudié les conséquences d'une surexpression de l'ATGL sur l'insulino-résistance ainsi que sur le contenu en lipides intermédiaires de myocytes humains en culture primaire. Nos résultats montrent qu'une surexpression de l'ATGL dans des myocytes traités à l'oléate conduit à une altération du signal et de la sensibilité à l'insuline associée à une accumulation de DAGs et de céramides. Afin de déterminer si ces deux espèces lipidiques étaient impliquées dans la perte de sensibilité à l'insuline de nos myocytes, nous avons traité les cellules surexprimant l'ATGL avec un inhibiteur des PKCs (la calphostine-C) ou un inhibiteur de la synthèse des céramides (la myriocine). De façon intéressante nous avons montré qu'un traitement à la calphostin-C contrecarre l'effet délétère de la surexpression de l'ATGL sur la sensibilité à l'insuline à l'inverse, d'un traitement à la myriocine. Comme les DAGs semblaient, au sein de notre modèle, l'espèce lipidique responsable de l'insulino-résistance, nous avons voulu étudier l'effet que pouvait avoir une modification de l'expression ou de l'activité de la LHS, principale DAGH, sur la sensibilité à l'insuline. De façon intéressante nous avons observé qu'une co-surexpression de la LHS avec l'ATGL permet de restaurer la sensibilité à l'insuline des myocytes. A l'inverse une inhibition pharmacologique de la LHS est suffisante pour augmenter le contenu en DAG des myocytes et diminuer la sensibilité à l'insuline. Ces résultats montrent pour la première fois le rôle clé de la balance lipolytique ATGL/LHS sur la genèse de l'insulino-résistance musculaire (Figure 10).

Ces données vont dans le sens d'une forte implication des DAGs dans l'insulino-résistance confirmant ainsi les nombreuses études menées *in vivo* chez l'homme et l'animal associant cette espèce lipidique à l'altération de la sensibilité à l'insuline musculaire et hépatique (Chibalin et al., 2008; Griffin et al., 1999; Itani et al., 2002; Samuel and Shulman, 2012). Il est intéressant de noter que nous montrons pour la première fois que dans certaines conditions, les AGs insaturés comme l'oléate peuvent se révéler toxiques. En effet nous observons qu'après dérégulation des lipases un traitement à l'oléate suffit à détériorer l'insulino-sensibilité des myocytes. Ces résultats confirment plusieurs travaux qui tendent à montrer que les DAGs insaturés pourraient être les plus aptes à activer les PKCs (Schmitz-Peiffer and Biden, 2008). De façon plus étonnante, et contrairement à ce qu'ont conclu plusieurs études réalisées sur myocytes (Chavez et al., 2003; Pickersgill et al., 2007), les céramides n'ont pas d'effet néfaste sur la sensibilité à l'insuline dans notre modèle de culture. Ceci peut s'expliquer par des différences dans le modèle utilisé, en effet nous avons travaillé sur une lignée primaire humaine, alors que les autres travaux ont été réalisés dans des cellules de souris d'une lignée immortalisée (C2C12). Outre la différence dans le modèle de culture utilisé, nos cellules ont été traitées avec un AG insaturé, l'oléate et non avec du palmitate classiquement utilisé dans ce type d'étude. En effet les AGs insaturés ne peuvent pas être utilisés par la SPT1 pour la synthèse *de novo* de céramides à l'inverse du palmitate (Schmitz-Peiffer, 2010). L'augmentation des céramides dans notre modèle serait donc due à la lipolyse des TAGs synthétisés à partir d'AGs issus de la lipogenèse *de novo*. De plus nous pouvons émettre l'hypothèse que le deuxième AG greffé pour former un dihydrocéramide (figure 5) est insaturé. Il est donc possible que les céramides composés à partir d'AGs insaturés soient moins aptes à activer la PP2A. Finalement, ce travail sur myocytes primaires humain nous a permis de prouver de manière causale qu'une augmentation de l'expression de l'ATGL, est suffisante pour déclencher l'insulino-résistance des myocytes. Ceci permet sans doute d'expliquer la corrélation inverse existant entre le niveau d'expression de l'ATGL et la sensibilité à l'insuline mesuré par clamp hyperinsulinémique-euglycémique. De plus nous avons montré que ce mécanisme était DAG-dépendant et pouvait être reversé par la surexpression de la LHS. Sur la base de ces données, il nous a semblé primordial d'aller mieux caractériser le contrôle de la lipolyse musculaire, en étudiant les

modifications d'expression des lipases durant un régime gras ainsi que le rôle de CGI-58 sur l'activité musculaire de l'ATGL.

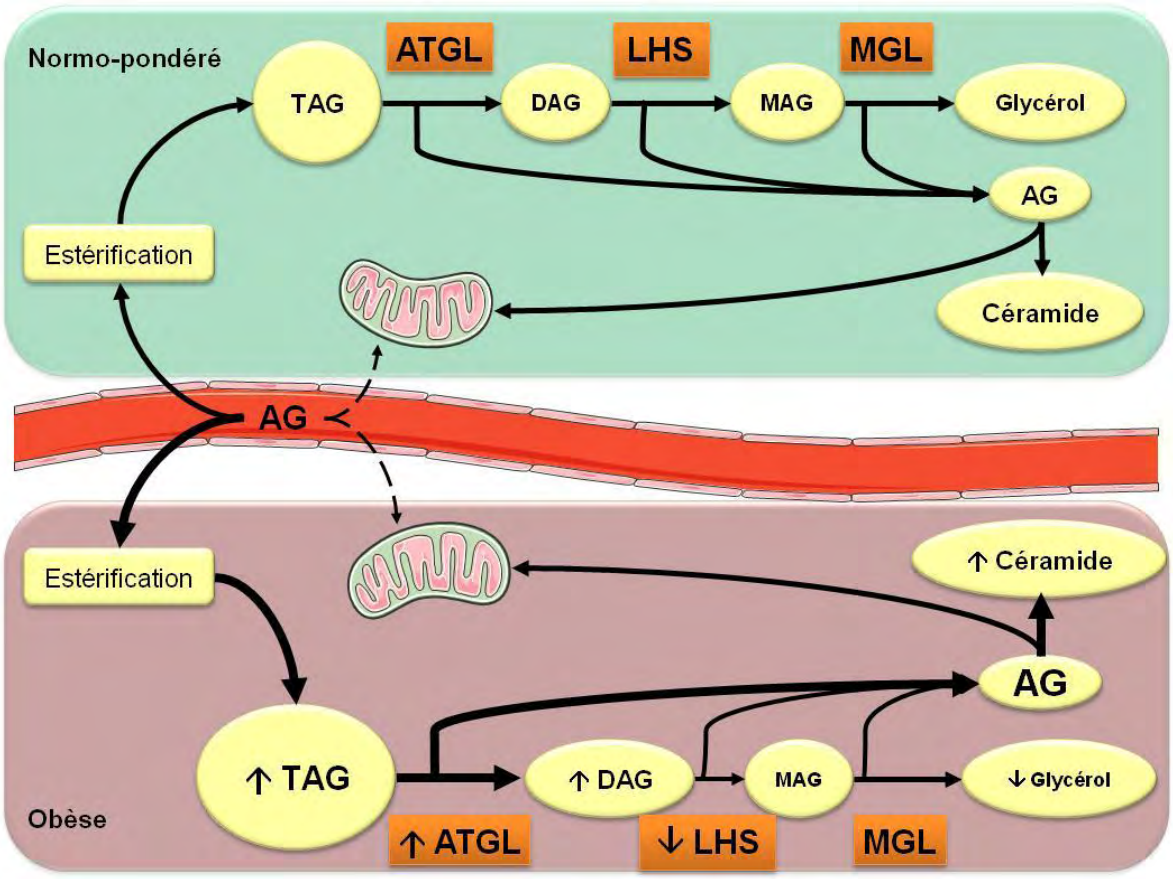

Figure 10. Implications de la dérégulation des lipases durant l'obésité

Chez l'obèse insulino-résistant, il existe une modification de l'expression des lipases, une hausse de l'expression de l'ATGL et une baisse de celle de la LHS. Nous avons montré dans un modèle cellulaire que ceci ce traduisant par une hausse de la production de lipides lipotoxiques et une perte de la sensibilité à l'insuline des myocytes.

6.2 PUBLICATION 2 : EFFET D'UN REGIME HYPER LIPIDIQUE SUR LA LIPOTOXICITE ET L'INSULINO-RESISTANCE : LIENS AVEC L'EXPRESSION DES LIPASES MUSCULAIRES CHEZ LA SOURIS

6.2.1 ARTICLE 2

Publication 2: High-fat diet-mediated lipotoxicity and insulin resistance is related to impaired lipase expression in mouse skeletal muscle

Badin PM, Vila IK, Louche K, Mairal A, Marques MA, Bourlier V, Tavernier G, Langin D, Moro C. *(2013). Endocrinology. 154(4):1444-53.*

Endocrinology. First published ahead of print March 7, 2013 as doi:10.1210/en.2012-2029

High-Fat Diet-Mediated Lipotoxicity and Insulin Resistance Is Related to Impaired Lipase Expression in Mouse Skeletal Muscle

Pierre-Marie Badin,* Isabelle K. Vila,* Katie Louche, Aline Mairal, Marie-Adeline Marques, Virginie Bourlier, Geneviève Tavernier, Dominique Langin, and Cedric Moro

Institut National de la Santé et de la Recherche Médicale (P.-M.B., I.K.V., K.L., A.M., M.-A.M., V.B., G.T., D.L., C.M.), Unité Mixte de Recherche 1048, Obesity Research Laboratory, Institute of Metabolic and Cardiovascular Diseases, 31432 Toulouse Cedex 4, France; University of Toulouse (P.-M.B., I.K.V., K.L., A.M., M.-A.M., V.B., G.T., D.L., C.M.), Paul Sabatier University, 31062 Toulouse Cedex 9, France; and Department of Clinical Biochemistry (D.L.), Toulouse University Hospitals, 31059 Toulouse Cedex 9, France

Elevated expression/activity of adipose triglyceride lipase (ATGL) and/or reduced activity of hormone-sensitive lipase (HSL) in skeletal muscle are causally linked to insulin resistance in vitro. We investigated here the effect of high-fat feeding on skeletal muscle lipolytic proteins, lipotoxicity, and insulin signaling in vivo. Five-week-old C3H mice were fed normal chow diet (NCD) or 45% kcal high-fat diet (HFD) for 4 weeks. Wild-type and HSL knockout mice fed NCD were also studied. Whole-body and muscle insulin sensitivity, as well as lipolytic protein expression, lipid levels, and insulin signaling in skeletal muscle, were measured. HFD induced whole-body insulin resistance and glucose intolerance and reduced skeletal muscle glucose uptake compared with NCD. HFD increased skeletal muscle total diacylglycerol (DAG) content, protein kinase Cθ and protein kinase Cϵ membrane translocation, and impaired insulin signaling as reflected by a robust increase of basal Ser1101 insulin receptor substrate 1 phosphorylation (2.8-fold, $P < .05$) and a decrease of insulin-stimulated v-Akt murine thymoma viral oncogene homolog Ser473 (-37%, $P < .05$) and AS160 Thr642 (-47%, $P < .01$) phosphorylation. We next showed that HFD strongly reduced HSL phosphorylation at Ser660. HFD significantly up-regulated the muscle protein content of the ATGL coactivator comparative gene identification 58 and triacylglycerol hydrolase activity, despite a lower ATGL protein content. We further show a defective skeletal muscle insulin signaling and DAG accumulation in HSL knockout compared with wild-type mice. Together, these data suggest a pathophysiological link between altered skeletal muscle lipase expression and DAG-mediated insulin resistance in mice. **(*Endocrinology* 154: 0000–0000, 2013)**

Obesity has become a major health problem worldwide. It constitutes a strong risk factor for other diseases, such as type 2 diabetes mellitus and cardiovascular diseases (1, 2). Obesity has been associated with ectopic fat deposition, and in sedentary populations, the level of intramyocellular triacylglycerol (TAG) (IMTG) is negatively correlated with insulin sensitivity (3, 4). However, studies on endurance athletes revealed a paradoxically elevated IMTG content in highly insulin sensitive subjects (5). It is now well established that skeletal muscle insulin resistance is mechanistically linked to accumulation of lipotoxic lipid species. Several studies show the detrimental

ISSN Print 0013-7227 ISSN Online 1945-7170
Printed in U.S.A.

Received October 8, 2012. Accepted February 12, 2013.

* P.-M.B. and I.K.V. contributed equally to this work.

Abbreviations: AAC, area above the curve; AMPK, 5′-AMP protein kinase; Akt, v-Akt murine thymoma viral oncogene homolog; ATGL, adipose triglyceride lipase; AU, arbitrary unit; AUC, area under the curve; CGI58, comparative gene identification 58; DAG, diacylglycerol; GTT, glucose tolerance test; HFD, high-fat diet; HSL, hormone-sensitive lipase; IMTG, intramyocellular TAG; IRS1, insulin receptor substrate-1; ITT, insulin tolerance test; NCD, normal chow diet; PKC, protein kinase C; PLIN, perilipin; TAG, triacylglycerol; TAGH, TAG hydrolase.

role of diacylglycerols (DAGs) and ceramides in cultured myotubes (6, 7), as well as in vivo in mice and human skeletal muscle (8–11).

DAG, a byproduct of lipolysis, is derived from TAG hydrolysis by adipose triglyceride lipase (ATGL) and is further hydrolyzed by the DAG hydrolase hormone-sensitive lipase (HSL) (12). Thus, HSL knockout mice accumulate DAG in several organs, such as skeletal muscle (13), whereas ATGL null mice appear more glucose tolerant (14). We recently demonstrated a causal relationship between defective lipolysis, lipotoxicity, and insulin resistance in human primary myotubes. Up-regulation of ATGL expression and/or inhibition of HSL activity both promoted DAG accumulation and impaired insulin signaling (7). Besides lipases, lipid droplet-associated proteins of the perilipin (PLIN) family (PLIN1–PLIN5) have been shown to play a major role in the control of TAG hydrolysis and lipolysis in multiple tissues (15, 16). It is still unclear whether skeletal muscle PLIN protein expression is disturbed in obesity and insulin-resistance states.

The aim of the present study was to test in vivo in mice the pathophysiological relevance of altered skeletal muscle lipolytic protein expression. We investigated here the impact of a high-fat diet (HFD) on the expression of lipases and PLIN proteins and its relationship with lipotoxicity and insulin resistance in skeletal muscle of C3H mice. This model has been previously used as a relevant model of diet-induced obesity and diabetes (17). We further examined this relationship in HSL knockout mice.

Materials and Methods

Animals

Animal protocols were performed according to Institut National de la Santé et de la Recherche Médicale and Institut des Maladies Métaboliques et Cardiovasculaires Animal Care Facility guidelines. All protocols were reviewed and approved by an Institutional Animal Care and Use Committee. Wild-type males C3H/HeOuJ and females B6D2 HSL null mice (kindly provided by Dr Cecilia Holm) were used and maintained on a 12-hour light, 12-hour dark cycle. They were housed 4 per cage, with ad libitum water and food. HFD (45% fat, Research Diets D12451; Research Diets, Inc, New Brunswick, New Jersey) or normal chow diet (NCD) (10% fat, D12450B) were initiated for 4 weeks right after weaning (5 wk of age) in C3H mice. HSL null mice were fed for 7 weeks under NCD.

Body mass and body composition

Body weight was measured weekly. For C3H mice, body composition was evaluated by quantitative nuclear magnetic resonance imaging (EchoMRI 3-in-1 system; Echo Medical Systems, Houston, Texas) before and at 4 weeks of each diet.

Glucose tolerance test (GTT) and insulin tolerance test (ITT)

For ip ITT and GTT, a bolus of insulin 0.5 mU/g of lean mass (Insuman Rapid, Sanofi Aventis, France) and D-glucose 2 mg/g of lean mass (Sigma-Aldrich, Saint-Quentin Fallavier, France) was injected to 6-hour-fasted mice, respectively. Blood glucose levels were monitored from the tip of the tail with a glucometer (Accucheck; Roche, Meylan, France) at 0, 15, 30, 45, 60, and 90 minutes after injection. Fasting insulin was measured using an ultrasensitive ELISA (ALPCO Diagnostics, Salem, New Hampshire). For ITTs, area above the curve (AAC) was calculated to account for differences in baseline fasting blood glucose concentrations as previously suggested (18).

Tissue-specific [2-^{3}H]deoxyglucose uptake during the GTT

To determine muscle-specific glucose uptake, [2-^{3}H]deoxyglucose (PerkinElmer, Boston, Massachusetts) (12 μCi/mouse) was mixed with 20% D-glucose to obtain a fixed specific activity before ip injection (2-mg/g lean body mass) as previously described with slight modifications (19). Animals were killed by cervical dislocation 45 minutes after injection, and soleus and gastrocnemius muscles were snap frozen in liquid nitrogen. Tissue-specific accumulation of 2-deoxyglucose-6-phosphate was determined as previously described, with minor modifications (20). The total of the [^{3}H]-radioactivity found in 2-deoxyglucose-6-phosphate was divided by the mean specific activity of glucose at 45 minutes to obtain the tissue-specific clearance index (Kg) (milliliter per 100 g of tissue per minute) as described elsewhere (21).

Tissue collection and preparation

After an overnight fast, mice were killed by cervical dislocation, and tissues were rapidly extracted and freeze clamped in liquid nitrogen before being stored at −80°C. For insulin signaling experiments, fresh tissues of C3H mice were incubated at 37°C for 20 minutes in Krebs-Henseleit buffer with or without 100nM insulin. After incubation, tissues were freeze clamped in liquid nitrogen and stored at −80°C. B6D2 wild-type and HSL null mice were injected ip with 10 mU/g of insulin 10 minutes before being killed.

Tissue fractionation

Plasma membrane and cytosol fractions were prepared as previously described with slight modifications (22, 23). Briefly, 50 mg of gastrocnemius muscles were extracted in buffer A (50mM Tris [pH 8.0] and 0.5mM dithiothreitol) containing 10-μL/mL protease inhibitor (Sigma-Aldrich), 10-μL/mL phosphatase I inhibitor (Sigma-Aldrich), and 10-μL/mL phosphatase II inhibitor (Sigma-Aldrich). Tissues were homogenized using a polytron and centrifuged at 1000*g* for 10 minutes at 4°C. The supernatant 1 was collected and kept on ice. The pellet was rinsed once in buffer A, centrifuged at 1000*g* for 10 minutes at 4°C, and the new pellet was resuspended in buffer B (buffer A plus Nonidet P-40 1%) and stood on ice for 1 hour with occasional mixing. The tube was then centrifuged at 16 000*g* for 20 minutes at 4°C, and the supernatant was used as the crude membrane fraction. The supernatant 1 was centrifuged at 16 000*g* for 20 minutes at 4°C, and the new supernatant was used as the cytosol fraction. A representative blot of 1 tissue fractionation experiment is shown in Supplemental Figure 1, published on The

Endocrine Society's Journals Online web site at http://endo.endojournals.org.

Western blot analysis

Soleus muscles were homogenized during 2 cycles of 30 seconds, 5500 rpm, 4°C using the Precellys 24 apparatus (Bertin Technologies, Montigny-le-Bretonneux, France) in a buffer containing 50mM Tris-HCl (pH 8.0), 150mM NaCl, 1% Nonidet P-40, 0.5% sodium deoxycholate, 0.1% sodium dodecyl sulfate, 10-μL/mL protease inhibitor, 10-μL/mL phosphatase I inhibitor, and 10-μL/mL phosphatase II inhibitor. Tissue lysates were centrifuged at 14 000*g* for 25 minutes, and supernatants were stored at −80°C. A total of 40 μg of solubilized proteins from muscle tissue were run on a 4%–20% gradient SDS-PAGE (Bio-Rad, Hercules, California), transferred onto nitrocellulose membrane (Hybond ECL; Amersham Biosciences, Piscataway, New Jersey), and incubated with the primary antibodies: ATGL, HSL, pSer660-HSL, and pSer565-HSL (Cell Signaling Technology, Beverly, Massachusetts) and comparative gene identification 58 (CGI58) (Abnova Corp, Tapei, Taiwan) for lipases; pSer473-Akt, v-Akt murine thymoma viral oncogene homolog (Akt), pSer1101-insulin receptor substrate-1 (IRS1), pTyr612-IRS1, IRS1, pThr642-AS160, and AS160 for insulin signaling (Cell Signaling Technology). For protein kinase C (PKC) translocation assays, PKCpan, PKCθ, and PKCϵ primary antibodies were from Santa Cruz Biotechnology, Inc (Santa Cruz, California). α-Tubulin (Sigma-Aldrich) was used as cytosolic marker, and caveolin1 (Cell Signaling Technology) was used as plasma membrane marker. Gels were loaded with equal amount of membrane and cytosol proteins. For detection of PLIN, membranes were also probed with PLIN2 and PLIN3 (Thermo Scientific, Illkirch, France) and PLIN5 (Progen, Heidelberg, Germany) antibodies. Subsequently, immunoreactive proteins were determined by enhanced chemiluminescence reagent (SuperSignal West Dura or SuperSignal West Femto; Thermo Scientific) and visualized by exposure to Hyperfilm ECL (GE Healthcare, Princeton, New Jersey). Glyceraldehyde-3-phosphate dehydrogenase (Cell Signaling Technology) was used as internal control.

Lipase activity assays

TAG hydrolase (TAGH) activity was measured on soleus lysates as previously described (24). Briefly, muscles were extracted in a lysis buffer containing 0.25M sucrose, 1mM EDTA, 1mM dithiothreitol, 20-μg/mL leupeptin, and 20-μg/mL antipain. [9, 10-^{3}H(N)]triolein (PerkinElmer) and cold triolein were emulsified with phospholipids by sonication. The data are expressed in nanomoles of oleic acid released per hour per milligram of protein.

Neutral lipid molecular species analysis

Soleus muscles were homogenized in 1 mL of methanol/5mM EGTA (2:1, vol/vol) with FAST-PREP (MP Biochemicals, Solon, Ohio). Lipids corresponding to 2 mg of tissue were extracted according to Bligh and Dyer (25) in methanol/water/dichloromethane (1.5:1.5:2, vol/vol/vol), in the presence of internal standards: 3 μg of stigmasterol, 3 μg of 1,3-dimyristine, 3 μg of cholesteryl heptadecanoate, and 20 μg of glyceryl trinonadecanoate. Dichloromethane phase was evaporated to dryness. Neutral lipid were separated on solid phase extraction columns (Macherey Nagel glass Chromabond pure silice, 200 mg) after washing cartridge with 2 mL of chloroform, crude extract was applied on the cartridge in 40 μL of chloroform, and neutral lipids were eluted in 2 mL of chloroform:methanol (9:1, vol/vol). The organic phase was evaporated to dryness and dissolved in 20 μL of ethyl acetate. One microliter of the lipid extract was analyzed by gas-liquid chromatography on a FOCUS Thermo Electron system using an Zebron-1 Phenomenex fused silica capillary columns (5 m × 0,32 mm inner diameter, 0.50 μm of film thickness) (26). Oven temperature was programmed from 200°C to 350°C at a rate of 5°C per minute, and the carrier gas was hydrogen (0.5 bar). The injector and the detector were at 315°C and 345°C, respectively. The equivalent of 0.3 mg of tissue was evaporated under nitrogen, the dry pellets were dissolved overnight in 0.2 mL of NaOH (0.1M), and proteins were measured with the Bio-Rad protein assay.

[1-^{14}C]palmitate incorporation

Whole solei were incubated for 2 hours in a modified sucrose-EDTA medium (250mM sucrose, 1mM EDTA, and 10mM Tris-HCl [pH 7.4]) with a combination of [1-^{14}C]palmitate (1 μCi/ml; PerkinElmer) and unlabeled palmitate (200μM final concentration). At the end of incubation, total lipids were extracted in chloroform/methanol (2volume/1volume) and separated by thin layer chromatography as previously described (27). Incorporation rates were normalized to wet tissue weight.

Statistics

All statistical analyses were performed using GraphPad Prism 5.0 for Windows (GraphPad Software, Inc, San Diego, California). Normal distribution of the data was tested with Kolmogorov-Smirnov tests. Unpaired Student's *t* tests were performed to determine differences between groups. Two-way ANOVA followed by Bonferonni's post hoc tests was applied when appropriate. Pearson correlations were applied when data were normally distributed and Spearman correlations for nonparametric data. All values in figures and tables are presented as mean ± SEM. Statistical significance was set at $P < .05$.

Results

Short-term HFD induces rapid weight gain and whole-body insulin resistance in C3H mice

As expected, 4 weeks of HFD 45% kcal from fat induced greater weight gain compared with NCD in C3H mice (NCD +25%, $P < .001$; HFD +60%, $P < .001$) mainly because of a robust increase in fat mass (NCD +61%, $P < .01$; HFD +382%, $P < .001$), whereas lean body mass was not significantly changed between NCD and HFD (Table 1). Importantly, 4 weeks of HFD in C3H mice were sufficient to induce a comparable body weight gain (about 60%) as is typically observed in C57Bl/6 mice after 8 weeks under the same diet (data not shown). In addition, HFD increased fasting blood glucose (+18%, $P < .001$) and fasting blood insulin (4.5-fold, $P < .001$) compared with NCD in C3H mice (Table 1). Whole-body insulin and glucose tolerance were measured (Figure 1, A

Table 1. Body Composition and Metabolic Variables in Fasted C3H Mice

	NCD	HFD	*P* value
Weight (g)	27.9 ± 0.38	35.5 ± 0.50	<.001
Fat mass (g)	2.6 ± 0.28	9.1 ± 0.33	<.001
Lean mass (g)	19.5 ± 0.20	19.7 ± 0.22	N.S.
Fasting insulin (ng/mL)	0.47 ± 0.08	2.1 ± 0.30	<.001
Fasting glucose (mg/dL)	140 ± 3.87	166 ± 4.21	<.001

N.S., not significant.

and B). The ITT AAC was reduced by −44% ($P < .01$) (Figure 1A), whereas the GTT area under the curve (AUC) was significantly increased in HFD-fed mice (3-fold, $P < .01$) (Figure 1B). Interestingly, plasma insulin concentration at 15 minutes during the GTT was significantly elevated in HFD-fed mice (2.8-fold, $P < .001$) (Figure 1C). Thus, C3H mice were strongly insulin resistant after 4 weeks of HFD and represent an interesting model to study the effect of short-term high-fat feeding on the mechanisms of fat-induced insulin resistance.

Short-term HFD promotes lipotoxicity and impairs insulin signaling in skeletal muscle

Because skeletal muscle is an important site of glucose disposal in the body, we examined the effects of short-term HFD on skeletal muscle glucose uptake, lipotoxicity, and insulin signaling. We first showed a reduced glucose uptake in both oxidative soleus and glycolytic gastrocnemius muscles of HFD-fed mice in vivo (Figure 2A). Of interest, glucose uptake in soleus was inversely correlated to the log(AUC) of the GTT ($r = -0.73$, $P = .01$). The reduced glucose uptake was associated with significant disturbances in muscle insulin signaling. Indeed, we noticed an increased basal Ser1101 phosphorylation of the IRS1 (2.8-fold, $P < .05$) (Figure 2, B and F), associated with an expected decrease of its activating phosphorylation on Tyr612 upon insulin stimulation (−68% $P < .01$) (Figure 2, C and F). Consistently, downstream insulin-stimulated phosphorylation of Akt at Ser473 residue (−37%, $P < .01$) (Figure 2, D and F) and AS160 at Thr642 (−88%, $P < .01$) (Figure 2, E and F) was reduced in HFD-fed mice, whereas their basal phosphorylation remained unaffected by the diet (Supplemental Figure 2). IRS1 phosphorylation at Ser1101 inhibits IRS1 function and is a primary target for DAG-activated PKC (28). This prompted us to examine PKC translocation to the plasma membrane and skeletal muscle lipid content. We found a higher membrane to cytosol ratio of all PKC isoforms (PKCpan) as well as of the main novel PKC isoforms, PKCθ and PKCϵ, in the muscle of HFD-fed compared with NCD-fed mice (Figure 3, A and B, and Supplemental Figure 3). As expected, the higher novel PKC membrane translocation was associated

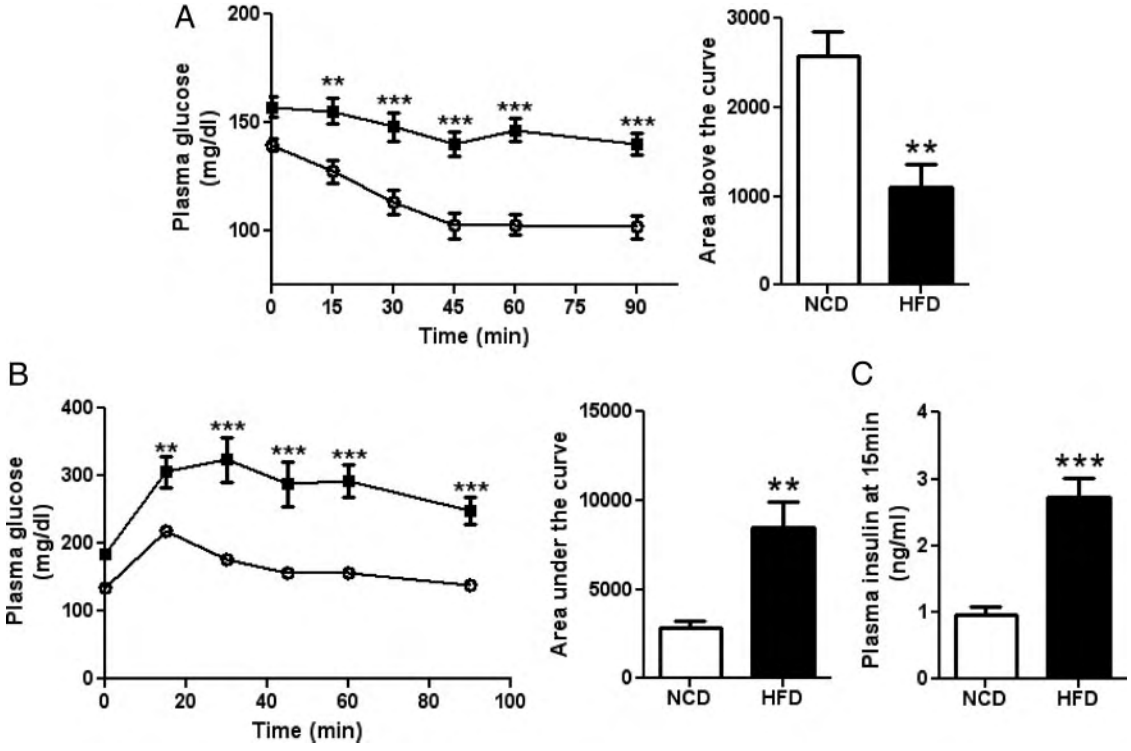

Figure 1. Short-term HFD induces whole-body insulin resistance in C3H mice. (A) (left panel) ITT in mice at 4 weeks of HFD (black square) or NCD (open circle); (right panel) AAC during the ITT. (B) (left panel) GTT in mice at 4 weeks of HFD or NCD; (right panel) AUC during the GTT. (C) Plasma insulin concentration measured 15 minutes after glucose injection. n = 8; $^{**}P < .01$, $^{***}P < .001$ vs NCD.

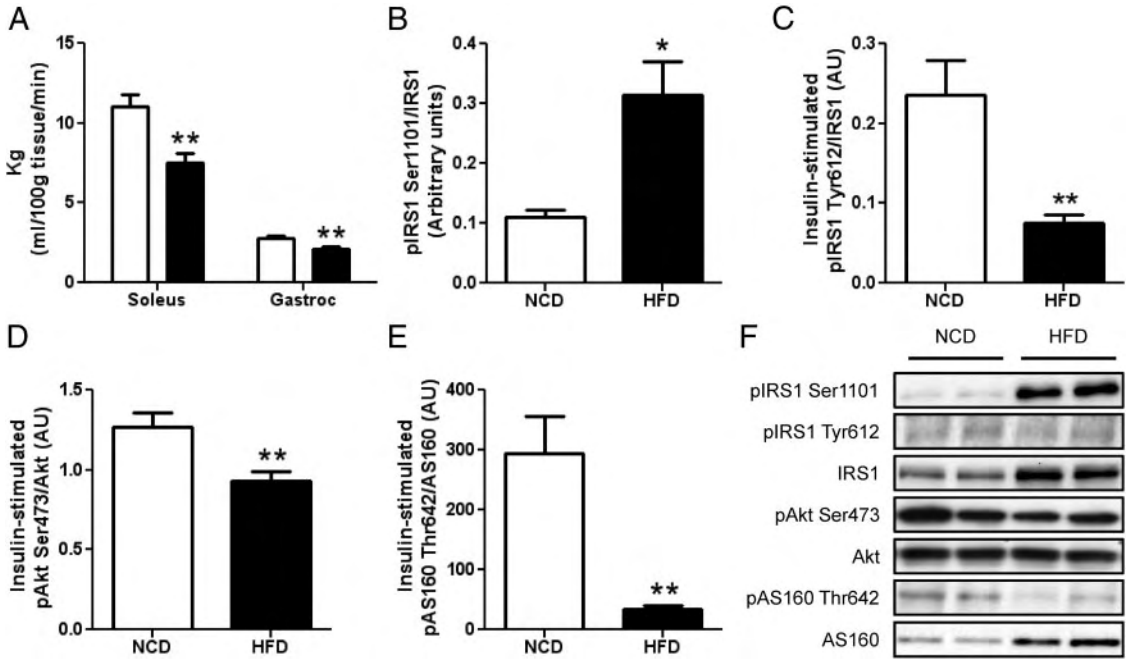

Figure 2. Impaired skeletal muscle insulin signaling after 4 weeks of HFD. (A) Tissue-specific glucose uptake in soleus and gastrocnemius muscles after 4 weeks of NCD or HFD (n = 6–8). (B) Quantitative bar graph of basal pIRS1 Ser1101 in mice soleus after 4 weeks of NCD or HFD (n = 4–5). (C) Quantitative bar graph of insulin-stimulated pIRS1 Tyr612 phosphorylation in mice soleus after 4 weeks of NCD or HFD (n = 8). (D) Quantitative bar graph of insulin-stimulated pAkt Ser473 phosphorylation in mice soleus after 4 weeks of NCD or HFD (n = 8). (E) Quantitative bar graph of insulin-stimulated pAS160 Thr642 phosphorylation in mice soleus after 4 weeks of NCD or HFD (n = 8). (F) Representative blots of 2 NCD- and 2 HFD-fed mice. $*P < .05$, $**P < .01$ vs NCD.

with a significantly elevated total DAG content (+39%, $P < .05$) (Figure 3C), whereas a trend for higher IMTG content (+35%, $P = .12$) (Figure 3D) was observed in HFD-fed mice. Interestingly, we noted a strong relationship between skeletal muscle DAG content and fasting blood insulin ($r = 0.60$, $P = .01$), as well as a negative correlation between muscle plasma membrane PKCpan and whole-body insulin sensitivity as measured by the ITT AAC ($r = -0.57$, $P = .03$). Additionally, IRS1 serine phosphorylation occurred without any significant change in c-Jun N-terminal kinase-1 phosphorylation (Supplemental Figure 4A), whereas 5′-AMP protein kinase (AMPK) Thr172 phosphorylation was significantly reduced in HFD-fed mice (Supplemental Figure 4B).

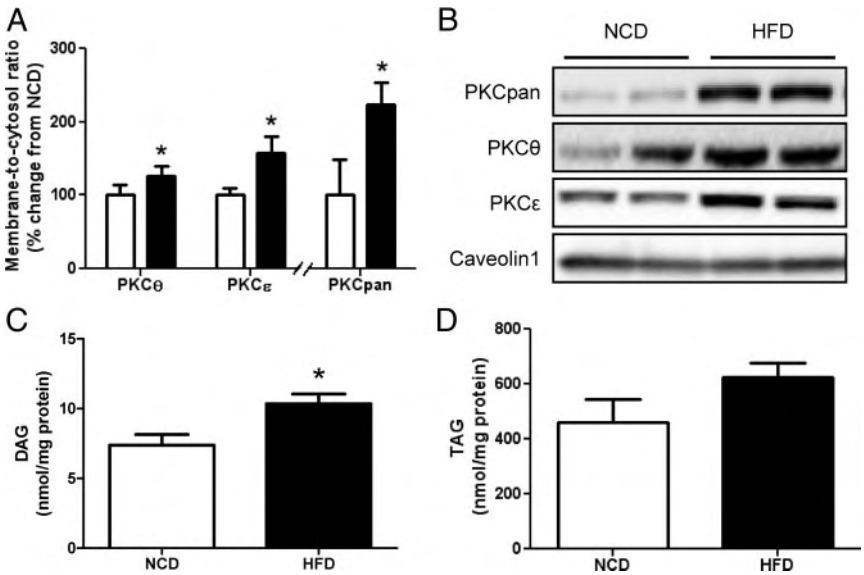

Figure 3. HFD-induced lipotoxicity in skeletal muscle. (A) Gastrocnemius muscle PKCs membrane to cytosol ratio of mice fed NCD (white bars) or HFD (black bars) during 4 weeks. (B) Representative blots of membrane PKCs (n = 6–8). (C and D) Neutral lipid content in soleus of mice after 4 weeks of NCD or HFD. (C) Total DAG content. (D) TAG content (n = 8). $*P < .05$ vs NCD.

Short-term HFD alters skeletal muscle lipolytic proteins

To gain further insight into the mechanisms of HFD-induced lipotoxicity, we examined lipase and PLIN protein expression in skeletal muscle. Interestingly, compared with NCD, HFD up-regulated the expression of the ATGL coactivator CGI58 both in soleus and gastrocnemius muscles (Figure 4B and Supplemental Figure 5B), whereas ATGL protein tended to decrease (Figure 4A and Supplemental Figure 5A). CGI58 protein level progressively

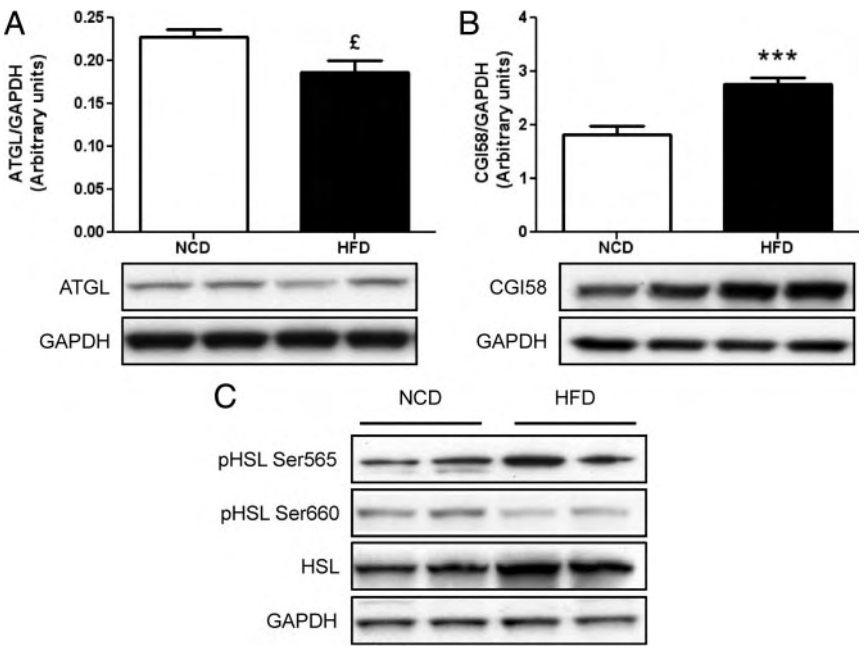

Figure 4. Altered skeletal muscle lipases expression in soleus of HFD-fed mice. (A–C) Lipase protein expression in mice fed with NCD or HFD for 4 weeks. (A) ATGL protein expression (n = 4–5). (B) CGI58 protein expression (n = 12–13). Insets show a representative blot of 2 NCD- and 2 HFD-fed mice. £ = 0.06, ***$P < .001$ vs NCD. (C) Representative blots of pHSL Ser660, pHSL Ser565, and total HSL protein. GAPDH, glyceraldehyde-3-phosphate dehydrogenase.

rose from the beginning of the HFD until 4 weeks, whereas ATGL expression was not significantly changed (Supplemental Figure 6). Importantly, we observed a very strong decrease in Ser660-HSL phosphorylation (NCD, 0.16 ± 0.02 arbitrary units [AU] vs HFD, 0.08 ± 0.01 AU, $P < .01$) (Figure 4C and Supplemental Figure 5C), whereas Ser565-HSL phosphorylation was not altered when adjusted to total HSL (NCD, 3.73 ± 0.76 AU vs HFD, 2.28 ± 0.62 AU, $P = .18$) (Figure 4C). The decrease in Ser660-HSL phosphorylation occurred despite a significant increase of total HSL protein (NCD, 0.90 ± 0.03 AU vs HFD, 1.21 ± 0.05 AU, $P < .01$) (Figure 4C). We also measured the protein content of PLINs that are lipid droplet related proteins involved in the control of lipid droplet dynamics and metabolism. PLIN2 and PLIN3 proteins were not affected by HFD (Figure 5, A and B), whereas PLIN5 was strongly up-regulated in HFD-fed mice compared with NCD (+86%, $P < .01$) (Figure 5C and Supplemental Figure 5D). Moreover, PLIN5 expression paralleled the increase of CGI58 protein during the time course of high-fat feeding (Supplemental Figure 7). In a larger cohort of mice, we found a very strong positive relationship between PLIN5 expression and total body weight (Figure 5D), as well as fat mass ($r = 0.81$, $P < .001$). Skeletal muscle lipase and PLIN protein expression responded similarly in B6D2 mice fed the same HFD for a longer period of 14 weeks (data not shown). These changes in lipolytic proteins were associated with a trend for increased TAGH activity (+53%) (NCD, 1.64 ± 0.24 nmol/h^{-1}·mg^{-1} vs HFD, 2.51 ± 0.41 nmol/h^{-1}·mg^{-1}, $P = .09$).

Increased DAG and disrupted insulin signaling in skeletal muscle of HSL knockout mice

To examine the link between reduced HSL activity in skeletal muscle and insulin resistance, we also studied HSL null mice on NCD (Figure 6A). We performed ex vivo studies in whole-soleus muscle and showed a higher incorporation rate of palmitate into DAG (+93%, $P < .05$) (Figure 6B), whereas the rate of incorporation of palmitate into TAG was not significantly affected (Figure 6C). This was accompanied by a reduced insulin activation of Akt on its Ser473 residue (−19%, $P < .05$) (Figure 6D), whereas basal Akt phosphorylation remained unaffected (data not shown). Thus, HSL deficiency in skeletal muscle promotes DAG accumulation and impairs insulin signaling.

Discussion

It is now well established that insulin resistance is related to accumulation of DAG and ceramides in skeletal muscle (6, 29). However, the mechanisms underlying their accumulation during the development of obesity are still discussed. In this study, we show that short-term HFD impairs skeletal muscle lipases and PLIN proteins and concomitantly promotes DAG accumulation, PKC membrane translocation, and insulin resistance in skeletal muscle. These findings are consistent with recent in vitro data, where we demonstrated a causal relationship between altered lipase expression, DAG accumulation, and insulin resistance in human primary myotubes (7).

In the present study, we used C3H mice, which represent an interesting model to study the effect of short-term high-fat feeding on skeletal muscle lipotoxicity and insulin resistance (17). A robust and fast body weight gain is observed in C3H mice within 4 weeks of HFD. Under the same diet, 8 weeks are required for C57Bl/6 mice to reach the same level of weight gain. We observed a strong deterioration of whole-body insulin sensitivity, glucose tolerance, and skeletal muscle glucose uptake in C3H mice

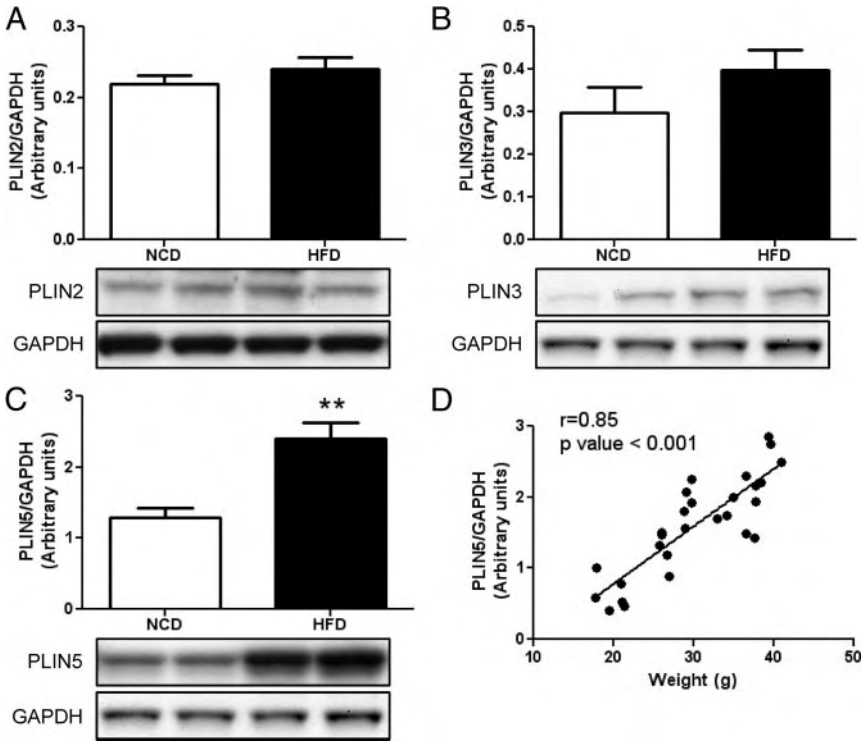

Figure 5. HFD-induced modulation of skeletal muscle PLINs. (A–C) PLIN protein expression in mice fed with NCD or HFD for 4 weeks. (A) PLIN2 protein expression. (B) PLIN3 protein expression. (C) PLIN5 protein expression (n = 4–5). Insets show a representative blot of 2 NCD- and 2 HFD-fed mice. $^{**}P < .01$ vs NCD. (D) Pearson correlation between body weight and PLIN5 protein expression (n = 28). GAPDH, glyceraldehyde-3-phosphate dehydrogenase.

within 4 weeks of HFD. Importantly, skeletal muscle insulin signaling was impaired in HFD-fed mice as reflected by an increased Ser1101-IRS1 phosphorylation and a decrease of Tyr612-IRS1 phosphorylation despite a significant increase of IRS1 protein. The higher expression of IRS1 protein could be explained by relatively higher fasting plasma insulin in HFD-fed mice. Insulin was shown to acutely induce IRS1 expression in mouse and human skeletal muscle to compensate for serine phosphorylation-induced IRS1 proteasomal degradation (30). As expected, downstream IRS1 signaling was strongly impaired as evidenced by reduced insulin-stimulated Ser473-Akt and Thr642-AS160 phosphorylation. We also showed impaired muscle AMPK activation, which could, together with reduced Akt activity, contribute to reduced AS160 activation, which is a downstream target of both Akt and AMPK signaling (31). These alterations of insulin signaling are consistent with other reports and confirm that skeletal muscle is a primary site of glucose disposal and insulin action (32).

Increased Ser1101 phosphorylation of IRS1 has been shown to inhibit IRS1 function and could be a specific target of PKCθ (28). We thus show a higher translocation of both PKCθ and PKCϵ at the plasma membrane of skeletal muscle in HFD-fed mice. DAGs are involved in activation of conventional PKC (α, βI, βII, γ) and novel PKC (δ, ϵ, η, θ), and DAG accumulation is known to be strongly associated with obesity and insulin resistance in humans (9, 24, 33) and mice (34). Interestingly, we noted that in parallel to insulin resistance, HFD-fed mice had elevated levels of DAG in skeletal muscle as previously described (35). HFD-induced impairments in skeletal muscle IRS1 function and insulin signaling were also independent of changes in c-Jun N-terminal kinase-1 activation in agreement with recent studies (36, 37). Our data are consistent with the view that HFD induces muscle insulin resistance through DAG-mediated novel PKC activation (9, 38).

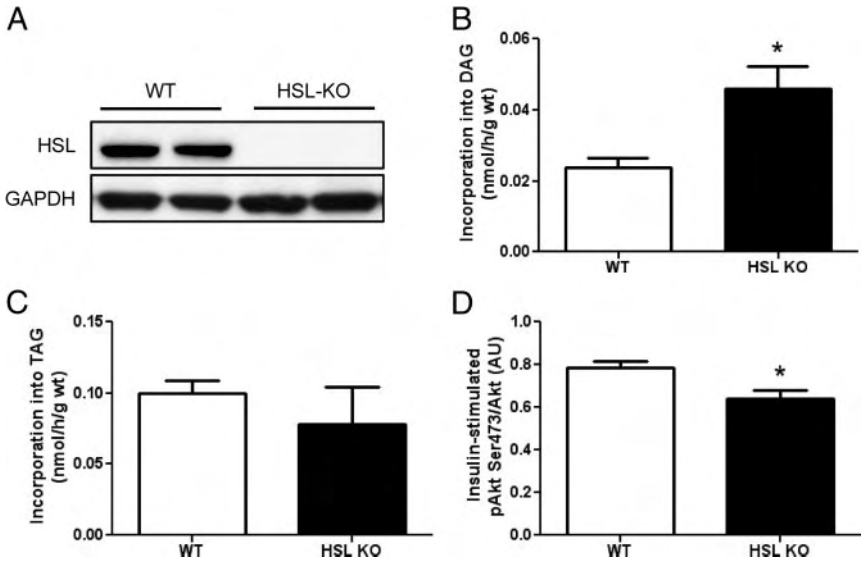

Figure 6. Elevated DAG and impaired insulin signaling in skeletal muscle of HSL null mice. (A) Representative blots of HSL protein and loading control in 2 wild-type (WT) and 2 HSL-knockout (KO) mice. (B and C) Incorporation of [1-^{14}C]palmitate in neutral lipid pools in soleus of WT and HSL-KO mice. (B) Incorporation rate into the DAG pool. (C) Incorporation rate into the TAG pool. (D) Insulin-stimulated Akt Ser473 phosphorylation in soleus of WT and HSL-KO mice (n = 5–6). $^{*}P < .05$ vs WT. GAPDH, glyceraldehyde-3-phosphate dehydrogenase.

Because DAG and TAG availability is highly regulated by lipolytic proteins (12), and that defective expression/activity of skeletal muscle lipases may promote DAG accumulation, we next investigated the influence of HFD on lipolytic proteins. This hypothesis is based on previous work, which demonstrate a strong association between obesity and defective skeletal muscle TAG and DAG hydrolysis (24) and related lipases in humans (7, 39). Although sn-1,2-DAG has been the most studied DAG in mammalian cells, it was shown that sn-1,3-DAG can promote PKCα binding to pure palmitoyl-2-oleoyl-sn-glycero-3-phosphoserine membrane vesicles (40). Thus, both sn-1,3-DAG and sn-1,2-DAG could activate PKC translocation to plasma membrane. In addition, we and others have recently shown that DAG produced from TAGHs, such as ATGL, can enter the pathway of phospholipid synthesis in normal human fibroblasts (41) and primary human myotubes (42). This suggests that ATGL-mediated TAG hydrolysis can provide sn-1,2-DAG capable of activating PKC. Of interest, ATGL protein content tended to be down-regulated, whereas its coactivator CGI58 was significantly up-regulated in skeletal muscle of HFD-fed mice. This inverse relationship has been previously observed in human myotubes (42) and in a human adipocyte cell line (43) and suggests that CGI58 and ATGL are reciprocally regulated in skeletal muscle and possibly in other tissues. Up-regulation of CGI58 despite the decrease of ATGL was sufficient to increase TAGH activity and lipolysis. This result confirms in vivo the central and limiting role of CGI58 in the regulation of skeletal muscle lipolysis (42).

An important finding of this study is that HSL Ser660 phosphorylation was dramatically reduced in the muscle of HFD-fed mice. No change in the phosphorylation level of the inhibitory HSL Ser565 residue was observed. Interestingly, HSL Ser660 phosphorylation is closely related to HSL activity in vitro (44). This serine residue is activated by cAMP-dependent protein kinase A (44). A similar down-regulation of HSL phosphorylation has been observed in adipose tissue during high-fat feeding (45). This may be explained by a reduction of protein kinase A activity through a down-regulation of its α-subunit in the obese state (46). Moreover, a reduced HSL Ser660 phosphorylation and partial resistance to catecholamine-induced lipolysis have been observed in skeletal muscle of obese insulin-resistant subjects (39, 47). Together, these data suggest that obesity and high-fat feeding may be associated with a low HSL activity in skeletal muscle.

We further investigated HSL null mice to understand the mechanistic link between low HSL activity and insulin resistance in skeletal muscle. We could show that HSL deficiency increases the rate of DAG accumulation without significant changes in skeletal muscle TAG dynamics. This finding is in agreement with a previous report (13). The higher DAG accumulation was associated with a lower insulin-stimulated activation of Akt on its Ser473 residue in the muscle of HSL null mice. Our data are in agreement with other reports showing a reduced insulin-mediated glucose transport in skeletal muscle of chow diet-fed HSL null mice (48, 49). It is important to note here that whole-body HSL deficiency may give a more complex phenotype than muscle-specific HSL deficiency. Thus, several phenotypic discrepancies have been observed in HSL knockout mice under different backgrounds and diet (48–50). This is also in line with recent findings showing an increased DAG accumulation and mild insulin resistance in human primary myotubes treated with a selective HSL inhibitor (7). Thus, the observed changes in DAG and insulin signaling were muscle autonomous. Together, these data suggest a causal link between low HSL activity, DAG accumulation, and insulin resistance in skeletal muscle.

The access of lipases to lipid droplets is partly controlled by PLIN proteins. In adipose tissue, PLIN1 is strongly expressed, and its role in lipolysis has been well studied (51, 52). Recent studies highlight the role of another member of the PLIN family, PLIN5, especially in oxidative tissues where PLIN1 is virtually not expressed (53). Wang et al (54, 55) and Granneman et al (56) showed that PLIN5 regulates negatively lipolysis and can link ATGL and CGI58 (54–56). PLIN5 protein expression increases in parallel of body fat mass during the HFD. This may be seen as an adaptive response to buffer excess dietary lipids into lipid droplets. This could be driven by increased FA flux and activation of peroxisome proliferator activated receptor signaling within the skeletal muscle (57, 58), because PLIN5 is a well-known target of peroxisome proliferator activated receptor α (16, 59). Futures studies will be necessary to understand the physiological role of PLIN5 in skeletal muscle in vivo and its association with insulin resistance.

One study limitation is that besides DAG, we cannot exclude a role of ceramides in fat-induced insulin resistance. Several studies have shown that ceramides contribute to the development of insulin resistance in palmitate-treated myocytes (6) and in mice fed lard diet and/or during saturated oil infusions (8, 35, 60). However, to the best of our knowledge, a direct effect of ceramide-activated Ser/Thr kinases on IRS1 serine phosphorylation has never been reported. We cannot dismiss either that other mechanisms might contribute to skeletal muscle DAG accumulation in obesity and diabetes, such as reduced DAG kinase activity and/or DAG-acyl-transferase-1 activity (34, 61).

In summary, our data show a pathophysiological link between altered lipase expression, lipotoxicity, and insulin resistance in skeletal muscle in vivo. These findings strengthen the relevance of in vitro results showing a causal association between altered lipase expression and insulin resistance in myotubes. Restoring a proper lipolytic control in skeletal muscle may alleviate obesity-related lipotoxicity and insulin resistance.

Acknowledgments

We thank M. Coonen, A. Girousse and A. Besse-Patin (Institut National de la Santé et de la Recherche Médicale [INSERM], Unité Mixte de Recherche [UMR] 1048) for outstanding help; J. Bertrand-Michel and V. Roques (Lipidomic Core Facility, INSERM, UMR 1048, part of Toulouse Metatoul Platform) for lipidomic analysis, advice, and technical assistance; and the Anexplo Mouse Phenotyping and Animal Care facility cores.

Address all correspondence and requests for reprints to: Cedric Moro, PhD, Institut National de la Santé et de la Recherche Médicale, Unité Mixte de Recherche 1048, Institut des Maladies Métaboliques et Cardiovasculaires, CHU Rangueil, BP 84225, 1 Avenue Jean Poulhès, 31432 Toulouse Cedex 4, France. E-mail: cedric.moro@inserm.fr.

This work was supported by grants from the European Foundation for the Study of Diabetes/Novo Nordisk, the National Research Agency Grant ANR-09-JCJC-0019-01, and the Société Francophone du Diabète (C.M.) and by the Fondation pour la Recherche Médicale (D.L.). I.K.V. was supported by a fellowship from the Midi-Pyrénées region.

Disclosure Summary: The authors have nothing to disclose.

References

1. **DeFronzo RA.** Pathogenesis of type 2 diabetes mellitus. *Med Clin North Am.* 2004;88:787–835, ix.
2. **McGarry JD.** Banting lecture 2001: dysregulation of fatty acid metabolism in the etiology of type 2 diabetes. *Diabetes*. 2002;51:7–18.
3. **Szczepaniak LS, Babcock EE, Schick F, et al.** Measurement of intracellular triglyceride stores by H spectroscopy: validation in vivo. *Am J Physiol*. 1999;276:E977–E989.
4. **Kelley DE, Goodpaster BH, Storlien L.** Muscle triglyceride and insulin resistance. *Annu Rev Nutr*. 2002;22:325–346.
5. **Moro C, Bajpeyi S, Smith SR.** Determinants of intramyocellular triglyceride turnover: implications for insulin sensitivity. *Am J Physiol*. 2008;294:E203–E213.
6. **Pickersgill L, Litherland GJ, Greenberg AS, Walker M, Yeaman SJ.** Key role for ceramides in mediating insulin resistance in human muscle cells. *J Biol Chem*. 2007;282:12583–12589.
7. **Badin PM, Louche K, Mairal A, et al.** Altered skeletal muscle lipase expression and activity contribute to insulin resistance in humans. *Diabetes*. 2011;60:1734–1742.
8. **Holland WL, Brozinick JT, Wang LP, et al.** Inhibition of ceramide synthesis ameliorates glucocorticoid-, saturated-fat-, and obesity-induced insulin resistance. *Cell Metab*. 2007;5:167–179.
9. **Itani SI, Ruderman NB, Schmieder F, Boden G.** Lipid-induced insulin resistance in human muscle is associated with changes in diacylglycerol, protein kinase C, and IκB-α. *Diabetes*. 2002;51:2005–2011.
10. **Dresner A, Laurent D, Marcucci M, et al.** Effects of free fatty acids on glucose transport and IRS-1-associated phosphatidylinositol 3-kinase activity. *J Clin Invest*. 1999;103:253–259.
11. **Adams JM 2nd, Pratipanawatr T, Berria R, et al.** Ceramide content is increased in skeletal muscle from obese insulin-resistant humans. *Diabetes*. 2004;53:25–31.
12. **Zechner R, Zimmermann R, Eichmann TO, et al.** FAT SIGNALS—lipases and lipolysis in lipid metabolism and signaling. *Cell Metab*. 2012;15:279–291.
13. **Haemmerle G, Zimmermann R, Hayn M, et al.** Hormone-sensitive lipase deficiency in mice causes diglyceride accumulation in adipose tissue, muscle, and testis. *J Biol Chem*. 2002;277:4806–4815.
14. **Haemmerle G, Lass A, Zimmermann R, et al.** Defective lipolysis and altered energy metabolism in mice lacking adipose triglyceride lipase. *Science*. 2006;312:734–737.
15. **Prats C, Donsmark M, Qvortrup K, et al.** Decrease in intramuscular lipid droplets and translocation of HSL in response to muscle contraction and epinephrine. *J Lipid Res*. 2006;47:2392–2399.
16. **Wolins NE, Quaynor BK, Skinner JR, et al.** OXPAT/PAT-1 is a PPAR-induced lipid droplet protein that promotes fatty acid utilization. *Diabetes*. 2006;55:3418–3428.
17. **Toye AA, Lippiat JD, Proks P, et al.** A genetic and physiological study of impaired glucose homeostasis control in C57BL/6J mice. *Diabetologia*. 2005;48:675–686.
18. **Ayala JE, Samuel VT, Morton GJ, et al.** Standard operating procedures for describing and performing metabolic tests of glucose homeostasis in mice. *Dis Model Mech*. 2010;3:525–534.
19. **Mauvais-Jarvis F, Virkamaki A, Michael MD, et al.** A model to explore the interaction between muscle insulin resistance and β-cell dysfunction in the development of type 2 diabetes. *Diabetes*. 2000;49:2126–2134.
20. **Virkamaki A, Rissanen E, Hamalainen S, Utriainen T, Yki-Jarvinen H.** Incorporation of [3–3H]glucose and 2-[1-14C]deoxyglucose into glycogen in heart and skeletal muscle in vivo: implications for the quantitation of tissue glucose uptake. *Diabetes*. 1997;46:1106–1110.
21. **Kraegen EW, James DE, Jenkins AB, Chisholm DJ.** Dose-response curves for in vivo insulin sensitivity in individual tissues in rats. *Am J Physiol*. 1985;248:E353–E362.
22. **Nishiumi S, Ashida H.** Rapid preparation of a plasma membrane fraction from adipocytes and muscle cells: application to detection of translocated glucose transporter 4 on the plasma membrane. *Biosci Biotechnol Biochem*. 2007;71:2343–2346.
23. **Bostrom P, Andersson L, Vind B, et al.** The SNARE protein SNAP23 and the SNARE-interacting protein Munc18c in human skeletal muscle are implicated in insulin resistance/type 2 diabetes. *Diabetes*. 2010;59:1870–1878.
24. **Moro C, Galgani JE, Luu L, et al.** Influence of gender, obesity, and muscle lipase activity on intramyocellular lipids in sedentary individuals. *J Clin Endocrinol Metab*. 2009;94:3440–3447.
25. **Bligh EG, Dyer WJ.** A rapid method of total lipid extraction and purification. *Can J Biochem Physiol*. 1959;37:911–917.
26. **Barrans A, Collet X, Barbaras R, et al.** Hepatic lipase induces the formation of pre-β 1 high density lipoprotein (HDL) from triacylglycerol-rich HDL2. A study comparing liver perfusion to in vitro incubation with lipases. *J Biol Chem*. 1994;269:11572–11577.
27. **Hessvik NP, Bakke SS, Fredriksson K, et al.** Metabolic switching of human myotubes is improved by n-3 fatty acids. *J Lipid Res*. 2010;51:2090–2104.
28. **Li Y, Soos TJ, Li X, et al.** Protein kinase Cθ inhibits insulin signaling by phosphorylating IRS1 at Ser(1101). *J Biol Chem*. 2004;279:45304–45307.
29. **Yu C, Chen Y, Cline GW, et al.** Mechanism by which fatty acids inhibit insulin activation of insulin receptor substrate-1 (IRS-1)-as-

sociated phosphatidylinositol 3-kinase activity in muscle. *J Biol Chem*. 2002;277:50230–50236.
30. **Ruiz-Alcaraz AJ, Liu HK, Cuthbertson DJ, et al.** A novel regulation of IRS1 (insulin receptor substrate-1) expression following short term insulin administration. *Biochem J*. 2005;392:345–352.
31. **Deshmukh AS, Hawley JA, Zierath JR.** Exercise-induced phosphoproteins in skeletal muscle. *Int J Obes (Lond)*. 2008;4(suppl 32): S18–S23.
32. **DeFronzo RA, Tripathy D.** Skeletal muscle insulin resistance is the primary defect in type 2 diabetes. *Diabetes Care*. 2009;2(suppl 32): S157–S163.
33. **Samuel VT, Shulman GI.** Mechanisms for insulin resistance: common threads and missing links. *Cell*. 2012;148:852–871.
34. **Chibalin AV, Leng Y, Vieira E, et al.** Downregulation of diacylglycerol kinase δ contributes to hyperglycemia-induced insulin resistance. *Cell*. 2008;132:375–386.
35. **Ussher JR, Koves TR, Cadete VJ, et al.** Inhibition of de novo ceramide synthesis reverses diet-induced insulin resistance and enhances whole-body oxygen consumption. *Diabetes*. 2010;59:2453–2464.
36. **Hage Hassan R, Hainault I, Vilquin JT, et al.** Endoplasmic reticulum stress does not mediate palmitate-induced insulin resistance in mouse and human muscle cells. *Diabetologia*. 2012;55:204–214.
37. **Rieusset J, Chauvin MA, Durand A, et al.** Reduction of endoplasmic reticulum stress using chemical chaperones or Grp78 overexpression does not protect muscle cells from palmitate-induced insulin resistance. *Biochem Biophys Res Commun*. 2012;417:439–445.
38. **Itani SI, Zhou Q, Pories WJ, MacDonald KG, Dohm GL.** Involvement of protein kinase C in human skeletal muscle insulin resistance and obesity. *Diabetes*. 2000;49:1353–1358.
39. **Jocken JW, Roepstorff C, Goossens GH, et al.** Hormone-sensitive lipase serine phosphorylation and glycerol exchange across skeletal muscle in lean and obese subjects: effect of β-adrenergic stimulation. *Diabetes*. 2008;57:1834–1841.
40. **Sanchez-Pinera P, Micol V, Corbalan-Garcia S, Gomez-Fernandez JC.** A comparative study of the activation of protein kinase Cα by different diacylglycerol isomers. *Biochem J*. 1999;337(pt 3):387–395.
41. **Igal RA, Coleman RA.** Acylglycerol recycling from triacylglycerol to phospholipid, not lipase activity, is defective in neutral lipid storage disease fibroblasts. *J Biol Chem*. 1996;271:16644–16651.
42. **Badin PM, Loubiere C, Coonen M, et al.** Regulation of skeletal muscle lipolysis and oxidative metabolism by the co-lipase CGI-58. *J Lipid Res*. 2012;53:839–848.
43. **Bezaire V, Mairal A, Ribet C, et al.** Contribution of adipose triglyceride lipase and hormone-sensitive lipase to lipolysis in hMADS adipocytes. *J Biol Chem*. 2009;284:18282–18291.
44. **Anthonsen MW, Ronnstrand L, Wernstedt C, Degerman E, Holm C.** Identification of novel phosphorylation sites in hormone-sensitive lipase that are phosphorylated in response to isoproterenol and govern activation properties in vitro. *J Biol Chem*. 1998;273:215–221.
45. **Gaidhu MP, Anthony NM, Patel P, Hawke TJ, Ceddia RB.** Dysregulation of lipolysis and lipid metabolism in visceral and subcutaneous adipocytes by high-fat diet: role of ATGL, HSL, and AMPK. *Am J Physiol Cell Physiol*. 2010;298:C961–C971.
46. **Rodriguez-Cuenca S, Carobbio S, Velagapudi VR, et al.** Peroxisome proliferator-activated receptor γ-dependent regulation of lipolytic nodes and metabolic flexibility. *Mol Cell Biol*. 2012;32:1555–1565.
47. **Blaak EE, Schiffelers SL, Saris WH, Mensink M, Kooi ME.** Impaired β-adrenergically mediated lipolysis in skeletal muscle of obese subjects. *Diabetologia*. 2004;47:1462–1468.
48. **Mulder H, Sorhede-Winzell M, Contreras JA, et al.** Hormone-sensitive lipase null mice exhibit signs of impaired insulin sensitivity whereas insulin secretion is intact. *J Biol Chem*. 2003;278:36380–36388.
49. **Park SY, Kim HJ, Wang S, et al.** Hormone-sensitive lipase knockout mice have increased hepatic insulin sensitivity and are protected from short-term diet-induced insulin resistance in skeletal muscle and heart. *Am J Physiol*. 2005;289:E30–E39.
50. **Harada K, Shen WJ, Patel S, et al.** Resistance to high-fat diet-induced obesity and altered expression of adipose-specific genes in HSL-deficient mice. *Am J Physiol*. 2003;285:E1182–E1195.
51. **Brasaemle DL, Rubin B, Harten IA, Gruia-Gray J, Kimmel AR, Londos C.** Perilipin A increases triacylglycerol storage by decreasing the rate of triacylglycerol hydrolysis. *J Biol Chem*. 2000;275:38486–38493.
52. **Subramanian V, Rothenberg A, Gomez C, et al.** Perilipin A mediates the reversible binding of CGI-58 to lipid droplets in 3T3-L1 adipocytes. *J Biol Chem*. 2004;279:42062–42071.
53. **Bosma M, Minnaard R, Sparks LM, et al.** The lipid droplet coat protein perilipin 5 also localizes to muscle mitochondria. *Histochem Cell Biol*. 2012;137:205–216.
54. **Wang H, Bell M, Sreenevasan U, et al.** Unique regulation of adipose triglyceride lipase (ATGL) by perilipin 5, a lipid droplet-associated protein. *J Biol Chem*. 2011;286:15707–15715.
55. **Wang H, Sreenevasan U, Hu H, et al.** Perilipin 5, a lipid droplet-associated protein, provides physical and metabolic linkage to mitochondria. *J Lipid Res*. 2011;52:2159–2168.
56. **Granneman JG, Moore HP, Mottillo EP, Zhu Z, Zhou L.** Interactions of perilipin-5 (Plin5) with adipose triglyceride lipase. *J Biol Chem*. 2011;286:5126–5135.
57. **Schmidt A, Endo N, Rutledge SJ, Vogel R, Shinar D, Rodan GA.** Identification of a new member of the steroid hormone receptor superfamily that is activated by a peroxisome proliferator and fatty acids. *Mol Endocrinol*. 1992;6:1634–1641.
58. **Garcia-Roves P, Huss JM, Han DH, et al.** Raising plasma fatty acid concentration induces increased biogenesis of mitochondria in skeletal muscle. *Proc Natl Acad Sci USA*. 2007;104:10709–10713.
59. **Dalen KT, Dahl T, Holter E, et al.** LSDP5 is a PAT protein specifically expressed in fatty acid oxidizing tissues. *Biochim Biophys Acta*. 2007;1771:210–227.
60. **Frangioudakis G, Garrard J, Raddatz K, Nadler JL, Mitchell TW, Schmitz-Peiffer C.** Saturated- and n-6 polyunsaturated-fat diets each induce ceramide accumulation in mouse skeletal muscle: reversal and improvement of glucose tolerance by lipid metabolism inhibitors. *Endocrinology*. 2010;151:4187–4196.
61. **Liu L, Zhang Y, Chen N, Shi X, Tsang B, Yu YH.** Upregulation of myocellular DGAT1 augments triglyceride synthesis in skeletal muscle and protects against fat-induced insulin resistance. *J Clin Invest*. 2007;117:1679–1689.

Supplemental Figure 1: Validation of skeletal muscle tissue fractionation. Representative blots of α-Tubulin (markers of cytosol), and caveolin1 (marker of membrane) on cytosol and membrane fractions of *gactrocnemius* extracts from two different mice.

Supplemental Figure 2: No change in basal phosphorylation of key insulin signaling proteins. This Figure is companion to Figure 2. A. Quantitative bar graph of basal pIRS1 Tyr612 phosphorylation in mice *soleus* after 4 weeks of NCD or HFD. B. Quantitative bar graph of basal pAkt Ser473 phosphorylation in mice *soleus* after 4 weeks of NCD or HFD. C. Quantitative bar graph of basal pAS160 Thr642 phosphorylation in mice *soleus* after 4 weeks of NCD or HFD. Insets show a representative blot of 2 NCD and 2 HFD fed mice. n=8; £=0.06

Supplemental Figure 3: Representative blots of cytosol PKC proteins. This figure is companion to Figure 3B and shows cytosolic PKCs from *gastrocnemius* muscle of C3H mice fed NCD and HFD during 4 weeks (n=6-8).

Supplemental Figure 4: No change in JNK1 phosphorylation in muscle of HFD-fed mice. A. Quantitative bar graph of pJNK1 and total JNK1 in *soleus* muscle of C3H mice fed NCD and HFD during 4 weeks. B. Quantitative bar graph of pAMPK and total AMPK in *soleus* muscle of C3H mice fed NCD and HFD during 4 weeks. Insets show a representative blot of 2 NCD and 2 HFD fed mice. n=4-5; *$p<0.05$.

Supplemental Figure 5: Altered skeletal muscle lipases and PLIN5 expression in *gastrocnemius* of HFD fed mice. A. ATGL protein expression. B. CGI58 protein expression. C. HSL Ser660 phosphorylation. D. PLIN5 protein expression. Insets show a representative blot of 2 NCD and 2 HFD fed mice. n=8 *$p<0.05$, **$p<0.01$ vs NCD. 2

Supplemental Figure 6: Time-course of ATGL and CGI-58 protein expression in skeletal muscle during 4 weeks of HFD. ATGL (black circle) and CGI58 protein (open square) at different time points during HFD on the top panel. A representative blot is shown on the bottom panel. n=6; ** $p<0.01$, ***$p<0.001$ vs 0 time point.

Supplemental Figure 7: Time-course of PLIN5 protein expression in skeletal muscle during 4 weeks of HFD in C3H mice. Western blot of PLIN5 protein on C3H mice at different time points during HFD on the top panel. A representative blot is shown on the bottom panel. n=6; ***$p<0.001$ vs 0 time point.

Supplemental Figure 1

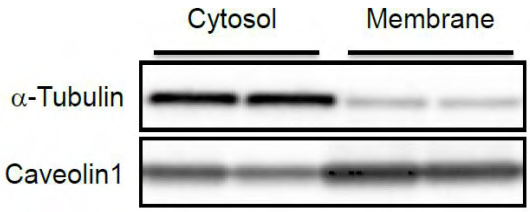

Supplemental Figure 2

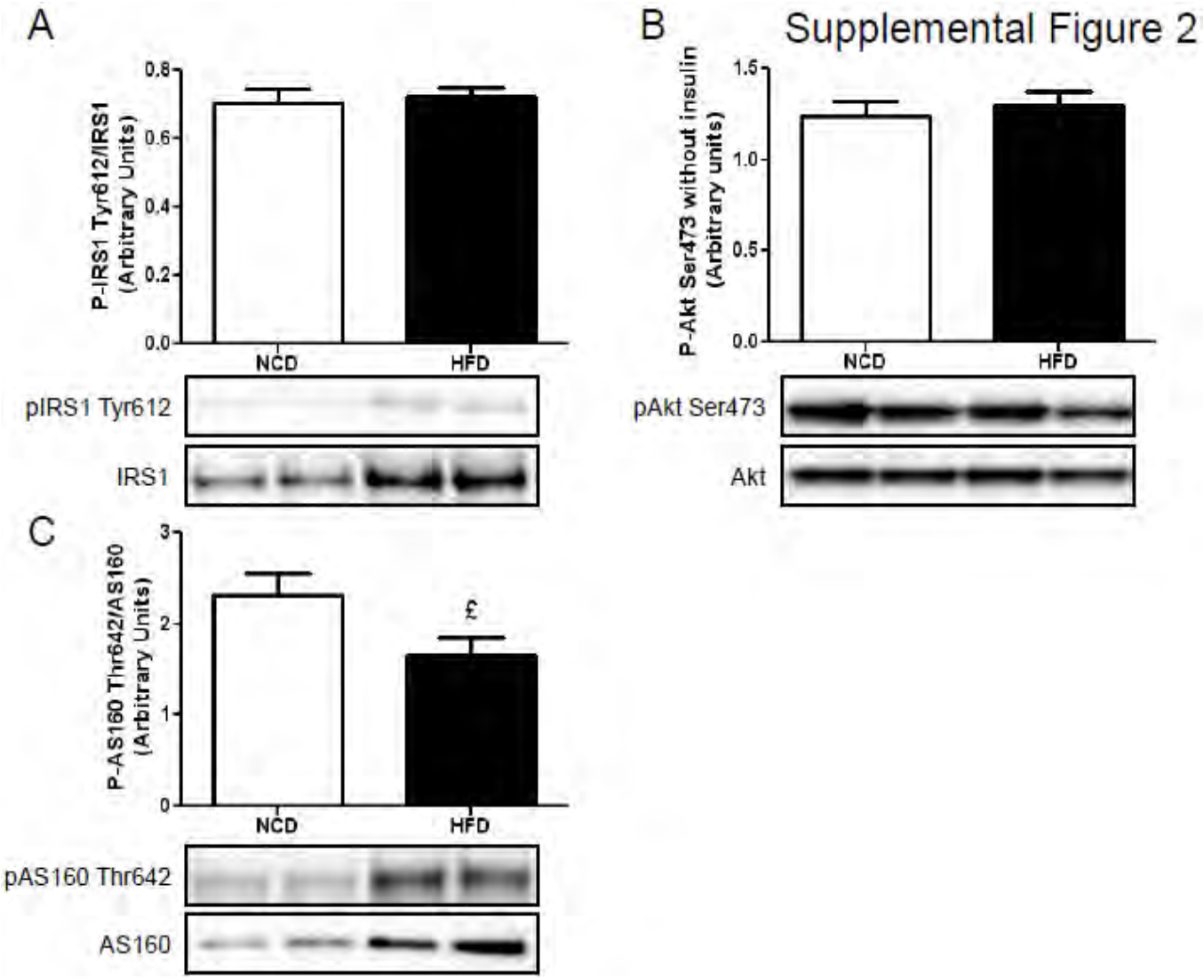

Supplemental Figure 3

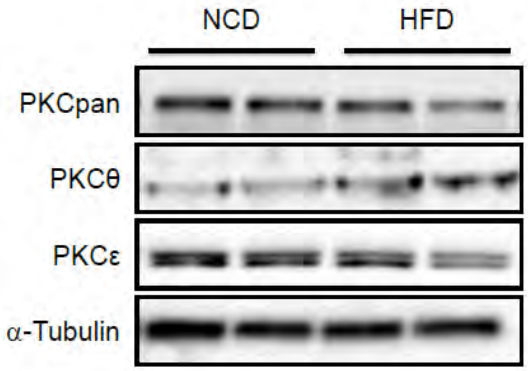

Supplemental Figure 4

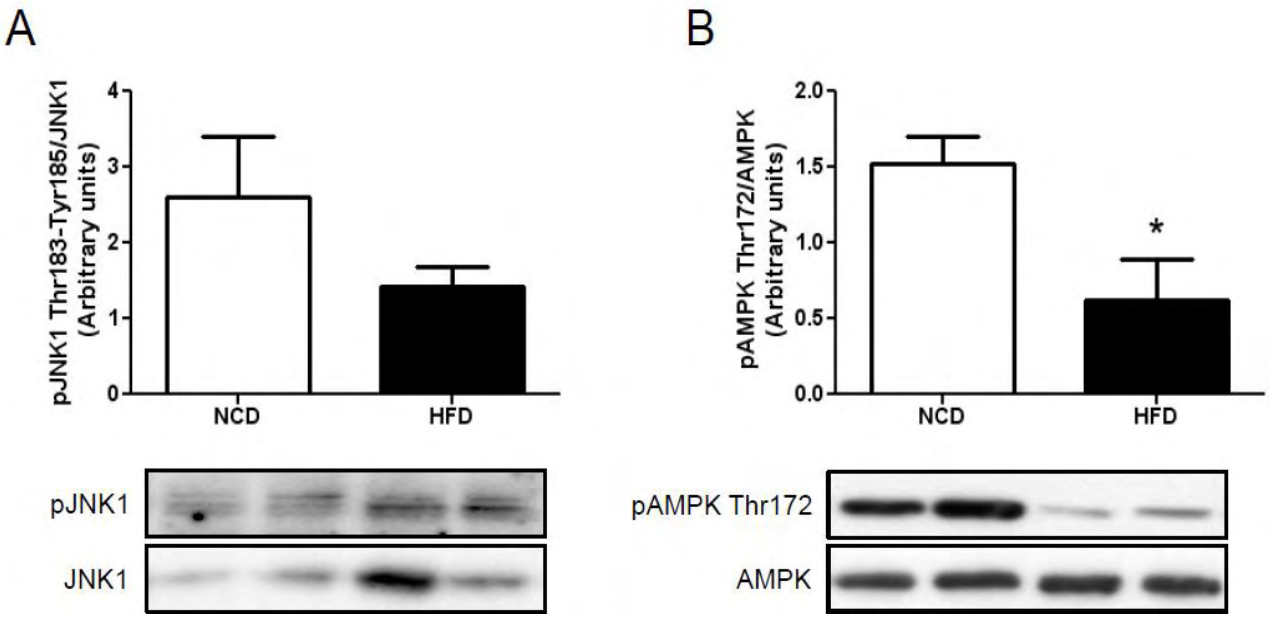

Supplemental Figure 5

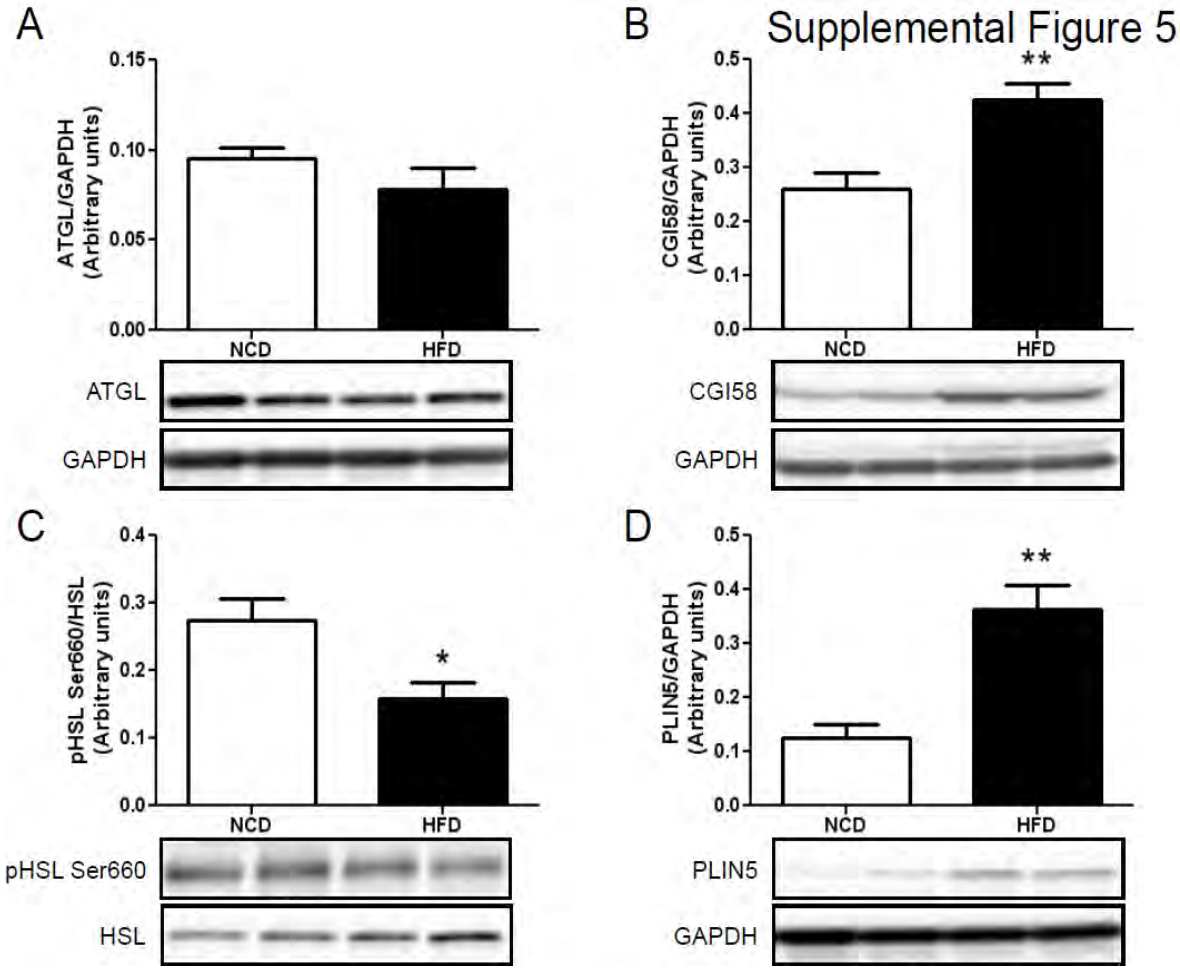

Supplemental Figure 6

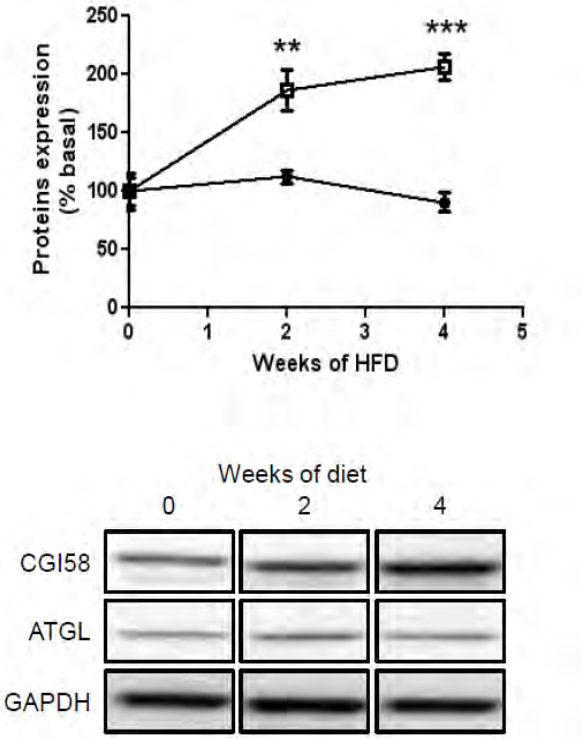

Supplemental Figure 7

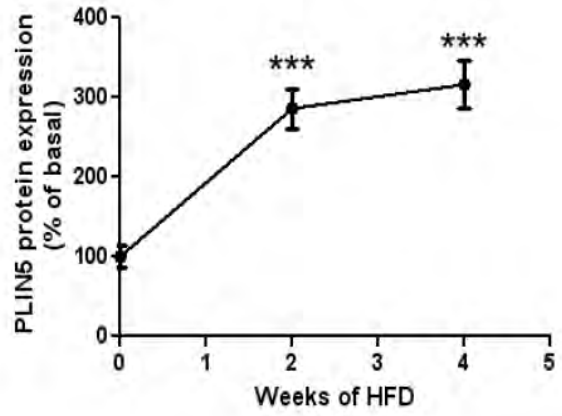

6.2.2 DISCUSSION

Ce travail a été réalisé dans un modèle murin particulièrement adapté à l'étude des troubles métaboliques induits par un régime riche en graisses. En effet le modèle de souris C3H a la particularité de prendre plus rapidement du poids que la souche de référence C57Bl/6. Nous avons évalué qu'en quatre semaines de régime gras (à 45%) nos souris C3H avaient pris autant de poids que des souris C57Bl/6 soumises au même régime depuis deux fois plus de temps. De plus ces souris présentent des dérégulations importantes de la sensibilité à l'insuline et de la tolérance au glucose dès deux semaines de régime hyperlipidique par rapport à leurs contrôles en régime standard. Cette détérioration du métabolisme glucidique s'explique en partie par une perte de la sensibilité musculaire à l'insuline reflétée par une diminution du transport de glucose médiée par l'insuline et par une augmentation de la phosphorylation d'IRS1 sur le résidu inhibiteur ser1101.

Le résidu ser1101 d'IRS1 a été décrit comme pouvant être phosphorylé par la kinase *c-Jun N-terminal kinase* (JNK) et certaines PKCs (Gual et al., 2005; Li et al., 2004; Yu et al., 2002). Nous avons mesuré le niveau de phosphorylation de JNK et réalisé des études de fractionnement cytosol/membrane afin d'évaluer le niveau d'activité respectif de JNK et des PKCs. De façon intéressante nous n'avons pas trouvé de modification de la phosphorylation de JNK dans le groupe de souris nourries en régime hyper lipidique. Ceci confirme les études récentes montrant que le stress du réticulum ne semble pas impliqué dans l'insulino-résistance musculaire (Hage Hassan et al., 2012; Rieusset et al., 2012). A l'inverse, nous avons retrouvé dans le groupe de souris soumises à un régime hyper lipidique une augmentation du contenu en PKCθ et PKCε à la membrane signe d'une plus grande activité de ces dernières. Cette hausse de la translocation des PKCs explique l'augmentation de la phosphorylation d'IRS1 en ser1101 (Li et al., 2004). Pour continuer notre travail nous avons dosé les DAGs, espèce lipidique très bien décrite pour activer les PKCs (Schmitz-Peiffer, 2010; Schmitz-Peiffer and Biden, 2008). Comme attendu nous avons trouvé une augmentation du contenu en DAGs dans le muscle de nos souris nourries en régime hyper lipidique comparées à celles placées en régime standard.

Nous avons précédemment montré qu'une dérégulation de l'expression et de l'activité des lipases musculaires pouvait participer à l'accumulation de DAGs et à l'insulino-résistance (Badin et al., 2011, 2012). Afin de continuer la caractérisation du modèle murin, nous avons donc étudié par western blot l'expression de l'ATGL, de CGI-58 et la phosphorylation de la LHS. De façon intéressante nous avons observé une forte augmentation de l'expression de CGI-58 alors que l'expression de l'ATGL tend, à l'inverse, à diminuer. Il est intéressant de noter que l'augmentation de CGI-58 malgré la diminution de l'ATGL suffit à augmenter l'hydrolyse des TAG au sein des myocytes (Badin et al., 2012). Nous avions, dans cette précédente étude, le même phénomène de régulation croisée de l'ATGL et de CGI-58. Ce type de contre régulation a également été observé dans des adipocytes (Bezaire et al., 2009). Il est probable que ceci soit dû à une régulation commune des deux gènes. Associée aux modifications d'expression de CGI-58 et d'ATGL, nous avons également noté une forte diminution de la phosphorylation activatrice de la LHS en ser660 or la phosphorylation de la LHS sur ce résidu est fortement liée à son activité (Anthonsen et al., 1998). Comme cette phosphorylation est dépendante de la PKA, sa diminution pourrait être due à une perte de sensibilité du muscle squelettique aux catécholamines comme précédemment observé chez l'obèse insulino-résistant (Blaak et al., 2004).

Pour confirmer qu'un déséquilibre de la balance lipolytique peut conduire à une perturbation du signal insulinique musculaire, nous avons utilisé des souris invalidées pour la LHS. Ces souris transgéniques présentent, en régime standard, une importante augmentation de la synthèse de DAGs au niveau musculaire. Associée à ces désordres lipidiques, nous avons observé une altération modérée du signal insulinique. Cette expérience confirme une insulino-résistance musculaire modérée de ces souris comme précédemment observée (Mulder et al., 2003). Ceci est sans doute lié à l'augmentation de la synthèse des DAGs (Haemmerle et al., 2002). Pour autant cela ne fait pas oublier que certaines souches de souris invalidées ou hétérozygotes pour la LHS sont protégées du développement de l'insulino-résistance lors d'un régime riche en lipides alors même que leur prise de poids n'est pas différente de celles des souris contrôles (Girousse and Langin, 2012;

Girousse et al., 2013; Park et al., 2005). Ceci s'expliquerait probablement par la diminution du flux d'AGs en provenance du tissu adipeux.

Cet article montre pour la première fois chez le rongeur qu'il existe une association entre l'insulino-résistance induite par un régime hyper lipidique et la dérégulation des lipases musculaires. Cette dérégulation de la lipolyse musculaire semble être responsable de l'accumulation de DAGs et de l'augmentation du contenu en PKCs membranaires. L'étude du signal insulinique menée sur le modèle invalidé pour la LHS montre le lien de causalité existant entre dérégulation de la lipolyse et insulino-résistance.

6.3 PUBLICATION 3 : LA REGULATION DE LA LIPOLYSE ET DU METABOLISME OXYDATIF MUSCULAIRE PAR LA CO-LIPASE CGI-58

6.3.1 ARTICLE 3

Publication 3 : Regulation of skeletal muscle lipolysis and oxidative metabolism by the co-lipase CGI-58. J. Lipid Res. *53*, 839–848.

Badin PM, Loubière C, Coonen M, Louche K, Tavernier G, Bourlier V, Mairal A, Rustan AC, Smith SR, Langin D, Moro C. *(2012) J. Lipid Res. 53(5):839-48.*

Regulation of skeletal muscle lipolysis and oxidative metabolism by the co-lipase CGI-58[S]

Pierre-Marie Badin,[1,*] Camille Loubière,[1,*] Maarten Coonen,[*] Katie Louche,[*] Geneviève Tavernier,[*] Virginie Bourlier,[*] Aline Mairal,[*] Arild C. Rustan,[†] Steven R. Smith,[§] Dominique Langin,[*] and Cedric Moro[2,*]

Inserm, 1048,* Obesity Research Laboratory, Institute of Metabolic and Cardiovascular Diseases, Paul Sabatier University, Toulouse, France; Department of Pharmaceutical Biosciences,† School of Pharmacy, University of Oslo, Oslo, Norway; and Translational Research Institute for Metabolism and Diabetes,§ Florida Hospital and the Burnham Institute for Medical Research, Winter Park, FL

Abstract **We investigated here the specific role of CGI-58 in the regulation of energy metabolism in skeletal muscle. We first examined CGI-58 protein expression in various muscle types in mice, and next modulated CGI-58 expression during overexpression and knockdown studies in human primary myotubes and evaluated the consequences on oxidative metabolism. We observed a preferential expression of CGI-58 in oxidative muscles in mice consistent with triacylglycerol hydrolase activity. We next showed by pulse-chase that CGI-58 overexpression increased by more than 2-fold the rate of triacylglycerol (TAG) hydrolysis, as well as TAG-derived fatty acid (FA) release and oxidation. Oppositely, CGI-58 silencing reduced TAG hydrolysis and TAG-derived FA release and oxidation (−77%, $P < 0.001$), whereas it increased glucose oxidation and glycogen synthesis. Interestingly, modulations of CGI-58 expression and FA release are reflected by changes in pyruvate dehydrogenase kinase 4 gene expression. This regulation involves the activation of the peroxisome proliferator activating receptor-δ (PPARδ) by lipolysis products.[JLR] Altogether, these data reveal that CGI-58 plays a limiting role in the control of oxidative metabolism by modulating FA availability and the expression of PPARδ-target genes, and highlight an important metabolic function of CGI-58 in skeletal muscle.**—Badin, P-M., C. Loubière, M. Coonen, K. Louche, G. Tavernier, V. Bourlier, A. Mairal, A. C. Rustan, S. R. Smith, D. Langin, and C. Moro. **Regulation of skeletal muscle lipolysis and oxidative metabolism by the co-lipase CGI-58.** ***J. Lipid Res.*** **2012.** 53: **839–848.**

Supplementary key words comparative gene identification 58 • fatty acid • substrate oxidation • intramyocellular triacylglycerol • peroxisome proliferator-activated receptor • mitochondria

Adipose triglyceride lipase (ATGL) is a novel adipose-enriched lipase that mediates the initial step in triacylglycerol (TAG) hydrolysis in various tissues of the body (1, 2). It was shown by Lass et al. (3) that ATGL activity is regulated by the product of the CGI-58 gene (comparative gene identification 58). Loss-of-function mutations in the human CGI-58 gene are sufficient to promote excessive lipid accumulation in most tissues leading to neutral lipid storage disease with ichtyosis (4). This clinical phenotype is more inconsistently associated with skeletal and cardiac myopathy, liver steatosis and hepatosplenomegaly as recently reviewed (5). CGI-58 mutant proteins are unable to induce ATGL activity, which results in cellular lipid accumulation in the form of TAG (3). Of interest, recent work indicates that the rate-limiting step for the mobilization of intracellular TAG is the release of CGI-58 from specific lipid droplet scaffold proteins such as Perilipin-A (6). Together, these data suggest that CGI-58 may be important for the control of lipolysis in several tissues.

Previous studies had shown the role of hormone sensitive lipase (HSL) in the regulation of intramyocellular TAG (IMTG) during exercise in humans (7, 8). However, HSL deficiency does not affect IMTG in skeletal muscle (9, 10). ATGL was recently shown to be expressed in human skeletal muscle predominantly in type I oxidative fibers (11). Thus, ATGL-deficient mice exhibit a defective TAG hydrolase activity in skeletal muscle and accumulate large amount of TAG in various tissues (1). These data suggest that ATGL may play an important role in the regulation of IMTG and lipolysis notably in skeletal muscle.

This study was supported by grants from the National Research Agency ANR-09-JCJC-0019-01 and from the European Federation for the Study of Diabetes/Novo Nordisk (C.M.); the Commission of the European Communities (Integrated Project HEPADIP (http://www.hepadip.org/), Contract LSHM-CT-2005-018734 (D.L.); and the National Insitutes of Health US 1P30 DK072476 (Pennington Biomedical Research Center/Nutrition Obesity Research Center) and R01AG030226 (S.R.S.). Its contents are solely the responsibility of the authors and do not necessarily represent the official views of the National Institutes of Health or other granting agencies.

Manuscript received 28 July 2012 and in revised form 10 February 2012.

Published, JLR Papers in Press, February 29, 2012
DOI 10.1194/jlr.M019182

Abbreviations: ATGL, adipose triglyceride lipase; DAG, diacylglycerol; HSL: hormone sensitive lipase; IMTG, intramyocellular triacylglycerol; MAG, monoacylglycerol; PLIN5: perilipin 5; LPAAT, lysophosphaditic acid acyltransferase; PL, phospholipids; SkM, skeletal muscle; TAG, triacylglycerol; TAGH, triacylglycerol hydrolase.

[1] These authors contributed equally to this work.
[2] To whom correspondence should be addressed.
e-mail: Cedric.Moro@inserm.fr

[S] The online version of this article (available at http://www.jlr.org) contains supplementary data in the form of three figures.

Furthermore, elevated ATGL activity and/or expression in human skeletal muscle was shown to play a role in the development of insulin resistance, a major risk factor for the development of type 2 diabetes (12). However, the regulation of ATGL activity in human skeletal muscle is currently poorly documented. We hypothesized that CGI-58 could be a critical regulator of human skeletal muscle TAG metabolism and substrate oxidation. The aim of the study was to examine the functional role of CGI-58 in human skeletal muscle by gain- and loss-of-function studies. We next measured the impact of elevated or reduced levels of CGI-58 on energy metabolism, mitochondrial activity, and gene expression in cultured human primary myotubes.

MATERIALS AND METHODS

Subjects

Six young healthy subjects, mean age 22.9 ± 0.4 yrs (18–29) and mean BMI 26.5 ± 0.5 kg/m^2 (20.1–34.7) were recruited in the study. The protocol was approved by the institutional review board of the Pennington Biomedical Research Center, and all volunteers gave written informed consent. The participants were asked to refrain from vigorous physical activity for 48 h before presenting to the Pennington inpatient clinic, and ate a weight-maintaining diet consisting of 35% fat, 16% protein, and 49% carbohydrate 2 days before the muscle biopsy. Samples of *vastus lateralis* weighing 60–100 mg were obtained using the Bergstrom technique, blotted, cleaned, and snap-frozen in liquid nitrogen (13). Human subcutaneous adipose tissue was obtained from six moderately overweight women undergoing plastic surgery. Their mean age was 44.6 ± 2.9 years and their mean BMI was 27.5 ± 1.2 kg/m^2. The study was in agreement with the Declaration of Helsinki, and the French National Institute of Health and Medical Research (INSERM) and the Toulouse University Hospital ethics regulation.

Animals

All experimental procedures were approved by a local ethical committee and performed according to INSERM animal core facility guidelines for the care and use of laboratory animals. Four- to five-week-old C57Bl/6 mice were housed in a pathogen-free barrier facility (12 h light/dark cycle) and fed a standard laboratory chow diet (D12450B) for 4 weeks before euthanasia and tissue collection.

Skeletal muscle cell culture

Satellite cells from *rectus abdominis* of healthy subjects (age 34.3 ± 2.5 years, BMI 26.0 ± 1.4 kg/m^2, fasting glucose 5.0 ± 0.2 mM) were isolated by trypsin digestion, preplated on an uncoated petri dish for 1 h to remove fibroblasts, and subsequently transferred to T-25 collagen-coated flasks in DMEM supplemented with 10% FBS and growth factors (human epidermal growth factor, BSA, dexamethasone, gentamycin, fungizone, fetuin) as previously described (12, 14). Cells were grown at 37°C in a humidified atmosphere of 5% CO_2. Differentiation of myoblasts into myotubes was initiated at ~80-90% confluence, by switching to α-MEM with antibiotics, 2% FBS, and fetuin. The medium was changed every other day and cells were grown up to 5 days.

Overexpression and knockdown studies

Human adipose tissue CGI-58 cDNA (Fwd: GCGGCTATGGCGGCGGAGGAGGA; Rev: GTGTTCAGTCCACAGTGTCGCAGAT) was cloned into the pcDNA3 vector (InVitrogen Corp., Carlsbad, CA). DNA sequencing was performed to check correct insertion of the cDNA using an ABI3100 automatic sequencer (Applied Biosystems, Courtaboeuf, France). For overexpression experiments, adenoviruses expressing bicistronic vectors containing in tandem GFP and hCGI-58 were constructed, purified, and titrated (Vector Biolabs, Philadelphia, PA). An adenovirus containing the GFP gene only was used as a control. Myotubes were infected with the control and hCGI-58 adenoviruses at day 4 of differentiation and remained exposed to the virus for 24 h in serum-free DMEM containing 150 μM of oleate complexed to BSA (ratio 4/1). For knockdown studies, lentiviral particles encoding for a shRNA of hCGI-58 (Sigma-Aldrich, France) or a scramble control (nontarget) were exposed for 24 h to the culture at the beginning of the differentiation. Infection efficiency was assessed using a TurboGFP control. Oleate was preferred to palmitate for lipid loading of the cells, to favor TAG synthesis and to avoid the intrinsic lipotoxic effect of palmitate (15, 16). No adenovirus-induced cellular toxicity was observed as determined by chemiluminescent quantification of adenylate kinase activity (ToxiLight, Lonza Group Ltd, Basel, Switzerland).

Determination of FA metabolism

Cells were pulsed overnight for 18 h with [1-^{14}C]oleate (1 μCi/ml; PerkinElmer, Boston, MA) and cold oleate (80 μM), to prelabel the endogenous TAG pool. Oleate was coupled to FA-free BSA in a molar ratio of 5:1. Some cells were harvested at the end of the pulse for the 0 time point. Following the pulse, myotubes were chased for 1, 3, and 6 h in DMEM containing 0.1 mM glucose, 0.5% FA-free BSA, and 10 μM triacsin C to block FA recycling into the TAG pool as described elsewhere (17, 18). TAG-derived FA oxidation (endogenous FA oxidation) measured by the sum of $^{14}CO_2$ and ^{14}C-ASM (acid soluble metabolites) was measured in absence of triacsin C as previously described (14). Myotubes were harvested in 0.2 ml SDS 0.1% at the end of the pulse and of the chase period to determine oleate incorporation into TAG, DAG, MAG (monoacylglycerol), FA, and protein content. The lipid extract was separated by TLC using heptane-isopropylether-acetic acid (60:40:4, v/v/v) as developing solvent. All assays were performed in duplicates, and data were normalized to cell protein content.

Determination of glucose metabolism

Cells were preincubated with a glucose- and serum-free medium for 90 min then exposed to DMEM supplemented with D[U-^{14}C]glucose (1 μCi/ml; PerkinElmer, Boston, MA) in the presence or absence of 100 nM insulin (Humulin®) for 3 h. Following incubation, glucose oxidation, and glycogen synthesis were determined as previously described (12).

Western blot analysis

Muscle tissues and cell extracts were homogenized in a buffer containing 50 mM HEPES, pH 7.4, 2 mM EDTA, 150 mM NaCl, 30 mM NaPPO4, 10 mM NaF, 1% Triton X-100, 10 μl/ml protease inhibitor (Sigma-Aldrich), 10 μl/ml phosphatase I inhibitor (Sigma-Aldrich), 10 μl/ml phosphatase II inhibitor (Sigma-Aldrich), and 1.5 mg/ml benzamidine HCl. Tissue homogenates were centrifuged for 25 min at 15,000 *g* and supernatants were stored at −80°C. Solubilized proteins from muscle tissue and myotubes were run on a 4-12% SDS-PAGE (Biorad), transferred onto nitrocellulose membrane (Hybond ECL, Amersham Biosciences), and incubated with the primary antibody CGI-58, (Abnova Corp., Tapei, Taiwan), PDK4 (Abnova), pAMPK, and AMPK (Cell Signaling Technology Inc., Beverly, MA). Subsequently, immunoreactive proteins were determined by enhanced chemiluminescence

reagent (GE Healthcare) and visualized by exposure to Hyperfilm ECL (GE Healthcare). GAPDH (Cell Signaling Technology) served as an internal control.

Lipase activity assays

Triacylglycerol hydrolase (TAGH) activity was measured on tissue and cell lysates as previously described (19). Briefly, tissue and cell lysates were extracted in a lysis buffer containing 0.25 M sucrose, 1 mM EDTA, 1 mM DTT, 20 μg/ml leupeptin, and 2 μg/ml antipain. [9, 10-^{3}H(N)]triolein and cold triolein were emulsified with phospholipids by sonication. The emulsion was incubated for 30 min at 37°C in the presence of 10–40 μg of total protein from tissue and cell lysates. After incubation, the reaction was terminated by adding 3.25 ml of methanol-chloroform-heptane (10:9:7) and 1 ml of 0.1 M potassium carbonate, 0.1 M boric acid, (pH 10.5). After centrifugation (800 *g*, 15 min), 0.5 ml of the upper phase was collected for scintillation counting. Stimulation of ATGL was achieved by coincubation of tissue lysates with 1.6 μg of recombinant human CGI-58 (rhCGI-58) (Abnova). The data are expressed in nmol of oleic acid released · min^{-1} · mg^{-1} of protein.

TAG determination by GC-MS

Total lipids were extracted from frozen muscle tissue samples and from myotubes harvested in water containing 0.25 ml 0.1% SDS. Lipids were extracted using the method of Folch et al. (20). The extracts were filtered and lipids recovered in the chloroform phase. TAGs were isolated using TLC on Silica Gel 60 A plates developed in petroleum ether- ethyl ether- acetic acid (80:20:1) and visualized by rhodamine 6G. The TAG band was scraped from the plate and methylated using BF_3 /methanol as described by Morrison and Smith (21). The methylated fatty acids were extracted with hexane and analyzed by GC using an HP 5890 gas chromatograph equipped with flame ionization detectors, an HP 3365 Chemstation, and a capillary column (SP2380, 0.25 mm × 30 m, 0.25 μm film, Supelco, Bellefonte, PA). Helium was used as a carrier gas. The oven temperature was programmed from 160°C to 230°C at 4°C/min. Fatty acid methyl esters were identified by comparing the retention times to those of known standards. Inclusion of the internal standards, 20:1 (trieicosenoin) and 17:0 (diheptadecanoin), permits quantitation of the amount of TAG in the sample.

Determination of mitochondrial content

For quantification of mitochondrial content, we measured the mitochondrial (mt) to nuclear DNA ratio as previously described (22). The sequences for the primer sets used for determination of mtDNA for NADH dehydrogenase subunit 1 (ND1) were forward primer CCCTAAAACCCGCCACATCT, reverse primer GAGCGATGGTGAGAGCTAAGGT, and of nuclear DNA for lipoprotein lipase (LPL) were forward primer CGAGTCGTCTTTCTCCTGATGAT, reverse primer TTCTGGATTCCAATGCTTCGA. We also determined mitochondrial mass in myotubes using Mitotracker Green FM (Invitrogen, Carlsbad, CA), which stains mitochondrial matrix protein irrespective of the membrane potential and thus provides an accurate assessment of mitochondrial mass. Similarly, we measured mitochondrial membrane potential using a Mitotracker Red CMX-Ros (Invitrogen), which stains mitochondria according to their membrane potential. Briefly, cells were washed with 1× PBS and incubated at 37°C for 30 min with 100 nM of each Mitotracker. Cells were then harvested using trypsin/EDTA and resuspended in 1× PBS. Fluorescence intensity was measured on a fluorometer and values corrected for total protein.

Real-time qRT-PCR

Total RNA from cultured myotubes was isolated in RNeasy Lysis Buffer + β-mercaptoethanol reagent (Qiagen GmbH, Hilden, Germany). The quantity of the RNA was determined on a Nanodrop ND-1000 (Thermo Scientific, Rockford, IL, USA). Reverse-transcriptase PCR was performed on a GeneAmp PCR System 9700 using the Multiscribe Reverse Transcriptase method (Applied Biosystems, Foster City, CA). Real-time quantitative PCR (qPCR) was performed to determine cDNA content. All primers were bought from Applied Biosystems. Primers used were: 18S (Taqman assay ID: Hs99999901_s1), PDK4 (Hs01037712_m1), GLUT4 (Hs00168966_m1), HSL (Hs00193510_m1), MYH1 (Hs00428600_m1). qPCR was then performed on a StepOnePLus real-time PCR system (Applied Biosystems). For each primer, a standard curve was made prior to mRNA quantification to assess the optimal total cDNA quantity. All expression data were normalized by the $2^{(\Delta\Delta Ct)}$ method using 18S as internal control.

Statistical analyses

All statistical analyses were performed using GraphPad Prism 5.0 for Windows (GraphPad Software Inc., San Diego, CA). One-way ANOVA followed by Tukey's posthoc tests were applied in time-course studies and paired Student's *t*-tests were performed to determine differences between treatments. Two-way ANOVA and Bonferroni's posthoc tests were used when appropriate. All values in figures and tables are presented as mean ± SEM. Statistical significance was set at $p < 0.05$.

RESULTS

CGI-58 expression and triglyceride hydrolase activity in different muscle types

We examined CGI-58 protein expression by western blot in various types of muscle in mice. The data show that CGI-58 is quantitatively more abundant in oxidative muscles. The expression pattern is as follow: heart>*soleus*> quadriceps>white *gastrocnemius* (**Fig. 1A**). This pattern was somehow consistent with the TAGH activity pattern observed in these muscles. TAGH activity was highest in heart and *soleus* when compared with quadriceps and *gastrocnemius* (Fig. 1B). TAGH activity was about 5 times lower in *soleus* and heart when compared with epididymal white adipose tissue ($P < 0.001$). We next investigated the ability of human recombinant CGI-58 (rhCGI-58) to induce TAGH activity (TAGH) in human adipose tissue (AT) and skeletal muscle (SkM) lysates (Fig. 1C). Exogenous rhCGI-58 almost doubled TAGH activity in hSkM (1.8-fold, $P = 0.004$) but did not induce TAGH activity in hAT. The validity of the system was checked by the ability of rhCGI-58 to induce TAGH activity in COS7 cell lysates stably overexpressing hATGL (8-fold, $P < 0.01$).

Overexpression of CGI-58 in human primary myotubes

Adenovirus-mediated overexpression of hCGI-58 led to a 2-fold increase in CGI-58 protein content in 5 day differentiated human myotubes ($P < 0.05$) (**Fig. 2A**). The adenovirus infection efficiency averaged 50% (GFP-positive myotubes to DAPI ratio) and was comparable between control (Ad-GFP) and Ad-CGI-58 (data not shown). Surprisingly, CGI-58 overexpression was paralleled by a down-regulation of ATGL protein (-34%, $P < 0.05$) (Fig. 2B). As expected, CGI-58 overexpression increased TAGH activity (2-fold, $P < 0.05$) (Fig. 2C) and reduced total TAG content (−51%, $P < 0.01$) (Fig. 2D).

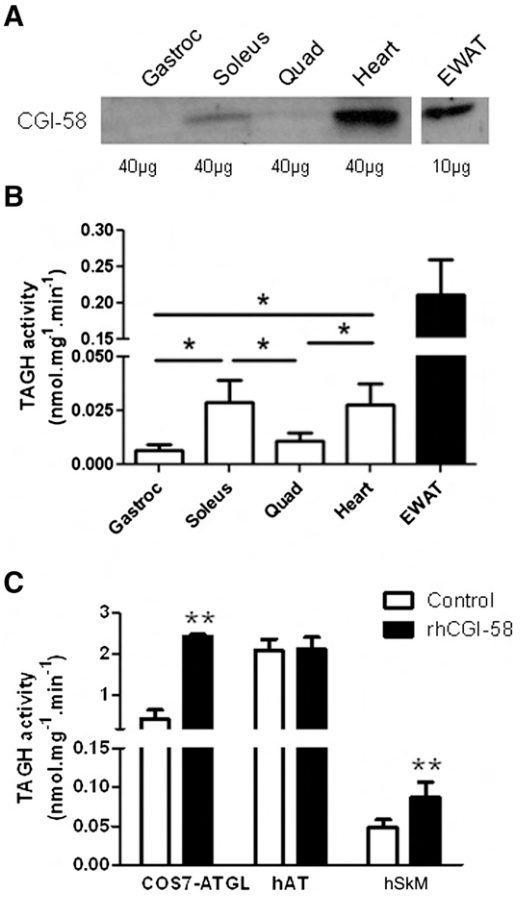

Fig. 1. Distribution and function of CGI-58 in skeletal muscle. A: Representative blot of CGI-58 protein expression in different types of muscle and EWAT [whole *gastrocnemius* (gastroc), *soleus*, quadriceps (quad) and heart, as well as epididimal white adipose tissue] in 20-week-old mice. Forty micrograms of total protein were loaded for the different muscles and 10 µg for EWAT (n = 3). B: Triacylglycerol hydrolase activity (TAGH) was measured in different types of muscle and EWAT in 20-week-old mice as previously (n = 6), One-way ANOVA * $P < 0.05$. C: TAGH was measured in human adipose tissue (hAT) and skeletal muscle (hSkM) in absence (control) or presence of recombinant human CGI-58 (rhCGI-58) (n = 6). A positive control experiment was performed in presence of COS7 cell extracts overexpressing human ATGL (COS7/ATGL), paired Student's *t*-test ** $P < 0.01$ when compared with control.

Impact of CGI-58 overexpression on lipolysis and FA oxidation

We performed pulse-chase experiments to evaluate the role of CGI-58 in the regulation of intracellular TAG hydrolysis and FA metabolism. Chase experiments were performed in the presence of 10 µM of triacsin C, which blocks 99.4% of TAG and 95.5% of DAG synthesis during 24 h loading with radiolabeled oleate in human primary myotubes (supplementary Fig. I). Endogenous TAGs were prelabeled with [1-^{14}C]oleate and subsequently, TAG hydrolysis and FA release into the culture medium were determined in GFP and CGI-58 overexpressing myotubes at different time points (**Fig. 3**). TAG depletion was increased at different time points in CGI-58 overexpressing myotubes compared with GFP controls (Fig. 3A). Consistent with an increased TAG hydrolysis, FA release into the medium was higher in CGI-58 overexpressing myotubes during the chase period (Fig. 3B). Of interest, CGI-58 overexpression increased the oxidation of endogenous FA originating from the TAG pool (2.2-fold, $P < 0.05$) (Fig. 3C). In line with an increased TAG hydrolysis, radiolabeled oleate incorporation into DAG, MAG, and intracellular FA was strongly upregulated in CGI-58 overexpressing myotubes (supplementary Fig. II A–C). Thus, because CGI-58 was reported to display a significant lysophosphaditic acid acyltransferase (LPAAT) activity (23, 24), we could show a robust increase in phospholipid synthesis in CGI-58 overexpressing myotubes (supplementary Fig. II D).

Impact of CGI-58 knockdown on lipolysis and FA oxidation

We used a lentiviral vector to knock down CGI-58 in differentiated myotubes and achieved 89% reduction of CGI-58 protein expression ($P < 0.01$) (**Fig. 4A**). Interestingly, CGI-58 knockdown induced important changes in neutral lipid dynamics and FA metabolism. CGI-58 knockdown robustly reduced TAG hydrolysis and protected endogenous TAG pools from lipolysis when compared with control (Fig. 4B). Consistently, FA release into the culture medium was significantly reduced (Fig. 4C), as well as the appearance of DAG, MAG, and intracellular FA consecutive to lipolysis (supplementary Fig. III A–C). The changes in FA release were paralleled by a robust drop in intracellular TAG-derived FA oxidation (−77%, $P < 0.001$) reflecting endogenous FA oxidation (Fig. 4D). As previously, phospholipid synthesis was slightly reduced (supplementary Fig. III D), suggesting that CGI-58 contributes to some extent to total skeletal muscle LPAAT activity.

Effects of CGI-58 knockdown on mitochondria

In light of the robust suppression of TAG-derived FA oxidation beyond the decrease of FA release from lipolysis, we sought to investigate whether modulations of CGI-58 expression alter mitochondrial activity. We first examined mitochondrial content using Mitotracker green, which stains mitochondrial matrix protein independently of the mitochondrial membrane potential and mainly reflects mitochondrial mass. We could show that mitochondrial mass is similar between control and siCGI-58 myotubes (**Fig. 5A**) and confirmed these results by the measure of the mitochondrial-to-nuclear DNA ratio (1.516 ± 0.008 vs. 1.540 ± 0.009 A.U. for control and siCGI-58 respectively, NS). Interestingly, mitochondrial membrane potential measured by fluorescence staining was reduced by 27% ($P = 0.016$) in siCGI-58 myotubes (Fig. 5B). This drop in membrane potential was paralleled by a 70% increase of the cellular energy-sensor AMPK phosphorylation state (pAMPK to AMPK ratio) despite a decrease in total AMPK protein content in siCGI-58 myotubes (−50%, $P < 0.05$) (Fig. 5C).

Effects of CGI-58 knockdown on glucose metabolism

We next evaluated the consequences of CGI-58 knockdown on glucose metabolism. Importantly, we observed a higher glucose oxidation in siCGI-58 myotubes (**Fig. 6A**), paralleled by an increased glucose incorporation into glycogen in the basal state and upon insulin stimulation (Fig. 6B).

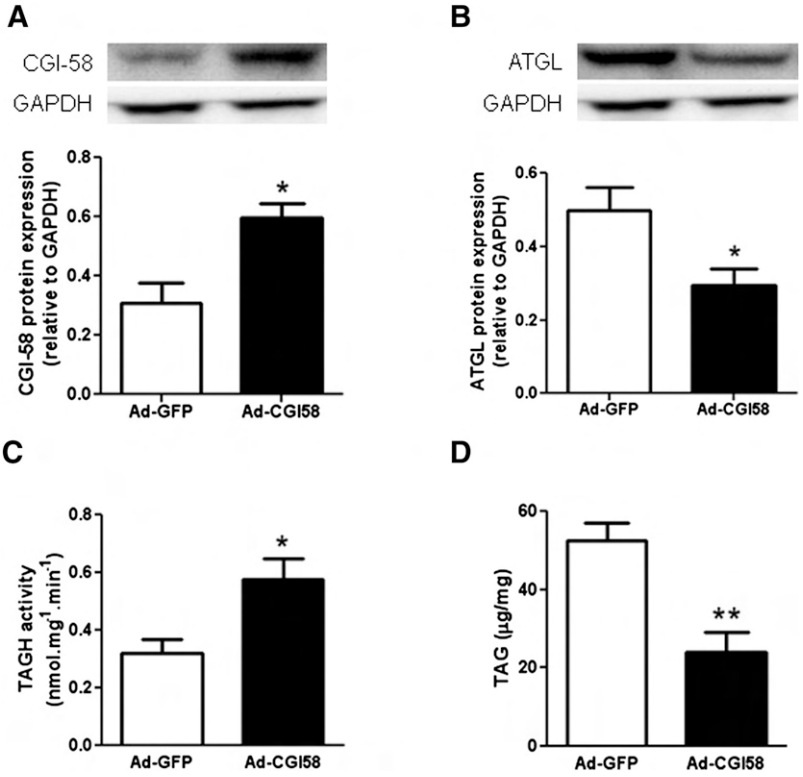

Fig. 2. CGI-58 overexpression promotes TAG breakdown. A: CGI-58 and (B) ATGL protein content were measured in control myotubes (Ad-GFP) and myotubes overexpressing CGI-58 (Ad-CGI58) (n = 5). Insets are showing representative blots and loading control of each protein, * $P < 0.05$ versus Ad-GFP. C: TAGH activity and (D) total TAG content were measured in control myotubes (Ad-GFP) and myotubes overexpressing CGI-58 (Ad-CGI58) (n = 5), paired Student's *t*-test * $P < 0.05$, ** $P < 0.01$ versus Ad-GFP.

To gain insight into the mechanism contributing to the substrate switch, we measured pyruvate dehydrogenase kinase 4 (PDK4) expression. PDK4 is a mitochondrial protein that inhibits the pyruvate dehydrogenase complex by phosphorylating one of its subunits, thereby inhibiting glucose oxidation (25). The data show that PDK4 protein expression was very significantly reduced by 41% in siCGI-58 myotubes (Fig. 6C). The downregulation of PDK4

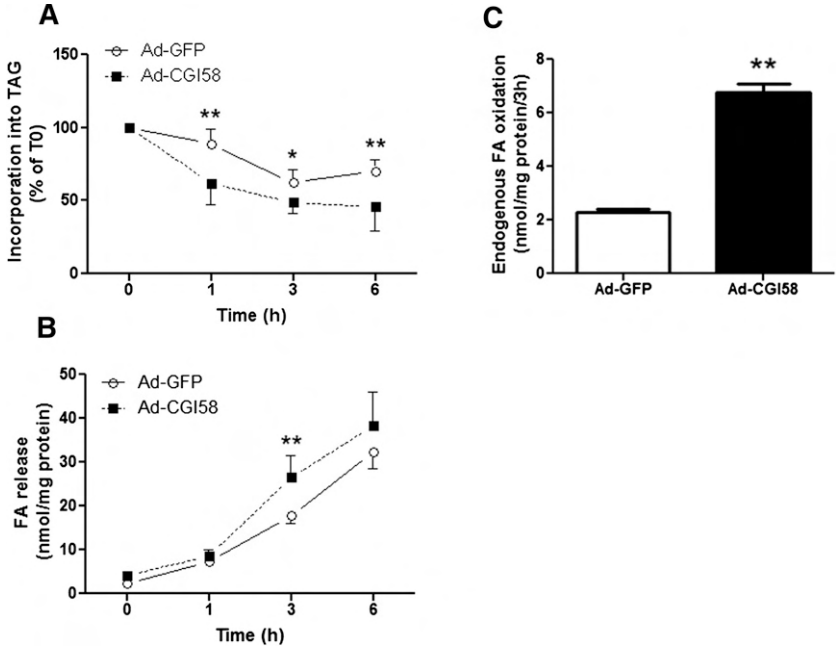

Fig. 3. CGI-58 increases TAG-derived FA release and oxidation. Pulse-chase experiments were performed to determine the time-course over 6 h of (A) TAG hydrolysis and (B) FA release into the culture medium, in control myotubes (Ad-GFP) and myotubes overexpressing CGI-58 (Ad-CGI58) (n = 6). TAG content was expressed as a function of the value at the 0 time point (% of T0). All parameters were measured at the end of the Pulse (0 time point) and during the Chase period (1, 3, and 6 h time points). Two-way ANOVA * $P < 0.05$, ** $P < 0.01$ when compared with Ad-GFP. C: Endogenous oxidation, i.e., TAG-derived FA oxidation was measured in absence of triacsin C after 3 h of Chase in the same conditions. Paired Student's *t*-test ** $P < 0.01$ when compared with Ad-GFP.

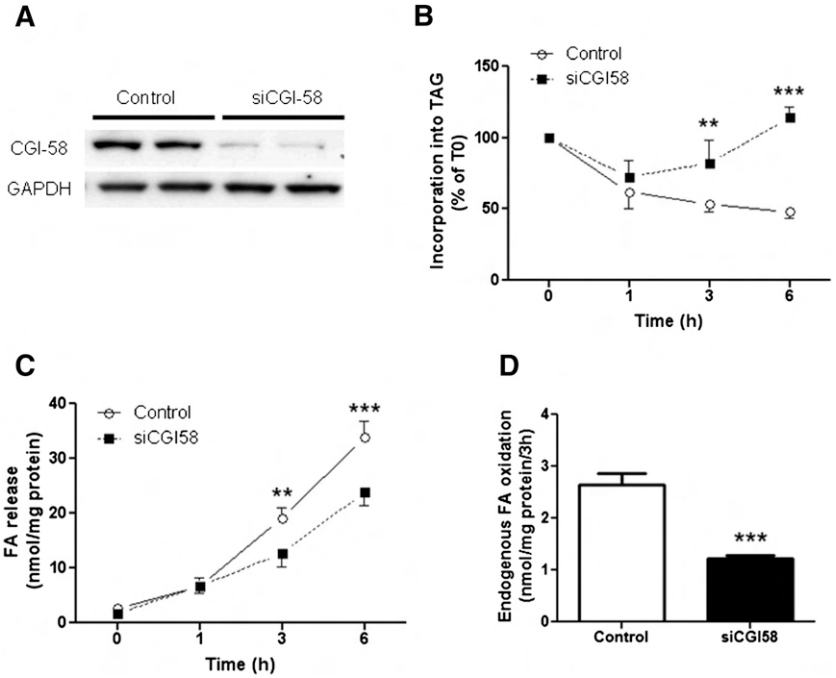

Fig. 4. CGI-58 silencing reduces lipolysis and TAG-derived FA oxidation. A: Representative blot of CGI-58 protein expression in control myotubes and myotubes knocked down for CGI-58 (siCGI58) (n = 2 lane per condition). We next measured by pulse-chase the time-course over 6 h of (B) TAG hydrolysis, (C) FA release into the culture medium in control myotubes and myotubes knocked down for CGI-58 (siCGI58) (n = 6). All parameters were measured at the end of the Pulse (0 time point) and during the Chase period (1, 3, and 6 h time points). TAG content was expressed as a function of the value at the 0 time point (% of T0). Two-way ANOVA ** $P < 0.01$, *** $P < 0.0001$ when compared with control. D: Endogenous oxidation, i.e., TAG-derived FA oxidation, was measured in absence of triacsin C after 3 h of Chase in the same conditions. Paired Student's *t*-test *** $P < 0.0001$ when compared with control.

was also observed at the mRNA level reflecting transcriptional modulations of the gene.

Modulations of CGI-58 and PPARδ target-genes

Because PDK4 has been described as a PPARδ-target gene (26), we examined the level of expression of several known PPARδ-target genes among other genes in skeletal muscle. We found that CGI-58 knockdown was associated with the downregulation of known PPARδ-target genes such as PDK4, GLUT4, HSL, and MYH1 gene expression (data not shown). Importantly, we validated that PDK4 gene expression was induced by a selective PPARδ agonist (GW0742) and efficiently blocked by a selective PPARδ antagonist (GSK0660) (**Fig. 7A**). We further show that PDK4 gene expression is strongly induced by oleate (Fig. 7B). This induction was almost completely abolished in presence of the selective PPARδ antagonist GSK0660. Thus, we also show that a selective PPARα agonist (GW7647) failed to induce PDK4 gene expression in human skeletal muscle cells. Interestingly, we next showed that CGI-58 overexpression was accompanied by an upregulation of PDK4 gene expression that was totally blunted by the PPARδ antagonist (Fig. 7C). Reciprocally, we observed a significant suppression of PDK4 mRNA level in myotubes invalidated for CGI-58 that was totally rescued by the selective PPARδ agonist (Fig. 7D).

DISCUSSION

Obesity and type 2 diabetes are associated with ectopic lipid deposition in insulin-sensitive tissue such as skeletal muscle (27, 28). The understanding of the regulation of IMTG metabolism has gained much interest because IMTG content inversely correlates with peripheral insulin sensitivity (19, 29–31). In this study, we identify that the ATGL coactivator CGI-58 has a master regulator of human skeletal muscle TAG metabolism. We first show that CGI-58 is mostly expressed in oxidative muscles (*soleus* and heart) where it coactivates ATGL to increase TAGH activity. Importantly, we demonstrate that CGI-58 is a limiting factor of skeletal muscle TAG metabolism and IMTG-derived FA oxidation. Thus, we also show that CGI-58 modulates skeletal muscle gene expression by regulating the availability of PPARδ FA ligands.

We identified a preferential expression of CGI-58 in oxidative muscle (heart and *soleus*) when compared with more glycolytic muscle (quadriceps and *gastrocnemius*). The highest expression was found in the heart. These findings are consistent with the strong TAGH activity predominantly observed in oxidative muscles in agreement with earlier studies (32). This result implies that CGI-58 may be mainly expressed in type I oxidative fibers as recently noted for ATGL (11). We further demonstrate that rhCGI-58

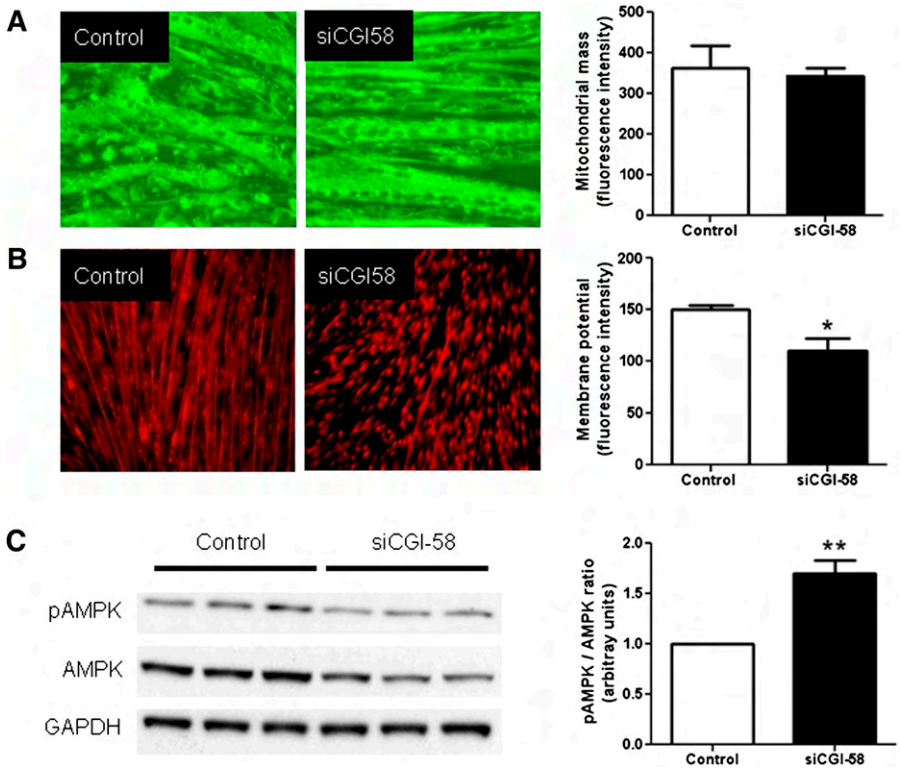

Fig. 5. CGI-58 silencing induces a cellular energy deficit. A: Mitochondrial mass was determined in control myotubes (left panel) and myotubes knocked down for CGI-58 (siCGI58) (middle panel) using the Mitotracker Green FM (20×). Quantitative bar graph of the fluorescence intensity signal (right panel) (n = 4). B: Mitochondrial membrane potential was determined in control myotubes (left panel) and myotubes knocked down for CGI-58 (siCGI58) (middle panel) using the Mitotracker Red CMX-Ros (10×). Quantitative bar graph of the fluorescence intensity signal (right panel) (n = 4). C: Representative blot (left panel) and quantitative bar graph (right panel) of phosphoAMPK to AMPK ratio in control myotubes (left panel) and myotubes knocked down for CGI-58 (siCGI58) (n = 5). Paired Student's *t*-test * $P < 0.05$, ** $P < 0.01$ versus control.

induces TAGH activity in human *vastus lateralis* muscle lysates, highlighting the limiting role of CGI-58 in this tissue. These data are in agreement with other reports (33). Interestingly, rhCGI-58 failed to induce TAGH in human subcutaneous adipose tissue and this suggests that ATGL may operate nearly maximally in human adipose tissue. This finding is consistent with a recent report showing that adipose-specific overexpression of CGI-58 fails to induce lipolysis in mice and suggests that CGI-58 is not limiting for adipose tissue lipolysis (34). ATGL and CGI-58 may interact at the surface of intramyocellular lipid droplets with lipid coat protein of the perilipin family to provide FA substrates for mitochondrial β-oxidation. Indeed, it was recently shown by Granneman et al. (35) that both CGI-58 and ATGL interacts with perilipin 5 (PLIN5, also called OXPAT or LSDP5) at the surface of the lipid droplet. The authors demonstrated that ATGL activity is strongly deficient in cells expressing PLIN5 mutant proteins able to bind CGI-58 but unable to bind ATGL (35). Thus PLIN5 was shown to be abundantly expressed in oxidative tissues such as skeletal muscle (36). Future studies will be required to unravel the molecular mechanisms regulating the interaction between ATGL, CGI-58, and PLIN5 in the control of lipolysis in skeletal muscle.

To gain further insight into the role of CGI-58 in skeletal muscle, we overexpressed CGI-58 in human primary myotubes. As expected, overexpression of CGI-58 induced TAGH activity and lipolysis as reflected by a reduced TAG content. Elevated CGI-58 protein expression induced a downregulation of ATGL protein expression. This observation suggests that CGI-58 and ATGL may be reciprocally regulated in skeletal muscle and possibly other tissues. Similar findings have been observed in a human white adipocyte cell model (37). This regulation could take place at the transcriptional level because CGI-58 knockdown was accompanied by a significant upregulation of ATGL gene expression. The transcription factor coordinating CGI-58 and ATGL expression is currently unknown. Consistent with an increased lipolytic rate, CGI-58 overexpression reduced the incorporation of oleate into TAG and increased FA release. CGI-58 specifically promoted the oxidation of IMTG-derived FA through increased intracellular FA release. Together, these data suggest that CGI-58-mediated IMTG hydrolysis provides FA substrates for mitochondrial β-oxidation. Conversely, CGI-58 knockdown increased the incorporation of the tracer into TAG reflecting a profound downregulation of TAG hydrolysis and lipolytic flux. Consistently, the reduced lipolytic rate was reflected by a reduced

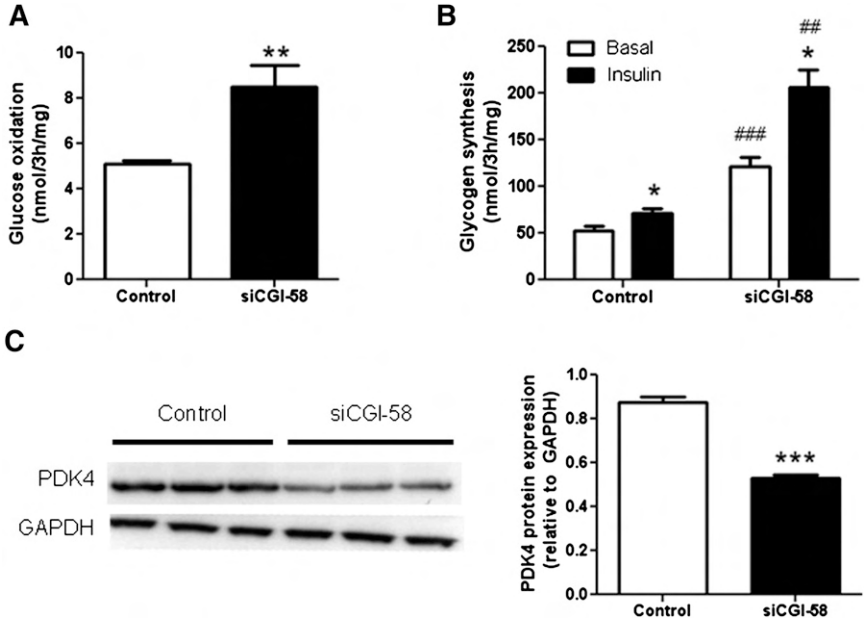

Fig. 6. CGI-58 silencing favors glucose metabolism. A: Basal glucose oxidation was measured in control myotubes and myotubes knocked down for CGI-58 (siCGI58). B: Glycogen synthesis was measured in absence (open bars) or presence (black bars) of 100 nM insulin. * $P < 0.05$, ** $P < 0.01$ versus basal; $^{\#\#}$ $P < 0.01$, $^{\#\#\#}$ $P < 0.001$ versus respective control (n = 6). C: Representative blot (left panel) and quantitative bar graph (right panel) of PDK4 protein in control myotubes and myotubes knocked down for CGI-58 (siCGI58) (n = 6), paired Student's *t*-test *** $P < 0.001$ versus control.

incorporation of the tracer into downstream lipolytic products such as DAG, MAG, and FA. Importantly, CGI-58 knockdown was associated with a robust downregulation of IMTG-derived FA oxidation. This effect is partly determined by the reduced intracellular FA release. Collectively, these data point toward a major limiting role of CGI-58 in the regulation of IMTG lipolysis and FA oxidation in human skeletal muscle. The data suggest that although ATGL is an important effector enzyme of lipolysis in skeletal muscle, ATGL cannot operate maximally without its coactivator CGI-58. These data also support the concept that increasing skeletal muscle lipolysis may favor mitochondrial FA oxidation.

Because the suppression of FA oxidation consecutive to CGI-58 knockdown exceeded the suppression of FA release, we sought to investigate whether CGI-58 deficiency altered mitochondrial activity. We could show that CGI-58 deficiency in myotubes reduced mitochondrial membrane potential independently of measurable changes in mitochondrial mass and DNA content. This result is consistent with a robust drop in mitochondrial FA oxidation and apparently not entirely compensated by other energy sources. This observed energy deficit induced AMPK activation, a cellular energy-sensor sensitive to the drop of ADP/ATP ratio (38). Interestingly, CGI-58 deficiency enhanced glucose nonoxidative and oxidative metabolism. The increase in basal glycogen synthesis may reflect a higher basal glucose transport induced by AMPK. Thus, consistent with a reduced incorporation into DAG, insulin-mediated glycogen synthesis tended to increase in siCGI-58 myotubes. These data are also in agreement with a recent study describing a potentially detrimental role of ATGL activity in human skeletal muscle (12). The rise in glucose oxidation might be the consequence of a classical substrate switch according to the Randle cycle (39). Moreover, this event was associated with a remarkable suppression of PDK4 gene and protein expression. PDK4 is a mitochondrial protein inhibiting glucose oxidation in response to elevated plasma FA availability as observed during fasting or high-fat feeding (40). Thus, the downregulation of PDK4 promotes glucose oxidation. Conversely, CGI-58 overexpression induced FA release, FA oxidation, and PDK4 expression. PDK4 has been reported as a classical PPARδ-target gene (26). We therefore hypothesized that CGI-58-mediated lipolysis provides FA ligands for activating PPARδ in muscle cells. Pioneer studies had shown the ability of PPAR to bind FA such as oleate and arachidonate (41). Thus, this hypothesis is in agreement with a recent study (42), and together they support the view that elevated TAG hydrolysis and the consequential release of FA modulates PPAR transcriptional activity. To test this hypothesis, we first showed that PDK4 expression was highly induced by a selective PPARδ agonist and by oleate in our cell model. This robust induction was completely abolished by a selective PPARδ antagonist. We showed that PDK4 expression can be fully normalized in presence of the PPARδ selective agonist GW0742 during CGI-58 silencing. Additionally, we further demonstrated that the induction of PDK4 by CGI-58 overexpression was totally suppressed by a selective PPARδ antagonist. Together, the data indicate that changes of PDK4 expression in response to changes in CGI-58-mediated lipolysis and FA availability are mediated by PPARδ in skeletal muscle.

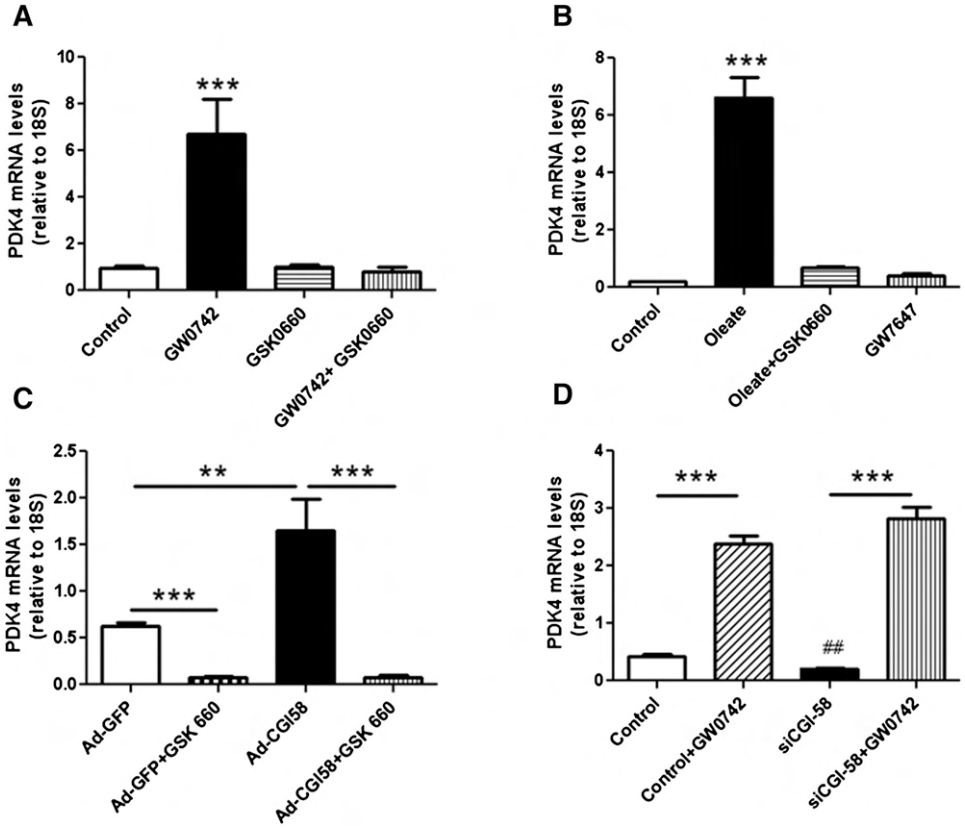

Fig. 7. CGI-58-mediated lipolysis specifically modulates PPARδ-target gene expression. A: PDK4 relative gene expression in myotubes treated for 24 h in absence (control) or presence of the selective PPARδ agonist GW0742 1 nM and the selective PPARδ antagonist GSK0660 500 nM (n = 6); One-way ANOVA *** $P < 0.001$ versus control. B: PDK4 relative gene expression in myotubes treated for 24 h in absence (control) or presence of 500 µM of oleate alone or in combination with the selective PPARδ antagonist GSK0660 2 µM, and with the selective PPARα agonist GW7647 100 nM (n = 8); One-way ANOVA ***$P < 0.001$ versus control. C: PDK4 relative gene expression in control myotubes (Ad-GFP) or overexpressing CGI-58 (Ad-CGI58) in absence or presence of the selective PPARδ antagonist GSK0660 500 nM; One-way ANOVA ** $P < 0.01$, *** $P < 0.001$ (n = 6). D: PDK4 relative gene expression in control myotubes (Ad-GFP) and myotubes knocked down for CGI-58 (siCGI58) in absence or presence of the selective PPARδ agonist GW0742 1 nM (n = 6), One-way ANOVA, *** $P < 0.001$ versus GW0742, $^{\#\#}$ $P < 0.01$ versus control.

In summary, our data show that CGI-58 is a limiting factor in the regulation of skeletal muscle TAG metabolism and substrate oxidation. Our results are consistent with the view that CGI-58-mediated lipolysis can modulate PPARδ transcriptional activity and the expression of the metabolic switch PDK4. Future studies using animal models with muscle-specific modulations of CGI-58 may help to unravel the specific role of CGI-58 in the regulation of skeletal muscle and whole-body energy metabolism in vivo.

The authors are very grateful to Shantele Thomas for excellent technical help.

REFERENCES

1. Haemmerle, G., A. Lass, R. Zimmermann, G. Gorkiewicz, C. Meyer, J. Rozman, G. Heldmaier, R. Maier, C. Theussl, S. Eder, et al. 2006. Defective lipolysis and altered energy metabolism in mice lacking adipose triglyceride lipase. *Science.* **312:** 734–737.
2. Zimmermann, R., J. G. Strauss, G. Haemmerle, G. Schoiswohl, R. Birner-Gruenberger, M. Riederer, A. Lass, G. Neuberger, F. Eisenhaber, A. Hermetter, et al. 2004. Fat mobilization in adipose tissue is promoted by adipose triglyceride lipase. *Science.* **306:** 1383–1386.
3. Lass, A., R. Zimmermann, G. Haemmerle, M. Riederer, G. Schoiswohl, M. Schweiger, P. Kienesberger, J. G. Strauss, G. Gorkiewicz, and R. Zechner. 2006. Adipose triglyceride lipase-mediated lipolysis of cellular fat stores is activated by CGI-58 and defective in Chanarin-Dorfman Syndrome. *Cell Metab.* **3:** 309–319.
4. Lefevre, C., F. Jobard, F. Caux, B. Bouadjar, A. Karaduman, R. Heilig, H. Lakhdar, A. Wollenberg, J. L. Verret, J. Weissenbach, et al. 2001. Mutations in CGI-58, the gene encoding a new protein of the esterase/lipase/thioesterase subfamily, in Chanarin-Dorfman syndrome. *Am. J. Hum. Genet.* **69:** 1002–1012.
5. Radner, F. P., S. Grond, G. Haemmerle, A. Lass, and R. Zechner. 2011. Fat in the skin: triacylglycerol metabolism in keratinocytes and its role in the development of neutral lipid storage disease. *Dermatoendocrinol.* **3:** 77–83.
6. Granneman, J. G., H. P. Moore, R. L. Granneman, A. S. Greenberg, M. S. Obin, and Z. Zhu. 2007. Analysis of lipolytic protein trafficking and interactions in adipocytes. *J. Biol. Chem.* **282:** 5726–5735.
7. Watt, M. J., G. J. Heigenhauser, M. O'Neill, and L. L. Spriet. 2003. Hormone-sensitive lipase activity and fatty acyl-CoA content in human skeletal muscle during prolonged exercise. *J. Appl. Physiol.* **95:** 314–321.
8. Watt, M. J., and L. L. Spriet. 2004. Regulation and role of hormone-sensitive lipase activity in human skeletal muscle. *Proc. Nutr. Soc.* **63:** 315–322.
9. Haemmerle, G., R. Zimmermann, M. Hayn, C. Theussl, G. Waeg, E. Wagner, W. Sattler, T. M. Magin, E. F. Wagner, and R. Zechner.

2002. Hormone-sensitive lipase deficiency in mice causes diglyceride accumulation in adipose tissue, muscle, and testis. *J. Biol. Chem.* **277:** 4806–4815.
10. Mulder, H., M. Sorhede-Winzell, J. A. Contreras, M. Fex, K. Strom, T. Ploug, H. Galbo, P. Arner, C. Lundberg, F. Sundler, et al. 2003. Hormone-sensitive lipase null mice exhibit signs of impaired insulin sensitivity whereas insulin secretion is intact. *J. Biol. Chem.* **278:** 36380–36388.
11. Jocken, J. W., E. Smit, G. H. Goossens, Y. P. Essers, M. A. van Baak, M. Mensink, W. H. Saris, and E. E. Blaak. 2008. Adipose triglyceride lipase (ATGL) expression in human skeletal muscle is type I (oxidative) fiber specific. *Histochem. Cell Biol.* **129:** 535–538.
12. Badin, P. M., K. Louche, A. Mairal, G. Liebisch, G. Schmitz, A. C. Rustan, S. R. Smith, D. Langin, and C. Moro. 2011. Altered skeletal muscle lipase expression and activity contribute to insulin resistance in humans. *Diabetes.* **60:** 1734–1742.
13. Bergstrom, J. 1975. Percutaneous needle biopsy of skeletal muscle in physiological and clinical research. *Scand. J. Clin. Lab. Invest.* **35:** 609–616.
14. Ukropcova, B., M. McNeil, O. Sereda, L. de Jonge, H. Xie, G. A. Bray, and S. R. Smith. 2005. Dynamic changes in fat oxidation in human primary myocytes mirror metabolic characteristics of the donor. *J. Clin. Invest.* **115:** 1934–1941.
15. Listenberger, L. L., X. Han, S. E. Lewis, S. Cases, R. V. Farese, Jr., D. S. Ory, and J. E. Schaffer. 2003. Triglyceride accumulation protects against fatty acid-induced lipotoxicity. *Proc. Natl. Acad. Sci. USA.* **100:** 3077–3082.
16. Turpin, S. M., G. I. Lancaster, I. Darby, M. A. Febbraio, and M. J. Watt. 2006. Apoptosis in skeletal muscle myotubes is induced by ceramides and is positively related to insulin resistance. *Am. J. Physiol. Endocrinol. Metab.* **291:** E1341–E1350.
17. Brasaemle, D. L., B. Rubin, I. A. Harten, J. Gruia-Gray, A. R. Kimmel, and C. Londos. 2000. Perilipin A increases triacylglycerol storage by decreasing the rate of triacylglycerol hydrolysis. *J. Biol. Chem.* **275:** 38486–38493.
18. Igal, R. A., and R. A. Coleman. 1996. Acylglycerol recycling from triacylglycerol to phospholipid, not lipase activity, is defective in neutral lipid storage disease fibroblasts. *J. Biol. Chem.* **271:** 16644–16651.
19. Moro, C., J. E. Galgani, L. Luu, M. Pasarica, A. Mairal, S. Bajpeyi, G. Schmitz, D. Langin, G. Liebisch, and S. R. Smith. 2009. Influence of gender, obesity, and muscle lipase activity on intramyocellular lipids in sedentary individuals. *J. Clin. Endocrinol. Metab.* **94:** 3440–3447.
20. Folch, J., M. Lees, and G. H. Sloane Stanley. 1957. A simple method for the isolation and purification of total lipides from animal tissues. *J. Biol. Chem.* **226:** 497–509.
21. Morrison, W. R., and L. M. Smith. 1964. Preparation of fatty acid methyl esters and dimethylacetals from lipids with boron fluoride-methanol. *J. Lipid Res.* **5:** 600–608.
22. Bonnard, C., A. Durand, S. Peyrol, E. Chanseaume, M. A. Chauvin, B. Morio, H. Vidal, and J. Rieusset. 2008. Mitochondrial dysfunction results from oxidative stress in the skeletal muscle of diet-induced insulin-resistant mice. *J. Clin. Invest.* **118:** 789–800.
23. Ghosh, A. K., G. Ramakrishnan, C. Chandramohan, and R. Rajasekharan. 2008. CGI-58, the causative gene for Chanarin-Dorfman syndrome, mediates acylation of lysophosphatidic acid. *J. Biol. Chem.* **283:** 24525–24533.
24. Montero-Moran, G., J. M. Caviglia, D. McMahon, A. Rothenberg, V. Subramanian, Z. Xu, S. Lara-Gonzalez, J. Storch, G. M. Carman, and D. L. Brasaemle. 2010. CGI-58/ABHD5 is a coenzyme A-dependent lysophosphatidic acid acyltransferase. *J. Lipid Res.* **51:** 709–719.
25. Pilegaard, H., and P. D. Neufer. 2004. Transcriptional regulation of pyruvate dehydrogenase kinase 4 in skeletal muscle during and after exercise. *Proc. Nutr. Soc.* **63:** 221–226.
26. Ehrenborg, E., and A. Krook. 2009. Regulation of skeletal muscle physiology and metabolism by peroxisome proliferator-activated receptor delta. *Pharmacol. Rev.* **61:** 373–393.
27. DeFronzo, R. A. 2004. Pathogenesis of type 2 diabetes mellitus. *Med. Clin. North Am.* **88:** 787–835 (ix.).
28. McGarry, J. D. 2002. Banting lecture 2001: dysregulation of fatty acid metabolism in the etiology of type 2 diabetes. *Diabetes.* **51:** 7–18.
29. Krssak, M., K. Falk Petersen, A. Dresner, L. DiPietro, S. M. Vogel, D. L. Rothman, M. Roden, and G. I. Shulman. 1999. Intramyocellular lipid concentrations are correlated with insulin sensitivity in humans: a 1H NMR spectroscopy study. *Diabetologia.* **42:** 113–116.
30. Pan, D. A., S. Lillioja, A. D. Kriketos, M. R. Milner, L. A. Baur, C. Bogardus, A. B. Jenkins, and L. H. Storlien. 1997. Skeletal muscle triglyceride levels are inversely related to insulin action. *Diabetes.* **46:** 983–988.
31. Perseghin, G., P. Scifo, F. De Cobelli, E. Pagliato, A. Battezzati, C. Arcelloni, A. Vanzulli, G. Testolin, G. Pozza, A. Del Maschio, et al. 1999. Intramyocellular triglyceride content is a determinant of in vivo insulin resistance in humans: a 1H–13C nuclear magnetic resonance spectroscopy assessment in offspring of type 2 diabetic parents. *Diabetes.* **48:** 1600–1606.
32. Langfort, J., T. Ploug, J. Ihlemann, M. Saldo, C. Holm, and H. Galbo. 1999. Expression of hormone-sensitive lipase and its regulation by adrenaline in skeletal muscle. *Biochem. J.* **340:** 459–465.
33. Alsted, T. J., L. Nybo, M. Schweiger, C. Fledelius, P. Jacobsen, R. Zimmermann, R. Zechner, and B. Kiens. 2009. Adipose triglyceride lipase in human skeletal muscle is upregulated by exercise training. *Am. J. Physiol. Endocrinol. Metab.* **296:** E445–E453.
34. Caviglia, J. M., J. L. Betters, D. H. Dapito, C. C. Lord, S. Sullivan, S. Chua, T. Yin, A. Sekowski, H. Mu, L. Shapiro, et al. 2011. Adipose-selective overexpression of ABHD5/CGI-58 does not increase lipolysis or protect against diet-induced obesity. *J. Lipid Res.* **52:** 2032–2042.
35. Granneman, J. G., H. P. Moore, E. P. Mottillo, Z. Zhu, and L. Zhou. 2011. Interactions of perilipin-5 (Plin5) with adipose triglyceride lipase. *J. Biol. Chem.* **286:** 5126–5135.
36. Wolins, N. E., B. K. Quaynor, J. R. Skinner, A. Tzekov, M. A. Croce, M. C. Gropler, V. Varma, A. Yao-Borengasser, N. Rasouli, P. A. Kern, et al. 2006. OXPAT/PAT-1 is a PPAR-induced lipid droplet protein that promotes fatty acid utilization. *Diabetes.* **55:** 3418–3428.
37. Bezaire, V., A. Mairal, C. Ribet, C. Lefort, A. Girousse, J. Jocken, J. Laurencikiene, R. Anesia, A. M. Rodriguez, M. Ryden, et al. 2009. Contribution of adipose triglyceride lipase and hormone-sensitive lipase to lipolysis in hMADS adipocytes. *J. Biol. Chem.* **284:** 18282–18291.
38. Hardie, D. G. 2007. AMP-activated/SNF1 protein kinases: conserved guardians of cellular energy. *Nat. Rev. Mol. Cell Biol.* **8:** 774–785.
39. Randle, P. J., P. B. Garland, C. N. Hales, and E. A. Newsholme. 1963. The glucose fatty-acid cycle. Its role in insulin sensitivity and the metabolic disturbances of diabetes mellitus. *Lancet.* **1:** 785–789.
40. Spriet, L. L., R. J. Tunstall, M. J. Watt, K. A. Mehan, M. Hargreaves, and D. Cameron-Smith. 2004. Pyruvate dehydrogenase activation and kinase expression in human skeletal muscle during fasting. *J. Appl. Physiol.* **96:** 2082–2087.
41. Schmidt, A., N. Endo, S. J. Rutledge, R. Vogel, D. Shinar, and G. A. Rodan. 1992. Identification of a new member of the steroid hormone receptor superfamily that is activated by a peroxisome proliferator and fatty acids. *Mol. Endocrinol.* **6:** 1634–1641.
42. Sapiro, J. M., M. T. Mashek, A. S. Greenberg, and D. G. Mashek. 2009. Hepatic triacylglycerol hydrolysis regulates peroxisome proliferator-activated receptor alpha activity. *J. Lipid Res.* **50:** 1621–1629.

Supplementary Figure 1. Effect of triacsin C on oleate incorporation into (A) TAG and (B) DAG in human primary myotubes. Four days differentiated human myotubes were incubated for 3 and 24h with 100 µM of [1-^{14}C]oleate in absence or presence of 10 µM of the acyl-coA synthase inhibitor triacsin C. *** $p<0.001$ when compared to control.

Supplementary Figure 2. CGI-58 overexpression increases lipolysis and phospholipid synthesis. Pulse-chase experiments were performed to determine the time-course over 6h of [1-^{14}C]oleate incorporation into (A) diacylglycerols (DAG), (B) monoacylglycerols (MAG), (C) intracellular FA, and (D) phospholipids (PL), in control myotubes (Ad-GFP) and myotubes overexpressing CGI-58 (Ad-CGI58) (n=6). The statistical difference was determined using Two-way ANOVA.

Supplementary Figure 3. CGI-58 silencing reduces lipolysis and phospholipid synthesis. Pulse-chase experiments were performed to determine the time-course over 6h of [1-^{14}C]oleate incorporation into (A) diacylglycerols (DAG), (B) monoacylglycerols (MAG), (C) intracellular FA, and (D) phospholipids (PL), in control myotubes and myotubes knocked down for CGI-58 (siCGI58) (n=6). The statistical difference was determined using Two-way ANOVA.

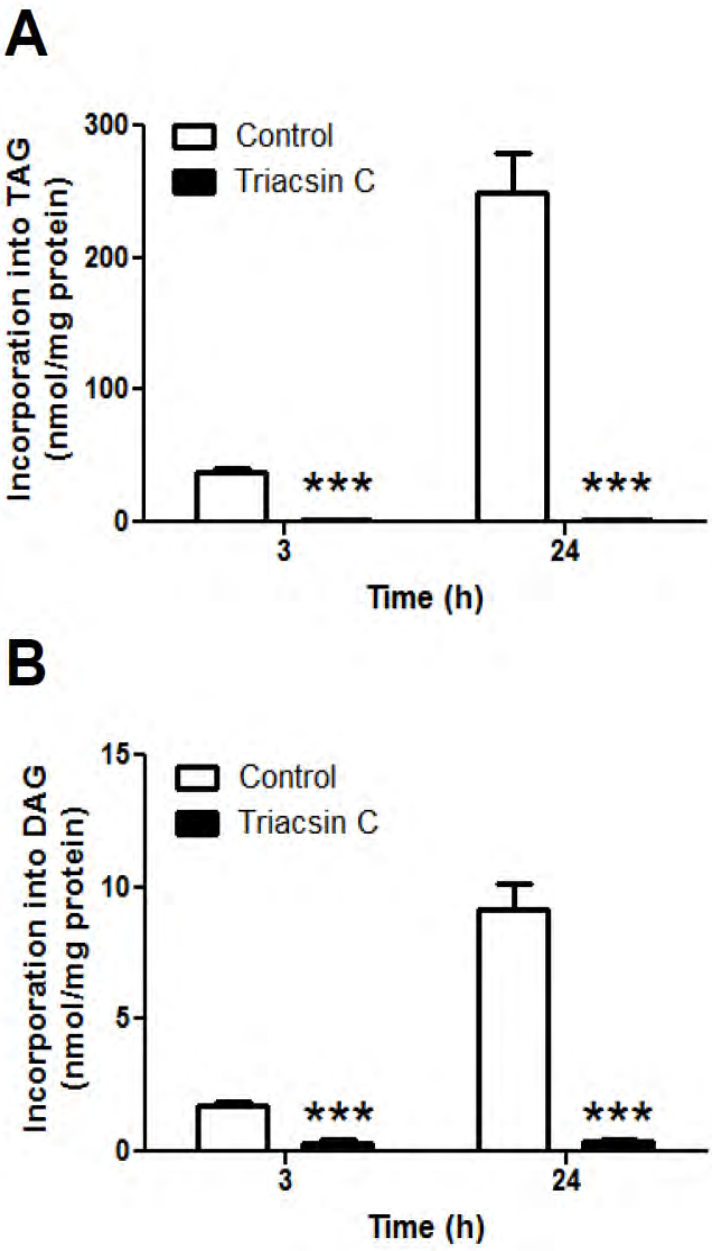
A
Incorporation into TAG (nmol/mg protein)
300
200
100
0
Control
Triacsin C
***
***
3
24
Time (h)
B
Incorporation into DAG (nmol/mg protein)
15
10
5
0
Control
Triacsin C
***
***
3
24
Time (h)

Figure S1

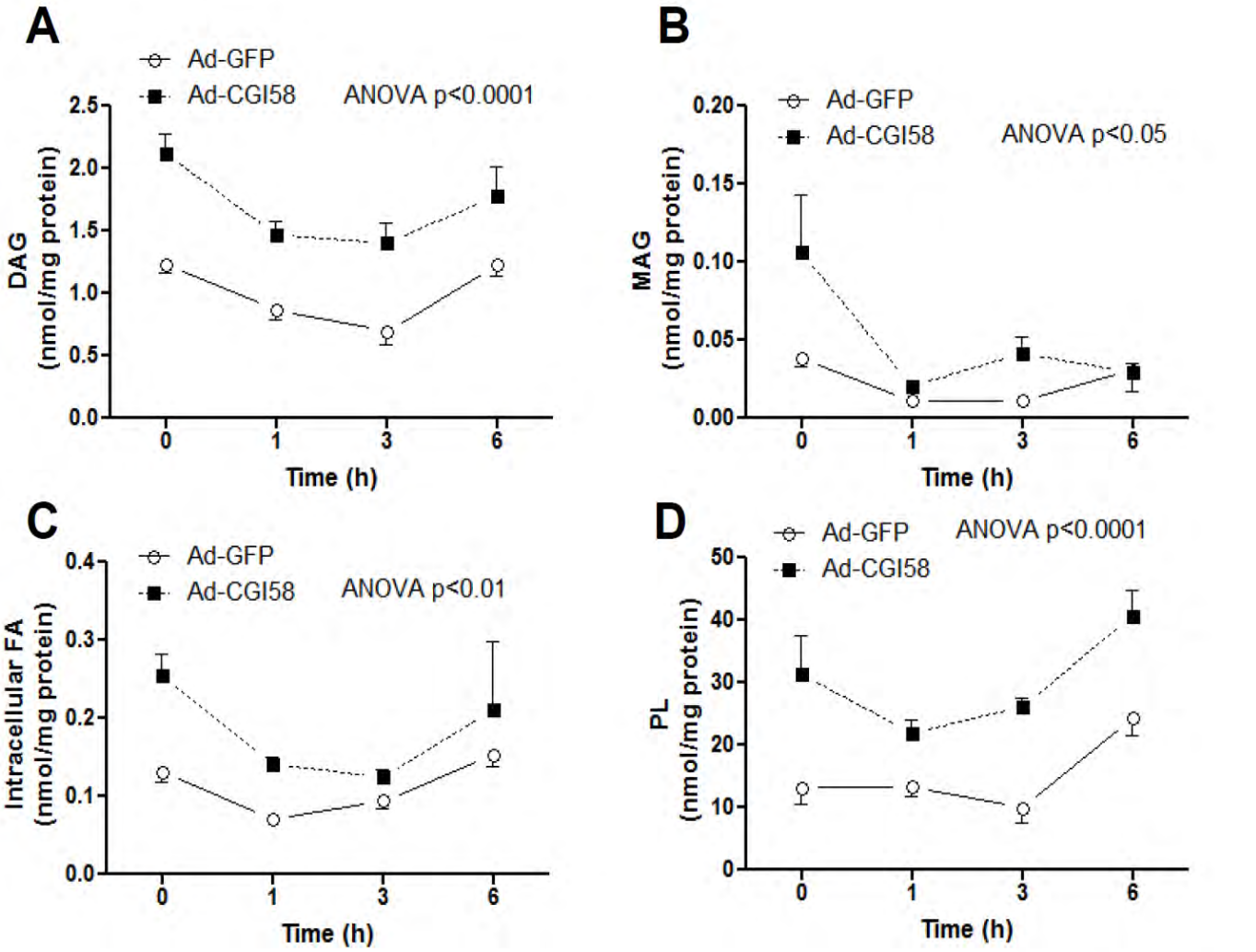
A
Ad-GFP
Ad-CGI58
ANOVA p<0.0001
DAG
(nmol/mg protein)
2.5
2.0
1.5
1.0
0.5
0.0
0
1
3
6
Time (h)
B
Ad-GFP
Ad-CGI58
ANOVA p<0.05
MAG
(nmol/mg protein)
0.20
0.15
0.10
0.05
0.00
0
1
3
6
Time (h)
C
Ad-GFP
Ad-CGI58
ANOVA p<0.01
Intracellular FA
(nmol/mg protein)
0.4
0.3
0.2
0.1
0.0
0
1
3
6
Time (h)
D
Ad-GFP
Ad-CGI58
ANOVA p<0.0001
PL
(nmol/mg protein)
50
40
30
20
10
0
0
1
3
6
Time (h)

Figure S2

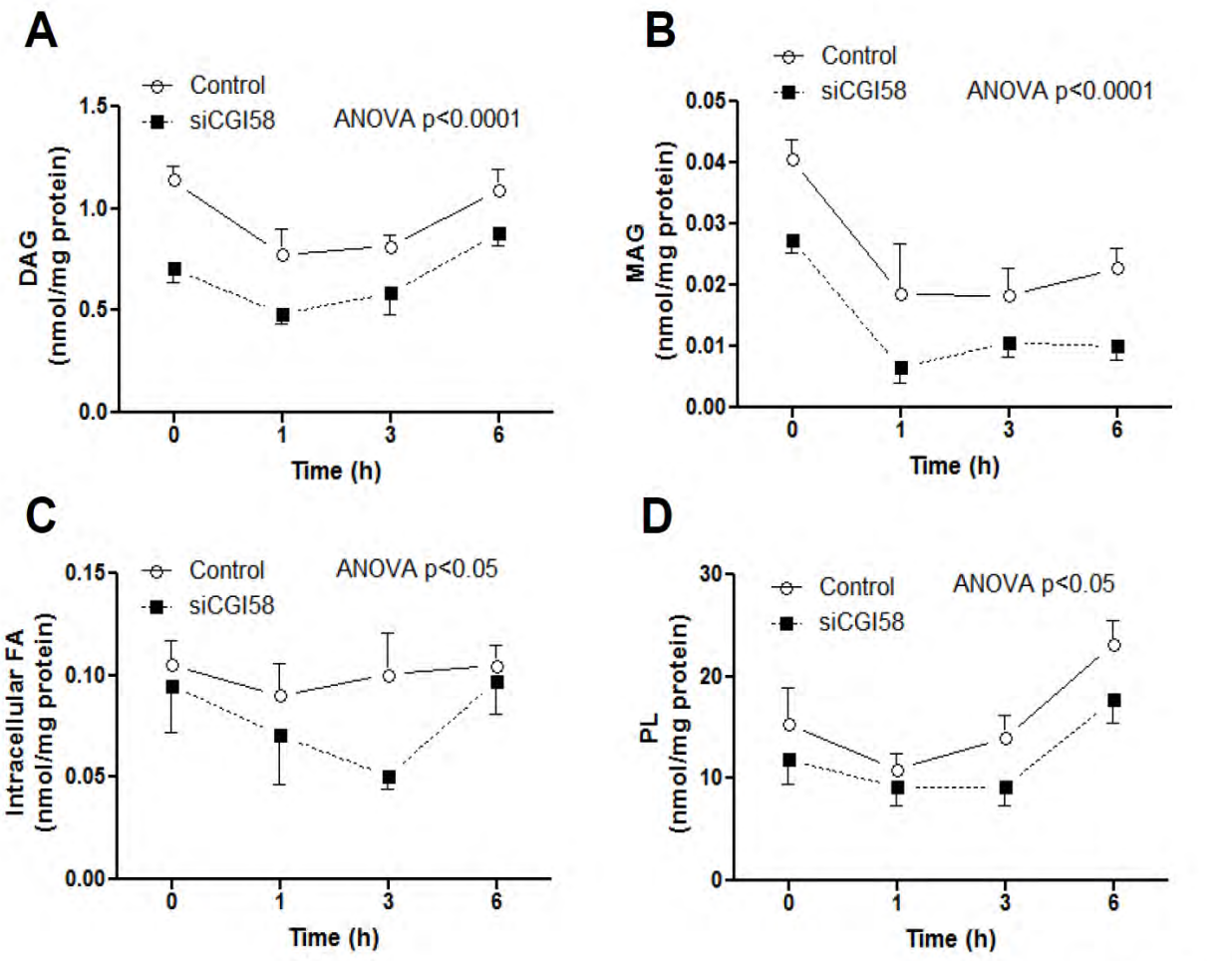
A
Control
siCGI58
ANOVA p<0.0001
DAG
(nmol/mg protein)
1.5
1.0
0.5
0.0
0
1
3
6
Time (h)
B
Control
siCGI58
ANOVA p<0.0001
MAG
(nmol/mg protein)
0.05
0.04
0.03
0.02
0.01
0.00
Time (h)
C
Control
siCGI58
ANOVA p<0.05
Intracellular FA
(nmol/mg protein)
0.15
0.10
0.05
0.00
Time (h)
D
Control
siCGI58
ANOVA p<0.05
PL
(nmol/mg protein)
30
20
10
0
Time (h)

Figure S3

6.3.2 DISCUSSION

Avant cette étude, le rôle de CGI-58 sur le contrôle lipolytique de l'adipocyte était bien décrit (Bezaire et al., 2009; Granneman et al., 2007), en revanche aucune étude n'avait évalué son implication au niveau musculaire. C'est pourquoi nous avons voulu déterminer pour la première fois le rôle de CGI-58 dans le métabolisme lipidique et oxydatif musculaire. Tout d'abord l'analyse par western blot de muscles murins nous a permis de confirmer que CGI-58 était exprimé au niveau musculaire. Le panel de muscles utilisé nous a permis de montrer, de façon intéressante que CGI-58, tout comme l'ATGL (Jocken et al., 2008), est plus exprimé au sein des muscles oxydatifs. Ainsi son expression corrèle parfaitement avec la capacité lipolytique des muscles comme nous avons pu le mesurer par l'activité TAGH.

L'action de CGI-58 a été étudié grâce au suivi d'AGs radio-marqués dans des myocytes sur-exprimant ou sous-exprimant cette protéine d'intérêt. Après une nuit de pré-marquage des lipides intra-myocellulaires par un AG radio-marqué nous avons retiré le milieu contenant la radioactivité et nous avons étudié à différents temps, la localisation de la radioactivité au sein des différentes espèces lipidiques. Lors d'une sous-expression de CGI-58, nous avons pu observer une diminution de la lipolyse musculaire reflétée par la baisse de la libération d'AGs radioactifs dans le milieu de culture. A l'inverse la surexpression augmente le niveau de lipolyse basale. De façon intéressante cette augmentation de la lipolyse se traduit par une diminution de la concentration en TGIM ce qui reflète que CGI-58 augmente la première étape de la lipolyse. Nous avons également montré pour la première fois que les AGs issus de la lipolyse étaient, dans notre modèle de myocyte, des ligands de PPARβ/δ et ainsi régulaient plusieurs gènes cibles de ce récepteur nucléaire (Figure 11). Ceci permet notamment de favoriser l'oxydation des lipides en augmentant le niveau d'expression de la protéine *pyruvate dehydrogenase kinase isozyme 4* (PDK4). En effet PDK4 inhibe la *pyruvate déshydrogénase* et donc l'oxydation du glucose. Récemment des travaux très intéressants de G. Haemmerle *et al* ont confirmé l'importance cruciale de l'ATGL dans l'activation de gènes mitochondriaux PPARα régulés dans le cœur (Haemmerle et al., 2011).

Nos résultats nous ont également permis de compléter les travaux obtenus précédemment montrant que la régulation de l'activité de l'ATGL est cruciale dans le contrôle de l'homéostasie glucidique (Badin et al., 2011, 2013). En effet, nous observons qu'une diminution de l'expression de CGI-58 diminue la production de DAGs et ainsi améliore la sensibilité à l'insuline.

Nous avons ainsi montré le rôle clé de CGI-58 dans la régulation de la lipolyse musculaire *via* son action de co-régulateur de l'ATGL. Il nous semble maintenant intéressant de caractériser le rôle physiologique de G0S2, de PLIN2 et de PLIN5 dans le muscle squelettique.

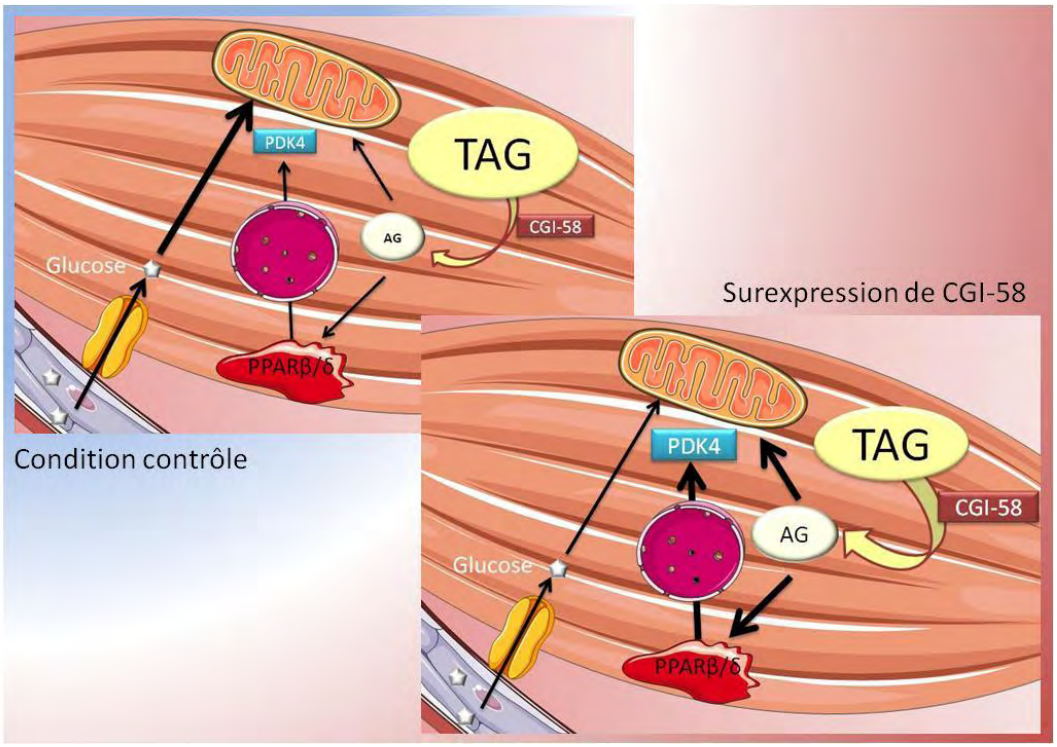

Figure 11. Régulation de la lipolyse et du métabolisme oxydatif par CGI-58

L'augmentation de l'expression de CGI-58 conduit à une forte augmentation de la lipolyse et donc de la production d'AGs. Lors d'une augmentation des concentrations d'AG l'expression de PDK4 est augmentée afin de favoriser leur oxydation. En effet, les AGs sont capables de réguler directement l'expression de PDK4 de par leur rôle de ligand du récepteur nucléaire PPARβ/δ.

7 CONCLUSION ET PERSPECTIVES

Mon travail de thèse a contribué à la compréhension des mécanismes moléculaires reliant l'activité des lipases musculaires à l'insulino-résistance ainsi qu'à la compréhension des mécanismes contrôlant la lipolyse musculaire.

7.1 QUELS LIPIDES INTERMEDIAIRES POUR L'INSULINO-RESISTANCE ?

Nos résultats ont permis d'établir qu'une surexpression de l'ATGL pouvait contribuer, chez l'homme et la souris à une diminution de la sensibilité à l'insuline. A l'inverse l'extinction de son co-activateur CGI-58 améliore la sensibilité à l'insuline des myocytes. Ces résultats vont dans le même sens, ils suggèrent que l'ATGL semble apte à produire des DAGs capables d'activer certaines PKCs. Ces résultats sont pourtant discutés dans une récente étude de Eichmann *et al* (Eichmann et al., 2012). Cette étude soutient sur la base de résultats de chromatographie en phase liquide à haute performance chirale que l'ATGL est incapable d'hydrolyser les TAGs en position trois pour former des 1,2 DAGs. De plus d'autres travaux montrent que les 1,2 DAGs sont seuls capables d'activer les PKCs à l'inverse des 2,3 DAG (Boni and Rando, 1985). Ensemble ces données tendent à démontrer que l'ATGL ne peut pas produire des DAGs lipotoxiques. Cependant plusieurs points cruciaux peuvent expliquer les discordances avec nos résultats.

Tout d'abord l'étude d'Eichmann *et al* a été réalisée sur des lysats de COS7 (cellules d'une lignée issu de rein de singe) surexprimants l'ATGL et CGI-58 mis en présence de trioléine (TAG dont tous les carbones sont radiomarqués). Nous pensons donc crucial de vérifier ces données dans un modèle cellulaire et dans des conditions plus physiologiques. Igal et Coleman ont, par exemple, montré sur des fibroblastes cutanés de patients atteint du syndrome Chanarin-Dorfman (déficients en CGI-58), une forte diminution de la synthèse de phospholipides après un conditionnement à l'oléate. Les phospholipides étant uniquement synthétisables à partir des 1,2 DAGs, il semblerait qu'en fonction du type cellulaire le couple ATGL/CGI58 puisse synthétiser cet isomère de DAG. Au sein du laboratoire, et afin de compléter nos précédents travaux, nous avons donc entrepris l'étude des espèces de DAGs

produites à la suite d'une surexpression de l'ATGL, de CGI-58 ou à l'inverse, d'une extinction de la LHS au sein de nos myocytes primaires. Dans un premier temps nous souhaitons évaluer, dans ces différentes conditions, la production de phospholipides issus des TAGs comme marqueur de la production de 1,2 DAG. Pour cela nous réaliserons au préalable un conditionnement des cellules à l'oléate radiomarqué.

Plusieurs études ont montré que les 1,2 DAGs étaient plus aptes à augmenter l'activité globale des PKCs que les 1,3 et les 2,3 DAGs. Cependant ces études n'ont pas évalué de manière spécifique l'activité des PKCs les plus probablement impliquées dans l'insulino-résistance tel que les PKCθ et ε. Il est envisageable que l'augmentation de l'activité de ces isoformes soit masquée par l'activité d'autres espèces majoritaires dont certaines peuvent être bénéfiques au signal insulinique (Schmitz-Peiffer and Biden, 2008). De plus les conditions expérimentales pour mesurer l'activité des PKCs semblent être très importantes. Ainsi Sanchez-Pinera *et al* ont montré qu'en changeant le type d'émulsion de phospholipides utilisée pour réaliser ce type d'expérimentation et/ou en changeant le type d'AGs composant les DAGs, les 1,3 DAGs étaient tout aussi capables d'activer la PKCα que les 1,2 DAGs (Sánchez-Piñera et al., 1999). Il est donc fortement probable que d'autres PKCs puissent être activées par les 1,3 DAG. Pour compléter nos expériences de mesure des phospholipides, nous souhaitons donc mesurer la translocation de PKCs à la membrane plasmique et ce dans nos myocytes surexprimant l'ATGL, CGI-58 ou invalidés pour la LHS. En effet, cette translocation étant un reflet de l'activité des PKCs, ceci nous permettra de clairement établir si les lipases sont capables de produire des DAGs lipotoxiques.

7.2 NOUVEAUX ACTEURS DU CONTROLE DE LA LIPOLYSE MUSCULAIRE

Les études que nous avons menées dans le laboratoire ont permis de montrer le rôle clé de CGI-58 dans la régulation de la lipolyse musculaire. Mieux comprendre la lipolyse musculaire est indispensable car elle fournit des AGs lipotoxiques néfastes pour la sensibilité à l'insuline, mais aussi car elle pourrait avoir un rôle clé dans l'acheminement des AGs à la mitochondrie. En effet Kanaley *et al* ont montré *in vivo*

dans le muscle humain qu'une large part des AGs transite par les TGIMs avant d'être oxydés (Kanaley et al., 2009).

L'étude de la lipolyse musculaire passe maintenant par une meilleure description du rôle de G0S2 et des PLIN2 et PLIN5. Pour cela des expériences de pré-conditionnement à l'oléate radiomarqué de myocytes ont été entreprises afin d'étudier l'effet d'une extinction ou d'une surexpression de G0S2 et des PLINs sur le re-largage d'oléate à la suite du conditionnement. Ceci permettra de décrire le rôle physiologique de G0S2 et des PLINs dans le muscle squelettique.

Des études de microscopie confocale pourraient également être envisagées afin d'appréhender les mécanismes moléculaires contrôlant la lipolyse musculaire. Ainsi nous pourrions par immuno-marquage de PLIN2 ou PLIN5, des lipases et de la gouttelette lipidique évaluer la colocalisation des différents acteurs dans des cultures primaires humaines. Wang *et al* ainsi que Granneman *et al* ont établi qu'il existait une colocalisation entre PLIN5 et l'ATGL dans des cellules non musculaires transfectées (Granneman et al., 2011; Wang et al., 2011b). De plus les travaux de MacPherson *et al* montrent une augmentation de l'interaction CGI-58/ATGL et une diminution de l'interaction ATGL/PLIN2 après stimulation électrique d'un muscle soléaire (Macpherson et al., 2013). Pour compléter ces travaux, il serait intéressant de réaliser les études d'immunofluorescence avant et après stimulations électriques des myocytes (Nikolić et al., 2012). Ceci pourrait également être réalisé avant et après un traitement avec un cocktail chimique mimant la contraction (Forskoline/Ionomycine) (Sparks et al., 2011).

L'étude du contrôle lipolytique musculaire devra également passer par des travaux *in vivo*. Nous disposons notamment au laboratoire d'un modèle de souris surexprimant CGI-58 dans le muscle squelettique. Si nous ne sommes qu'au début de la caractérisation de ce modèle, il nous a déjà permis d'identifier quelques informations importantes. Premièrement, nous avons montré que la surexpression musculaire de CGI-58 conduit à une augmentation de l'activité TAGH. Ces informations confirment ceux précédemment obtenu sur myocytes humains (Badin et al., 2012). Nous pouvons donc clairement affirmer que contrairement à l'adipocyte ou son expression n'est pas limitante (Caviglia et al., 2011), CGI-58 semble avoir un rôle clé dans la régulation de la lipolyse musculaire *in vivo.* Pour compléter ces travaux il serait

également intéressant de développer certaines études chez l'animal. Si les résultats de Bosma *et al* sur PLIN2 ont clairement montré le rôle de la protéine dans le contrôle de la lipolyse et un rôle clé dans le développement de l'insulino-résistance, les travaux de surexpression de PLIN5 dans le *tibialis anterior* et le cœur sont moins concluants (Bosma et al., 2013; Pollak et al., 2013; Wang et al., 2013). Ceci peut être dû à la très forte expression de PLIN5 dans les tissus oxydatifs comme le cœur et les muscles (Dalen et al., 2007; Wolins et al., 2006). Pour établir définitivement le rôle musculaire de PLIN5 nous pensons donc préférable d'envisager une stratégie de perte de fonction spécifique au muscle squelettique. Ceci pourrait être réalisé en croisant des animaux dont le gène de PLIN5 a été entouré par des séquences LoxP avec des souris exprimant la recombinase Cre sous le contrôle du promoteur de l'*human α-skeletal actin* (proteine strictement exprimé dans le muscle squelettique). Il serait aussi intéressant de développer un modèle murin invalidé pour G0S2, cependant, vu le rôle probable de cette protéine dans le cycle cellulaire, l'apoptose et la différenciation (Russell and Forsdyke, 1991; Welch et al., 2009; Yamada et al., 2012), il pourrait être préférable de réaliser une invalidation conditionnelle afin d'éviter tout problème lié au développement des souris. Pour cela la meilleure stratégie serait sans doute d'utiliser des souris exprimant un système HSA-Cre inductible par le Tamoxifène. Ces souris seront alors croisées avec des animaux G0S2-LoxP. Il suffira, par la suite, de traiter la descendance à l'âge adulte avec du Tamoxifène afin d'entraîner la délétion muscle spécifique de G0S2. La caractérisation de ces trois modèles devra passer par le suivi de poids et la mesure de la masse grasse par une technique de résonnance nucléaire magnétique. Afin d'analyser l'impact de l'invalidation de G0S2 et de PLIN5 sur la lipolyse, des études de chromatographie sur couche mince menées *ex vivo* sur le muscle squelettique après une incubation à l'oléate marqué ainsi que la mesure des TAGs, DAGs et céramides par chromatographie gazeuse seront nécessaires. Nous souhaitons également soumettre les animaux à des tests d'endurance, afin d'établir si les modifications d'expression de protéines lipolytiques régulent les capacités d'endurance en changeant les types de substrats préférentiellement utilisés. Enfin il serait intéressant d'analyser les possibles implications d'une augmentation de l'hydrolyse des TAGs possiblement attendu dans ces modèles sur la sensibilité à l'insuline. Pour cela des études de clamp hyperinsulinique-euglycémique associées à une analyse plus physiologique comme un test de tolérance au glucose couplé au

dosage de l'insulinémie au pic de glycémie et à une mesure de transport de 2-deoxyglucose au sein du muscle squelettique pourraient être envisagés. Il sera nécessaire afin de bien caractériser ces trois modèles transgéniques de réaliser ces expériences dans différentes cohortes d'animaux soumis à différents protocoles. Nous pensons notamment à placer les animaux dans des conditions modifiant le contenu en lipides intra-myocellulaire et l'activité/expression des lipases. Ceci passe par la mise en régime hyperlipidique mais aussi par des protocoles d'entraînement de plusieurs semaines.

7.3 CONCLUSION

Durant ma thèse, nous avons montré le rôle clé de la lipolyse dans l'insulino-résistance. En effet nos résultats montrent l'implication, chez l'homme et la souris, d'une augmentation d'activité de l'ATGL ainsi que d'une baisse d'activité de la LHS dans l'insulino-résistance. Ces dérégulations conduisent à l'accumulation de DAGs et à l'activation des PKCs connus pour inhiber la voie de signalisation de l'insuline.

Nous avons également, grâce à nos travaux, montré le rôle central de CGI-58 dans la régulation de la lipolyse musculaire. Cet effet passe comme dans le tissu adipeux par son rôle de co-activateur de l'ATGL. En parallèle nous avons montré l'implication des AGs issus de la lipolyse musculaire dans l'activation de gènes PPAR régulés.

BIBLIOGRAPHIE

Adams, J.M., 2nd, Pratipanawatr, T., Berria, R., Wang, E., DeFronzo, R.A., Sullards, M.C., and Mandarino, L.J. (2004). Ceramide content is increased in skeletal muscle from obese insulin-resistant humans. Diabetes *53*, 25–31.

Aerts, J.M., Ottenhoff, R., Powlson, A.S., Grefhorst, A., van Eijk, M., Dubbelhuis, P.F., Aten, J., Kuipers, F., Serlie, M.J., Wennekes, T., et al. (2007). Pharmacological inhibition of glucosylceramide synthase enhances insulin sensitivity. Diabetes *56*, 1341–1349.

Aguer, C., Mercier, J., Man, C.Y.W., Metz, L., Bordenave, S., Lambert, K., Jean, E., Lantier, L., Bounoua, L., Brun, J.F., et al. (2010). Intramyocellular lipid accumulation is associated with permanent relocation ex vivo and in vitro of fatty acid translocase (FAT)/CD36 in obese patients. Diabetologia *53*, 1151–1163.

Ahmadian, M., Abbott, M.J., Tang, T., Hudak, C.S.S., Kim, Y., Bruss, M., Hellerstein, M.K., Lee, H.-Y., Samuel, V.T., Shulman, G.I., et al. (2011). Desnutrin/ATGL is regulated by AMPK and is required for a brown adipose phenotype. Cell Metab. *13*, 739–748.

Amati, F., Dubé, J.J., Alvarez-Carnero, E., Edreira, M.M., Chomentowski, P., Coen, P.M., Switzer, G.E., Bickel, P.E., Stefanovic-Racic, M., Toledo, F.G.S., et al. (2011). Skeletal muscle triglycerides, diacylglycerols, and ceramides in insulin resistance: another paradox in endurance-trained athletes? Diabetes *60*, 2588–2597.

Anthonsen, M.W., Rönnstrand, L., Wernstedt, C., Degerman, E., and Holm, C. (1998). Identification of novel phosphorylation sites in hormone-sensitive lipase that are phosphorylated in response to isoproterenol and govern activation properties in vitro. J. Biol. Chem. *273*, 215–221.

Asmann, Y.W., Stump, C.S., Short, K.R., Coenen-Schimke, J.M., Guo, Z., Bigelow, M.L., and Nair, K.S. (2006). Skeletal muscle mitochondrial functions, mitochondrial DNA copy numbers, and gene transcript profiles in type 2 diabetic and nondiabetic subjects at equal levels of low or high insulin and euglycemia. Diabetes *55*, 3309–3319.

Badin, P.-M., Louche, K., Mairal, A., Liebisch, G., Schmitz, G., Rustan, A.C., Smith, S.R., Langin, D., and Moro, C. (2011). Altered skeletal muscle lipase expression and activity contribute to insulin resistance in humans. Diabetes *60*, 1734–1742.

Badin, P.-M., Loubière, C., Coonen, M., Louche, K., Tavernier, G., Bourlier, V., Mairal, A., Rustan, A.C., Smith, S.R., Langin, D., et al. (2012). Regulation of skeletal muscle lipolysis and oxidative metabolism by the co-lipase CGI-58. J. Lipid Res. *53*, 839–848.

Badin, P.-M., Vila, I.K., Louche, K., Mairal, A., Marques, M.-A., Bourlier, V., Tavernier, G., Langin, D., and Moro, C. (2013). High-fat diet-mediated lipotoxicity and insulin resistance is related to impaired lipase expression in mouse skeletal muscle. Endocrinology *154*, 1444–1453.

Bajpeyi, S., Pasarica, M., Moro, C., Conley, K., Jubrias, S., Sereda, O., Burk, D.H., Zhang, Z., Gupta, A., Kjems, L., et al. (2011). Skeletal muscle mitochondrial capacity and insulin resistance in type 2 diabetes. J. Clin. Endocrinol. Metab. *96*, 1160–1168.

Belfrage, P., Jergil, B., Strålfors, P., and Tornqvist, H. (1977). Hormone-sensitive lipase of rat adipose tissue: identification and some properties of the enzyme protein. FEBS Lett. *75*, 259–264.

Bergman, B.C., Perreault, L., Hunerdosse, D.M., Koehler, M.C., Samek, A.M., and Eckel, R.H. (2010). Increased intramuscular lipid synthesis and low saturation relate to insulin sensitivity in endurance-trained athletes. J. Appl. Physiol. *108*, 1134–1141.

Bergman, B.C., Hunerdosse, D.M., Kerege, A., Playdon, M.C., and Perreault, L. (2012). Localisation and composition of skeletal muscle diacylglycerol predicts insulin resistance in humans. Diabetologia *55*, 1140–1150.

Bezaire, V., Mairal, A., Ribet, C., Lefort, C., Girousse, A., Jocken, J., Laurencikiene, J., Anesia, R., Rodriguez, A.-M., Ryden, M., et al. (2009). Contribution of adipose triglyceride lipase and hormone-sensitive lipase to lipolysis in hMADS adipocytes. J. Biol. Chem. *284*, 18282–18291.

Blaak, E.E., Wagenmakers, A.J., Glatz, J.F., Wolffenbuttel, B.H., Kemerink, G.J., Langenberg, C.J., Heidendal, G.A., and Saris, W.H. (2000). Plasma FFA utilization

and fatty acid-binding protein content are diminished in type 2 diabetic muscle. Am. J. Physiol. Endocrinol. Metab. *279*, E146–154.

Blaak, E.E., Schiffelers, S.L., Saris, W.H., Mensink, M., and Kooi, M.E. (2004). Impaired beta-adrenergically mediated lipolysis in skeletal muscle of obese subjects. Diabetologia *47*, 1462–1468.

Blachnio-Zabielska, A., Baranowski, M., Zabielski, P., and Gorski, J. (2010). Effect of high fat diet enriched with unsaturated and diet rich in saturated fatty acids on sphingolipid metabolism in rat skeletal muscle. J. Cell. Physiol. *225*, 786–791.

Van Blitterswijk, W.J., and Houssa, B. (2000). Properties and functions of diacylglycerol kinases. Cell. Signal. *12*, 595–605.

Boini, K.M., Zhang, C., Xia, M., Poklis, J.L., and Li, P.-L. (2010). Role of sphingolipid mediator ceramide in obesity and renal injury in mice fed a high-fat diet. J. Pharmacol. Exp. Ther. *334*, 839–846.

Bonen, A., Parolin, M.L., Steinberg, G.R., Calles-Escandon, J., Tandon, N.N., Glatz, J.F.C., Luiken, J.J.F.P., Heigenhauser, G.J.F., and Dyck, D.J. (2004). Triacylglycerol accumulation in human obesity and type 2 diabetes is associated with increased rates of skeletal muscle fatty acid transport and increased sarcolemmal FAT/CD36. FASEB J. *18*, 1144–1146.

Bonen, A., Han, X.-X., Habets, D.D.J., Febbraio, M., Glatz, J.F.C., and Luiken, J.J.F.P. (2007). A null mutation in skeletal muscle FAT/CD36 reveals its essential role in insulin- and AICAR-stimulated fatty acid metabolism. Am. J. Physiol. Endocrinol. Metab. *292*, E1740–1749.

Boni, L.T., and Rando, R.R. (1985). The nature of protein kinase C activation by physically defined phospholipid vesicles and diacylglycerols. J. Biol. Chem. *260*, 10819–10825.

Bonnard, C., Durand, A., Peyrol, S., Chanseaume, E., Chauvin, M.-A., Morio, B., Vidal, H., and Rieusset, J. (2008). Mitochondrial dysfunction results from oxidative stress in the skeletal muscle of diet-induced insulin-resistant mice. J. Clin. Invest. *118*, 789–800.

Bosma, M., Hesselink, M.K.C., Sparks, L.M., Timmers, S., Ferraz, M.J., Mattijssen, F., van Beurden, D., Schaart, G., de Baets, M.H., Verheyen, F.K., et al. (2012). Perilipin 2 improves insulin sensitivity in skeletal muscle despite elevated intramuscular lipid levels. Diabetes *61*, 2679–2690.

Bosma, M., Sparks, L.M., Hooiveld, G.J., Jorgensen, J.A., Houten, S.M., Schrauwen, P., Kersten, S., and Hesselink, M.K.C. (2013). Overexpression of PLIN5 in skeletal muscle promotes oxidative gene expression and intramyocellular lipid content without compromising insulin sensitivity. Biochim. Biophys. Acta *1831*, 844–852.

Bruce, C.R., Thrush, A.B., Mertz, V.A., Bezaire, V., Chabowski, A., Heigenhauser, G.J.F., and Dyck, D.J. (2006). Endurance training in obese humans improves glucose tolerance and mitochondrial fatty acid oxidation and alters muscle lipid content. Am. J. Physiol. Endocrinol. Metab. *291*, E99–E107.

Bruce, C.R., Risis, S., Babb, J.R., Yang, C., Kowalski, G.M., Selathurai, A., Lee-Young, R.S., Weir, J.M., Yoshioka, K., Takuwa, Y., et al. (2012). Overexpression of sphingosine kinase 1 prevents ceramide accumulation and ameliorates muscle insulin resistance in high-fat diet-fed mice. Diabetes *61*, 3148–3155.

Bush, N.C., Basu, R., Rizza, R.A., Nair, K.S., Khosla, S., and Jensen, M.D. (2012). Insulin-mediated FFA suppression is associated with triglyceridemia and insulin sensitivity independent of adiposity. J. Clin. Endocrinol. Metab. *97*, 4130–4138.

Caviglia, J.M., Betters, J.L., Dapito, D.-H., Lord, C.C., Sullivan, S., Chua, S., Yin, T., Sekowski, A., Mu, H., Shapiro, L., et al. (2011). Adipose-selective overexpression of ABHD5/CGI-58 does not increase lipolysis or protect against diet-induced obesity. J. Lipid Res. *52*, 2032–2042.

Chalkley, S.M., Hettiarachchi, M., Chisholm, D.J., and Kraegen, E.W. (1998). Five-hour fatty acid elevation increases muscle lipids and impairs glycogen synthesis in the rat. Metab. Clin. Exp. *47*, 1121–1126.

Chavez, J.A., and Summers, S.A. (2012). A ceramide-centric view of insulin resistance. Cell Metab. *15*, 585–594.

Chavez, J.A., Knotts, T.A., Wang, L.-P., Li, G., Dobrowsky, R.T., Florant, G.L., and Summers, S.A. (2003). A role for ceramide, but not diacylglycerol, in the antagonism of insulin signal transduction by saturated fatty acids. J. Biol. Chem. *278*, 10297–10303.

Chavez, J.A., Holland, W.L., Bär, J., Sandhoff, K., and Summers, S.A. (2005). Acid ceramidase overexpression prevents the inhibitory effects of saturated fatty acids on insulin signaling. J. Biol. Chem. *280*, 20148–20153.

Chen, M.T., Kaufman, L.N., Spennetta, T., and Shrago, E. (1992). Effects of high fat-feeding to rats on the interrelationship of body weight, plasma insulin, and fatty acyl-coenzyme A esters in liver and skeletal muscle. Metab. Clin. Exp. *41*, 564–569.

Chibalin, A.V., Leng, Y., Vieira, E., Krook, A., Björnholm, M., Long, Y.C., Kotova, O., Zhong, Z., Sakane, F., Steiler, T., et al. (2008). Downregulation of diacylglycerol kinase delta contributes to hyperglycemia-induced insulin resistance. Cell *132*, 375–386.

Coen, P.M., Dubé, J.J., Amati, F., Stefanovic-Racic, M., Ferrell, R.E., Toledo, F.G.S., and Goodpaster, B.H. (2010). Insulin resistance is associated with higher intramyocellular triglycerides in type I but not type II myocytes concomitant with higher ceramide content. Diabetes *59*, 80–88.

Colberg, S.R., Simoneau, J.A., Thaete, F.L., and Kelley, D.E. (1995). Skeletal muscle utilization of free fatty acids in women with visceral obesity. J. Clin. Invest. *95*, 1846–1853.

Coleman, R.A., and Lee, D.P. (2004). Enzymes of triacylglycerol synthesis and their regulation. Prog. Lipid Res. *43*, 134–176.

Coleman, R.A., Lewin, T.M., and Muoio, D.M. (2000). Physiological and nutritional regulation of enzymes of triacylglycerol synthesis. Annu. Rev. Nutr. *20*, 77–103.

Cornaciu, I., Boeszoermenyi, A., Lindermuth, H., Nagy, H.M., Cerk, I.K., Ebner, C., Salzburger, B., Gruber, A., Schweiger, M., Zechner, R., et al. (2011). The minimal domain of adipose triglyceride lipase (ATGL) ranges until leucine 254 and can be activated and inhibited by CGI-58 and G0S2, respectively. PLoS ONE *6*, e26349.

Dalen, K.T., Dahl, T., Holter, E., Arntsen, B., Londos, C., Sztalryd, C., and Nebb, H.I. (2007). LSDP5 is a PAT protein specifically expressed in fatty acid oxidizing tissues. Biochim. Biophys. Acta *1771*, 210–227.

Deevska, G.M., Rozenova, K.A., Giltiay, N.V., Chambers, M.A., White, J., Boyanovsky, B.B., Wei, J., Daugherty, A., Smart, E.J., Reid, M.B., et al. (2009). Acid Sphingomyelinase Deficiency Prevents Diet-induced Hepatic Triacylglycerol Accumulation and Hyperglycemia in Mice. J. Biol. Chem. *284*, 8359–8368.

DeFronzo, R.A. (1988). Lilly lecture 1987. The triumvirate: beta-cell, muscle, liver. A collusion responsible for NIDDM. Diabetes *37*, 667–687.

DeFronzo, R.A., and Tripathy, D. (2009). Skeletal muscle insulin resistance is the primary defect in type 2 diabetes. Diabetes Care *32 Suppl 2*, S157–163.

Dobrzyń, A., Zendzian-Piotrowska, M., and Górski, J. (2004). Effect of endurance training on the sphingomyelin-signalling pathway activity in the skeletal muscles of the rat. J. Physiol. Pharmacol. *55*, 305–313.

Donsmark, M., Langfort, J., Holm, C., Ploug, T., and Galbo, H. (2003). Contractions activate hormone-sensitive lipase in rat muscle by protein kinase C and mitogen-activated protein kinase. J. Physiol. (Lond.) *550*, 845–854.

Dubé, J.J., Amati, F., Stefanovic-Racic, M., Toledo, F.G.S., Sauers, S.E., and Goodpaster, B.H. (2008). Exercise-induced alterations in intramyocellular lipids and insulin resistance: the athlete's paradox revisited. Am. J. Physiol. Endocrinol. Metab. *294*, E882–888.

Dubé, J.J., Amati, F., Toledo, F.G.S., Stefanovic-Racic, M., Rossi, A., Coen, P., and Goodpaster, B.H. (2011). Effects of weight loss and exercise on insulin resistance, and intramyocellular triacylglycerol, diacylglycerol and ceramide. Diabetologia *54*, 1147–1156.

Eichmann, T.O., Kumari, M., Haas, J.T., Farese, R.V., Jr, Zimmermann, R., Lass, A., and Zechner, R. (2012). Studies on the substrate and stereo/regioselectivity of adipose triglyceride lipase, hormone-sensitive lipase, and diacylglycerol-O-acyltransferases. J. Biol. Chem. *287*, 41446–41457.

Ellis, B.A., Poynten, A., Lowy, A.J., Furler, S.M., Chisholm, D.J., Kraegen, E.W., and Cooney, G.J. (2000). Long-chain acyl-CoA esters as indicators of lipid metabolism and insulin sensitivity in rat and human muscle. Am. J. Physiol. Endocrinol. Metab. *279*, E554–560.

Erion, D.M., and Shulman, G.I. (2010). Diacylglycerol-mediated insulin resistance. Nat. Med. *16*, 400–402.

Fabbrini, E., Mohammed, B.S., Magkos, F., Korenblat, K.M., Patterson, B.W., and Klein, S. (2008). Alterations in adipose tissue and hepatic lipid kinetics in obese men and women with nonalcoholic fatty liver disease. Gastroenterology *134*, 424–431.

Ferreira, L.F., Moylan, J.S., Gilliam, L.A.A., Smith, J.D., Nikolova-Karakashian, M., and Reid, M.B. (2010). Sphingomyelinase stimulates oxidant signaling to weaken skeletal muscle and promote fatigue. Am. J. Physiol., Cell Physiol. *299*, C552–560.

Finck, B.N., and Kelly, D.P. (2006). PGC-1 coactivators: inducible regulators of energy metabolism in health and disease. J. Clin. Invest. *116*, 615–622.

Fox, T.E., Houck, K.L., O'Neill, S.M., Nagarajan, M., Stover, T.C., Pomianowski, P.T., Unal, O., Yun, J.K., Naides, S.J., and Kester, M. (2007). Ceramide recruits and activates protein kinase C zeta (PKC zeta) within structured membrane microdomains. J. Biol. Chem. *282*, 12450–12457.

Frangioudakis, G., Garrard, J., Raddatz, K., Nadler, J.L., Mitchell, T.W., and Schmitz-Peiffer, C. (2010). Saturated- and n-6 polyunsaturated-fat diets each induce ceramide accumulation in mouse skeletal muscle: reversal and improvement of glucose tolerance by lipid metabolism inhibitors. Endocrinology *151*, 4187–4196.

Fredrikson, G., Strålfors, P., Nilsson, N.O., and Belfrage, P. (1981). Hormone-sensitive lipase of rat adipose tissue. Purification and some properties. J. Biol. Chem. *256*, 6311–6320.

Fredrikson, G., Tornqvist, H., and Belfrage, P. (1986). Hormone-sensitive lipase and monoacylglycerol lipase are both required for complete degradation of adipocyte triacylglycerol. Biochim. Biophys. Acta *876*, 288–293.

Fried, S.K., Russell, C.D., Grauso, N.L., and Brolin, R.E. (1993). Lipoprotein lipase regulation by insulin and glucocorticoid in subcutaneous and omental adipose tissues of obese women and men. J. Clin. Invest. *92*, 2191–2198.

Fueger, P.T., Shearer, J., Bracy, D.P., Posey, K.A., Pencek, R.R., McGuinness, O.P., and Wasserman, D.H. (2005). Control of muscle glucose uptake: test of the rate-limiting step paradigm in conscious, unrestrained mice. J. Physiol. (Lond.) *562*, 925–935.

Galgani, J.E., Vasquez, K., Watkins, G., Dupuy, A., Bertrand-Michel, J., Levade, T., and Moro, C. (2013). Enhanced Skeletal Muscle Lipid Oxidative Efficiency in Insulin-Resistant vs Insulin-Sensitive Nondiabetic, Nonobese Humans. J. Clin. Endocrinol. Metab.

Girousse, A., and Langin, D. (2012). Adipocyte lipases and lipid droplet-associated proteins: insight from transgenic mouse models. Int J Obes (Lond) *36*, 581–594.

Girousse, A., Tavernier, G., Valle, C., Moro, C., Mejhert, N., Dinel, A.-L., Houssier, M., Roussel, B., Besse-Patin, A., Combes, M., et al. (2013). Partial inhibition of adipose tissue lipolysis improves glucose metabolism and insulin sensitivity without alteration of fat mass. PLoS Biol. *11*, e1001485.

Golay, A., Swislocki, A.L., Chen, Y.D., Jaspan, J.B., and Reaven, G.M. (1986). Effect of obesity on ambient plasma glucose, free fatty acid, insulin, growth hormone, and glucagon concentrations. J. Clin. Endocrinol. Metab. *63*, 481–484.

Goodpaster, B.H. (2013). Mitochondrial deficiency is associated with insulin resistance. Diabetes *62*, 1032–1035.

Goodpaster, B.H., Thaete, F.L., Simoneau, J.A., and Kelley, D.E. (1997). Subcutaneous abdominal fat and thigh muscle composition predict insulin sensitivity independently of visceral fat. Diabetes *46*, 1579–1585.

Goodpaster, B.H., He, J., Watkins, S., and Kelley, D.E. (2001). Skeletal muscle lipid content and insulin resistance: evidence for a paradox in endurance-trained athletes. J. Clin. Endocrinol. Metab. *86*, 5755–5761.

Gordon, E. (1960). Non-Esterified Fatty Acids in the Blood of Obese and Lean Subjects. Am J Clin Nutr *8*, 740–747.

Goudriaan, J.R., Dahlmans, V.E.H., Teusink, B., Ouwens, D.M., Febbraio, M., Maassen, J.A., Romijn, J.A., Havekes, L.M., and Voshol, P.J. (2003). CD36 deficiency increases insulin sensitivity in muscle, but induces insulin resistance in the liver in mice. J. Lipid Res. *44*, 2270–2277.

Granneman, J.G., Moore, H.-P.H., Granneman, R.L., Greenberg, A.S., Obin, M.S., and Zhu, Z. (2007). Analysis of lipolytic protein trafficking and interactions in adipocytes. J. Biol. Chem. *282*, 5726–5735.

Granneman, J.G., Moore, H.-P.H., Krishnamoorthy, R., and Rathod, M. (2009). Perilipin controls lipolysis by regulating the interactions of AB-hydrolase containing 5 (Abhd5) and adipose triglyceride lipase (Atgl). J. Biol. Chem. *284*, 34538–34544.

Granneman, J.G., Moore, H.-P.H., Mottillo, E.P., Zhu, Z., and Zhou, L. (2011). Interactions of perilipin-5 (Plin5) with adipose triglyceride lipase. J. Biol. Chem. *286*, 5126–5135.

Greenberg, A.S., Shen, W.J., Muliro, K., Patel, S., Souza, S.C., Roth, R.A., and Kraemer, F.B. (2001). Stimulation of lipolysis and hormone-sensitive lipase via the extracellular signal-regulated kinase pathway. J. Biol. Chem. *276*, 45456–45461.

Griffin, M.E., Marcucci, M.J., Cline, G.W., Bell, K., Barucci, N., Lee, D., Goodyear, L.J., Kraegen, E.W., White, M.F., and Shulman, G.I. (1999). Free fatty acid-induced insulin resistance is associated with activation of protein kinase C theta and alterations in the insulin signaling cascade. Diabetes *48*, 1270–1274.

Gual, P., Le Marchand-Brustel, Y., and Tanti, J.-F. (2005). Positive and negative regulation of insulin signaling through IRS-1 phosphorylation. Biochimie *87*, 99–109.

Haemmerle, G., Zimmermann, R., Strauss, J.G., Kratky, D., Riederer, M., Knipping, G., and Zechner, R. (2002). Hormone-sensitive lipase deficiency in mice changes the plasma lipid profile by affecting the tissue-specific expression pattern of lipoprotein lipase in adipose tissue and muscle. J. Biol. Chem. *277*, 12946–12952.

Haemmerle, G., Lass, A., Zimmermann, R., Gorkiewicz, G., Meyer, C., Rozman, J., Heldmaier, G., Maier, R., Theussl, C., Eder, S., et al. (2006). Defective lipolysis and altered energy metabolism in mice lacking adipose triglyceride lipase. Science *312*, 734–737.

Haemmerle, G., Moustafa, T., Woelkart, G., Büttner, S., Schmidt, A., van de Weijer, T., Hesselink, M., Jaeger, D., Kienesberger, P.C., Zierler, K., et al. (2011). ATGL-mediated fat catabolism regulates cardiac mitochondrial function via PPAR-α and PGC-1. Nat. Med. *17*, 1076–1085.

Hage Hassan, R., Hainault, I., Vilquin, J.-T., Samama, C., Lasnier, F., Ferré, P., Foufelle, F., and Hajduch, E. (2012). Endoplasmic reticulum stress does not mediate palmitate-induced insulin resistance in mouse and human muscle cells. Diabetologia *55*, 204–214.

Handschin, C., Choi, C.S., Chin, S., Kim, S., Kawamori, D., Kurpad, A.J., Neubauer, N., Hu, J., Mootha, V.K., Kim, Y.-B., et al. (2007). Abnormal glucose homeostasis in skeletal muscle-specific PGC-1alpha knockout mice reveals skeletal muscle-pancreatic beta cell crosstalk. J. Clin. Invest. *117*, 3463–3474.

Hannun, Y.A., and Obeid, L.M. (2008). Principles of bioactive lipid signalling: lessons from sphingolipids. Nat. Rev. Mol. Cell Biol. *9*, 139–150.

Harada, K., Shen, W.-J., Patel, S., Natu, V., Wang, J., Osuga, J., Ishibashi, S., and Kraemer, F.B. (2003). Resistance to high-fat diet-induced obesity and altered expression of adipose-specific genes in HSL-deficient mice. Am. J. Physiol. Endocrinol. Metab. *285*, E1182–1195.

He, J., Watkins, S., and Kelley, D.E. (2001). Skeletal muscle lipid content and oxidative enzyme activity in relation to muscle fiber type in type 2 diabetes and obesity. Diabetes *50*, 817–823.

Heptulla, R., Smitten, A., Teague, B., Tamborlane, W.V., Ma, Y.Z., and Caprio, S. (2001). Temporal patterns of circulating leptin levels in lean and obese adolescents: relationships to insulin, growth hormone, and free fatty acids rhythmicity. J. Clin. Endocrinol. Metab. *86*, 90–96.

Holland, W.L., Brozinick, J.T., Wang, L.-P., Hawkins, E.D., Sargent, K.M., Liu, Y., Narra, K., Hoehn, K.L., Knotts, T.A., Siesky, A., et al. (2007). Inhibition of ceramide synthesis ameliorates glucocorticoid-, saturated-fat-, and obesity-induced insulin resistance. Cell Metab. *5*, 167–179.

Holloszy, J.O. (2013). “Deficiency” of mitochondria in muscle does not cause insulin resistance. Diabetes *62*, 1036–1040.

Holloway, G.P., Benton, C.R., Mullen, K.L., Yoshida, Y., Snook, L.A., Han, X.-X., Glatz, J.F.C., Luiken, J.J.F.P., Lally, J., Dyck, D.J., et al. (2009). In obese rat muscle transport of palmitate is increased and is channeled to triacylglycerol storage despite an increase in mitochondrial palmitate oxidation. Am. J. Physiol. Endocrinol. Metab. *296*, E738–747.

Hu, W., Ross, J., Geng, T., Brice, S.E., and Cowart, L.A. (2011). Differential regulation of dihydroceramide desaturase by palmitate versus monounsaturated fatty acids: implications for insulin resistance. J. Biol. Chem. *286*, 16596–16605.

Huijsman, E., van de Par, C., Economou, C., van der Poel, C., Lynch, G.S., Schoiswohl, G., Haemmerle, G., Zechner, R., and Watt, M.J. (2009). Adipose triacylglycerol lipase deletion alters whole body energy metabolism and impairs exercise performance in mice. Am. J. Physiol. Endocrinol. Metab. *297*, E505–513.

Imamura, M., Inoguchi, T., Ikuyama, S., Taniguchi, S., Kobayashi, K., Nakashima, N., and Nawata, H. (2002). ADRP stimulates lipid accumulation and lipid droplet formation in murine fibroblasts. Am. J. Physiol. Endocrinol. Metab. *283*, E775–783.

Itani, S.I., Zhou, Q., Pories, W.J., MacDonald, K.G., and Dohm, G.L. (2000). Involvement of protein kinase C in human skeletal muscle insulin resistance and obesity. Diabetes *49*, 1353–1358.

Itani, S.I., Pories, W.J., Macdonald, K.G., and Dohm, G.L. (2001). Increased protein kinase C theta in skeletal muscle of diabetic patients. Metab. Clin. Exp. *50*, 553–557.

Itani, S.I., Ruderman, N.B., Schmieder, F., and Boden, G. (2002). Lipid-induced insulin resistance in human muscle is associated with changes in diacylglycerol, protein kinase C, and IkappaB-alpha. Diabetes *51*, 2005–2011.

Jacob, S., Machann, J., Rett, K., Brechtel, K., Volk, A., Renn, W., Maerker, E., Matthaei, S., Schick, F., Claussen, C.D., et al. (1999). Association of increased intramyocellular lipid content with insulin resistance in lean nondiabetic offspring of type 2 diabetic subjects. Diabetes *48*, 1113–1119.

Jenkins, C.M., Mancuso, D.J., Yan, W., Sims, H.F., Gibson, B., and Gross, R.W. (2004). Identification, cloning, expression, and purification of three novel human calcium-independent phospholipase A2 family members possessing triacylglycerol lipase and acylglycerol transacylase activities. J. Biol. Chem. *279*, 48968–48975.

Jensen, M.D., Haymond, M.W., Gerich, J.E., Cryer, P.E., and Miles, J.M. (1987). Lipolysis during fasting. Decreased suppression by insulin and increased stimulation by epinephrine. J. Clin. Invest. *79*, 207–213.

Jensen, M.D., Haymond, M.W., Rizza, R.A., Cryer, P.E., and Miles, J.M. (1989). Influence of body fat distribution on free fatty acid metabolism in obesity. J. Clin. Invest. *83*, 1168–1173.

Jocken, J.W.E., Smit, E., Goossens, G.H., Essers, Y.P.G., van Baak, M.A., Mensink, M., Saris, W.H.M., and Blaak, E.E. (2008). Adipose triglyceride lipase (ATGL) expression in human skeletal muscle is type I (oxidative) fiber specific. Histochem. Cell Biol. *129*, 535–538.

Jocken, J.W.E., Moro, C., Goossens, G.H., Hansen, D., Mairal, A., Hesselink, M.K.C., Langin, D., van Loon, L.J.C., and Blaak, E.E. (2010). Skeletal muscle lipase content and activity in obesity and type 2 diabetes. J. Clin. Endocrinol. Metab. *95*, 5449–5453.

Joza, N., Oudit, G.Y., Brown, D., Bénit, P., Kassiri, Z., Vahsen, N., Benoit, L., Patel, M.M., Nowikovsky, K., Vassault, A., et al. (2005). Muscle-specific loss of apoptosis-inducing factor leads to mitochondrial dysfunction, skeletal muscle atrophy, and dilated cardiomyopathy. Mol. Cell. Biol. *25*, 10261–10272.

Kanaley, J.A., Shadid, S., Sheehan, M.T., Guo, Z., and Jensen, M.D. (2009). Relationship between plasma free fatty acid, intramyocellular triglycerides and long-chain acylcarnitines in resting humans. J. Physiol. (Lond.) *587*, 5939–5950.

Karlsson, M., Contreras, J.A., Hellman, U., Tornqvist, H., and Holm, C. (1997). cDNA cloning, tissue distribution, and identification of the catalytic triad of monoglyceride lipase. Evolutionary relationship to esterases, lysophospholipases, and haloperoxidases. J. Biol. Chem. *272*, 27218–27223.

Karpe, F., Dickmann, J.R., and Frayn, K.N. (2011). Fatty acids, obesity, and insulin resistance: time for a reevaluation. Diabetes *60*, 2441–2449.

Kelley, D.E., Goodpaster, B., Wing, R.R., and Simoneau, J.A. (1999). Skeletal muscle fatty acid metabolism in association with insulin resistance, obesity, and weight loss. Am. J. Physiol. *277*, E1130–1141.

Kelley, D.E., He, J., Menshikova, E.V., and Ritov, V.B. (2002). Dysfunction of mitochondria in human skeletal muscle in type 2 diabetes. Diabetes *51*, 2944–2950.

Kiens, B. (2006). Skeletal muscle lipid metabolism in exercise and insulin resistance. Physiol. Rev. *86*, 205–243.

Kim, J.K., Fillmore, J.J., Sunshine, M.J., Albrecht, B., Higashimori, T., Kim, D.-W., Liu, Z.-X., Soos, T.J., Cline, G.W., O'Brien, W.R., et al. (2004a). PKC-theta knockout mice are protected from fat-induced insulin resistance. J. Clin. Invest. *114*, 823–827.

Kim, J.K., Gimeno, R.E., Higashimori, T., Kim, H.-J., Choi, H., Punreddy, S., Mozell, R.L., Tan, G., Stricker-Krongrad, A., Hirsch, D.J., et al. (2004b). Inactivation of fatty acid transport protein 1 prevents fat-induced insulin resistance in skeletal muscle. J. Clin. Invest. *113*, 756–763.

Kjaer, M., Howlett, K., Langfort, J., Zimmerman-Belsing, T., Lorentsen, J., Bulow, J., Ihlemann, J., Feldt-Rasmussen, U., and Galbo, H. (2000). Adrenaline and glycogenolysis in skeletal muscle during exercise: a study in adrenalectomised humans. J. Physiol. (Lond.) *528 Pt 2*, 371–378.

Koves, T.R., Ussher, J.R., Noland, R.C., Slentz, D., Mosedale, M., Ilkayeva, O., Bain, J., Stevens, R., Dyck, J.R.B., Newgard, C.B., et al. (2008). Mitochondrial overload and incomplete fatty acid oxidation contribute to skeletal muscle insulin resistance. Cell Metab. *7*, 45–56.

Krintel, C., Osmark, P., Larsen, M.R., Resjö, S., Logan, D.T., and Holm, C. (2008). Ser649 and Ser650 are the major determinants of protein kinase A-mediated activation of human hormone-sensitive lipase against lipid substrates. PLoS ONE *3*, e3756.

Krssak, M., Falk Petersen, K., Dresner, A., DiPietro, L., Vogel, S.M., Rothman, D.L., Roden, M., and Shulman, G.I. (1999). Intramyocellular lipid concentrations are correlated with insulin sensitivity in humans: a 1H NMR spectroscopy study. Diabetologia *42*, 113–116.

Lafontan, M., and Langin, D. (2009). Lipolysis and lipid mobilization in human adipose tissue. Prog. Lipid Res. *48*, 275–297.

Langfort, J., Ploug, T., Ihlemann, J., Saldo, M., Holm, C., and Galbo, H. (1999). Expression of hormone-sensitive lipase and its regulation by adrenaline in skeletal muscle. Biochem. J. *340 (Pt 2)*, 459–465.

Langfort, J., Ploug, T., Ihlemann, J., Holm, C., and Galbo, H. (2000). Stimulation of hormone-sensitive lipase activity by contractions in rat skeletal muscle. Biochem. J. *351*, 207–214.

Langin, D., Dicker, A., Tavernier, G., Hoffstedt, J., Mairal, A., Rydén, M., Arner, E., Sicard, A., Jenkins, C.M., Viguerie, N., et al. (2005). Adipocyte lipases and defect of lipolysis in human obesity. Diabetes *54*, 3190–3197.

Larigauderie, G., Furman, C., Jaye, M., Lasselin, C., Copin, C., Fruchart, J.-C., Castro, G., and Rouis, M. (2004). Adipophilin enhances lipid accumulation and prevents lipid efflux from THP-1 macrophages: potential role in atherogenesis. Arterioscler. Thromb. Vasc. Biol. *24*, 504–510.

Lass, A., Zimmermann, R., Haemmerle, G., Riederer, M., Schoiswohl, G., Schweiger, M., Kienesberger, P., Strauss, J.G., Gorkiewicz, G., and Zechner, R. (2006). Adipose triglyceride lipase-mediated lipolysis of cellular fat stores is activated by CGI-58 and defective in Chanarin-Dorfman Syndrome. Cell Metab. *3*, 309–319.

Lee, D.P., Deonarine, A.S., Kienetz, M., Zhu, Q., Skrzypczak, M., Chan, M., and Choy, P.C. (2001). A novel pathway for lipid biosynthesis: the direct acylation of glycerol. J. Lipid Res. *42*, 1979–1986.

Lehner, R., and Kuksis, A. (1995). Triacylglycerol synthesis by purified triacylglycerol synthetase of rat intestinal mucosa. Role of acyl-CoA acyltransferase. J. Biol. Chem. *270*, 13630–13636.

Lessard, S.J., Rivas, D.A., Chen, Z.-P., Bonen, A., Febbraio, M.A., Reeder, D.W., Kemp, B.E., Yaspelkis, B.B., 3rd, and Hawley, J.A. (2007). Tissue-specific effects of rosiglitazone and exercise in the treatment of lipid-induced insulin resistance. Diabetes *56*, 1856–1864.

Levin, M.C., Monetti, M., Watt, M.J., Sajan, M.P., Stevens, R.D., Bain, J.R., Newgard, C.B., Farese, R.V., Sr, and Farese, R.V., Jr (2007). Increased lipid accumulation and insulin resistance in transgenic mice expressing DGAT2 in glycolytic (type II) muscle. Am. J. Physiol. Endocrinol. Metab. *293*, E1772–1781.

Lewin, T.M., Granger, D.A., Kim, J.H., and Coleman, R.A. (2001). Regulation of mitochondrial sn-glycerol-3-phosphate acyltransferase activity: response to feeding status is unique in various rat tissues and is discordant with protein expression. Arch. Biochem. Biophys. *396*, 119–127.

Li, H., Song, Y., Zhang, L.-J., Gu, Y., Li, F.-F., Pan, S.-Y., Jiang, L.-N., Liu, F., Ye, J., and Li, Q. (2012). LSDP5 enhances triglyceride storage in hepatocytes by influencing lipolysis and fatty acid β-oxidation of lipid droplets. PLoS ONE *7*, e36712.

Li, M., Paran, C., Wolins, N.E., and Horowitz, J.F. (2011a). High muscle lipid content in obesity is not due to enhanced activation of key triglyceride esterification enzymes or the suppression of lipolytic proteins. Am. J. Physiol. Endocrinol. Metab. *300*, E699–707.

Li, Y., Soos, T.J., Li, X., Wu, J., Degennaro, M., Sun, X., Littman, D.R., Birnbaum, M.J., and Polakiewicz, R.D. (2004). Protein kinase C Theta inhibits insulin signaling by phosphorylating IRS1 at Ser(1101). J. Biol. Chem. *279*, 45304–45307.

Li, Z., Zhang, H., Liu, J., Liang, C.-P., Li, Y., Li, Y., Teitelman, G., Beyer, T., Bui, H.H., Peake, D.A., et al. (2011b). Reducing plasma membrane sphingomyelin increases insulin sensitivity. Mol. Cell. Biol. *31*, 4205–4218.

Lipina, C., and Hundal, H.S. (2011). Sphingolipids: agents provocateurs in the pathogenesis of insulin resistance. Diabetologia *54*, 1596–1607.

Listenberger, L.L., Ostermeyer-Fay, A.G., Goldberg, E.B., Brown, W.J., and Brown, D.A. (2007). Adipocyte differentiation-related protein reduces the lipid droplet association of adipose triglyceride lipase and slows triacylglycerol turnover. J. Lipid Res. *48*, 2751–2761.

Liu, L., Zhang, Y., Chen, N., Shi, X., Tsang, B., and Yu, Y.-H. (2007). Upregulation of myocellular DGAT1 augments triglyceride synthesis in skeletal muscle and protects against fat-induced insulin resistance. J. Clin. Invest. *117*, 1679–1689.

Lowell, B.B., and Shulman, G.I. (2005). Mitochondrial dysfunction and type 2 diabetes. Science *307*, 384–387.

Luiken, J.J., Arumugam, Y., Dyck, D.J., Bell, R.C., Pelsers, M.M., Turcotte, L.P., Tandon, N.N., Glatz, J.F., and Bonen, A. (2001). Increased rates of fatty acid uptake and plasmalemmal fatty acid transporters in obese Zucker rats. J. Biol. Chem. *276*, 40567–40573.

Macpherson, R.E., Ramos, S., Vandenboom, R., Roy, B.D., and Peters, S.J. (2013). Skeletal muscle PLIN proteins, ATGL and CGI-58, interactions at rest and following stimulated contraction. Am. J. Physiol. Regul. Integr. Comp. Physiol.

Mason, R.R., Meex, R.C.R., Lee-Young, R., Canny, B.J., and Watt, M.J. (2012). Phosphorylation of adipose triglyceride lipase Ser(404) is not related to 5’-AMPK activation during moderate-intensity exercise in humans. Am. J. Physiol. Endocrinol. Metab. *303*, E534–541.

McQuaid, S.E., Hodson, L., Neville, M.J., Dennis, A.L., Cheeseman, J., Humphreys, S.M., Ruge, T., Gilbert, M., Fielding, B.A., Frayn, K.N., et al. (2011). Downregulation of adipose tissue fatty acid trafficking in obesity: a driver for ectopic fat deposition? Diabetes *60*, 47–55.

Merrill, A.H., Jr (2002). De novo sphingolipid biosynthesis: a necessary, but dangerous, pathway. J. Biol. Chem. *277*, 25843–25846.

Miele, C., Paturzo, F., Teperino, R., Sakane, F., Fiory, F., Oriente, F., Ungaro, P., Valentino, R., Beguinot, F., and Formisano, P. (2007). Glucose regulates diacylglycerol intracellular levels and protein kinase C activity by modulating diacylglycerol kinase subcellular localization. J. Biol. Chem. *282*, 31835–31843.

Mitsutake, S., Date, T., Yokota, H., Sugiura, M., Kohama, T., and Igarashi, Y. (2012). Ceramide kinase deficiency improves diet-induced obesity and insulin resistance. FEBS Lett. *586*, 1300–1305.

Mittendorfer, B., Magkos, F., Fabbrini, E., Mohammed, B.S., and Klein, S. (2009). Relationship between body fat mass and free fatty acid kinetics in men and women. Obesity (Silver Spring) *17*, 1872–1877.

Miyoshi, H., Souza, S.C., Zhang, H.-H., Strissel, K.J., Christoffolete, M.A., Kovsan, J., Rudich, A., Kraemer, F.B., Bianco, A.C., Obin, M.S., et al. (2006). Perilipin promotes hormone-sensitive lipase-mediated adipocyte lipolysis via phosphorylation-dependent and -independent mechanisms. J. Biol. Chem. *281*, 15837–15844.

Miyoshi, H., Perfield, J.W., 2nd, Souza, S.C., Shen, W.-J., Zhang, H.-H., Stancheva, Z.S., Kraemer, F.B., Obin, M.S., and Greenberg, A.S. (2007). Control of adipose triglyceride lipase action by serine 517 of perilipin A globally regulates protein kinase A-stimulated lipolysis in adipocytes. J. Biol. Chem. *282*, 996–1002.

Moore, H.-P.H., Silver, R.B., Mottillo, E.P., Bernlohr, D.A., and Granneman, J.G. (2005). Perilipin targets a novel pool of lipid droplets for lipolytic attack by hormone-sensitive lipase. J. Biol. Chem. *280*, 43109–43120.

Mootha, V.K., Lindgren, C.M., Eriksson, K.-F., Subramanian, A., Sihag, S., Lehar, J., Puigserver, P., Carlsson, E., Ridderstråle, M., Laurila, E., et al. (2003). PGC-1alpha-responsive genes involved in oxidative phosphorylation are coordinately downregulated in human diabetes. Nat. Genet. *34*, 267–273.

Morino, K., Petersen, K.F., Dufour, S., Befroy, D., Frattini, J., Shatzkes, N., Neschen, S., White, M.F., Bilz, S., Sono, S., et al. (2005). Reduced mitochondrial density and

increased IRS-1 serine phosphorylation in muscle of insulin-resistant offspring of type 2 diabetic parents. J. Clin. Invest. *115*, 3587–3593.

Moro, C., Bajpeyi, S., and Smith, S.R. (2008). Determinants of intramyocellular triglyceride turnover: implications for insulin sensitivity. Am. J. Physiol. Endocrinol. Metab. *294*, E203–213.

Moro, C., Galgani, J.E., Luu, L., Pasarica, M., Mairal, A., Bajpeyi, S., Schmitz, G., Langin, D., Liebisch, G., and Smith, S.R. (2009). Influence of gender, obesity, and muscle lipase activity on intramyocellular lipids in sedentary individuals. J. Clin. Endocrinol. Metab. *94*, 3440–3447.

Mulder, H., Sörhede-Winzell, M., Contreras, J.A., Fex, M., Ström, K., Ploug, T., Galbo, H., Arner, P., Lundberg, C., Sundler, F., et al. (2003). Hormone-sensitive lipase null mice exhibit signs of impaired insulin sensitivity whereas insulin secretion is intact. J. Biol. Chem. *278*, 36380–36388.

Muoio, D.M., Seefeld, K., Witters, L.A., and Coleman, R.A. (1999). AMP-activated kinase reciprocally regulates triacylglycerol synthesis and fatty acid oxidation in liver and muscle: evidence that sn-glycerol-3-phosphate acyltransferase is a novel target. Biochem. J. *338 (Pt 3)*, 783–791.

Nagle, C.A., An, J., Shiota, M., Torres, T.P., Cline, G.W., Liu, Z.-X., Wang, S., Catlin, R.L., Shulman, G.I., Newgard, C.B., et al. (2007). Hepatic overexpression of glycerol-sn-3-phosphate acyltransferase 1 in rats causes insulin resistance. J. Biol. Chem. *282*, 14807–14815.

Neschen, S., Morino, K., Hammond, L.E., Zhang, D., Liu, Z.-X., Romanelli, A.J., Cline, G.W., Pongratz, R.L., Zhang, X.-M., Choi, C.S., et al. (2005). Prevention of hepatic steatosis and hepatic insulin resistance in mitochondrial acyl-CoA:glycerol-sn-3-phosphate acyltransferase 1 knockout mice. Cell Metab. *2*, 55–65.

Nikolić, N., Bakke, S.S., Kase, E.T., Rudberg, I., Flo Halle, I., Rustan, A.C., Thoresen, G.H., and Aas, V. (2012). Electrical pulse stimulation of cultured human skeletal muscle cells as an in vitro model of exercise. PLoS ONE *7*, e33203.

Nishizuka, Y. (1995). Protein kinase C and lipid signaling for sustained cellular responses. FASEB J. *9*, 484–496.

Okazaki, H., Osuga, J.-I., Tamura, Y., Yahagi, N., Tomita, S., Shionoiri, F., Iizuka, Y., Ohashi, K., Harada, K., Kimura, S., et al. (2002). Lipolysis in the absence of hormone-sensitive lipase: evidence for a common mechanism regulating distinct lipases. Diabetes *51*, 3368–3375.

Ong, J.M., and Kern, P.A. (1989). Effect of feeding and obesity on lipoprotein lipase activity, immunoreactive protein, and messenger RNA levels in human adipose tissue. J. Clin. Invest. *84*, 305–311.

Pagnon, J., Matzaris, M., Stark, R., Meex, R.C.R., Macaulay, S.L., Brown, W., O'Brien, P.E., Tiganis, T., and Watt, M.J. (2012). Identification and functional characterization of protein kinase A phosphorylation sites in the major lipolytic protein, adipose triglyceride lipase. Endocrinology *153*, 4278–4289.

Pan, D.A., Lillioja, S., Kriketos, A.D., Milner, M.R., Baur, L.A., Bogardus, C., Jenkins, A.B., and Storlien, L.H. (1997). Skeletal muscle triglyceride levels are inversely related to insulin action. Diabetes *46*, 983–988.

Park, S.-Y., Kim, H.-J., Wang, S., Higashimori, T., Dong, J., Kim, Y.-J., Cline, G., Li, H., Prentki, M., Shulman, G.I., et al. (2005). Hormone-sensitive lipase knockout mice have increased hepatic insulin sensitivity and are protected from short-term diet-induced insulin resistance in skeletal muscle and heart. Am. J. Physiol. Endocrinol. Metab. *289*, E30–39.

Patti, M.E., Butte, A.J., Crunkhorn, S., Cusi, K., Berria, R., Kashyap, S., Miyazaki, Y., Kohane, I., Costello, M., Saccone, R., et al. (2003). Coordinated reduction of genes of oxidative metabolism in humans with insulin resistance and diabetes: Potential role of PGC1 and NRF1. Proc. Natl. Acad. Sci. U.S.A. *100*, 8466–8471.

Petersen, K.F., Dufour, S., Befroy, D., Garcia, R., and Shulman, G.I. (2004). Impaired mitochondrial activity in the insulin-resistant offspring of patients with type 2 diabetes. N. Engl. J. Med. *350*, 664–671.

Petersen, K.F., Dufour, S., and Shulman, G.I. (2005). Decreased insulin-stimulated ATP synthesis and phosphate transport in muscle of insulin-resistant offspring of type 2 diabetic parents. PLoS Med. *2*, e233.

Pickersgill, L., Litherland, G.J., Greenberg, A.S., Walker, M., and Yeaman, S.J. (2007). Key role for ceramides in mediating insulin resistance in human muscle cells. J. Biol. Chem. *282*, 12583–12589.

Pollak, N.M., M., Schweiger, M., Jaeger, D., Kolb, D., Kumari, M., Schreiber, R., Kolleritsch, S., Markolin, P., Grabner, G.F., Heier, C., et al. (2013). Cardiac-specific overexpression of perilipin 5 provokes severe cardiac steatosis via the formation of a lipolytic barrier. J. Lipid Res.

Pospisilik, J.A., Knauf, C., Joza, N., Benit, P., Orthofer, M., Cani, P.D., Ebersberger, I., Nakashima, T., Sarao, R., Neely, G., et al. (2007). Targeted deletion of AIF decreases mitochondrial oxidative phosphorylation and protects from obesity and diabetes. Cell *131*, 476–491.

Powell, D.J., Hajduch, E., Kular, G., and Hundal, H.S. (2003). Ceramide disables 3-phosphoinositide binding to the pleckstrin homology domain of protein kinase B (PKB)/Akt by a PKCzeta-dependent mechanism. Mol. Cell. Biol. *23*, 7794–7808.

Prats, C., Donsmark, M., Qvortrup, K., Londos, C., Sztalryd, C., Holm, C., Galbo, H., and Ploug, T. (2006). Decrease in intramuscular lipid droplets and translocation of HSL in response to muscle contraction and epinephrine. J. Lipid Res. *47*, 2392–2399.

Ravichandran, L.V., Esposito, D.L., Chen, J., and Quon, M.J. (2001). Protein kinase C-zeta phosphorylates insulin receptor substrate-1 and impairs its ability to activate phosphatidylinositol 3-kinase in response to insulin. J. Biol. Chem. *276*, 3543–3549.

Reaven, G.M., Hollenbeck, C., Jeng, C.Y., Wu, M.S., and Chen, Y.D. (1988). Measurement of plasma glucose, free fatty acid, lactate, and insulin for 24 h in patients with NIDDM. Diabetes *37*, 1020–1024.

Rieusset, J., Chauvin, M.-A., Durand, A., Bravard, A., Laugerette, F., Michalski, M.-C., and Vidal, H. (2012). Reduction of endoplasmic reticulum stress using chemical

chaperones or Grp78 overexpression does not protect muscle cells from palmitate-induced insulin resistance. Biochem. Biophys. Res. Commun. *417*, 439–445.

Roepstorff, C., Vistisen, B., Donsmark, M., Nielsen, J.N., Galbo, H., Green, K.A., Hardie, D.G., Wojtaszewski, J.F.P., Richter, E.A., and Kiens, B. (2004). Regulation of hormone-sensitive lipase activity and Ser563 and Ser565 phosphorylation in human skeletal muscle during exercise. J. Physiol. (Lond.) *560*, 551–562.

Roepstorff, C., Donsmark, M., Thiele, M., Vistisen, B., Stewart, G., Vissing, K., Schjerling, P., Hardie, D.G., Galbo, H., and Kiens, B. (2006). Sex differences in hormone-sensitive lipase expression, activity, and phosphorylation in skeletal muscle at rest and during exercise. Am. J. Physiol. Endocrinol. Metab. *291*, E1106–1114.

Roust, L.R., and Jensen, M.D. (1993). Postprandial free fatty acid kinetics are abnormal in upper body obesity. Diabetes *42*, 1567–1573.

Russell, L., and Forsdyke, D.R. (1991). A human putative lymphocyte G0/G1 switch gene containing a CpG-rich island encodes a small basic protein with the potential to be phosphorylated. DNA Cell Biol. *10*, 581–591.

Samuel, V.T., and Shulman, G.I. (2012). Mechanisms for insulin resistance: common threads and missing links. Cell *148*, 852–871.

Sánchez-Piñera, P., Micol, V., Corbalán-García, S., and Gómez-Fernández, J.C. (1999). A comparative study of the activation of protein kinase C alpha by different diacylglycerol isomers. Biochem. J. *337 (Pt 3)*, 387–395.

Schenk, S., and Horowitz, J.F. (2007). Acute exercise increases triglyceride synthesis in skeletal muscle and prevents fatty acid-induced insulin resistance. J. Clin. Invest. *117*, 1690–1698.

Schmitz-Peiffer, C. (2010). Targeting ceramide synthesis to reverse insulin resistance. Diabetes *59*, 2351–2353.

Schmitz-Peiffer, C., and Biden, T.J. (2008). Protein kinase C function in muscle, liver, and beta-cells and its therapeutic implications for type 2 diabetes. Diabetes *57*, 1774–1783.

Schoiswohl, G., Schweiger, M., Schreiber, R., Gorkiewicz, G., Preiss-Landl, K., Taschler, U., Zierler, K.A., Radner, F.P.W., Eichmann, T.O., Kienesberger, P.C., et al. (2010). Adipose triglyceride lipase plays a key role in the supply of the working muscle with fatty acids. J. Lipid Res. *51*, 490–499.

Schrauwen-Hinderling, V.B., Schrauwen, P., Hesselink, M.K.C., van Engelshoven, J.M.A., Nicolay, K., Saris, W.H.M., Kessels, A.G.H., and Kooi, M.E. (2003). The increase in intramyocellular lipid content is a very early response to training. J. Clin. Endocrinol. Metab. *88*, 1610–1616.

Schweiger, M., Paar, M., Eder, C., Brandis, J., Moser, E., Gorkiewicz, G., Grond, S., Radner, F.P.W., Cerk, I., Cornaciu, I., et al. (2012). G0/G1 switch gene-2 regulates human adipocyte lipolysis by affecting activity and localization of adipose triglyceride lipase. J. Lipid Res. *53*, 2307–2317.

Sekiya, M., Osuga, J., Okazaki, H., Yahagi, N., Harada, K., Shen, W.-J., Tamura, Y., Tomita, S., Iizuka, Y., Ohashi, K., et al. (2004). Absence of hormone-sensitive lipase inhibits obesity and adipogenesis in Lep ob/ob mice. J. Biol. Chem. *279*, 15084–15090.

Shepherd, S.O., Cocks, M., Tipton, K.D., Ranasinghe, A.M., Barker, T.A., Burniston, J.G., Wagenmakers, A.J.M., and Shaw, C.S. (2013). Sprint interval and traditional endurance training increase net intramuscular triglyceride breakdown and expression of perilipin 2 and 5. J. Physiol. (Lond.) *591*, 657–675.

Shi, Y., and Cheng, D. (2009). Beyond triglyceride synthesis: the dynamic functional roles of MGAT and DGAT enzymes in energy metabolism. Am. J. Physiol. Endocrinol. Metab. *297*, E10–18.

Simoneau, J.A., and Kelley, D.E. (1997). Altered glycolytic and oxidative capacities of skeletal muscle contribute to insulin resistance in NIDDM. J. Appl. Physiol. *83*, 166–171.

Simoneau, J.A., Colberg, S.R., Thaete, F.L., and Kelley, D.E. (1995). Skeletal muscle glycolytic and oxidative enzyme capacities are determinants of insulin sensitivity and muscle composition in obese women. FASEB J. *9*, 273–278.

Simoneau, J.A., Veerkamp, J.H., Turcotte, L.P., and Kelley, D.E. (1999). Markers of capacity to utilize fatty acids in human skeletal muscle: relation to insulin resistance and obesity and effects of weight loss. FASEB J. *13*, 2051–2060.

Skovbro, M., Baranowski, M., Skov-Jensen, C., Flint, A., Dela, F., Gorski, J., and Helge, J.W. (2008). Human skeletal muscle ceramide content is not a major factor in muscle insulin sensitivity. Diabetologia *51*, 1253–1260.

Sparks, L.M., Moro, C., Ukropcova, B., Bajpeyi, S., Civitarese, A.E., Hulver, M.W., Thoresen, G.H., Rustan, A.C., and Smith, S.R. (2011). Remodeling lipid metabolism and improving insulin responsiveness in human primary myotubes. PLoS ONE *6*, e21068.

Straczkowski, M., Kowalska, I., Nikolajuk, A., Dzienis-Straczkowska, S., Kinalska, I., Baranowski, M., Zendzian-Piotrowska, M., Brzezinska, Z., and Gorski, J. (2004). Relationship between insulin sensitivity and sphingomyelin signaling pathway in human skeletal muscle. Diabetes *53*, 1215–1221.

Straczkowski, M., Kowalska, I., Baranowski, M., Nikolajuk, A., Otziomek, E., Zabielski, P., Adamska, A., Blachnio, A., Gorski, J., and Gorska, M. (2007). Increased skeletal muscle ceramide level in men at risk of developing type 2 diabetes. Diabetologia *50*, 2366–2373.

Subramanian, V., Rothenberg, A., Gomez, C., Cohen, A.W., Garcia, A., Bhattacharyya, S., Shapiro, L., Dolios, G., Wang, R., Lisanti, M.P., et al. (2004). Perilipin A mediates the reversible binding of CGI-58 to lipid droplets in 3T3-L1 adipocytes. J. Biol. Chem. *279*, 42062–42071.

Tagami, S., Inokuchi Ji, J., Kabayama, K., Yoshimura, H., Kitamura, F., Uemura, S., Ogawa, C., Ishii, A., Saito, M., Ohtsuka, Y., et al. (2002). Ganglioside GM3 participates in the pathological conditions of insulin resistance. J. Biol. Chem. *277*, 3085–3092.

Talanian, J.L., Tunstall, R.J., Watt, M.J., Duong, M., Perry, C.G.R., Steinberg, G.R., Kemp, B.E., Heigenhauser, G.J.F., and Spriet, L.L. (2006). Adrenergic regulation of HSL serine phosphorylation and activity in human skeletal muscle during the onset of exercise. Am. J. Physiol. Regul. Integr. Comp. Physiol. *291*, R1094–1099.

Teruel, T., Hernandez, R., and Lorenzo, M. (2001). Ceramide mediates insulin resistance by tumor necrosis factor-alpha in brown adipocytes by maintaining Akt in an inactive dephosphorylated state. Diabetes *50*, 2563–2571.

Thiebaud, D., Jacot, E., DeFronzo, R.A., Maeder, E., Jequier, E., and Felber, J.P. (1982). The effect of graded doses of insulin on total glucose uptake, glucose oxidation, and glucose storage in man. Diabetes *31*, 957–963.

Thompson, A.L., and Cooney, G.J. (2000). Acyl-CoA inhibition of hexokinase in rat and human skeletal muscle is a potential mechanism of lipid-induced insulin resistance. Diabetes *49*, 1761–1765.

Thrush, A.B., Brindley, D.N., Chabowski, A., Heigenhauser, G.J., and Dyck, D.J. (2009). Skeletal muscle lipogenic protein expression is not different between lean and obese individuals: a potential factor in ceramide accumulation. J. Clin. Endocrinol. Metab. *94*, 5053–5061.

Timmers, S., de Vogel-van den Bosch, J., Hesselink, M.K.C., van Beurden, D., Schaart, G., Ferraz, M.J., Losen, M., Martinez-Martinez, P., De Baets, M.H., Aerts, J.M.F.G., et al. (2011). Paradoxical increase in TAG and DAG content parallel the insulin sensitizing effect of unilateral DGAT1 overexpression in rat skeletal muscle. PLoS ONE *6*, e14503.

Tippett, P.S., and Neet, K.E. (1982). An allosteric model for the inhibition of glucokinase by long chain acyl coenzyme A. J. Biol. Chem. *257*, 12846–12852.

Topham, M.K., and Epand, R.M. (2009). Mammalian diacylglycerol kinases: molecular interactions and biological functions of selected isoforms. Biochim. Biophys. Acta *1790*, 416–424.

Villena, J.A., Roy, S., Sarkadi-Nagy, E., Kim, K.-H., and Sul, H.S. (2004). Desnutrin, an adipocyte gene encoding a novel patatin domain-containing protein, is induced by fasting and glucocorticoids: ectopic expression of desnutrin increases triglyceride hydrolysis. J. Biol. Chem. *279*, 47066–47075.

Wang, H., Sreenevasan, U., Hu, H., Saladino, A., Polster, B.M., Lund, L.M., Gong, D., Stanley, W.C., and Sztalryd, C. (2011a). Perilipin 5, a lipid droplet-associated

protein, provides physical and metabolic linkage to mitochondria. J. Lipid Res. *52*, 2159–2168.

Wang, H., Bell, M., Sreenevasan, U., Hu, H., Liu, J., Dalen, K., Londos, C., Yamaguchi, T., Rizzo, M.A., Coleman, R., et al. (2011b). Unique regulation of adipose triglyceride lipase (ATGL) by perilipin 5, a lipid droplet-associated protein. J. Biol. Chem. *286*, 15707–15715.

Wang, H., Sreenivasan, U., Gong, D.-W., O'Connell, K.A., Dabkowski, E.R., Hecker, P.A., Ionica, N., Konig, M., Mahurkar, A., Sun, Y., et al. (2013). Cardiomyocyte specific perilipin 5 over expression leads to myocardial steatosis, and modest cardiac dysfunction. J. Lipid Res.

Watson, M.L., Coghlan, M., and Hundal, H.S. (2009). Modulating serine palmitoyl transferase (SPT) expression and activity unveils a crucial role in lipid-induced insulin resistance in rat skeletal muscle cells. Biochem. J. *417*, 791–801.

Watt, M.J., and Spriet, L.L. (2010). Triacylglycerol lipases and metabolic control: implications for health and disease. Am. J. Physiol. Endocrinol. Metab. *299*, E162–168.

Watt, M.J., Stellingwerff, T., Heigenhauser, G.J.F., and Spriet, L.L. (2003). Effects of plasma adrenaline on hormone-sensitive lipase at rest and during moderate exercise in human skeletal muscle. J. Physiol. (Lond.) *550*, 325–332.

Watt, M.J., Holmes, A.G., Pinnamaneni, S.K., Garnham, A.P., Steinberg, G.R., Kemp, B.E., and Febbraio, M.A. (2006). Regulation of HSL serine phosphorylation in skeletal muscle and adipose tissue. Am. J. Physiol. Endocrinol. Metab. *290*, E500–508.

Welch, C., Santra, M.K., El-Assaad, W., Zhu, X., Huber, W.E., Keys, R.A., Teodoro, J.G., and Green, M.R. (2009). Identification of a protein, G0S2, that lacks Bcl-2 homology domains and interacts with and antagonizes Bcl-2. Cancer Res. *69*, 6782–6789.

Wolins, N.E., Quaynor, B.K., Skinner, J.R., Tzekov, A., Croce, M.A., Gropler, M.C., Varma, V., Yao-Borengasser, A., Rasouli, N., Kern, P.A., et al. (2006). OXPAT/PAT-1

is a PPAR-induced lipid droplet protein that promotes fatty acid utilization. Diabetes *55*, 3418–3428.

Yamada, T., Park, C.S., Burns, A., Nakada, D., and Lacorazza, H.D. (2012). The cytosolic protein G0S2 maintains quiescence in hematopoietic stem cells. PLoS ONE *7*, e38280.

Yamaguchi, T., Matsushita, S., Motojima, K., Hirose, F., and Osumi, T. (2006). MLDP, a novel PAT family protein localized to lipid droplets and enriched in the heart, is regulated by peroxisome proliferator-activated receptor alpha. J. Biol. Chem. *281*, 14232–14240.

Yamaguchi, T., Omatsu, N., Morimoto, E., Nakashima, H., Ueno, K., Tanaka, T., Satouchi, K., Hirose, F., and Osumi, T. (2007). CGI-58 facilitates lipolysis on lipid droplets but is not involved in the vesiculation of lipid droplets caused by hormonal stimulation. J. Lipid Res. *48*, 1078–1089.

Yamashita, T., Hashiramoto, A., Haluzik, M., Mizukami, H., Beck, S., Norton, A., Kono, M., Tsuji, S., Daniotti, J.L., Werth, N., et al. (2003). Enhanced insulin sensitivity in mice lacking ganglioside GM3. Proc. Natl. Acad. Sci. U.S.A. *100*, 3445–3449.

Yang, X., Lu, X., Lombès, M., Rha, G.B., Chi, Y.-I., Guerin, T.M., Smart, E.J., and Liu, J. (2010). The G(0)/G(1) switch gene 2 regulates adipose lipolysis through association with adipose triglyceride lipase. Cell Metab. *11*, 194–205.

Yen, C.-L.E., Stone, S.J., Cases, S., Zhou, P., and Farese, R.V., Jr (2002). Identification of a gene encoding MGAT1, a monoacylglycerol acyltransferase. Proc. Natl. Acad. Sci. U.S.A. *99*, 8512–8517.

Yen, C.-L.E., Stone, S.J., Koliwad, S., Harris, C., and Farese, R.V., Jr (2008). Thematic review series: glycerolipids. DGAT enzymes and triacylglycerol biosynthesis. J. Lipid Res. *49*, 2283–2301.

Yu, C., Chen, Y., Cline, G.W., Zhang, D., Zong, H., Wang, Y., Bergeron, R., Kim, J.K., Cushman, S.W., Cooney, G.J., et al. (2002). Mechanism by which fatty acids inhibit insulin activation of insulin receptor substrate-1 (IRS-1)-associated phosphatidylinositol 3-kinase activity in muscle. J. Biol. Chem. *277*, 50230–50236.

Zandbergen, F., Mandard, S., Escher, P., Tan, N.S., Patsouris, D., Jatkoe, T., Rojas-Caro, S., Madore, S., Wahli, W., Tafuri, S., et al. (2005). The G0/G1 switch gene 2 is a novel PPAR target gene. Biochem. J. *392*, 313–324.

Zimmermann, R., Strauss, J.G., Haemmerle, G., Schoiswohl, G., Birner-Gruenberger, R., Riederer, M., Lass, A., Neuberger, G., Eisenhaber, F., Hermetter, A., et al. (2004). Fat mobilization in adipose tissue is promoted by adipose triglyceride lipase. Science *306*, 1383–1386.

ANNEXES

PUBLICATION 4: LA DYNAMIQUE DE LA GOUTTELETTE LIPIDIQUE DU MUSCLE SQUELETTIQUE

Publication 4 : Dynamics of skeletal muscle lipid pools

Badin PM, Langin D, Moro C. (2013) Trends Endocrinol. Metab. In press.

Review

Cell PRESS

Dynamics of skeletal muscle lipid pools

Pierre-Marie Badin[1,2], Dominique Langin[1,2,3], and Cedric Moro[1,2]

[1] Obesity Research Laboratory, Institut National de la Santé et de la Recherche Médicale (INSERM) Unité Mixte de Recherche (UMR) 1048, Institute of Metabolic and Cardiovascular Diseases (I2MC), Toulouse, France
[2] University of Toulouse, UMR1048, Paul Sabatier University, Toulouse, France
[3] Toulouse University Hospitals, Department of Clinical Biochemistry, Toulouse, France

Intramyocellular triacylglycerol (IMTG) is emerging as an important energy fuel source during muscle contraction and are adaptively increased in response to exercise, without adverse physiological effects. Paradoxically, elevated IMTG content in obese and type 2 diabetics has been linked to insulin resistance, highlighting the importance of IMTG pools in physiology and pathology. Two separate views suggest that IMTG dynamics are determinant for skeletal muscle fat oxidation, and that disruption of IMTG dynamics facilitates the accumulation of lipotoxic intermediates such as diacylglycerols and ceramides that interfere with insulin signaling. Thus, understanding the factors that control IMTG dynamics is crucial. Here we discuss recent literature describing the regulation of IMTG pools with a particular emphasis on lipases and lipid droplet (LD)-associated proteins.

IMTGs: dynamic lipid droplets

Skeletal muscle is an important site for glucose storage and lipid utilization. Lipids are stored as triacylglycerols (TAG) in LDs within skeletal muscle, called IMTG (see Glossary), and are used by healthy subjects as a substrate source during exercise [1,2]. Indeed, IMTG pools are adaptively increased in endurance-trained individuals and in response to exercise-training interventions [3,4]. Interestingly, this increase in intramyocellular lipid content does not adversely affect insulin sensitivity or oxidative capacity, both of which remain high, accounting for a phenomenon referred to as athlete's paradox [3]. Currently, the physiological regulation of this lipid pool remains incompletely understood.

By contrast, IMTG content also increases linearly with body fat and is elevated in obesity and type 2 diabetes mellitus (T2DM) [5] without intrinsically inducing insulin resistance. Elevated content of IMTG is accompanied by higher availability of lipotoxic intermediates such as diacylglycerols (DAG) and ceramides that inhibit insulin signaling [6]. However, how IMTG mediates lipotoxicity in obese sedentary subjects is unclear.

Corresponding author: Moro, C. (cedric.moro@inserm.fr).
Keywords: intramyocellular lipids; lipolysis; exercise; fat oxidation; insulin sensitivity; type 2 diabetes; ATGL.

1043-2760/$ – see front matter
 http://dx.doi.org/10.1016/j.tem.2013.08.001

LDs are dynamic organelles resulting from the balance between storage and breakdown of TAG by lipases. In resting humans, fatty acids (FAs) largely traffic through IMTG pools before being oxidized [7]. Moreover, lipase-mediated TAG hydrolysis could generate lipid ligands for the peroxisome proliferator-activated receptors (PPAR) family of nuclear receptors in cardiac [8] and skeletal [9] muscles, thereby increasing oxidative capacity through transcriptional regulation of key target genes. We therefore propose that skeletal muscle LD dynamics may be an important determinant of fat oxidative metabolism, lipotoxicity, and insulin sensitivity.

In this review we critically examine the current knowledge regarding the regulation of IMTG pools during exercise and its pathophysiological implication for metabolic diseases. Particular emphasis is given to lipases and LDs-associated proteins.

Physiological regulation of IMTG pools

IMTG is used as fuel during exercise

Although IMTG stores represent a small fraction of whole-body lipid stores (about 1%) in sedentary subjects, recent studies show that IMTG constitutes an important energy fuel source during exercise [1]. IMTG utilization could

Glossary

Adipose triglyceride lipase (ATGL): also known as patatin-like phospholipase domain-containing protein – PNAPL2, or desnutrin, is the rate-limiting enzyme in TAG hydrolysis in several metabolic tissues.
Diacylglycerol hydrolase (DAGH): this refers to DAG hydrolase activity measured *ex vivo* using a 1(3)-mono[3H]oleyl-2-*O*-mono-oleylglycerol (MOME).
Diacylglycerol *O*-acyltransferase 1 (DGAT1): this is a microsomal rate-limiting enzyme of TAG synthesis. It uses DAG and fatty acyl-CoA as substrates for TAG synthesis in most tissues of the body.
Ectopic lipids: this term defines lipid storage/accumulation in tissues other than adipose tissue. Although present in small quantity in healthy muscle, IMTG content increases during obesity and may contribute to insulin resistance.
Hormone-sensitive lipase (HSL): an enzyme expressed in several metabolic and steroidogenic tissues that displays high affinity for DAG as substrate.
Intramyocellular triacylglycerols (IMTG): the most abundant form of lipid storage within the myocyte. This lipid pool represents an important energy source to supply muscle contraction during exercise.
Mitochondrial glycerol-3-phosphate acyltransferase 1 (mtGPAT): this enzyme is attached to the external membrane of mitochondria and catalyzes the initial step in the glycerolipid biosynthesis pathway.
Monoacylglycerol lipase (MGL): the last enzyme in the lipolytic cascade and is widely distributed across the body.
Perilipins (PLIN): a family of five proteins (PLIN1–5) with varying tissue distribution. They serve as structural components of the lipid droplet.
Triacylglycerol hydrolase (TAGH): TAG hydrolase activity measured *ex vivo* using [9,10-^{3}H(N)] triolein.

provide up to 25% of total energy during moderate intensity exercise; it has been suggested that IMTG stores are selectively depleted by about half in type I oxidative fibers following 1 h of exercise at 65% of peak oxygen uptake [10] and are replenished within 48 h during post-exercise recovery in subjects fed a standard diet [11]. This likely depends on a higher FA availability and uptake by skeletal muscle during the post-exercise recovery [12]. IMTG content, as determined by immunohistochemistry, appears to be 2–3-fold higher in type I oxidative compared to type II glycolytic fibers, suggesting that it represents an important fuel source for type I fibers [13,14]. Indeed, IMTG content is adaptively increased in type I oxidative fibers in response to chronic exercise training [4,13,15]. The underlying molecular mechanism likely involves an increase in the expression and/or activity of FA transporter proteins (cluster of differentiation 36, CD36) and TAG esterification enzymes such as mitochondrial glycerol-3-phosphate acyltransferase 1 (mtGPAT) and diglyceride acyltransferase 1 (DGAT1) [16,17]. In summary, IMTG pools are tightly controlled during acute and chronic exercise to supply energy fuel during muscle contraction, particularly in oxidative type I fibers.

IMTG breakdown: the role of lipases

TAG breakdown is operated by lipases. Monoacylglycerol (MAG) lipase (MGL) and hormone-sensitive lipase (HSL) were the first lipases identified, and both are highly expressed in skeletal muscle [18]. MGL specifically hydrolyzes MAG to produce glycerol, and has no apparent activity against either DAG or TAG. Although MGL deficiency has little effect on adipose tissue mass in mice [19], its exact role in skeletal muscle has not been assessed. HSL displays a 10-fold higher specificity for DAG compared to TAG, MAG and cholesterol esters [18]. Targeted disruption of HSL in transgenic mice revealed that HSL is a major DAG hydrolase (DAGH) in both adipose tissue and skeletal muscle [20–22]. Indeed, HSL null mice display normal TAG but elevated DAG synthesis rate in skeletal muscle. These findings raised question of whether a second, TAG specific, hydrolase exists, and led to the identification of a novel lipase of the PNPLA (patatin-like phospholipase domain-containing protein) family, PNPLA2, also known as adipose triglyceride lipase (ATGL) or desnutrin [23–25]. This enzyme is expressed in the skeletal muscle of mice [25] and humans [26] and ATGL mutations in humans lead to neutral lipid storage diseases with myopathy, indicating a role for ATGL in muscle function [27]. Genetic inactivation of ATGL in mouse leads to massive TAG accumulation in skeletal and cardiac muscle [28], suggesting that ATGL is a dominant TAG hydrolase (TAGH) in muscle. ATGL is also important for adipose-tissue lipolysis because exercise-induced lipid mobilization is severely blunted in ATGL null mice [29,30]. In addition, ATGL overexpression drastically reduces TAG content, and increases FA release and oxidation in human primary myotubes [31]. Interestingly, the two majors lipases, HSL and ATGL, are predominantly expressed in type I oxidative fibers [2,26]. These data confirm that ATGL is the dominant TAG hydrolase, whereas HSL is a major DAG hydrolase in human skeletal muscle, both actively controlling IMTG mobilization.

Turnover of IMTG pools in humans at rest and during exercise

Determination of IMTG kinetics in humans is challenging and studies are rather scarce. However, Sacchetti *et al.* indicated that IMTG pools turn over at a high rate in resting human skeletal muscle [32]. Elegant studies from Jensen's group demonstrated significant IMTG turnover both at rest [7] and during submaximal exercise (45% VO_2 max) [33] in healthy volunteers. The latter studies provided evidence that plasma-derived FAs are esterified into IMTG pools before being oxidized at rest and during exercise. Others reported higher IMTG fractional synthesis rate and decreased saturation of skeletal muscle diacylglycerol in athletes [34], whereas obese male subjects with prediabetes [35] displayed lower IMTG oxidation and turnover with subsequent accumulation of IMTG. In addition, IMTG fractional turnover rate appears to be higher in glycolytic (tibialis anterior) and mixed (gastrocnemius) muscle compared to oxidative (soleus) muscle in rats, in a pattern reciprocal to their IMTG pool size [36]. In summary, IMTG may represent a dynamic lipid pool both at rest and during exercise in humans and disturbances in IMTG turnover are associated with obesity.

Regulation of muscle lipase activity

HSL activity

HSL activity in skeletal muscle is mostly regulated by phosphorylation on five serine residues that are conserved in rats [serines (Ser) 563, 565, 600, 659 and 660) and humans (Ser552, 554, 589, 649 and 650) [37]. Studies of rat soleus muscle revealed that HSL activity is strongly induced by epinephrine and contraction [2]. Prats *et al.* further showed, by confocal imaging of single muscle fibers, that HSL translocates to IMTGs in response to epinephrine or contraction [38]. Epinephrine, through binding to β_2 adrenergic receptors, induces cAMP-dependent protein kinase (PKA) which is known to activate HSL through phosphorylation of Ser563, 659 and 660. Ser659 and 660 are specifically phosphorylated in skeletal muscle during exercise and induce HSL activity *in vitro* [2,39]. In adrenalectomized humans, acute exercise does not induce HSL activity in skeletal muscle, confirming that epinephrine plays a permissive role in exercise-induced HSL activation [40]. Other studies demonstrated that muscle contraction induces HSL activity through calcium-dependent PKC activation (rodent study) [41] and ERK (human study) [42]. By contrast, 5′-AMP-activated protein kinase (AMPK) was shown to inhibit HSL activity through phosphorylation at Ser565 in adipose tissue, although this effect is still a matter of debate when it comes to human skeletal muscle [2]. In summary, acute exercise-mediated HSL activation requires epinephrine and muscle contraction (Figure 1).

ATGL activity

Similarly to HSL, ATGL can also be phosphorylated on Ser404 and 428 in humans, and Ser406 and 430 in mice [43,44]. AMPK induces ATGL Ser406 phosphorylation and increases its TAG hydrolase activity in murine adipocytes [45]. However, studies in human skeletal muscle have dissociated ATGL Ser406 phosphorylation from AMPK activation *in vitro* and *in vivo* during exercise

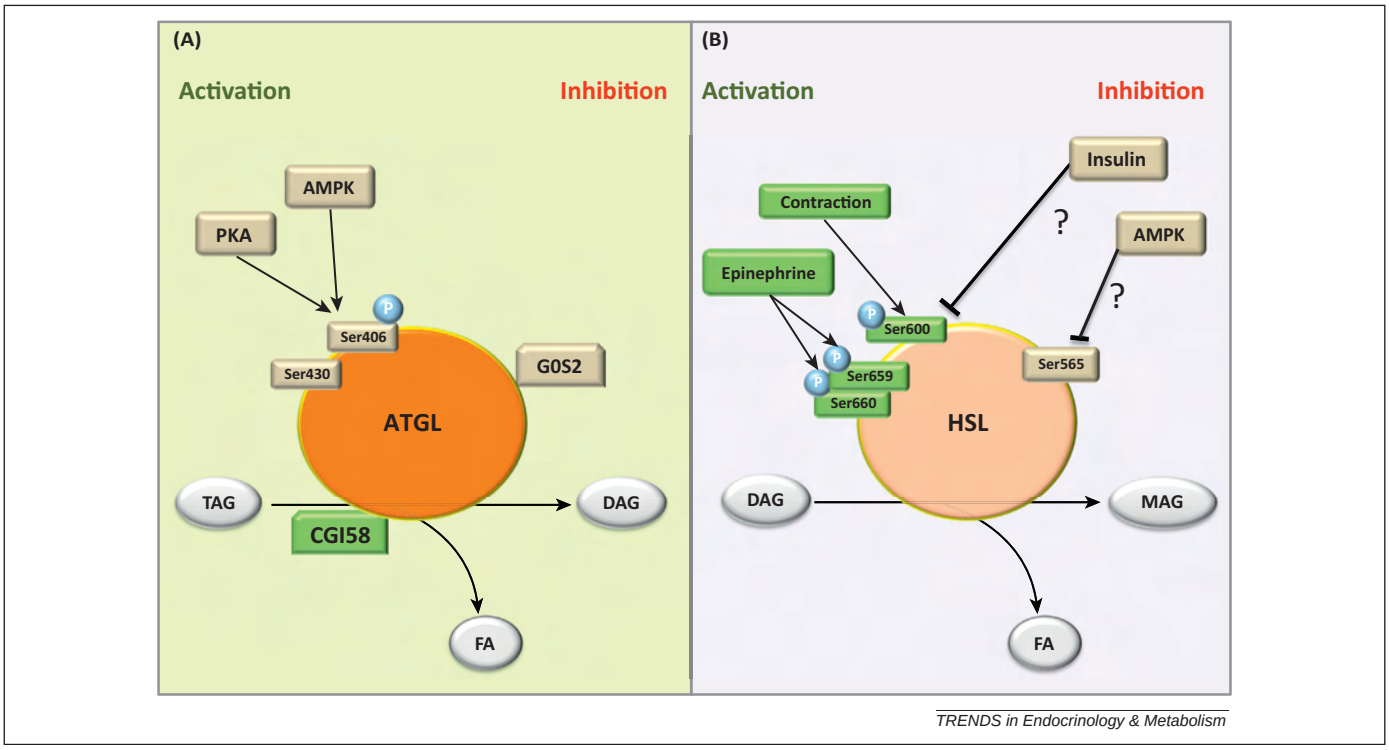

Figure 1. Molecular regulation of lipase activity in skeletal muscle. ATGL appears to be rate-limiting for the hydrolysis of TAG into DAG, whereas HSL mainly hydrolyzes DAG into MAG. Each step releases one FA molecule. **(A)** ATGL activity appears to be regulated positively by CGI-58 and negatively by G0S2. ATGL could also be activated by phosphorylation (P) on Ser406 by AMPK and potentially PKA. The role of Ser430 is currently unknown. **(B)** Muscle contraction activates HSL by phosphorylation on Ser600, and epinephrine does the same via the phosphorylation of Ser659 and Ser660. Unlike in adipose tissue, the inhibitory role of insulin and AMPK on HSL activity is still a matter of debate in muscle. Green boxes indicate what has been demonstrated in skeletal muscle whereas gray boxes highlight what remains to be investigated. Abbreviations: AMPK, 5′-AMP-activated protein kinase; ATGL, adipose triglyceride lipase; DAG, diacylglycerol; FA, fatty acid; HSL, hormone-sensitive lipase; MAG, monoacylglycerol; PKA/PKC, protein kinases A/C; TAG, triacylglycerol.

[46]. Zimmerman *et al.* first demonstrated that ATGL is not phosphorylated by PKA in human HepG2 cells [25], whereas recent data from Pagnon *et al.* show that ATGL can be phosphorylated by PKA at Ser406 in murine adipocytes. β-Adrenergic mediated-ATGL activation resulting in Ser404 phosphorylation induces a modest increase of lipolysis in human adipose tissue explants [47]. Thus, PKA may activate ATGL in a tissue dependent manner. The functional role of Ser430 is currently unknown. In summary, the regulation of ATGL by phosphorylation differs according to species and/or tissue. The regulation and physiological function of ATGL serine phosphorylation in skeletal muscle remain unclear and requires further work.

ATGL activity is regulated by the ATGL coactivator, comparative gene identification 58 (CGI-58). Loss-of-function mutations of CGI-58 are associated with a severe clinical phenotype referred to as the Chanarin–Dorfman syndrome, associated with severe ichtyosis and muscular weakness [48]. CGI-58 is a powerful activator of ATGL in mammalian cells [49] and is coexpressed with ATGL in human skeletal muscle [9,50]. It was recently reported that CGI-58 induces TAG hydrolase activity in human and mouse skeletal muscle extracts [9]. CGI-58 is predominantly expressed in oxidative muscles, where TAG hydrolase activity is the greatest. Upregulation of CGI-58 expression in human primary myotubes accelerates TAG depletion and increases lipolysis and FA oxidation [9]. By contrast, CGI-58 knockdown reduces lipolysis and promotes TAG accumulation. Interestingly, Macpherson *et al.* have shown increased CGI-58/ATGL protein interaction in soleus muscle during contraction versus rest [51]. This suggests that CGI-58 plays a pivotal role in the regulation of skeletal muscle ATGL activity and TAG dynamics, particularly during exercise. By contrast, ATGL activity is inhibited by the G0/G1 switch gene 2 (G0S2) in murine and human adipocytes [52,53]. Because G0S2 appears to be expressed in mouse skeletal muscle [52], future studies should investigate its functional role and physiological relevance in human muscle. Collectively, current data suggest that human skeletal muscle ATGL activity is constitutively controlled by CGI-58 at rest and during contraction, and that ATGL activity may be acutely regulated by phosphorylation in response to hormonal stimulation during exercise (Figure 1).

Perilipins

Proteins of the perilipin (PLIN) family are major structural components of LDs. PLINs are proposed to control lipolysis and lipid storage in most mammalian cells as recently reviewed [54]. Currently there are five members of the PLIN family, and these are widely distributed across the body and have different expression patterns. Although the role of PLIN1 and its interactions with HSL and CGI-58 are well established in adipocytes [54], several studies failed to detect a significant expression of PLIN1 protein in human skeletal muscle, questioning the role of PLIN1 in the regulation of lipolysis in this tissue [55,56]. Other PLIN species, in other words PLIN2 (also known as adipose-related differentiation protein or adipophilin), PLIN3 (also

known as Tail interacting protein of 47 kDa), and PLIN5 (also known as OXPAT), are associated with intermyofibrillar LDs in skeletal muscle [38,55,57,58]. A recent study showed that PLIN4 null mice do not accumulate more IMTG compared to wild type mice, thus excluding a major role of PLIN4 in the regulation of lipid storage and lipolysis in skeletal muscle [59]. However, overexpression of PLIN2 and PLIN5 in mice promotes TAG accumulation in skeletal and cardiac muscle [60–63]. By contrast, PLIN5 null mice lack detectable LDs in their cardiac muscle, thus confirming an important role for PLIN5 in the control of muscle lipolysis [64]. IMTG accumulation in these mouse models could be driven by the antilipolytic effect of PLIN as already described for PLIN1 and PLIN5 [65]. As mentioned above, epinephrine stimulation and contraction reduced IMTG content by more than 50% and increased HSL activity and also promoted HSL and PLIN2 colocalization in rat skeletal muscle [38]. More recently, Shepherd *et al.* reported that only PLIN2- and PLIN5-positive LDs are depleted in response to 1 h of exercise at 65% of peak oxygen consumption in skeletal muscle of healthy volunteers [4]. Interestingly, PLIN2 and PLIN5 are predominantly expressed in type I oxidative fibers, and protein expression is increased in response to either endurance training or sprint-interval training, together with IMTG content, as determined by immunohistochemistry [4,66]. Thus, net IMTG breakdown appeared to be preferentially increased during acute exercise in PLIN5-positive LDs in response to both types of exercise-training interventions, suggesting a specific role for PLIN5 in the control of lipolysis and FA oxidation in skeletal muscle [4]. Of note, colocalization of PLIN5 and mitochondria has been reported in human skeletal muscle [67], suggesting an involvement of PLIN5 in FA channeling toward mitochondria during lipolysis. Of interest, oxidative and lipolytic capacity in skeletal muscle appear to be correlated because muscle-specific overexpression of the transcriptional coactivator peroxisome proliferator-activated receptor γ coactivator 1α (PGC1α) in mice increases concomitantly mitochondrial oxidative capacity as well as the expression of lipases (ATGL and HSL), co-lipases (CGI-58 and G0S2), and PLIN5 [16].

In summary, despite the presence of numerous PLIN in skeletal muscle, the modulation of PLIN function during contractions and hormonal stimuli is still unclear, as is the interaction between PLIN and other proteins involved in IMTG breakdown. Further investigation of the molecular mechanisms linking lipolysis and mitochondrial FA oxidation in skeletal muscle is warranted.

Lipid pools and insulin resistance

Obesity has been associated with ectopic fat deposition in non-adipose, insulin-sensitive tissues, such as skeletal muscle and liver, both of which play an important role in the etiology of insulin resistance and T2DM [68]. As mentioned above, lipids are stored as TAG within LDs (i.e., IMTG). Unlike in active lean individuals, IMTG content is inversely related to peripheral glucose disposal in sedentary subjects [5,69]. In obesity, IMTG content is also associated with elevated levels of lipotoxic intermediates such as DAG and ceramides, which inhibit insulin signaling and interfere with insulin-stimulated glucose metabolism [6]. We will discuss the molecular mechanisms by which DAG and ceramides induce insulin resistance in skeletal muscle.

DAG pools

Several clinical studies demonstrated that total DAG content is elevated in vastus lateralis of obese and T2DM individuals compared to lean controls [5,70]. In addition, interventional studies show a decrease of skeletal muscle DAG content and improvement of insulin sensitivity after several weeks of endurance training [15]. Lipid-infusion studies have helped gain further insight into the molecular mechanisms of DAG-induced insulin resistance. In this experimental setting, TAG/heparin infusion typically raises plasma FA levels in a supra-physiological range, between 1.5 and 2 mM, and promotes a strong reduction of insulin-stimulated glucose disposal within 4 h [71]. This impairment in insulin signaling is associated with an increase in skeletal muscle total DAG content. Defects were mainly observed at the level of insulin receptor susbtrate-1 (IRS1), which exhibits reduced tyrosine phosphorylation, thus leading to a downregulation of PI3K activity and glucose uptake in response to insulin [6]. Causal relationships between DAG accumulation and insulin resistance have been also reported in culture of human primary myotubes [31].

DAGs are well-known allosteric activators of the conventional members of protein kinase C (PKC) (α, βI, βII, γ) and novel PKC (δ, ε, η, θ), whereas the atypical PKC (ζ,λ) devoid of a C1 binding site are not DAG-responsive. Activation of PKC by DAG induces serine phosphorylation of IRS1 and inhibits insulin signaling [72]. A few studies have shown that PKCθ activation is strongly associated with skeletal muscle insulin resistance in humans and rodents [73–75]. The role of other PKC isoforms remains unclear. Itani *et al.* reported an increase of membrane PKCδ and β isoforms in biopsies of vastus lateralis during lipid infusion in healthy individuals. Although PKCε has been associated with insulin resistance in rodent skeletal muscle [75,76], no study has confirmed this finding in humans.

Collectively, current evidence suggests that elevated DAG content in skeletal muscle might promote insulin resistance through the activation of PKCθ and other PKC isoforms. However, as total DAG may not be an accurate marker of insulin resistance in skeletal muscle (Box 1), further studies are needed to address this question (see outstanding question).

Ceramide pools

Ceramides have also been described as potential lipid mediators of skeletal muscle insulin resistance. Inhibition of ceramide synthesis by administration of the pharmacological inhibitor myriocin protects against high-fat diet-induced insulin resistance in rodents [77]. A positive association between total ceramide content and insulin resistance has been shown in human skeletal muscle. Adams *et al.* found a higher level of ceramides in obese insulin resistant patients [78], whereas Straczkowski *et al.* observed an increased ceramide content in response to lard oil infusion in healthy subjects [79]. Other

Box 1. Cellular origin of diacylglycerols and ceramides

Although the relationship between ectopic lipids and insulin resistance is an extensive area of research, several conflicting findings have been reported. Experimental conditions and particularly the type of FA (chain length, saturation degree) may explain some of the discrepancies between findings during lipid-infusion studies: for example, are ceramides exclusively produced from saturated FA? Discrepancies in the relationship between DAG, ceramides, and insulin resistance in cohort studies were also reported [95–97]. This raises the possibility that all DAG and ceramide species are not equal in skeletal muscle. Interestingly, it was recently shown that the majority of DAG are found at the membrane (about 80%), and that membrane DAG content is a better predictor of insulin resistance than total DAG content in skeletal muscle [70]. In addition, membrane DAG content in muscle was significantly increased in obese and T2DM when compared to endurance-trained subjects. This study clearly highlights that cellular localization of DAG is a significant determinant of insulin sensitivity. It is now well-established that both FA composition and cellular localization of DAG and potentially ceramides are of crucial importance [70,95]. Because IMTG stored within LDs represent a dynamic pool, and FAs largely traffic through IMTG pools before being oxidized [7], it is possible that alterations in IMTG dynamics might contribute to lipotoxicity and insulin resistance.

cross-sectional studies reported an elevated level of muscle ceramides in obese and T2DM subjects [5] and in lean insulin-resistant versus matched insulin-sensitive subjects [80]. Those data were corroborated by interventional studies employing chronic and acute training that showed an increase in insulin sensitivity which was paralleled by a decrease in skeletal muscle ceramide content [15,81].

The molecular mechanism of ceramide-induced insulin resistance has been studied in vitro. Ceramides block the translocation of Akt to the plasma membrane and further activation by insulin, in cells culture models, via two separate mechanism; ceramides activate PKCζ, and phosphatase protein phosphatase 2A (PP2A), which phosphorylate Akt on a serine residue, and dephosphorylate active Akt on Ser473, respectively, thus inhibiting of Akt activation in response to insulin [77]. This second mechanism might also explain palmitate-mediated insulin resistance in human skeletal muscle cells [82]. However, based on current data, it is unclear if total ceramide content in skeletal muscle may serve as a marker of insulin resistance (Box 1).

Dynamics of IMTG pools, lipotoxicity and insulin resistance

Dysregulation of lipase expression/activity in metabolic diseases

Recent studies have investigated the relationship between skeletal muscle lipolysis and insulin resistance in human cohorts. A consistent decrease of HSL protein expression has been reported in obese and T2DM men [31,83,84], associated with a reduction of DAG hydrolase activity [5,84]. The expression of muscle ATGL also appears to be dysregulated in obesity and T2DM. A strong negative correlation between whole-body insulin sensitivity, measured by hyperinsulinemic–euglycemic clamp, and ATGL protein expression in human skeletal muscle has been observed [31]. Several studies have shown that ATGL protein expression is markedly increased in obese and T2DM patients, whereas the ratio of DAG-to-TAG hydrolase activities is significant decreased [5,31,84]. One study, however, failed to detect a significant difference in muscle ATGL and HSL protein content in obese versus lean women [85], and this could be potentially explained by a gender effect. This is in agreement with an apparent sexual dimorphism of IMTG and lipolytic enzymes in skeletal muscle [5]. Of importance, the ratio of DAG to TAG hydrolase activities predicts respectively 54% and 38% of the variance in intramyocellular DAG and ceramides [5]. Collectively, these data show that disturbances of lipase expression and/or activity in skeletal muscle are associated with lipotoxicity and insulin resistance (Figure 2).

Molecular mechanisms of lipase-mediated lipotoxicity

Investigation of the causal relationship between dysregulation of lipolysis, lipotoxicity, and insulin resistance in human primary myotubes, has shown that overexpression of ATGL induces insulin resistance through a DAG/PKC-dependent pathway [31], which is rescued by pharmacological inhibition of PKC. Myriocin, an inhibitor of serine palmitoyl-CoA transferase-I, blocked ATGL-mediated ceramide synthesis but did not rescue insulin resistance in this model [31]. Interestingly, inhibition of HSL with a selective inhibitor induced a mild inhibition of insulin signaling. Further supporting a crucial role of the balance between ATGL and HSL, it was shown that restoration of a proper lipolytic balance, by augmenting HSL expression in ATGL-overexpressing myotubes, rescued insulin resistance in this model. Altogether, these data support the concept that disturbances of IMTG breakdown by lipases induce insulin resistance through DAG-mediated activation of PKC (Box 2).

Box 2. Is lipolysis-derived DAG linked to insulin resistance?

Although mounting evidence evokes a role for DAG in insulin resistance, there has been a controversy with respect to the stereospecificity and subcellular localization of DAG species [6,98]. The major controversy is whether or not DAG-derived from LD breakdown by ATGL can activate PKC and induce insulin resistance. The debate may be summarized via two key questions described below:

(i) Can ATGL-mediated lipolysis supply DAG capable of activating PKC? ATGL may promote DAG accumulation and induce insulin resistance in human primary myotubes and treatment with a non-selective inhibitor of PKC can reverse ATGL-mediated insulin resistance [31]. However, recent data from the Zechner's group indicate that ATGL cannot produce signaling *sn*-1,2-DAG capable of activating PKC [99]. In addition, contrary to human, muscle-specific modulations of ATGL have apparently no effect on fat oxidation and insulin sensitivity in mice [90].

(ii) Is only *sn*-1,2-DAG able to activate PKC? Although *sn*-1,2-diacylglycerol has been the most studied DAG in mammalian cells, it was reported that *sn*-1,3-DAG can promote PKCα binding to pure palmitoyl-2-oleoyl-*sn*-glycero-3-phosphoserine (POPS) membrane vesicles [100]. However, it is unlikely that plasma membrane and/or membrane-bound LDs are only composed of phosphatidylserine in intact cells.

As discussed in Box 1, the subcellular compartmentalization of LDs and lipid species appears crucial. Because LDs are found both in the intermyofibrillar and subsarcolemmal compartments, subsarcolemmal LDs could supply plasma membrane with DAG. More research efforts are needed to understand the molecular mechanisms linking disturbances of lipolysis and insulin resistance.

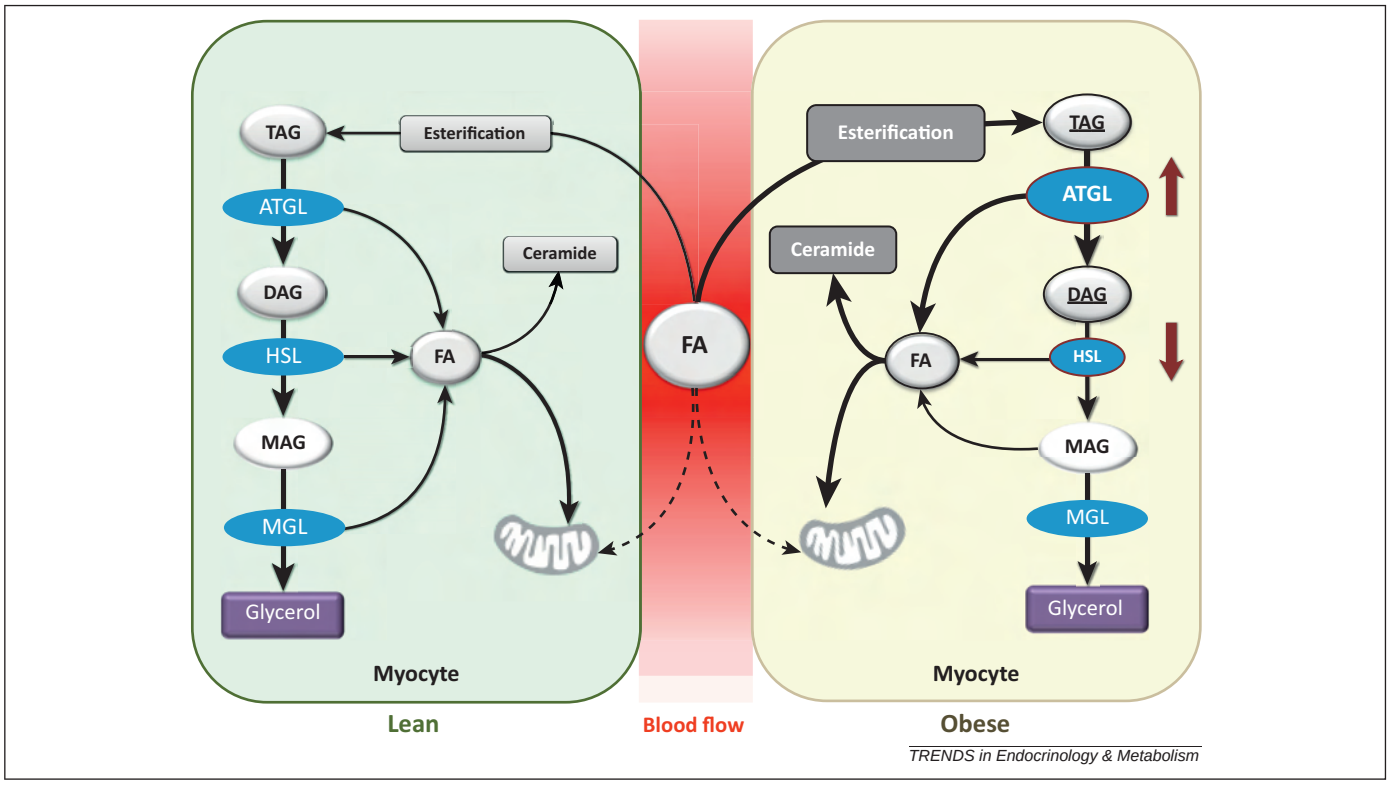

Figure 2. Regulation of skeletal muscle lipid pools in lean and obese subjects. This cartoon illustrates that IMTG are important lipid pools to supply FA fuels to skeletal muscle mitochondria during exercise in lean healthy subjects. Recent evidence suggests that FAs are largely esterified into intramyocellular triacylglycerols (IMTG) pools before being hydrolyzed by lipases and oxidized by mitochondria. IMTG pools can also be a source of intracellular ceramides. Chronic higher FA availability and uptake in obese subjects lead to a higher IMTG content. A potential imbalance of ATGL activity relative to HSL activity in obese individuals could increase intramyocellular DAG and ceramide levels. Abbreviations: MGL; monoacylglycerol lipase; other abbreviations as in Figure 1 legend.

The pathophysiological relevance of these findings is illustrated in several mouse models. First, HSL knockout mice exhibit a strong increase of skeletal muscle DAG in parallel with a mild insulin-resistant phenotype [21,22,86]. However, this relationship between HSL deficiency and insulin sensitivity is not unanimously found [21,87] and might be influenced by the background of the mouse strain [88]. Second, ATGL null mice remain insulin-sensitive and glucose-tolerant despite massive accumulation of TAG in skeletal muscle [28,89]. Interestingly, ATGL null mice are resistant to high-fat diet-induced lipotoxicity (increase of muscle DAG) and insulin resistance compared to their wild type littermates [89]. In addition, a pathophysiological link between disturbances of muscle lipase expression and insulin resistance has been observed in mice. High-fat diet-mediated insulin resistance was associated with higher total DAG content and higher membrane translocation of PKCθ and ε in skeletal muscle. Of interest, DAG accumulation was associated with an increase of CGI-58 expression whereas HSL Ser660 phosphorylation was dramatically reduced [75].

However, recent data indicate that skeletal muscle-specific modulations of ATGL in mice do not have significant impact on fat oxidation and insulin sensitivity, despite marked changes in IMTG [90]. The discrepancies between *in vitro* and *in vivo* findings with respect to the role of ATGL are still unclear. Differences in FA flux, energy demand, and species (humans vs mice) could be involved, and functional compensations attenuating the phenotype could also occur. In the same line, increasing IMTG content through modulations of esterification enzymes provided similarly conflicting results. Indeed, mouse models with muscle-specific overexpression of DGAT1 [17] and DGAT2 [91] confer protection and susceptibility to fat-induced insulin resistance, respectively.

Potential role of perilipins

As discussed above, PLIN proteins are key regulators of IMTG dynamics in skeletal muscle. PLIN2 and PLIN5 are predominantly expressed in skeletal muscle [55], and a few studies have evaluated their relationship with insulin sensitivity. Two independent studies reported a positive relationship between muscle PLIN2 protein expression and insulin sensitivity [14,92], whereas another study found an inverse correlation [93]. Another recent study indicates that overexpression of PLIN2 in human primary myotubes and *in vivo* in mice improves insulin sensitivity despite accumulation of IMTG [63]. In addition, a polymorphism in PLIN2 has been recently described in human and is associated with reduced circulating levels of TGs and VLDL-TG [94]. By contrast, muscle PLIN5 protein content correlates well with IMTG volume, but seems unchanged between lean and obese individuals [58,95]. No change in muscle PLIN5 protein expression was found in obese T2DM volunteers compared to matched-controls [93]. More recently, the Hesselink group demonstrated that PLIN5 overexpression in mouse tibialis anterior increases IMTG content without compromising insulin sensitivity, thus underlying a role of PLIN5 in IMTG storage and inhibition of muscle lipolysis [60]. Together

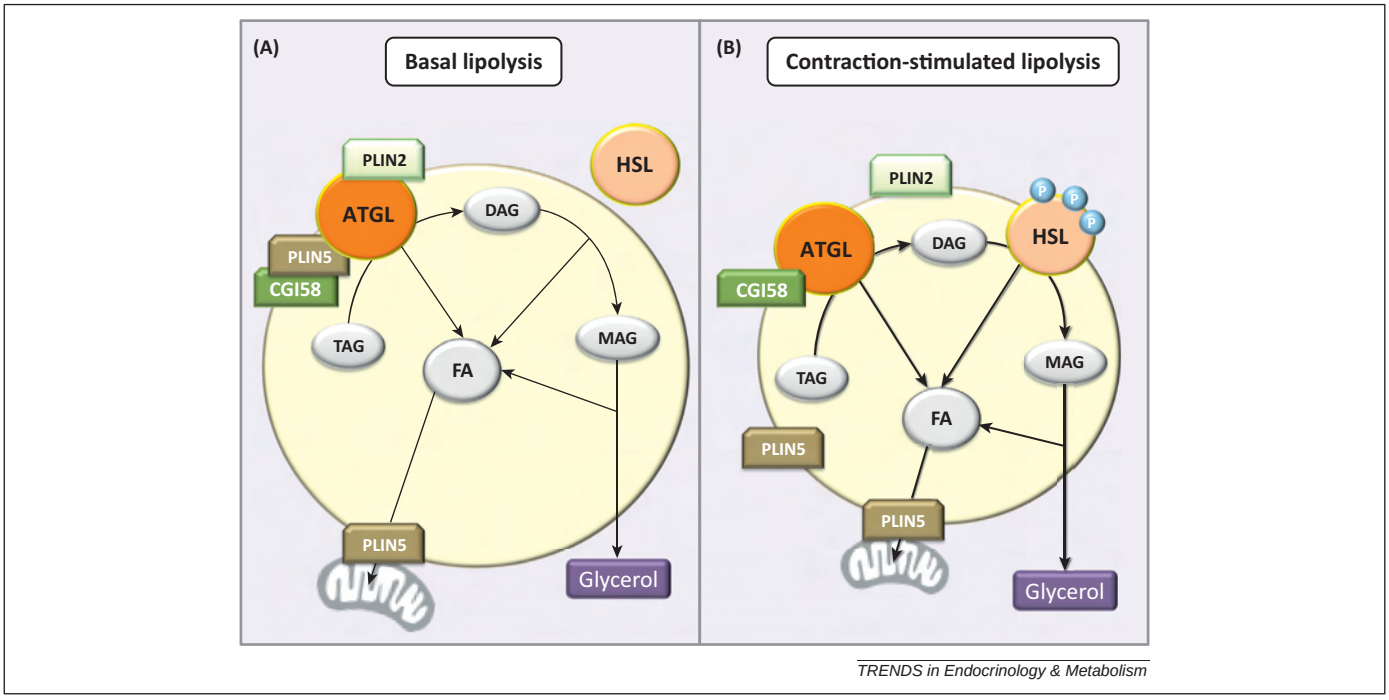

Figure 3. Hypothetical model of contraction-induced lipolysis in skeletal muscle. In the basal state **(A)**, ATGL binds to perilipins PLIN2 and PLIN5. In response to muscle contraction **(B)**, ATGL dissociates from PLIN proteins and interacts specifically with its coactivator CGI-58, while HSL is being activated by phosphorylation (P) and is translocated to the lipid droplet. CGI-58 could be preferentially linked to PLIN5 but it is still unclear how contraction induces its physical interaction with ATGL. These molecular events increase intracellular FA flux to supply energy fuels for the working muscle and as a consequence, the lipid droplet size decreases. PLIN5 may also channel IMTG-derived FA to mitochondria for β-oxidation.

these data show a possible involvement of skeletal muscle PLIN in the regulation of lipotoxicity and insulin resistance that needs to be explored further.

Concluding remarks

IMTG is an important site of energy storage and a fuel source in skeletal muscle. IMTG breakdown through the interplay of various partners (lipases, co-lipases, perilipins) reflects the dynamic nature of the LD. Contraction-mediated activation of lipases is pivotal and supplies energy fuels to the working muscle during exercise (Figure 3). Although exercise- and/or contraction-mediated IMTG breakdown has been studied extensively, the precise molecular mechanisms by which lipolysis is activated remains unclear (Box 3). The role of ATGL in this process could be dominant, in comparison to HSL. Future studies focusing on the role of lipase coactivators/corepressors and LD-associated proteins such as PLIN will be useful in understanding their contributions to IMTG dynamics. Importantly, the major role of lipases in resting condition is supported by the trafficking of FAs which occurs chiefly through IMTG pools before mitochondrial FA β-oxidation. An imbalance between IMTG breakdown and FA oxidation might lead to lipotoxicity and insulin resistance, whereas an imbalance between ATGL and HSL activity in skeletal muscle favors a state of lipotoxicity and insulin resistance. Disturbances of IMTG dynamics in the resting state may represent a novel mechanism of lipotoxicity in skeletal muscle, and targeting skeletal muscle lipases could be potentially helpful to alleviate obesity-related insulin resistance. Collectively, IMTG is not simply a passive fuel depot but has emerged as a highly dynamic pool, and maintaining proper IMTG homeostasis through exercise appears crucial to prevent the emergence of metabolic diseases.

Box 3. Outstanding questions

- What are the molecular mechanisms of contraction-mediated IMTG breakdown?
- What is the effect of ATGL serine phosphorylation on its activity? Is G0S2 an important cofactor of ATGL activity in skeletal muscle?
- Do PLIN proteins actively control IMTG dynamics or are they simply innocent bystanders?
- Can IMTG breakdown mediate some of the physiological adaptations to physical exercise?
- Which DAG and ceramide subspecies are the most detrimental for insulin signaling in skeletal muscle?
- Is DAG-mediated lipotoxicity only driven by PKCθ in muscle?
- Can ATGL-mediated lipolysis supply DAG capable of activating PKC?
- Is only *sn*-1,2-DAG able to activate PKC?

Acknowledgments

Studies from our laboratory were supported by grants from the European Foundation for the Study of Diabetes/Novo Nordisk and the National Research Agency ANR-12-JSV1-0010-01 (C.M.). The authors are very grateful to Dr François Crampes for outstanding discussion and critical reading of the manuscript. The authors are also grateful to Gabriel Badin for expert assistance with figure design.

References

1 van Loon, L.J. (2004) Use of intramuscular triacylglycerol as a substrate source during exercise in humans. *J. Appl. Physiol.* 97, 1170–1187
2 Kiens, B. (2006) Skeletal muscle lipid metabolism in exercise and insulin resistance. *Physiol. Rev.* 86, 205–243
3 Goodpaster, B.H. *et al.* (2001) Skeletal muscle lipid content and insulin resistance: evidence for a paradox in endurance-trained athletes. *J. Clin. Endocrinol. Metab.* 86, 5755–5761

4 Shepherd, S.O. *et al.* (2013) Sprint interval and traditional endurance training increase net intramuscular triglyceride breakdown and expression of perilipin 2 and 5. *J. Physiol.* 591, 657–675
5 Moro, C. *et al.* (2009) Influence of gender, obesity, and muscle lipase activity on intramyocellular lipids in sedentary individuals. *J. Clin. Endocrinol. Metab.* 94, 3440–3447
6 Samuel, V.T. and Shulman, G.I. (2012) Mechanisms for insulin resistance: common threads and missing links. *Cell* 148, 852–871
7 Kanaley, J.A. *et al.* (2009) Relationship between plasma free fatty acid, intramyocellular triglycerides and long-chain acylcarnitines in resting humans. *J. Physiol.* 587, 5939–5950
8 Haemmerle, G. *et al.* (2011) ATGL-mediated fat catabolism regulates cardiac mitochondrial function via PPAR-alpha and PGC-1. *Nat. Med.* 17, 1076–1085
9 Badin, P.M. *et al.* (2012) Regulation of skeletal muscle lipolysis and oxidative metabolism by the co-lipase CGI-58. *J. Lipid Res.* 53, 839–848
10 Shepherd, S.O. *et al.* (2012) Preferential utilization of perilipin 2-associated intramuscular triglycerides during 1 h of moderate-intensity endurance-type exercise. *Exp. Physiol.* 97, 970–980
11 van Loon, L.J. *et al.* (2003) Influence of prolonged endurance cycling and recovery diet on intramuscular triglyceride content in trained males. *Am. J. Physiol.* 285, E804–E811
12 Newsom, S.A. *et al.* (2011) High fatty acid availability after exercise alters the regulation of muscle lipid metabolism. *Metabolism* 60, 852–859
13 Shaw, C.S. *et al.* (2012) Prolonged exercise training increases intramuscular lipid content and perilipin 2 expression in type I muscle fibers of patients with type 2 diabetes. *Am. J. Physiol.* 303, E1158–E1165
14 Coen, P.M. *et al.* (2010) Insulin resistance is associated with higher intramyocellular triglycerides in type I but not type II myocytes concomitant with higher ceramide content. *Diabetes* 59, 80–88
15 Dube, J.J. *et al.* (2011) Effects of weight loss and exercise on insulin resistance, and intramyocellular triacylglycerol, diacylglycerol and ceramide. *Diabetologia* 54, 1147–1156
16 Koves, T.R. *et al.* (2013) PPARgamma coactivator-1alpha contributes to exercise-induced regulation of intramuscular lipid droplet programming in mice and humans. *J. Lipid Res.* 54, 522–534
17 Liu, L. *et al.* (2007) Upregulation of myocellular DGAT1 augments triglyceride synthesis in skeletal muscle and protects against fat-induced insulin resistance. *J. Clin. Invest.* 117, 1679–1689
18 Lass, A. *et al.* (2011) Lipolysis – a highly regulated multi-enzyme complex mediates the catabolism of cellular fat stores. *Prog. Lipid Res.* 50, 14–27
19 Taschler, U. *et al.* (2011) Monoglyceride lipase deficiency in mice impairs lipolysis and attenuates diet-induced insulin resistance. *J. Biol. Chem.* 286, 17467–17477
20 Harada, K. *et al.* (2003) Resistance to high-fat diet-induced obesity and altered expression of adipose-specific genes in HSL-deficient mice. *Am. J. Physiol.* 285, E1182–E1195
21 Park, S.Y. *et al.* (2005) Hormone-sensitive lipase knockout mice have increased hepatic insulin sensitivity and are protected from short-term diet-induced insulin resistance in skeletal muscle and heart. *Am. J. Physiol.* 289, E30–E39
22 Haemmerle, G. *et al.* (2002) Hormone-sensitive lipase deficiency in mice causes diglyceride accumulation in adipose tissue, muscle, and testis. *J. Biol. Chem.* 277, 4806–4815
23 Villena, J.A. *et al.* (2004) Desnutrin, an adipocyte gene encoding a novel patatin domain-containing protein, is induced by fasting and glucocorticoids: ectopic expression of desnutrin increases triglyceride hydrolysis. *J. Biol. Chem.* 279, 47066–47075
24 Jenkins, C.M. *et al.* (2004) Identification, cloning, expression, and purification of three novel human calcium-independent phospholipase A2 family members possessing triacylglycerol lipase and acylglycerol transacylase activities. *J. Biol. Chem.* 279, 48968–48975
25 Zimmermann, R. *et al.* (2004) Fat mobilization in adipose tissue is promoted by adipose triglyceride lipase. *Science* 306, 1383–1386
26 Jocken, J.W. *et al.* (2008) Adipose triglyceride lipase (ATGL) expression in human skeletal muscle is type I (oxidative) fiber specific. *Histochem. Cell Biol.* 129, 535–538
27 Fischer, J. *et al.* (2007) The gene encoding adipose triglyceride lipase (PNPLA2) is mutated in neutral lipid storage disease with myopathy. *Nat. Genet.* 39, 28–30
28 Haemmerle, G. *et al.* (2006) Defective lipolysis and altered energy metabolism in mice lacking adipose triglyceride lipase. *Science* 312, 734–737
29 Huijsman, E. *et al.* (2009) Adipose triacylglycerol lipase deletion alters whole body energy metabolism and impairs exercise performance in mice. *Am. J. Physiol.* 297, E505–E513
30 Schoiswohl, G. *et al.* (2010) Adipose triglyceride lipase plays a key role in the supply of the working muscle with fatty acids. *J. Lipid Res.* 51, 490–499
31 Badin, P.M. *et al.* (2011) Altered skeletal muscle lipase expression and activity contribute to insulin resistance in humans. *Diabetes* 60, 1734–1742
32 Sacchetti, M. *et al.* (2004) High triacylglycerol turnover rate in human skeletal muscle. *J. Physiol.* 561, 883–891
33 Guo, Z. *et al.* (2000) Kinetics of intramuscular triglyceride fatty acids in exercising humans. *J. Appl. Physiol.* 89, 2057–2064
34 Bergman, B.C. *et al.* (2010) Increased intramuscular lipid synthesis and low saturation relate to insulin sensitivity in endurance-trained athletes. *J. Appl. Physiol.* 108, 1134–1141
35 Perreault, L. *et al.* (2010) Altered intramuscular lipid metabolism relates to diminished insulin action in men, but not women, in progression to diabetes. *Obesity (Silver Spring)* 18, 2093–2100
36 Guo, Z. and Zhou, L. (2005) Muscle type-dependent responses to insulin in intramyocellular triglyceride turnover in obese rats. *Obes. Res.* 13, 2081–2087
37 Contreras, J.A. *et al.* (1998) Human hormone-sensitive lipase: expression and large-scale purification from a baculovirus/insect cell system. *Protein Expr. Purif.* 12, 93–99
38 Prats, C. *et al.* (2006) Decrease in intramuscular lipid droplets and translocation of HSL in response to muscle contraction and epinephrine. *J. Lipid Res.* 47, 2392–2399
39 Krintel, C. *et al.* (2008) Ser649 and Ser650 are the major determinants of protein kinase A-mediated activation of human hormone-sensitive lipase against lipid substrates. *PLoS ONE* 3, e3756
40 Kjaer, M. *et al.* (2000) Adrenaline and glycogenolysis in skeletal muscle during exercise: a study in adrenalectomised humans. *J. Physiol.* 528 (Pt 2), 371–378
41 Donsmark, M. *et al.* (2003) Contractions activate hormone-sensitive lipase in rat muscle by protein kinase C and mitogen-activated protein kinase. *J. Physiol.* 550, 845–854
42 Watt, M.J. *et al.* (2003) Effects of plasma adrenaline on hormone-sensitive lipase at rest and during moderate exercise in human skeletal muscle. *J. Physiol.* 550, 325–332
43 Bartz, R. *et al.* (2007) Dynamic activity of lipid droplets: protein phosphorylation and GTP-mediated protein translocation. *J. Proteome Res.* 6, 3256–3265
44 Duncan, R.E. *et al.* (2010) Characterization of desnutrin functional domains: critical residues for triacylglycerol hydrolysis in cultured cells. *J. Lipid Res.* 51, 309–317
45 Ahmadian, M. *et al.* (2011) Desnutrin/ATGL is regulated by AMPK and is required for a brown adipose phenotype. *Cell Metab.* 13, 739–748
46 Mason, R.R. *et al.* (2012) Phosphorylation of adipose triglyceride lipase Ser404 is not related to 5′-AMPK activation during moderate-intensity exercise in humans. *Am. J. Physiol.* 303, E534–E541
47 Pagnon, J. *et al.* (2012) Identification and functional characterization of protein kinase a phosphorylation sites in the major lipolytic protein, adipose triglyceride lipase. *Endocrinology* 153, 4278–4289
48 Lefevre, C. *et al.* (2001) Mutations in CGI-58, the gene encoding a new protein of the esterase/lipase/thioesterase subfamily, in Chanarin–Dorfman syndrome. *Am. J. Hum. Genet.* 69, 1002–1012
49 Lass, A. *et al.* (2006) Adipose triglyceride lipase-mediated lipolysis of cellular fat stores is activated by CGI-58 and defective in Chanarin–Dorfman Syndrome. *Cell Metab.* 3, 309–319
50 Alsted, T.J. *et al.* (2009) Adipose triglyceride lipase in human skeletal muscle is upregulated by exercise training. *Am. J. Physiol.* 296, E445–E453
51 Macpherson, R.E. *et al.* (2013) Skeletal muscle PLIN proteins, ATGL and CGI-58, interactions at rest and following stimulated contraction. *Am. J. Physiol. Regul. Integr. Comp. Physiol.* 304, 644–650

52 Yang, X. *et al.* (2010) The G0/G1 switch gene 2 regulates adipose lipolysis through association with adipose triglyceride lipase. *Cell Metab.* 11, 194–205
53 Schweiger, M. *et al.* (2012) G0/G1 switch gene-2 regulates human adipocyte lipolysis by affecting activity and localization of adipose triglyceride lipase. *J. Lipid Res.* 53, 2307–2317
54 Kimmel, A.R. *et al.* (2010) Adoption of PERILIPIN as a unifying nomenclature for the mammalian PAT-family of intracellular lipid storage droplet proteins. *J. Lipid Res.* 51, 468–471
55 Wolins, N.E. *et al.* (2006) OXPAT/PAT-1 is a PPAR-induced lipid droplet protein that promotes fatty acid utilization. *Diabetes* 55, 3418–3428
56 Moro, C. *et al.* (2008) Determinants of intramyocellular triglyceride turnover: implications for insulin sensitivity. *Am. J. Physiol.* 294, E203–E213
57 Dalen, K.T. *et al.* (2007) LSDP5 is a PAT protein specifically expressed in fatty acid oxidizing tissues. *Biochim. Biophys. Acta* 1771, 210–227
58 Peters, S.J. *et al.* (2012) Perilipin family (PLIN) proteins in human skeletal muscle: the effect of sex, obesity, and endurance training. *Appl. Physiol. Nutr. Metab.* 37, 724–735
59 Chen, W. *et al.* (2013) Inactivation of Plin4 downregulates Plin5 and reduces cardiac lipid accumulation in mice. *Am. J. Physiol.* 304, E770–E779
60 Bosma, M. *et al.* (2013) Overexpression of PLIN5 in skeletal muscle promotes oxidative gene expression and intramyocellular lipid content without compromising insulin sensitivity. *Biochim. Biophys. Acta* 1831, 844–852
61 Wang, H. *et al.* (2013) Cardiomyocyte-specific perilipin 5 overexpression leads to myocardial steatosis and modest cardiac dysfunction. *J. Lipid Res.* 54, 953–965
62 Pollak, N.M. *et al.* (2013) Cardiac-specific overexpression of perilipin 5 provokes severe cardiac steatosis via the formation of a lipolytic barrier. *J. Lipid Res.* 54, 1092–1102
63 Bosma, M. *et al.* (2012) Perilipin 2 improves insulin sensitivity in skeletal muscle despite elevated intramuscular lipid levels. *Diabetes* 61, 2679–2690
64 Kuramoto, K. *et al.* (2012) Perilipin 5, a lipid droplet-binding protein, protects heart from oxidative burden by sequestering fatty acid from excessive oxidation. *J. Biol. Chem.* 287, 23852–23863
65 Brasaemle, D.L. (2013) Perilipin 5: putting the brakes on lipolysis. *J. Lipid Res.* 54, 876–877
66 Shaw, C.S. *et al.* (2009) Adipophilin distribution and colocalization with lipid droplets in skeletal muscle. *Histochem. Cell Biol.* 131, 575–581
67 Bosma, M. *et al.* (2012) The lipid droplet coat protein perilipin 5 also localizes to muscle mitochondria. *Histochem. Cell Biol.* 137, 205–216
68 DeFronzo, R.A. (2004) Pathogenesis of type 2 diabetes mellitus. *Med. Clin. North Am.* 88, 787–835
69 Perseghin, G. *et al.* (1999) Intramyocellular triglyceride content is a determinant of in vivo insulin resistance in humans: a ^{1}H-^{13}C nuclear magnetic resonance spectroscopy assessment in offspring of type 2 diabetic parents. *Diabetes* 48, 1600–1606
70 Bergman, B.C. *et al.* (2012) Localisation and composition of skeletal muscle diacylglycerol predicts insulin resistance in humans. *Diabetologia* 55, 1140–1150
71 Roden, M. *et al.* (1996) Mechanism of free fatty acid-induced insulin resistance in humans. *J. Clin. Invest.* 97, 2859–2865
72 Schmitz-Peiffer, C. and Biden, T.J. (2008) Protein kinase C function in muscle, liver, and beta-cells and its therapeutic implications for type 2 diabetes. *Diabetes* 57, 1774–1783
73 Itani, S.I. *et al.* (2001) Increased protein kinase C theta in skeletal muscle of diabetic patients. *Metabolism* 50, 553–557
74 Kim, J.K. *et al.* (2004) PKC-theta knockout mice are protected from fat-induced insulin resistance. *J. Clin. Invest.* 114, 823–827
75 Badin, P.M. *et al.* (2013) High-fat diet-mediated lipotoxicity and insulin resistance is related to impaired lipase expression in mouse skeletal muscle. *Endocrinology* 154, 1444–1453
76 Laybutt, D.R. *et al.* (1999) Muscle lipid accumulation and protein kinase C activation in the insulin-resistant chronically glucose-infused rat. *Am. J. Physiol.* 277, E1070–E1076
77 Chavez, J.A. and Summers, S.A. (2012) A ceramide-centric view of insulin resistance. *Cell Metab.* 15, 585–594
78 Adams, J.M., 2nd *et al.* (2004) Ceramide content is increased in skeletal muscle from obese insulin-resistant humans. *Diabetes* 53, 25–31
79 Straczkowski, M. *et al.* (2004) Relationship between insulin sensitivity and sphingomyelin signaling pathway in human skeletal muscle. *Diabetes* 53, 1215–1221
80 Galgani, J.E. *et al.* (2013) Enhanced skeletal muscle lipid oxidative efficiency in insulin-resistant vs insulin-sensitive nondiabetic, nonobese humans. *J. Clin. Endocrinol. Metab.* 98, 646–653
81 Schenk, S. and Horowitz, J.F. (2007) Acute exercise increases triglyceride synthesis in skeletal muscle and prevents fatty acid-induced insulin resistance. *J. Clin. Invest.* 117, 1690–1698
82 Chavez, J.A. *et al.* (2003) A role for ceramide, but not diacylglycerol, in the antagonism of insulin signal transduction by saturated fatty acids. *J. Biol. Chem.* 278, 10297–10303
83 Jocken, J.W. *et al.* (2008) Hormone-sensitive lipase serine phosphorylation and glycerol exchange across skeletal muscle in lean and obese subjects: effect of beta-adrenergic stimulation. *Diabetes* 57, 1834–1841
84 Jocken, J.W. *et al.* (2010) Skeletal muscle lipase content and activity in obesity and type 2 diabetes. *J. Clin. Endocrinol. Metab.* 95, 5449–5453
85 Li, M. *et al.* (2011) High muscle lipid content in obesity is not due to enhanced activation of key triglyceride esterification enzymes or the suppression of lipolytic proteins. *Am. J. Physiol.* 300, E699–E707
86 Mulder, H. *et al.* (2003) Hormone-sensitive lipase null mice exhibit signs of impaired insulin sensitivity whereas insulin secretion is intact. *J. Biol. Chem.* 278, 36380–36388
87 Voshol, P.J. *et al.* (2003) Increased hepatic insulin sensitivity together with decreased hepatic triglyceride stores in hormone-sensitive lipase-deficient mice. *Endocrinology* 144, 3456–3462
88 Girousse, A. and Langin, D. (2012) Adipocyte lipases and lipid droplet-associated proteins: insight from transgenic mouse models. *Int. J. Obesity* 36, 581–594
89 Hoy, A.J. *et al.* (2011) Adipose triglyceride lipase-null mice are resistant to high-fat diet-induced insulin resistance despite reduced energy expenditure and ectopic lipid accumulation. *Endocrinology* 152, 48–58
90 Sitnick, M.T. *et al.* (2013) Skeletal muscle triacylglycerol hydrolysis does not influence metabolic complications of obesity. *Diabetes* http://dx.doi.org/10.2337/db13-0500
91 Levin, M.C. *et al.* (2007) Increased lipid accumulation and insulin resistance in transgenic mice expressing DGAT2 in glycolytic (type II) muscle. *Am. J. Physiol.* 293, E1772–E1781
92 Phillips, S.A. *et al.* (2005) Adipocyte differentiation-related protein in human skeletal muscle: relationship to insulin sensitivity. *Obes. Res.* 13, 1321–1329
93 Minnaard, R. *et al.* (2009) Adipocyte differentiation-related protein and OXPAT in rat and human skeletal muscle: involvement in lipid accumulation and type 2 diabetes mellitus. *J. Clin. Endocrinol. Metab.* 94, 4077–4085
94 Magne, J. *et al.* (2013) The minor allele of the missense polymorphism Ser251Pro in perilipin 2 (PLIN2) disrupts an α-helix, affects lipolysis, and is associated with reduced plasma triglyceride concentration in humans. *FASEB J.* 27, 3090–3099
95 Amati, F. *et al.* (2011) Skeletal muscle triglycerides, diacylglycerols, and ceramides in insulin resistance: another paradox in endurance-trained athletes? *Diabetes* 60, 2588–2597
96 Skovbro, M. *et al.* (2008) Human skeletal muscle ceramide content is not a major factor in muscle insulin sensitivity. *Diabetologia* 51, 1253–1260
97 Jocken, J.W. *et al.* (2011) Skeletal muscle lipase content and activity in obesity and type 2 diabetes. *J. Clin. Endocrinol. Metab.* 95, 5449–5453
98 Zechner, R. *et al.* (2012) FAT SIGNALS – lipases and lipolysis in lipid metabolism and signaling. *Cell Metab.* 15, 279–291
99 Eichmann, T.O. *et al.* (2012) Studies on the substrate and stereo/regioselectivity of adipose triglyceride lipase, hormone-sensitive lipase, and diacylglycerol-O-acyltransferases. *J. Biol. Chem.* 287, 41446–41457
100 Sanchez-Pinera, P. *et al.* (1999) A comparative study of the activation of protein kinase C alpha by different diacylglycerol isomers. *Biochem. J.* 337, 387–395

PUBLICATION 5: L'ACIDE PALMITIQUE SUIT UNE VOIE METABOLIQUE DIFFERENTE DE L'ACIDE OLEIQUE AU SEIN DE CELLULES DE MUSCLE SQUELETTIQUE HUMAIN ; LA LIPOLYSE EST DIMINUEE MALGRE UNE AUGMENTATION DE L'EXPRESSION DE L'ADIPOSE TRIGLYCERIDE LIPASE

Publication 5: Palmitic acid follows a different metabolic pathway than oleic acid in human skeletal muscle cells; lower lipolysis rate despite an increased level of adipose triglyceride lipase

Bakke SS, Moro C, Nikolić N, Hessvik NP, Badin PM, Lauvhaug L, Fredriksson K, Hesselink MKC, Boekschoten MV, Kersten S, Gaster M, Thoresen GH, Rustan AC. *(2012) Biochim Biophys Acta. 1821(10):1323-33.*

Biochimica et Biophysica Acta 1821 (2012) 1323–1333

Contents lists available at SciVerse ScienceDirect

Biochimica et Biophysica Acta

journal homepage: www.elsevier.com/locate/bbalip

Palmitic acid follows a different metabolic pathway than oleic acid in human skeletal muscle cells; lower lipolysis rate despite an increased level of adipose triglyceride lipase

Siril S. Bakke [a,*], Cedric Moro [b], Nataša Nikolić [a], Nina P. Hessvik [a], Pierre-Marie Badin [b], Line Lauvhaug [a], Katarina Fredriksson [c], Matthijs K.C. Hesselink [c], Mark V. Boekschoten [d,e], Sander Kersten [d,e], Michael Gaster [f,g], G. Hege Thoresen [a], Arild C. Rustan [a]

[a] Department of Pharmaceutical Biosciences, School of Pharmacy, University of Oslo, Norway
[b] Inserm 1048, Institute of Metabolic and Cardiovascular Diseases, Paul Sabatier University, Toulouse, France
[c] Nutrim School for Nutrition, Toxicology and Metabolism, Department of Human Movement Sciences, Maastricht University, Maastricht, The Netherlands
[d] Division of Human Nutrition, Wageningen University, Wageningen, The Netherlands
[e] Nutrigenomics Centre, TI Food and Nutrition, Wageningen, The Netherlands
[f] Laboratory for Molecular Physiology, Dept. of Pathology, Odense University Hospital, Odense, Denmark
[g] Department of Endocrinology, Odense University Hospital, Odense, Denmark

ARTICLE INFO

Article history:
Received 16 October 2011
Received in revised form 31 May 2012
Accepted 3 July 2012
Available online 13 July 2012

Keywords:
Human myotube
Lipid oxidation
Lipolysis
Adipose triglyceride lipase
Lipid droplet
Fatty acid

ABSTRACT

Development of insulin resistance is positively associated with dietary saturated fatty acids and negatively associated with monounsaturated fatty acids. To clarify aspects of this difference we have compared the metabolism of oleic (OA, monounsaturated) and palmitic acids (PA, saturated) in human myotubes. Human myotubes were treated with 100 μM OA or PA and the metabolism of [^{14}C]-labeled fatty acid was studied. We observed that PA had a lower lipolysis rate than OA, despite a more than two-fold higher protein level of adipose triglyceride lipase after 24 h incubation with PA. PA was less incorporated into triacylglycerol and more incorporated into phospholipids after 24 h. Supporting this, incubation with compounds modifying lipolysis and reesterification pathways suggested a less influenced PA than OA metabolism. In addition, PA showed a lower accumulation than OA, though PA was oxidized to a relatively higher extent than OA. Gene set enrichment analysis revealed that 24 h of PA treatment upregulated lipogenesis and fatty acid β-oxidation and downregulated oxidative phosphorylation compared to OA. The differences in lipid accumulation and lipolysis between OA and PA were eliminated in combination with eicosapentaenoic acid (polyunsaturated fatty acid). In conclusion, this study reveals that the two most abundant fatty acids in our diet are partitioned toward different metabolic pathways in muscle cells, and this may be relevant to understand the link between dietary fat and skeletal muscle insulin resistance.

1. Introduction

Development of insulin resistance and type 2 diabetes is associated with the type of dietary fat in both human and animal studies. There is a positive correlation by intake of saturated fatty acids (SFA) whereas mono- and polyunsaturated fatty acids (MUFA and PUFA) show beneficial effects [1–4]. Dietary short-chain and unsaturated fatty acids are more rapidly oxidized than dietary long-chain and SFA in healthy subjects [5]. These findings suggest that unsaturated fatty acids are more channeled towards mitochondria for oxidation than SFA, which in turn are stored preferentially as triacylglycerol (TAG). In contrast to this, in human skeletal muscle cells (myotubes), it has been reported that palmitic acid (SFA, PA, 16:0) oxidation was greater than oleic acid (MUFA, OA, 18:1 n−9) oxidation [6]. There is a growing body of data that suggests that the incorporation of unsaturated fatty acids and SFAs into complex lipids

Abbreviations: ASMs, acid soluble metabolites; ACSL, long-chain fatty acyl-CoA synthetase; ATGL, adipose triglyceride lipase; BSA, bovine serum albumin; CA, cell-associated; CD36/FAT, fatty acid translocase; FDR, false discovery rate; CE, cholesteryl ester; CRAT, carnitine O-acetyltransferase; CPT1, carnitine palmitoyltransferase 1; DAG, diacylglycerol; DGAT, diacylglycerol acyltransferase; ECM, extracellular matrix; EPA, eicosapentaenoic acid; FADS2, fatty acid desaturase 2; FFA, free fatty acid; GSEA, gene set enrichment analysis; HADHA, mitochondrial trifunctional protein, alpha subunit; HSL, hormone-sensitive lipase; LD, lipid droplet; LMM, linear mixed models; MUFA, monounsaturated fatty acid; OA, oleic acid; PA, palmitic acid; PDK4, pyruvate dehydrogenase kinase isozyme 4; PL, phospholipid; PLIN, perilipin; PUFA, polyunsaturated fatty acid; SCD1, stearoyl-CoA desaturase 1; SFA, saturated fatty acid; SLC25A20, solute carrier family 25 (carnitine/acylcarnitine translocase), member 20; SPA, scintillation proximity assay; TAG, triacylglycerol

* Corresponding author at: School of Pharmacy, P.O. Box 1068 Blindern, 0316 Oslo, Norway. Tel.: +47 22857578; fax: +47 22854402.
E-mail address: s.s.bakke@farmasi.uio.no (S.S. Bakke).

1388-1981/$ – see front matter © 2012 Elsevier B.V. All rights reserved.
doi:10.1016/j.bbalip.2012.07.001

markedly differ [6–8]. Data from cultured myotubes suggest that TAG biosynthesis is lower in cells exposed to SFA compared to unsaturated fatty acids and consequently PA has a lower rate of incorporation into TAG, which in turn may lead to abnormal accumulation of lipid intermediates such as diacylglycerol (DAG) and/or ceramide [9–11]. In accordance with this, Just et al. [12] reported that long-chain acyl-CoA accumulated only during 24 h exposure to PA but not during exposure to OA in myotubes. We have previously shown that after 4 h incubation of human skeletal muscle cells with OA and PA, PA accumulated primarily more as DAG and TAG, whereas OA accumulated mostly as free fatty acid (FFA) [8]. Moreover, after 20 h incubation of human myotubes with labeled PA, stearate and OA, Montell et al. [7] also found a preferential incorporation of SFA into DAG. However, as opposed to the reports from Gaster et al. [8], Montell et al. [7] observed a lower incorporation of SFA into TAG whereas unsaturated fatty acids accumulated in TAG and in very minor proportions in DAG. García-Martínez et al. [6] also found after 16 h incubation, a lower PA incorporation in TAG compared to OA.

Once the fatty acids are stored as TAG in lipid droplets (LDs), they can, on stimuli for energy demand, undergo lipolysis and become available substrates for oxidation. The majority of the studies have been performed in adipocytes or in muscle in animal models, while studies using cultured human skeletal muscle cells are rarer [13–18]. PLINs (Perilipins) coat and regulate LD biogenesis, and in human skeletal muscle, all five PLINs are present, where 2, 4 and 5 are expressed higher than the others [19,20]. Despite this, Gjelstad et al. [20] examined mRNA expression in cultured human myotubes and found that PLIN2 and 3 were dominant, whereas the expressions of PLIN4 and PLIN1 were very low and no expression of PLIN5 was found. PLIN2 covers 62% of intramyocellular lipids in C2C12 mouse skeletal muscle cells [21] and is anticipated to protect the LD against lipolysis in non-adipose tissues [22,23]. PLIN3 suppression in HeLa cells resulted in a blocked LD maturation and decreased incorporation of TAG into LDs [24].

Adipose triglyceride lipase (ATGL) is expressed in human skeletal muscle [16,18,25–27] and is proposed as the major lipase that initiates lipolysis by hydrolyzing TAG to DAG [28]. Studies showing TAG accumulation in patients suffering from neutral lipid storage disease where ATGL function is impaired clearly demonstrate an important role of ATGL in skeletal muscle lipid metabolism [29–31]. Hormone-sensitive lipase (HSL) is also expressed in human skeletal muscle [32,33] and has the function to hydrolyze DAG to monoacylglycerol and, to a small extent, TAG to DAG [34]. β-Adrenergic stimuli or contraction may increase lipolysis by phosphorylation of PLIN1 and HSL via protein kinase A in adipose tissue [35–37] and by phosphorylation of HSL in skeletal muscle [38–40]. However, the biological role and regulation of the PLINs and lipases in skeletal muscle are not yet fully elucidated.

Previously we found that incubation of myotubes with 100 μM OA and PA for 24 h had no influence on glucose metabolism (insulin-stimulated glycogen synthesis) and insulin action (phosphorylation of Akt/protein kinase B) [41]. We observed that fatty acid accumulation curve flattens out after 24 h incubation with 100 μM fatty acid [15]. Therefore, our experiments were performed using the same concentration of fatty acid and an incubation period up to 24 h. To obtain a more complete picture of the handling and metabolism of PA and OA in human myotubes, accumulation, lipolysis, reesterification and oxidation were investigated. Moreover, we also studied glucose accumulation and oxidation, and glycerol accumulation in the presence of PA and OA. Finally, OA and PA were also added in combination with eicosapentaenoic acid (EPA) due to the effects of this polyunsaturated fatty acid to positively influence energy metabolism in myotubes as shown in earlier reports [41–43]. We here show that PA underwent lipolysis to a lesser degree than OA despite an increased protein level of ATGL. In addition, PA had a lower cellular accumulation compared to OA, while PA was incorporated into phospholipids (PL) and oxidized to a relatively higher extent.

2. Materials and methods

2.1. Materials

Dulbecco's modified Eagles medium (DMEM-Glutamax™), DMEM without phenol red, heat-inactivated fetal calf serum (FCS), and penicillin–streptomycin–amphotericin B were purchased from Gibco Invitrogen (Gibco, Life Technologies, Paisley, UK). Ultroser G was purchased from PALL Life Science (Port Washington, NY, US), insulin (Actrapid®) from NovoNordisk (Bagsvaerd, Denmark), BSA (bovine serum albumin) (essentially fatty acid-free), L-carnitine, Dulbecco's phosphate-buffered saline (DPBS with Mg^{2+} and Ca^{2+}), eicosapentaenoic acid (EPA, 20:5, n−3), oleic acid (OA, 18:1, n−9), palmitic acid (PA, 16:0), extracellular matrix (ECM) gel, glucose, HEPES, protease inhibitor and phosphatase I and II inhibitors, were all obtained from Sigma (St Louis, MO, US). [1-^{14}C]oleic acid (58.2 mCi/mmol), [1-^{14}C]palmitic acid (60.0 mCi/mmol), [^{14}C(U)]glycerol (142 mCi/mmol) and D-[^{14}C(U)]glucose (2.9 mCi/mmol) were from PerkinElmer NEN® (Boston, MA, US). Corning® CellBIND® tissue culture plates (96-well plates and 60 mm dishes) were obtained from Corning Life-Sciences (Schiphol-Rijk, The Netherlands). Glass bottom 12-well plates were purchased from MatTek (Ashland, MA, US), 96-well plates with V-bottom from Nunc (Thermo Scientific, Rochester, MA, US), Biocoat ™ 25 cm^2 cell flask from BD Biosciences (Franklin Lakes, NJ, US) and 12-well plate from Corning Life-Sciences (Lowell, MA, US). Ecoscint A scintillation solution was from National Diagnostics (Hessle, England, UK). OptiPhase Supermix, UniFilter®-96 GF/B, ScintiPlate®-96 TC plates and all liquid scintillation was performed by the 1450 MicroBeta TriLux scintillation counter, were obtained from PerkinElmer (Shelton, CT, US). Thin layer chromatography plates were purchased from Merck (Darmstadt, Germany), nitrocellulose membrane from Hybond ECL (Amersham Biosciences, Boston, MA, US) and chemiluminescence reagent and hyperfilm ECL from GE Healthcare. Antibodies for ATGL, HSL and glyceraldehyde-3-phosphate dehydrogenase (GAPDH) were purchased from Cell Signaling Technology (Beverly, MA, US) and PLIN2 and PLIN3 from Thermo Fisher Scientific (Waltham, MA, US). Bodipy 493/503 (4.4-difluoro-1.3.5.7.8-pentamethyl-4-bora-3a.4a-diaza-s-indacene), MitoTracker®Red FM, Hoechst 33258 and the primers for TaqMan qPCR were obtained from Molecular Probes, Invitrogen (Carlsbad, CA, US). NuGO human Genechip arrays were obtained from Affymetrix (Santa Clara, CA, US). RNeasy minikit was from Qiagen (Venlo, The Netherlands). SYBR green and TaqMan reverse transcription kit reagents were obtained from Applied Biosystems (Warrington, UK). Agilent Total RNA isolation Kit was purchased from Agilent Technologies (Santa Clara, CA, US). Salbutamol and triacsin C were purchased from Sigma (St Louis, MO, US) and A922500 (DGAT-1 inhibitor) (cat. no. 10012708) was purchased from Cayman Chemicals (Ann Arbor, MI, US). Protein assay reagent was purchased from BioRad (Copenhagen, Denmark) and protein content in each experiment was determined by the use of Coomassie reagent [44] and results were standardized according to this value for each well. All other chemicals used were of standard commercial high-purity quality.

2.2. Methods

2.2.1. Cell culture and fatty acid incubation

Satellite cells were isolated as previously described [45] from the *M. obliquus internus abdominis* of 15 healthy donors. Donors were 48 ± 3 years old, had a body mass index of 25.0 ± 1.0 kg/m^2 and fasting glucose 5.4 ± 0.2 mM, plasma lipids and blood pressure within normal range, and no family history of diabetes. The biopsies were obtained with informed consent and approved by the National Committee for Research Ethics, Oslo, Norway. The western blot experiments were performed on a different set of cells isolated from the *M. vastus lateralis* of 5 healthy donors. Donors were aged 50 ±

2 years, had a body mass index of 23.5 ± 1.0 kg/m^2, fasting glucose of 5.5 ± 0.1 mM, insulin and plasma lipids within normal range and no family history of diabetes. The biopsies were obtained with informed consent and approved by the local ethics committee of Funen and Vejle County, Denmark. In the complete set of donors used in this study there were 3 men and 12 women (western blot experiments; 2 women and 3 men). In most of the experiments myotubes from men were in minority and excluding them did not change the results.

The cells were cultured on 60 mm dishes, 12- or 96-well plates or 25 cm^2 flasks in DMEM-Glutamax™ (5.5 mM glucose), 2% fetal calf serum (FCS), 2% Ultroser G, 25 IU penicillin, 25 μg/ml streptomycin, and 1.25 μg/ml amphotericin B. At 70–80% confluence, the growth medium was replaced by DMEM-Glutamax™ supplemented with 2% FCS, 25 IU penicillin, 25 μg/ml streptomycin, 1.25 μg/ml amphotericin B, and 25 pM insulin to induce differentiation. The cells were cultured in humidified 5% CO_2 atmosphere at 37 °C, and the media were changed every 2–3 days. Experiments were performed after 7 days of differentiation. Stock solutions of fatty acid sodium salts (6 mM) were bound to albumin (BSA, 2.4 mM) (ratio FA/BSA 2.5/1) and they were heated to 45 °C and rapidly mixed. Only optically clear solutions were used. There were no differences between the myotubes after incubation with fatty acids for 24 h as evaluated by microscopic inspection searching for floating cells as well as by measurement of cell protein content and counting of number of nuclei.

2.2.2. Lipid distribution

Myotubes were cultured as described in Section 2.2.1 on 12-well plates coated with extracellular matrix (ECM) gel and incubated with 100 μM OA or PA supplemented with [^{14}C]OA, [^{14}C]PA (0.5 μCi/ml) or 25 μM [^{14}C]glycerol (1 μCi/ml) for 24 h. Myotubes were then washed twice with PBS (1 ml), harvested into a tube with two additions of 250 μl distilled water, and frozen at −20 °C. Cellular lipids were extracted as described earlier [46]. Briefly, homogenized cell fractions were extracted, lipids were separated by thin layer chromatography, and radioactivity was quantified by liquid scintillation. The amount of neutral lipids was calculated by using total protein levels for standardization.

2.2.3. Live imaging of lipid droplets (LDs)

Myotubes were cultured as described in Section 2.2.1 and pretreated with 100 μM OA or PA, with the exception of using 12-well glass bottom plates coated with ECM gel. The cells were incubated in 37 °C and 5% CO_2 with Bodipy 493/503 (2 μg/ml) for 5 min to stain LDs, with Hoechst 33258 (2.5 μg/ml) for 15 min to stain nuclei, with MitoTracker®Red FM (100 nM) for 15 min to stain mitochondria. Automated image acquisition was performed in culture medium without phenol red with a Scan^R platform (Olympus IX81 inverted fluorescence microscope) equipped with a temperature and CO_2-enrichment incubator for long-term live imaging, as described in Hessvik et al. [41]. We used a 20× objective and images were taken in 25 positions per well. The background-subtracted maximal intensity projection from 12 images taken in z-direction (1 μm apart) was used for each color channel at each position. Scan^R software was used for automated image analysis, using edge detection algorithm for object segmentation to quantify the intensity of MitoTracker®Red FM (mitochondrial content), number of nuclei and packing, area and number of LDs. LD volume was estimated from the measured area and packing was measured as fluorescence intensity per LD. After gating out aggregates and dead cells the results were determined from about 200 images (average of 38 ± 4 nuclei per image). Parameters were related to the number of nucleus to account for cell density.

2.2.4. Scintillation proximity assay

Radiolabeled substrates taken up and accumulated by adherent cells will be concentrated close to the scintillator embedded in the plastic bottom of each well (ScintiPlate®-96 TC, PerkinElmer) and provide a stronger signal than the radiolabel dissolved in the medium alone [47]. Myotubes were cultured as described in Section 2.2.1 and measurements of fatty acids present in the cell by scintillation proximity assay (SPA) were performed in medium without phenol red with [^{14}C]OA or [^{14}C]PA (0.5 μCi/ml, 100 μM) and were liquid scintillation monitored for 0, 2, 4, 6, 8 and 24 h during the incubation. Thereafter, the media were changed to DPBS with 10 mM HEPES, 0.5% BSA, 1 mM L-carnitine and 0.1 mM glucose and liquid scintillation measurements were monitored at 0, 1, 2, 4 and 6 h. The decline in [^{14}C]OA or [^{14}C]PA present in the cells in the absence and presence of triacsin C (10 μM) was then studied. Triacsin C inhibits long-chain fatty acyl-CoA synthetase (ACSL) and will therefore inhibit, among other pathways, reesterification. Earlier reports in human skeletal myotubes have shown that TAG synthesis is efficiently blocked with incubation of 10 μM triacsin C for 3 h [18]. Reesterification can be measured as fatty acid present in the cells, calculating the difference with and without triacsin C present, as previously reported by Bezaire et al. [48]. Salbutamol has been shown to induce lipolysis in human skeletal muscle [49] and was used to increase lipolysis via β2-adrenergic stimulation at a concentration of 100 nM.

2.2.5. Substrate oxidation assay and acid soluble metabolites

The muscle cells were cultured on 96-well CellBIND® microplates as described in Section 2.2.1. Substrate, [^{14}C]OA or [^{14}C]PA (0.5 or 1 μCi/ml, 100 μM) was given either for incubation for 24 h in culture media prior to the experiment (chronic exposure) with no fatty acid present during 4 h CO_2 trapping or in DPBS with 10 mM HEPES and 1 mM L-carnitine bound to BSA (40 μM) at a ratio of 2.5:1 during the 4 h CO_2 trapping experiment (acute exposure). A 96-well UniFilter®-96 GF/B microplate was mounted on top of the CellBIND® plate as described before [47], and the cells were incubated for 4 h at 37 °C. The [^{14}C]CO_2 trapped in the filter was counted by liquid scintillation, and the result reflects CO_2 production. DGAT-1 (diacylglycerol acyltransferase 1) inhibitor (A922500, 1 μM) or ACSL inhibitor (triacsin C, 10 μM) was added during these 4 h.

The muscle cells were also cultured on 96-well CellBIND® microplates or ScintiPlate®-96 TC as described in Section 2.2.1 and substrate, [^{14}C]glucose (0.58 μCi/ml, 200 μM) was given for incubation for 3 h. The labeled glucose was in the presence of 100 μM OA or PA in DPBS buffer with 10 mM HEPES during the CO_2 trapping experiment. A 96-well UniFilter®-96 GF/B microplate was mounted on top of the CellBIND® plate as described before [47], and the cells were incubated for 3 h at 37 °C. The [^{14}C]CO_2 trapped in the filter was counted by liquid scintillation, and the result reflects CO_2 production.

After the experiments (substrate oxidation assay or SPA) were finished, measurement of acid soluble metabolites (ASMs) was performed using a method modified from Skrede et al. [50]. Incubation media (30 μl) were transferred to a new Nunc multiwell V plate, precipitated with 100 μl $HClO_4$ (1 M) and 10 μl BSA (6%), and centrifuged (Sorvall RC-3C plus, Block Scientific, Inc., Bohemia, NY, US) at 900 *g* for 10 min at 4 °C. Then, 30–50 μl of the supernatant was counted by liquid scintillation. ASMs consist mainly of tricarboxylic acid cycle metabolites and reflect incomplete fatty acid oxidation in the mitochondria.

The remaining cell-associated (CA) radioactivity was assessed by liquid scintillation in every experiment. Myotubes were also treated with 25 μM [^{14}C]glycerol (1 μCi/ml) and 100 μM OA or PA for 24 h for measurement of cellular accumulation of this substrate.

2.2.6. Microarray

Human myotubes were cultured as described in Section 2.2.1 on 25 cm^2 flasks and preincubated with 100 μM OA, PA or EPA for 24 h. Thereafter the cells were harvested and the experiment was carried through as described by Hessvik et al. [41]. Gene set enrichment analysis

(GSEA) was performed for functional analysis of changes in gene expression. GSEA is focused on predefined gene sets, that is, groups of genes that share biological function, chromosomal location, or regulation [51]. In this study the microarray data was related to OA, contrary to Hessvik et al. [41] who related the data to BSA as a control. Gene sets with an FDR<0.2 were considered significantly regulated. All microarray data have been submitted to Gene Expression Omnibus (accession number: GSE18589).

2.2.7. RNA isolation and analysis of gene expression by TaqMan® qPCR

Cells were cultured as described in Section 2.2.1 on 25 cm^2 flasks and harvested and total RNA was isolated by Agilent Total RNA isolation kit according to the supplier's total RNA isolation protocol. Total RNA was reverse-transcribed with oligo primers using a PerkinElmer Thermal Cycler 9600 (25 °C for 10 min, 37 °C for 1 h 20 min, and 85 °C for 5 min) and a TaqMan reverse transcription reagents kit. Two micrograms of total RNA was added per 20 μl of total TaqMan reaction solution. qPCR was performed using an ABI PRISMT 7000 Detection System (Applied Biosystems, Warrington, UK). RNA expression was determined by SYBRT Green, and primers were designed using Primer ExpressT (Applied Biosystems, Warrington, UK). Each target gene was quantified in triplicate and carried out in a reaction volume of 25 μl according to the supplier's protocol. All assays were run for 40 cycles (95 °C for 12 s followed by 60 °C for 60 s). The transcription levels were normalized to the average of the housekeeping control genes 36B4 and GAPDH. The following forward and reverse primers were used at a concentration of 30 μM:

36B4 (acc_no M17885): F:CCATTCTATCATCAACGGGTACAA,
R:AGCAAGTGGGAAGGTGTAATCC;
GAPDH (acc_no NM_002046): F:TGCACCACCAACTGCTTAGC,
R:GGCATGGACTGTGGTCATGAG;
CD36 (acc_no L06850): F: AGTCACTGC GACATG ATTAATGGT,
R:CTGCAATACCTGGCTTTTCTCAA;
SCD (acc_no AB032261): F: CTCCCCTGCCACACTGATG,
R: GAGCGCTTGGCTTCTCATG;
FADS2 (acc_no NM_004265.2): F:5CCCGGCCTGGCTTCAC,
R:TGTAACAAAGCAGGCCTCTCTATG;
PLIN2 (Perilipin 2) (acc_no NM_001122): F:GGTGATGGCAGG CGCAT,
R: TAGAAGTGAGGAGGCTGTCAGACA;
PLIN3 (Perilipin 3) (acc_no NM_001164189.1): F:CACTCGCTGGG CAAGCTT,
R:CTTGACAGTTTCCATCAGGCTTAG;
PDK4 (acc_no BC040239): F:TTTCCAGACCAACCAATTCACA,
R: TGCCCGCATTGCATTCTTA.

2.2.8. Western blots

Myotubes were cultured as described in Section 2.2.1 on 60 mm dishes and harvested and homogenized in a buffer containing 50 mM HEPES, pH 7.4, 2 mM EDTA, 150 mM NaCl, 30 mM $NaPO_4$, 10 mM NaF, 1% Triton X-100, 10 μl/ml protease inhibitor, 10 μl/ml phosphatase I inhibitor, 10 μl/ml phosphatase II inhibitor, and 1.5 mg/ml benzamidine HCl. Cell extracts were centrifuged for 25 min at 15,000 *g*, and supernatants were stored at −80 °C. Solubilized proteins from myotubes were run on a 4–12% SDS-PAGE, transferred onto nitrocellulose membrane and incubated with the primary antibodies for PLIN2, PLIN3, ATGL and HSL. Subsequently, immunoreactive proteins were determined by enhanced chemiluminescence reagent and visualized by exposure to Hyperfilm ECL. GAPDH served as an internal control.

The antibodies were validated by the use of recombinant human PLIN2 protein and detection of PLIN3 in different muscle types in mice. ATGL and HSL antibodies have been previously validated in overexpression and knockdown studies in human myotubes [16].

2.2.9. Presentation of data and statistics

Statistical analyses were performed using GraphPad Prism 5.0 for Windows (GraphPad Software Inc., San Diego, CA, US). All values are reported as means ± SEM. The value n usually represents the number of different donors used each with at least triplicate samples. Two-tailed paired Student's t-tests were performed to determine the difference between OA and PA or between fatty acid and control. Linear mixed models (LMM) (SPSS Inc., Chicago, IL, US) were used to compare the effects of PA and OA over time when SPA was used in accumulation and lipolysis experiments. A p-value<0.05 was considered significant.

3. Results

3.1. Fatty acid and glycerol accumulations were lower in myotubes exposed to PA than OA

To explore the accumulation of OA and PA in human myotubes, the cells were treated with 100 μM [^{14}C]OA (18:1, n−9) or [^{14}C]PA (16:0), and cell-associated (CA) radioactivity was measured during 24 h by scintillation proximity assay (SPA). The results showed that PA incubation caused lower accumulation of radiolabeled fatty acid in the cells over time than OA ($p<0.05$, Fig. 1A). Quantification of lipid droplets (LDs) by live cell imaging (representative images are presented in Fig. 1C) showed that PA treatment for 24 h resulted in half the number of LDs compared to OA pretreatment ($p<0.05$, Fig. 1B), while LD volume and packing were similar (data not shown). When myotubes were treated with 25 μM [^{14}C]glycerol and 100 μM OA or PA for 24 h, cells incubated with PA resulted in a lower amount of CA-labeled glycerol than cells incubated with OA ($p<0.05$, Fig. 1B).

3.2. Incubation of myotubes with PA resulted in a different lipid distribution than incubation with OA

Myotubes were treated with 100 μM [^{14}C]OA or [^{14}C]PA for 24 h to examine lipid distribution. Incubation with PA resulted in relatively less PA incorporated into triacylglycerol (TAG), while relatively more PA was incorporated into phospholipid (PL) and cholesteryl ester (CE) in comparison to incubation with OA ($p<0.05$, Fig. 2A). The ratio between PA and OA for the lipid classes also revealed a lower incorporation into total lipids, TAG, DAG and free fatty acid (FFA) for PA when related to OA ($p<0.05$, Fig. 2B, data presented in Supplemental Table S-1). We achieved similar results for TAG, DAG and monoacylglycerol using [^{14}C]glycerol as label (data not shown).

Calculating ratios between the different lipid classes revealed that DAG related to TAG (DAG/TAG ratio) was significantly higher after incubation with PA than after OA incubation ($p<0.05$, Fig. 2C). Another calculated ratio, representing the reesterification and lipolysis pathway via LDs in relation to accumulation in membranes (TAG/PL), was significantly higher after incubation with OA than after PA incubation ($p<0.05$, Fig. 2C).

3.3. Lipolysis was lower in cells exposed to PA than to OA

To study the different metabolic fates of OA and PA, we measured reesterification and lipolysis of these fatty acids with and without triacsin C (ACSL inhibitor). Triacsin C increased lipolysis for both fatty acids to the same extent (data not shown). After 24 h treatment with of [^{14}C]OA or [^{14}C]PA, lipolysis was measured by SPA at 0, 1, 2, 4 and 6 h. Cells incubated with PA showed a lower lipolysis rate than cells incubated with OA, but a similar reesterification rate ($p<0.05$ for lipolysis, Fig. 3A). In addition to measuring lipolysis as decline of radioactive label in the cells, this finding was also confirmed by measuring lipolysis rate as radioactive label release into the culture medium (data not shown). If the lipolysis rate was related to

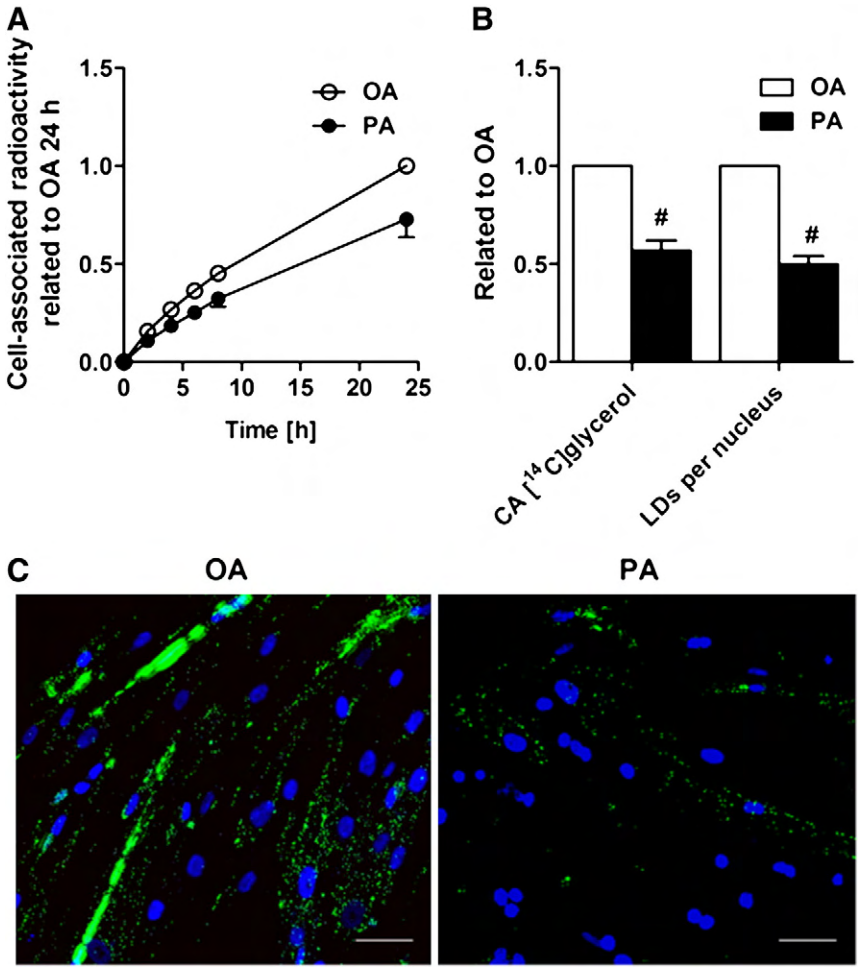

Fig. 1. Fatty acid and glycerol accumulation in myotubes. Human skeletal muscle cells were treated with 100 μM OA and PA for 24 h. A) Real-time accumulation of OA and PA in myotubes over time. Human myotubes were incubated with 0.5 μCi/ml [^{14}C]OA and [^{14}C]PA and accumulation of radiolabel monitored by SPA as described in Section 2.2.4. Results represent mean ± SEM for n = 7 donors related to OA at 24 h, LMM test, $p<0.05$ (74 ± 31 nmol/mg for OA and 39 ± 12 nmol/mg for PA at 24 h). B) Glycerol accumulation and number of LDs in the presence of OA or PA. Cells were treated with 25 μM [^{14}C]glycerol (1 μCi/ml) for 24 h as described in Section 2.2.5. CA [^{14}C]glycerol, presented as mean ± SEM related to OA, n = 8 donors, t-test, $p<0.05$(4.4 ± 0.5 nmol/mg for OA and 2.5 ± 0.5 nmol/mg for PA). Number of LDs per nucleus. Human skeletal muscle cells were stained and LDs and nuclei quantified as described in Section 2.2.3. Results represent mean ± SEM related to OA for n = 4 donors, t-test, $p<0.05$ (151 ± 25 LDs/nucleus for OA and 78 ± 13 LDs/nucleus for PA). C) Live cell imaging of LDs and nuclei in human myotubes. Human skeletal muscle cells were stained with Bodipy 493/503 (neutral lipid, green) and Hoechst 33258 (nuclei, blue) as described in Section 2.2.3. Representative images presented. Scale bar is 50 μm. The notation "#" represents statistics OA versus PA. CA, cell-associated; LD, lipid droplet; LMM, linear mixed model; OA, oleic acid; PA, palmitic acid; SPA, scintillation proximity assay.

cell-associated (CA) radioactivity there was no significant difference between the two fatty acid treatments (data not shown).

To evaluate this further, lipolysis- and reesterification rates of OA and PA were measured using a selective β_2-adrenergic agonist, salbutamol. Incubation with 100 nM salbutamol over 6 h after fatty acid pretreatment increased lipolysis for cells prelabelled with OA (≈50%, $p<0.05$, Fig. 3B), but this was not observed for cells prelabelled with PA. Fatty acid reesterification rate was unchanged for both fatty acids after incubation with salbutamol (data not shown).

3.4. Differential endogenous and exogenous fatty acid oxidation in PA and OA-treated myotubes

To further explore the metabolic fate of OA and PA, especially why PA was stored to a lesser extent than OA, we studied both exogenous (acute FA exposure) and endogenous (chronic FA exposure/TAG-derived) fatty acid oxidation in muscle cells. Myotubes were treated with 100 μM [^{14}C]OA or [^{14}C]PA for 24 h, and acid-soluble metabolites (ASMs) which give an indication of incomplete fatty acid oxidation, were measured. ASMs were found to be 45 ± 15% higher for PA than for OA during the 24 h pretreatment (OA: 200 ± 82 nmol/mg, $p<0.05$). Fatty acid oxidation data presented in this study were related to cell-associated (CA) labeled fatty acid to study how much fatty acid was oxidized compared to what was available as a substrate in the cell at the given time point. Measurement of [^{14}C]ASM formation and [^{14}C]CO_2 production during 4 h after fatty acid 24 h pretreatment showed that PA derived from the intracellular endogenous lipid pool was oxidized to a greater extent than OA ($p<0.05$ for both ASM and CO_2, Fig. 4A). However, the mitochondrial content measured by MitoTracker®Red FM staining after 24 h fatty acid incubation was similar between the two fatty acids (data not shown).

We also measured exogenous FA oxidation during acute exposure with either radiolabeled PA or OA. Myotubes were treated with 100 μM [^{14}C]OA and [^{14}C]PA for 4 h, and during this time period CO_2 production was about 70% higher for PA than for OA when related to intracellular CA ($p<0.05$, Fig. 4B). ASM formation during 4 h did not differ significantly (Fig. 4B).

Myotubes were also treated with 200 μM [^{14}C]glucose in the presence of 100 μM OA or PA for 3 h, revealing that cells incubated with PA and OA had a similar amount of cell-associated (CA) labeled

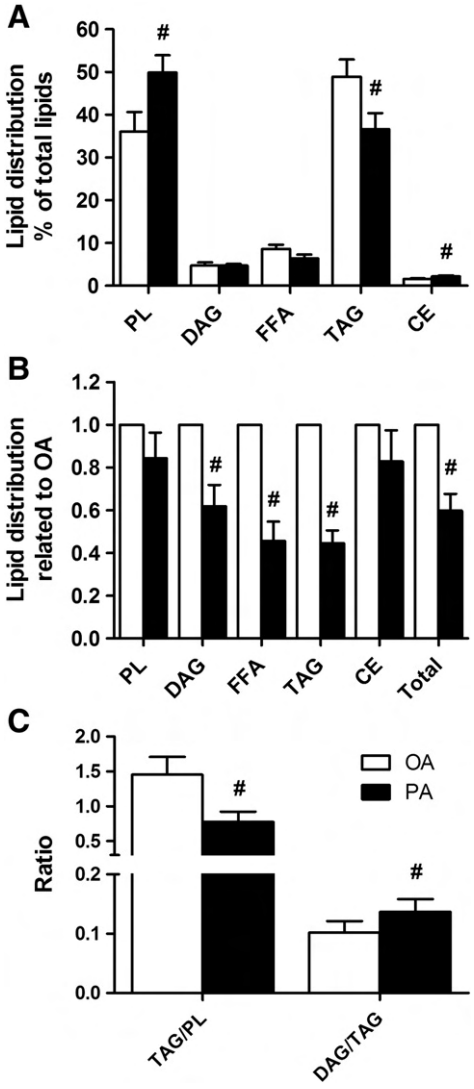

Fig. 2. Lipid distribution in myotubes. Human skeletal muscle cells were pretreated with 0.5 μCi/ml, 100 μM [^{14}C]OA and [^{14}C]PA for 24 h. Cellular lipids were extracted and separated by thin-layer chromatography, and radioactivity was quantified by liquid scintillation as described in Section 2.2.2. A) Lipid distribution as % of total lipids in the cell. Results represent mean ± SEM for n = 6 donors (4 experiments), t-test, $p<0.05$ for TAG, PL and CE (absolute values presented in Supplemental Table S-1). B) Lipid distribution as PA related to OA. Results represent mean ± SEM for n = 6 donors (4 experiments), t-test, $p<0.05$ for DAG, FFA, TAG and total lipids (absolute values presented in Supplemental Table S-1). C) DAG/TAG and TAG/PL ratio. Results represent mean ratio ± SEM for n = 6 donors (4 experiments), t-test, $p<0.05$. The notation "#" represents statistics OA versus PA. CE, cholesteryl ester; DAG, diacylglycerol; FFA, free fatty acid; OA, oleic acid; PA, palmitic acid; PL, phospholipid; TAG, triacylglycerol.

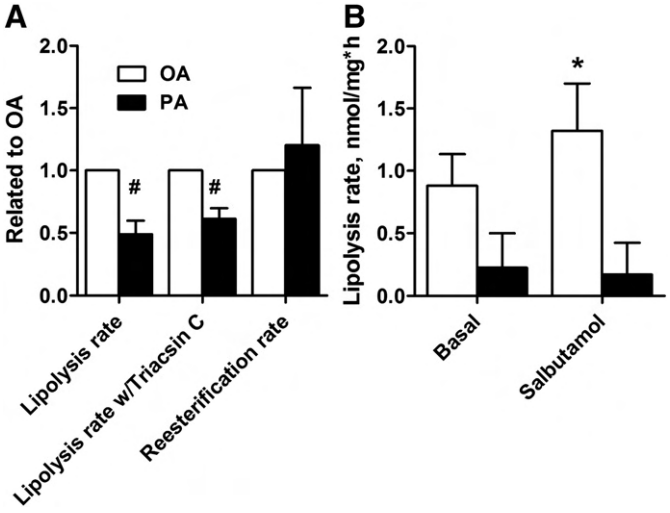

Fig. 3. Lipolysis and reesterification rates. Human myotubes were pretreated with 0.5 μCi/ml, 100 μM [^{14}C]OA and [^{14}C]PA for 24 h, washed and reincubated and lipolysis measured as described in Section 2.2.4. Reesterification was calculated as the difference between lipolysis in the presence and absence of triacsin C. A) Lipolysis- and reesterification rates of OA and PA. Data from measurements at 1, 2, 4, and 6 h with SPA are pooled. Results represent mean ± SEM related to OA for n = 7 donors, LMM test, $p<0.05$ (OA; 3.0 ± 1.3, 5.8 ± 2.6, 7.8 ± 3.5 nmol/mg·h, PA; 1.4 ± 0.6, 3.0 ± 1.1, 5.3 ± 1.3 nmol/mg·h). B) Lipolysis rate after cell incubation with OA and PA with and without salbutamol (100 nM, β-adrenergic agonist). Data from measurements at 1, 2, 4, and 6 h with SPA are pooled. Results represent mean ± SEM for n = 3 donors, LMM, $p<0.05$ for OA lipolysis vs. basal. The notation "#" represents statistics OA versus PA, while the notation "*" represents statistics fatty acid versus basal. LMM, linear mixed model; OA, oleic acid; PA, palmitic acid; SPA, scintillation proximity assay.

glucose (data not shown). In line with this, there were no significant differences in glucose oxidation between the two fatty acid incubations, also when related to CA (data not shown).

Myotubes were treated with 100 μM fatty acid and 25 μM [^{14}C] glycerol with and without the DGAT-1 inhibitor (1 μM A922500) for 4 h. Measurement of lipid distribution showed approximately 90% decrease in incorporation into TAG in the presence of A922500 (data not shown). In addition, myotubes were treated with 100 μM [^{14}C]OA and [^{14}C]PA for 4 h, with and without DGAT-1 inhibitor or ACSL inhibitor (10 μM triacsin C). CO_2 production from OA and PA increased in the presence of DGAT-1 inhibitor (for OA; $p<0.05$, Fig. 4C) and the increase was significantly higher for OA-treated cells than PA-treated cells ($p<0.05$, Fig. 4C). Incubation with ACSL inhibitor resulted in a decreased CO_2 production from OA and PA (for OA; $p<0.05$, Fig. 4C).

3.5. Exposure of the cells to PA upregulated several metabolic pathway, among them fatty acid β-oxidation and lipogenesis, while downregulated oxidative phosphorylation

Microarray analysis was performed to examine whether treatment with 100 μM OA or PA for 24 h regulated gene expression differently in the myotubes. Gene set enrichment analysis (GSEA) was performed for functional analysis of changes in gene expression. Pathways with FDR (q-value) <0.2, that is -log q > 0.7, were considered as significantly regulated. Compared to treatment with OA, treatment with PA significantly upregulated several pathways, such as lipogenesis, fatty acid β-oxidation and cholesterol synthesis and downregulated pathways such as oxidative phosphorylation (Fig. 5). Genes involved in these pathways are presented in Supplemental Table S-2. The genes ACSL1, ACSL5, SLC25A20, HADHA and CRAT were ranked high by the GSEA analysis of the fatty acid β-oxidation pathway. ACSL catalyzes long-chain fatty acids (LCFA) to LCFA-acyl CoA esters, which, among other pathways, are substrate for carnitine palmitoyltransferase 1 (CPT1) before crossing the mitochondrial membrane via carnitine/acylcarnitine translocase (encoded by SLC25A20) in skeletal muscle [52]. ACSL5 is suggested to provide acyl-CoA for β-oxidation rather than TAG synthesis, although this might not be the case in skeletal muscle (reviewed in [53]). Once inside the mitochondria LCFA-acyl-CoA goes through β-oxidation where chain-shortening reactions are catalyzed by mitochondrial trifunctional protein (alfa subunit encoded by HADHA) (reviewed in [54]), while carnitine O-acetyltransferase (CRAT) is a mitochondrial matrix enzyme that plays a key role in the synthesis and efflux of short-chain carnitine conjugates, such as acetyl-carnitine.

The expression of some genes playing important roles in lipid metabolism, CD36, SCD-1, FADS2, PLIN2, PLIN3 and PDK4 was studied by qPCR after 24 h incubation of 100 μM OA or PA. None of these genes were significantly different expressed between the two treatments (Fig. 6); although PLIN2 mRNA expression (relative to GAPDH and

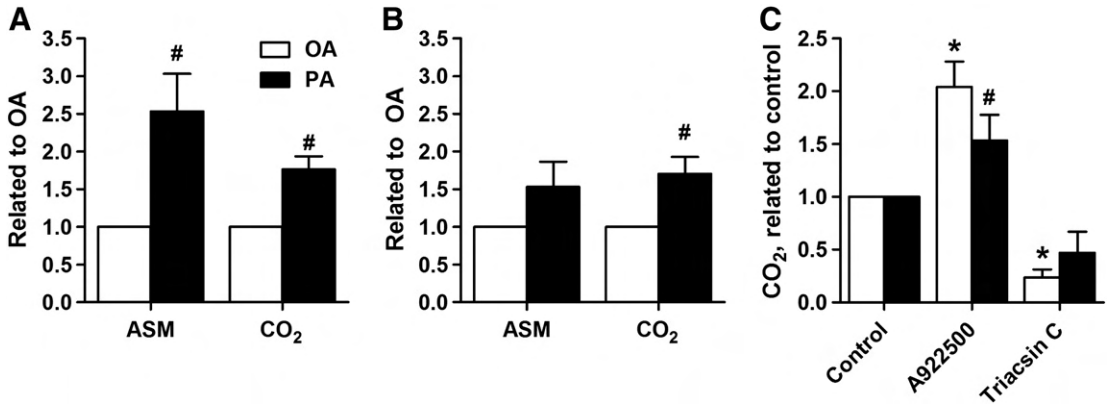

Fig. 4. Fatty acid oxidation. Human myotubes were treated with 0.5 or 1 μCi/ml, 100 μM [^{14}C]OA and [^{14}C]PA and [^{14}C]ASMs and [^{14}C]CO_2 production was measured as explained in Section 2.2.5. A) Measurement of ASM and CO_2 production from endogenous intramyocellular lipids in myotubes related to CA and OA. Human myotubes were pretreated with fatty acids for 24 h, thereafter the cells were reincubated with fatty acid-free media for 4 h and ASM and CO_2 production was measured during this time. Results represent mean ± SEM for n = 17 and 13 donors, t-test, $p<0.05$ (for OA: ASM/CA: 0.10 ± 0.03, CO_2/CA: 0.045 ± 0.007, for PA: ASM/CA: 0.15 ± 0.02, CO_2/CA: 0.071 ± 0.011). B) Measurement of ASM and CO_2 production from exogenous lipids in myotubes related to CA radioactivity and OA. Human myotubes were treated with fatty acids for 4 h and ASM was measured and CO_2 production was measured during this time. Results represent mean ± SEM for n = 11 and 16 donors, t-test, $p=0.14$ for ASM and $p<0.05$ for CO_2 (for OA: ASM/CA: 1.51 ± 0.53, CO_2/CA: 0.067 ± 0.010, for PA: ASM/CA: 1.47 ± 0.55, CO_2/CA: 0.096 ± 0.012). C) CO_2 production from exogenous lipids in myotubes in the presence of inhibitors related to CA radioactivity and control. Human myotubes were treated with fatty acids for 4 h with A922500 (1 μM, DGAT-1 inhibitor) or triacsin C (10 μM, ACSL inhibitor) present and CO_2 production was measured. Results represent mean ± SEM for n = 3 donors, t-test, $p<0.05$. The notation "#" represents statistics OA versus PA, while the notation "*" represents statistics fatty acid versus control. ASMs, acid soluble metabolites; CA, cell-associated; DGAT, diacylglycerol acyltransferase; ACSL, long-chain fatty acyl-CoA synthetase; OA, oleic acid; PA, palmitic acid.

36B4) related to the number of LDs revealed a more than two-fold higher ratio for PA- than OA-treated cells (data not shown).

3.6. Exposure of the cells with PA upregulated adipose triglyceride lipase protein level to a higher extent compared to OA

Western blot analysis was performed to examine whether treatment with 100 μM OA or PA for 24 h regulated levels of proteins involved in lipolysis (PLINs and lipases). The results showed no difference in PLIN2 and PLIN3 protein levels. ATGL had a more than two-fold higher protein level in cells incubated with PA compared to OA ($p<0.05$, Fig. 7), while HSL showed an unchanged protein level after fatty acid treatment. An upregulation of ATGL by PA compared to OA was seen both in myotubes established from *M. vastus lateralis* (Fig. 7) and from *M. obliquus internus abdominis* (data not shown). ATGL mRNA level (based on microarray data) was unchanged between OA and PA conditions (data not shown).

3.7. Coincubation with eicosapentaenoic acid eliminated the difference in fatty acid accumulation and lipolysis between PA and OA

Eicosapentaenoic acid (EPA) has been shown to positively influence energy metabolism in myotubes [41,43] and this fatty acid was coincubated with OA and PA to see if it would have an impact on the discrepancy between them. Myotubes were treated with a mixture of 100 μM fatty acids for 24 h and cell-associated (CA) radioactivity was measured during 24 h by SPA. The results showed that

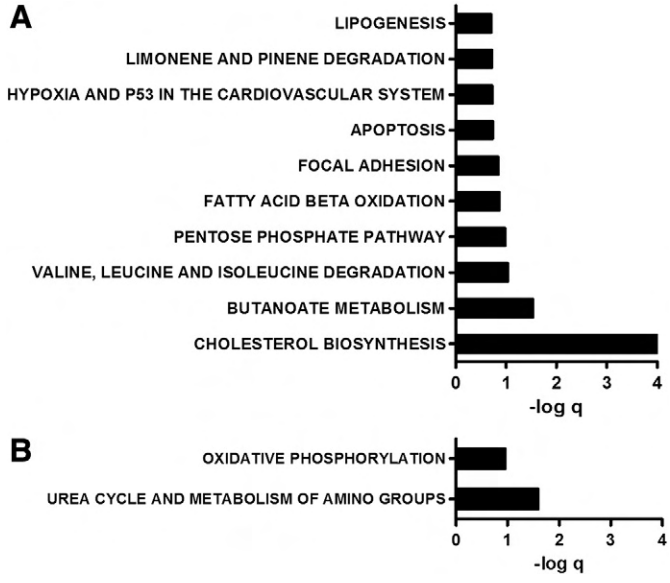

Fig. 5. Microarray pathway analysis. Pathways involved in metabolic processes upregulated A) and downregulated B) by PA related to OA in myotubes. Myotubes were incubated with OA or PA (100 μM) for 24 h and then harvested for RNA isolation. Gene expression was measured by Affymetrix human NuGO GeneChip arrays, and GSEA was performed to identify pathways regulated by PA compared with OA in three donors as explained in Section 2.2.6. Pathways with FDR (q-value) <0.2 (that is, log (q) >0.7) were considered significantly regulated and only these are presented. Genes included in some of these pathways are presented in Supplemental Table S-2. GSEA, gene set enrichment analysis; OA, oleic acid; PA, palmitic acid.

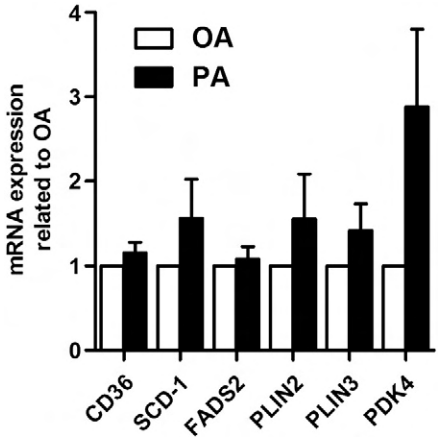

Fig. 6. Gene regulation. Human skeletal muscle cells were pretreated with 100 μM OA or 100 μM PA for 24 h and harvested for RNA isolation. qPCR was performed as described in Section 2.2.7. Results represent mean ± SEM related to OA for 4–6 donors, t-test, $p=0.13$ for PDK4, (values related to 36B4 and GAPDH; CD36; 0.84 ± 0.13 and 0.93 ± 0.10, SCD1; 1.03 ± 0.32 and 1.42 ± 0.47, FADS2; 1.07 ± 0.35 and 1.14 ± 0.45, PLIN2 (Perilipin 2); 1.17 ± 0.62 and 1.52 ± 0.61, PLIN3 (Perilipin 3); 1.81 ± 0.58 and 1.79 ± 0.76, PDK4; 0.94 ± 0.37 and 1.85 ± 0.32 for OA and PA respectively). CD36, fatty acid translocase; FADS2, fatty acid desaturase 2; OA, oleic acid; PA, palmitic acid; PDK4, pyruvate dehydrogenase kinase isozyme 4; SCD1, stearoyl-CoA desaturase 1.

the presence of EPA increased the CA radioactivity of labeled PA during 24 h ($p<0.05$ for [^{14}C]PA in addition to EPA versus [^{14}C]PA, Fig. 8A), recovering the difference between OA and PA observed in Fig. 1. Lipolysis of OA and PA was also measured using SPA after 24 h pretreatment with these fatty acid mixtures. The decay of [^{14}C] OA or [^{14}C]PA was measured during 6 h in fatty acid-free medium. The results revealed that EPA increased lipolysis of PA ($p<0.05$ for [^{14}C]PA in combination with EPA versus [^{14}C]PA alone, Fig. 8B), and thus eliminating the differences between OA and PA on lipolysis observed in Fig. 3A. The combination with EPA also increased reesterification similarly for both OA and PA. We also examined the mixture of trace amounts of [^{14}C]PA (9 μM) and non-labeled OA and the results showed that the presence of OA neither had an effect on CA radioactivity nor lipolysis in PA treated cells (data not shown).

Microarray analysis was performed to examine whether treatment for 24 h with 100 μM EPA regulated gene expression differently in the myotubes than 24 h with 100 μM OA. Gene set enrichment analysis (GSEA) was performed for functional analysis of changes in gene expression. Compared to treatment with OA, treatment with EPA significantly upregulated several pathways, such as glycolysis, gluconeogenesis, fructose and mannose metabolism and cholesterol synthesis (Fig. 8C). Genes involved in these pathways are presented in Supplemental Table S-3.

4 . Discussion and conclusion

4.1 . Discussion

In cultured human myotubes we observed that labeled PA was accumulated and stored in TAG to a lower extent than OA, and incorporated PA underwent a lower lipolysis rate compared to OA. On the other hand, relatively more PA was oxidized, and stored mainly as PL, and PA increased ATGL protein content to a greater extent than OA. Interestingly, the differences in lipid accumulation and lipolysis between these two fatty acids were drastically reduced in combination with EPA.

The main new finding in this study is that the lipolysis rate of PA was lower than that of OA. In addition, lipid distribution showed that PA was also incorporated to a lesser extent into TAG and DAG; also indicating that PA may undergo less lipolysis from this pool. PA was, on the other hand, incorporated to a higher extent into PL and CE, which are lipid pools not supposed to undergo lipolysis to the same extent as TAG. The number of LDs after PA exposure was 50% lower compared to OA exposure. Because PLIN2 protein level was similar in OA and PA-treated myotubes, the relative amount of PLIN2 per LD was higher for PA-treated cells, potentially indicating a LD surface more protected against lipolysis [22,23]. This might be in accordance with the results of a lower lipolysis rate of PA than OA.

Although treatment of myotubes with PA induced more than two-fold higher ATGL protein level than OA, our results with labeled fatty acids revealed that PA had a lower lipolysis rate than OA. This may be due to a lower pool of total TAG in PA-treated myotubes, suggesting that the size of the TAG pool determines the rate of lipolysis. This is in agreement with studies showing a higher depletion of the intramyocellular TAG pool during exercise in the skeletal muscle of women having a larger intramyocellular TAG pool than men [55]. In this study, ATGL mRNA level was unchanged between OA and PA treatments. Post-transcriptional regulation of ATGL has been observed in human adipocytes [48] demonstrating that mRNA and protein level of lipases are not always correlated, and this might also be the case for skeletal muscle cells. Another hypothesis is that ATGL is not active. Indeed the regulation of ATGL depends on coregulators like comparative gene identification-58 (CGI-58) [18,56]. Recent studies in human myotubes clearly show the limiting role of CGI-58 in the control of lipolysis and ATGL activity [18].

HSL protein level did not differ between OA and PA treatments, this protein is most likely activated by phosphorylation and needs to translocate from the cytoplasm, thus neither for this enzyme the full picture of the function from the protein level might be revealed [34,39].

Surprisingly, although LD number was lower after PA than after OA treatment, the fatty acid reesterification rate for PA- and OA-treated cells was not different. This might be due to that PA was more incorporated into PL and CE rather than into DAG and TAG. The enzyme DGAT-1 catalyzes the formation of DAG from TAG (reviewed in [57]). Incubation for 4 h of the myotubes with a DGAT-1 inhibitor markedly decreased fatty acid incorporation into the TAG-pool. In addition, when DGAT-1 was inhibited, fatty acid oxidation was increased, and oxidation of OA was increased to a higher extent than oxidation of PA. Combined with the higher DAG/TAG ratio after 24 h PA treatment than after OA treatment, this might reflect a higher affinity for OA-CoA or unsaturated fatty acids by DGAT-1. In line with this, Thörn et al. [58] hypothesized that DGAT expression was dependent on the degree of fatty acid saturation in a pancreatic β cell line, while Cases et al. [59] found that DGAT-1 appeared to prefer oleoyl-CoA over palmitoyl-CoA in vitro in insect cells.

EPA in combination with PA had an effect on increasing PA accumulation and lipolysis rate. We have previously reported that this fatty acid

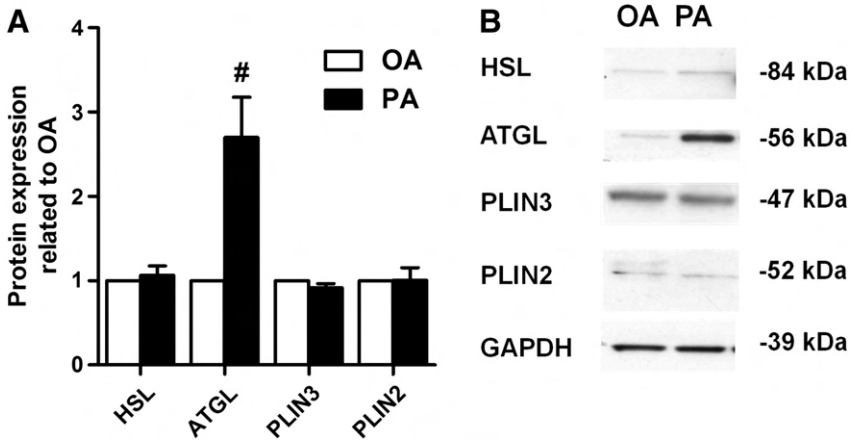

Fig. 7. Protein regulation. Human skeletal muscle cells were pretreated with 100 μM OA and PA for 24 h and cells were harvested as described in Section 2.2.8. Protein expression was measured by Western blot. A) Protein expression. Results represent mean ± SEM related to OA for 5 donors, t-test, $p<0.05$ for ATGL, (values related to GAPDH; HSL; 0.54 ± 0.20 and 0.62 ± 0.29, ATGL; 0.29 ± 0.05 and 0.70 ± 0.04, PLIN3 (Perilipin 3); 0.45 ± 0.09 and 0.41 ± 0.09, PLIN2 (Perilipin 2); 0.22 ± 0.03 and 0.22 ± 0.05 for OA and PA respectively). The notation "#" represents statistics OA versus PA. B) Representative Western blots for the proteins examined. GAPDH served as an internal control. ATGL, adipose triglyceride lipase; GAPDH, Glyceraldehyde 3-phosphate dehydrogenase; HSL, hormone-sensitive lipase; OA, oleic acid; PA, palmitic acid.

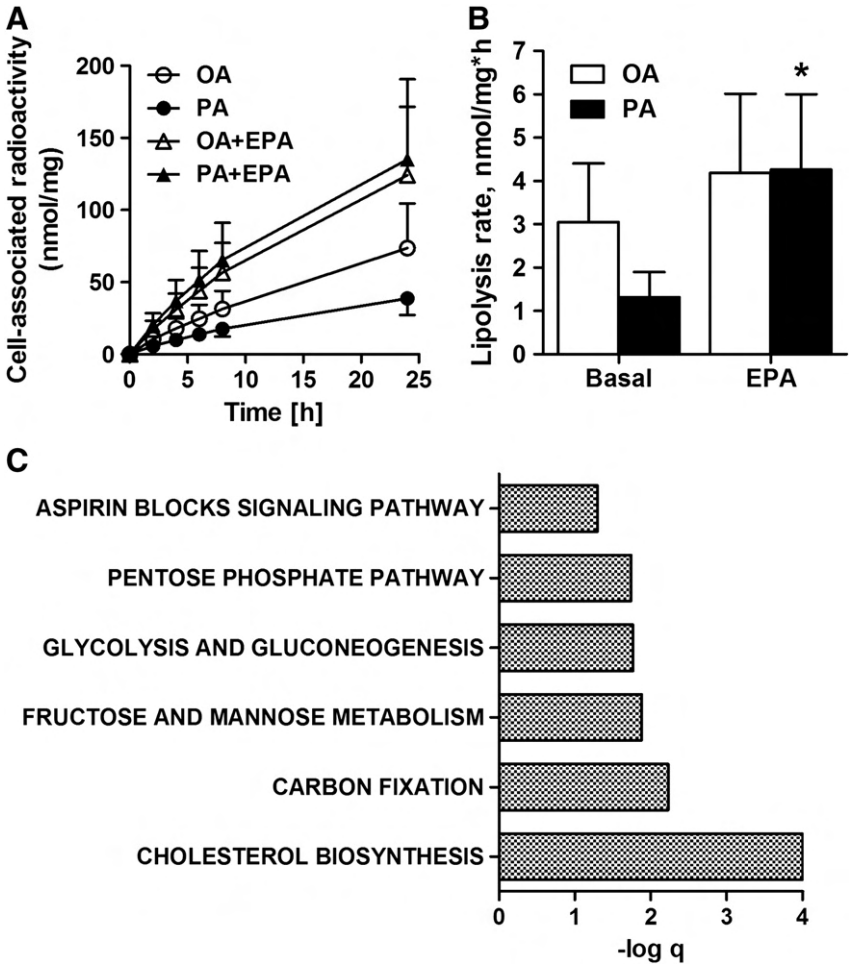

Fig. 8. Effects of eicosapentaenoic acid (EPA). A) Effect of EPA on OA and PA accumulation in cells over time. Human myotubes were incubated with 0.5 μCi/ml, 100 μM [^{14}C]OA and OA or EPA, or with [^{14}C]PA and PA or EPA for 24 h, and accumulation of [^{14}C]fatty acid was measured by SPA as described in Section 2.2.4. Results represent mean ± SEM for n = 7 donors, LMM, $p<0.05$ for [^{14}C]PA in addition to EPA versus [^{14}C]PA. B) Effect of EPA on OA and PA lipolysis rate. Human myotubes were reincubated in fatty acid-free media for 6 h after 24 h fatty acid pretreatment (as described in A) and data from measurements at 1, 2, 4, and 6 h by SPA were pooled. Results represent mean ± SEM for n = 7 donors, LMM, $p<0.05$ for and [^{14}C]PA in addition to EPA versus [^{14}C]PA. C) Pathways involved in metabolic processes upregulated by EPA related to OA in myotubes. Myotubes were incubated with OA or EPA (100 μM) for 24 h and then harvested for RNA isolation. Gene expression was measured by Affymetrix human NuGO GeneChip arrays, and GSEA was performed to identify pathways regulated by EPA compared with OA in three donors as explained in Section 2.2.6. Pathways with FDR (q-value) <0.2 (that is, log (q) >0.7) were considered significantly regulated and only these are presented. Genes included in some of these pathways are presented in Supplemental Table S-3. The notation "#" represents statistics OA versus PA, while the notation "*" represents statistics fatty acid versus basal. EPA, eicosapentaenoic acid; GSEA, gene set enrichment analysis; LMM, linear mixed model; OA, oleic acid; PA, palmitic acid.

can increase PA accumulation in human myotubes as well as positively influence glucose metabolism [42,43]. This is also in agreement with a study in β-pancreatic cells where EPA restored PA-induced inhibition of insulin secretion [60]. From the microarray GSEA pathway analysis, we observed that treatment with EPA significantly upregulated glycolysis and gluconeogenesis pathways related to OA. Moreover, EPA (300 μM) has been shown to stimulate lipolysis in 3T3-L1 mouse adipocytes after 24 h incubation [61]. On the other side, another study in cultured primary rat adipocytes has shown that EPA (100 and 200 μM) decreased lipolysis in an AMP-kinase-dependent way. The same study also observed that EPA incubation resulted in stimulation of HSL phosphorylation in Ser-565 and a decrease in ATGL protein levels in 3T3-L1 mouse cells. At the same time, in vivo in rats, EPA had no effect on mRNA HSL and ATGL levels in adipose tissue [62]. The observation that EPA increases the lipolysis of PA in myotubes might be a result of a higher accumulation of TAG, supported by earlier reports that observed that EPA incubation in myotubes results in about twice as many LDs than PA [41]. In this study we mostly examined skeletal muscle cells in culture supplied with only one fatty acid, while in vivo the diet is a mixture of different fatty acids. Nevertheless, our study may indicate that if a diet is composed of mainly SFA, it may require consumption of more PUFA to increase storage of PA in LDs. This may eliminate possible undesirable effects of SFA on skeletal muscle lipid metabolism such as accumulation of ceramides and other potentially lipotoxic intermediates ([9–11], reviewed in [63]).

Our data showed that PA was oxidized to CO_2 to a relatively higher extent than OA; both from exo- and endogenous lipids, and PA also underwent incomplete oxidation (ASMs) to a higher degree than OA when derived from endogene lipids. This is in line with the report of García-Martínez et al. [6], where human myotubes incubated with PA and OA for 16 h showed higher incomplete and complete oxidation of fatty acids when exposed to PA compared to OA. Also in accordance with this, Koves et al. [64] found that palmitoylcarnitine content was higher than oleoylcarnitine in L6 rat myotubes after incubation for 24 h, indicating a higher uptake of PA into the mitochondria than OA. CPT1 is the main fatty acid transporter into the mitochondria, and CPT1 has also been shown to have a higher affinity for palmitoyl-CoA than oleoyl-CoA in vivo in rats [65]. Despite a higher oxidation of PA than OA, mitochondrial content did not differ between the two treatments. Mitochondrial content has in different studies been shown to

correlate both negatively and positively with fatty acid oxidation in myotubes [15,66] and is perhaps in this context not a reliable measure of mitochondrial activity.

Microarray pathway analysis showed that PA treatment of myotubes upregulated genes involved in lipogenesis, fatty acid β-oxidation and cholesterol synthesis, while downregulated oxidative phosphorylation compared to OA. Upregulation of fatty acid β-oxidation is in accordance with the observed higher PA oxidation than OA oxidation. Furthermore, the upregulation of lipogenesis might be to promote increased desaturation and TAG formation and cholesterol synthesis to increase cholesterol ester (CE) formation, while downregulation of oxidative phosphorylation might be to prevent formation of superoxide. Up- and downregulation of these pathways could therefore work as protective mechanisms to sequester fatty acids and lipotoxic intermediates to prevent lipotoxic effects [67–72].

4.2 . Conclusion

Results from the present study indicate that less PA compared to OA is accumulated and incorporated into TAG, while relatively more PA was incorporated into PL. PA underwent lipolysis to a lesser degree than OA, despite an increased protein level of ATGL, but showed a higher mitochondrial fatty acid oxidation. Furthermore, the differences in accumulation and lipolysis between OA and PA were eliminated in combination with EPA. This study reveals that the two most abundant fatty acids in our diet have a different metabolic fate in skeletal muscle cells, which might be of relevance in understanding the link between dietary fat and development of skeletal muscle insulin resistance.

Acknowledgements

The authors are thankful to Gerbrand Koster and Oddmund Bakke of the NORMIC-UiO imaging platform, Department of Molecular Biosciences, University of Oslo, for the support and use of equipment and to Camilla Stensrud and Åse-Karine Fjeldheim for the excellent technical assistance. Kurt Højlund and Klaus Levin are thanked for muscle biopsies and Katie Louche for the help with protein analysis, while Eili T. Kase is thanked for reading the manuscript and giving constructive criticism.

This work was supported by grants from the Norwegian Research Council, the Norwegian Diabetes Foundation, Freia Chocolade Fabriks Medical Foundation, the Anders Jahre's Foundation, the National Research Agency ANR-09-JCJC-0019-01, the European Foundation for the Study of Diabetes/Novo Nordisk, the Danish Medical Research Council and Novo Nordisk Foundation, Denmark.

Appendix A. Supplementary data

Supplementary data to this article can be found online at http://dx.doi.org/10.1016/j.bbalip.2012.07.001.

References

[1] E.J. Feskens, J.G. Loeber, D. Kromhout, Diet and physical activity as determinants of hyperinsulinemia: the Zutphen Elderly Study, Am. J. Epidemiol. 140 (4) (1994) 350–360.
[2] J.A. Marshall, D.H. Bessesen, R.F. Hamman, High saturated fat and low starch and fibre are associated with hyperinsulinaemia in a non-diabetic population: the San Luis Valley Diabetes Study, Diabetologia 40 (4) (1997) 430–438.
[3] B. Vessby, M. Uusitupa, K. Hermansen, G. Riccardi, A.A. Rivellese, L.C. Tapsell, C. Nalsen, L. Berglund, A. Louheranta, B.M. Rasmussen, G.D. Calvert, A. Maffetone, E. Pedersen, I.B. Gustafsson, L.H. Storlien, Substituting dietary saturated for monounsaturated fat impairs insulin sensitivity in healthy men and women: the KANWU Study, Diabetologia 44 (3) (2001) 312–319.
[4] N. Tardif, J. Salles, J.F. Landrier, I. Mothe-Satney, C. Guillet, C. Boue-Vaysse, L. Combaret, C. Giraudet, V. Patrac, J. Bertrand-Michel, C. Migne, J.M. Chardigny, Y. Boirie, S. Walrand, Oleate-enriched diet improves insulin sensitivity and restores muscle protein synthesis in old rats, Clin. Nutr. 30 (6) (2011) 799–806.
[5] J.P. DeLany, M.M. Windhauser, C.M. Champagne, G.A. Bray, Differential oxidation of individual dietary fatty acids in humans, Am. J. Clin. Nutr. 72 (4) (2000) 905–911.
[6] C. García-Martínez, M. Marotta, R. Moore-Carrasco, M. Guitart, M. Camps, S. Busquets, E. Montell, A.M. Gomez-Foix, Impact on fatty acid metabolism and differential localization of FATP1 and FAT/CD36 proteins delivered in cultured human muscle cells, Am. J. Physiol. Cell Physiol. 288 (6) (2005) C1264–C1272.
[7] E. Montell, M. Turini, M. Marotta, M. Roberts, V. Noe, C.J. Ciudad, K. Mace, A.M. Gomez-Foix, DAG accumulation from saturated fatty acids desensitizes insulin stimulation of glucose uptake in muscle cells, Am. J. Physiol. Endocrinol. Metab. 280 (2) (2001) E229–E237.
[8] M. Gaster, A.C. Rustan, H. Beck-Nielsen, Differential utilization of saturated palmitate and unsaturated oleate: evidence from cultured myotubes, Diabetes 54 (3) (2005) 648–656.
[9] J.A. Chavez, T.A. Knotts, L.P. Wang, G. Li, R.T. Dobrowsky, G.L. Florant, S.A. Summers, A role for ceramide, but not diacylglycerol, in the antagonism of insulin signal transduction by saturated fatty acids, J. Biol. Chem. 278 (12) (2003) 10297–10303.
[10] J.S. Lee, S.K. Pinnamaneni, S.J. Eo, I.H. Cho, J.H. Pyo, C.K. Kim, A.J. Sinclair, M.A. Febbraio, M.J. Watt, Saturated, but not n−6 polyunsaturated, fatty acids induce insulin resistance: role of intramuscular accumulation of lipid metabolites, J. Appl. Physiol. 100 (5) (2006) 1467–1474.
[11] G. Kewalramani, P.J. Bilan, A. Klip, Muscle insulin resistance: assault by lipids, cytokines and local macrophages, Curr. Opin. Clin. Nutr. Metab. Care 13 (4) (2010) 382–390.
[12] M. Just, N.J. Faergeman, J. Knudsen, H. Beck-Nielsen, M. Gaster, Long-chain Acyl-CoA is not primarily increased in myotubes established from type 2 diabetic subjects, Biochim. Biophys. Acta 1762 (7) (2006) 666–672.
[13] C. Moro, S. Bajpeyi, S.R. Smith, Determinants of intramyocellular triglyceride turnover: implications for insulin sensitivity, Am. J. Physiol. Endocrinol. Metab. 294 (2) (2008) E203–E213.
[14] M. Gaster, Reduced lipid oxidation in myotubes established from obese and type 2 diabetic subjects, Biochem. Biophys. Res. Commun. 382 (4) (2009) 766–770.
[15] E. Corpeleijn, N.P. Hessvik, S.S. Bakke, K. Levin, E.E. Blaak, G.H. Thoresen, M. Gaster, A.C. Rustan, Oxidation of intramyocellular lipids is dependent on mitochondrial function and the availability of extracellular fatty acids, Am. J. Physiol. Endocrinol. Metab. 299 (1) (2010) E14–E22.
[16] P.M. Badin, K. Louche, A. Mairal, G. Liebisch, G. Schmitz, A.C. Rustan, S.R. Smith, D. Langin, C. Moro, Altered skeletal muscle lipase expression and activity contribute to insulin resistance in humans, Diabetes 60 (6) (2011) 1734–1742.
[17] L.M. Sparks, C. Moro, B. Ukropcova, S. Bajpeyi, A.E. Civitarese, M.W. Hulver, G.H. Thoresen, A.C. Rustan, S.R. Smith, Remodeling lipid metabolism and improving insulin responsiveness in human primary myotubes, PLoS One 6 (7) (2011) e21068.
[18] P.M. Badin, C. Loubiere, M. Coonen, K. Louche, G. Tavernier, V. Bourlier, A. Mairal, A.C. Rustan, S.R. Smith, D. Langin, C. Moro, Regulation of skeletal muscle lipolysis and oxidative metabolism by the co-lipase CGI-58, J. Lipid Res. 53 (5) (2012) 839–848.
[19] R. Minnaard, P. Schrauwen, G. Schaart, J.A. Jorgensen, E. Lenaers, M. Mensink, M.K. Hesselink, Adipocyte differentiation-related protein and OXPAT in rat and human skeletal muscle: involvement in lipid accumulation and type 2 diabetes mellitus, J. Clin. Endocrinol. Metab. 94 (10) (2009) 4077–4085.
[20] I.M. Gjelstad, F. Haugen, H.L. Gulseth, F. Norheim, A. Jans, S.S. Bakke, T. Raastad, A.E. Tjonna, U. Wisloff, E.E. Blaak, U. Riserus, M. Gaster, H.M. Roche, K.I. Birkeland, C.A. Drevon, Expression of perilipins in human skeletal muscle in vitro and in vivo in relation to diet, exercise and energy balance, Arch. Physiol. Biochem. 118 (1) (2012) 22–30.
[21] C.S. Shaw, M. Sherlock, P.M. Stewart, A.J. Wagenmakers, Adipophilin distribution and colocalization with lipid droplets in skeletal muscle, Histochem. Cell Biol. 131 (5) (2009) 575–581.
[22] C. Londos, C. Sztalryd, J.T. Tansey, A.R. Kimmel, Role of PAT proteins in lipid metabolism, Biochimie 87 (1) (2005) 45–49.
[23] T.F. Lee, K.M. Mak, O. Rackovsky, Y.L. Lin, A.J. Kwong, J.C. Loke, S.L. Friedman, Downregulation of hepatic stellate cell activation by retinol and palmitate mediated by adipose differentiation-related protein (ADRP), J. Cell. Physiol. 223 (3) (2010) 648–657.
[24] A.V. Bulankina, A. Deggerich, D. Wenzel, K. Mutenda, J.G. Wittmann, M.G. Rudolph, K.N. Burger, S. Honing, TIP47 functions in the biogenesis of lipid droplets, J. Cell Biol. 185 (4) (2009) 641–655.
[25] J.W. Jocken, E. Smit, G.H. Goossens, Y.P. Essers, M.A. van Baak, M. Mensink, W.H. Saris, E.E. Blaak, Adipose triglyceride lipase (ATGL) expression in human skeletal muscle is type I (oxidative) fiber specific, Histochem. Cell Biol. 129 (4) (2008) 535–538.
[26] T.J. Alsted, L. Nybo, M. Schweiger, C. Fledelius, P. Jacobsen, R. Zimmermann, R. Zechner, B. Kiens, Adipose triglyceride lipase in human skeletal muscle is upregulated by exercise training, Am. J. Physiol. Endocrinol. Metab. 296 (3) (2009) E445–E453.
[27] A. Yao-Borengasser, V. Varma, R.H. Coker, G. Ranganathan, B. Phanavanh, N. Rasouli, P.A. Kern, Adipose triglyceride lipase expression in human adipose tissue and muscle. Role in insulin resistance and response to training and pioglitazone, Metab. Clin. Exp. 60 (7) (2011) 1012–1020.
[28] R. Zimmermann, J.G. Strauss, G. Haemmerle, G. Schoiswohl, R. Birner-Gruenberger, M. Riederer, A. Lass, G. Neuberger, F. Eisenhaber, A. Hermetter, R. Zechner, Fat mobilization in adipose tissue is promoted by adipose triglyceride lipase, Science 306 (5700) (2004) 1383–1386.

[29] C. Lefevre, F. Jobard, F. Caux, B. Bouadjar, A. Karaduman, R. Heilig, H. Lakhdar, A. Wollenberg, J.L. Verret, J. Weissenbach, M. Ozguc, M. Lathrop, J.F. Prud'homme, J. Fischer, Mutations in CGI-58, the gene encoding a new protein of the esterase/lipase/thioesterase subfamily, in Chanarin-Dorfman syndrome, Am. J. Hum. Genet. 69 (5) (2001) 1002–1012.
[30] M. Akiyama, K. Sakai, M. Ogawa, J.R. McMillan, D. Sawamura, H. Shimizu, Novel duplication mutation in the patatin domain of adipose triglyceride lipase (PNPLA2) in neutral lipid storage disease with severe myopathy, Muscle Nerve 36 (6) (2007) 856–859.
[31] J. Fischer, C. Lefevre, E. Morava, J.M. Mussini, P. Laforet, A. Negre-Salvayre, M. Lathrop, R. Salvayre, The gene encoding adipose triglyceride lipase (PNPLA2) is mutated in neutral lipid storage disease with myopathy, Nat. Genet. 39 (1) (2007) 28–30.
[32] M.J. Watt, G.J. Heigenhauser, M. O'Neill, L.L. Spriet, Hormone-sensitive lipase activity and fatty acyl-CoA content in human skeletal muscle during prolonged exercise, J. Appl. Physiol. 95 (1) (2003) 314–321.
[33] M.J. Watt, T. Stellingwerff, G.J. Heigenhauser, L.L. Spriet, Effects of plasma adrenaline on hormone-sensitive lipase at rest and during moderate exercise in human skeletal muscle, J. Physiol. 550 (Pt 1) (2003) 325–332.
[34] G. Fredrikson, H. Tornqvist, P. Belfrage, Hormone-sensitive lipase and monoacylglycerol lipase are both required for complete degradation of adipocyte triacylglycerol, Biochim. Biophys. Acta 876 (2) (1986) 288–293.
[35] L.R. Liu, S.P. Lin, C.C. Chen, Y.J. Chen, C.C. Tai, S.C. Chang, R.H. Juang, Y.W. Tseng, B.H. Liu, H.J. Mersmann, T.L. Shen, S.T. Ding, Serum amyloid A induces lipolysis by downregulating perilipin through ERK1/2 and PKA signaling pathways, Obesity 19 (12) (2011) 2301–2309.
[36] C. Sztalryd, G. Xu, H. Dorward, J.T. Tansey, J.A. Contreras, A.R. Kimmel, C. Londos, Perilipin A is essential for the translocation of hormone-sensitive lipase during lipolytic activation, J. Cell Biol. 161 (6) (2003) 1093–1103.
[37] J. Langfort, T. Ploug, J. Ihlemann, C. Holm, H. Galbo, Stimulation of hormone-sensitive lipase activity by contractions in rat skeletal muscle, Biochem. J. 351 (Pt 1) (2000) 207–214.
[38] J. Langfort, T. Ploug, J. Ihlemann, M. Saldo, C. Holm, H. Galbo, Expression of hormone-sensitive lipase and its regulation by adrenaline in skeletal muscle, Biochem. J. 340 (Pt 2) (1999) 459–465.
[39] C. Prats, M. Donsmark, K. Qvortrup, C. Londos, C. Sztalryd, C. Holm, H. Galbo, T. Ploug, Decrease in intramuscular lipid droplets and translocation of HSL in response to muscle contraction and epinephrine, J. Lipid Res. 47 (11) (2006) 2392–2399.
[40] J.W. Jocken, C. Roepstorff, G.H. Goossens, P. van der Baan, M. van Baak, W.H. Saris, B. Kiens, E.E. Blaak, Hormone-sensitive lipase serine phosphorylation and glycerol exchange across skeletal muscle in lean and obese subjects: effect of beta-adrenergic stimulation, Diabetes 57 (7) (2008) 1834–1841.
[41] N.P. Hessvik, S.S. Bakke, K. Fredriksson, M.V. Boekschoten, A. Fjorkenstad, G. Koster, M.K. Hesselink, S. Kersten, E.T. Kase, A.C. Rustan, G.H. Thoresen, Metabolic switching of human myotubes is improved by n − 3 fatty acids, J. Lipid Res. 51 (8) (2010) 2090–2104.
[42] V. Aas, M.H. Rokling-Andersen, E.T. Kase, G.H. Thoresen, A.C. Rustan, Eicosapentaenoic acid (20:5 n − 3) increases fatty acid and glucose uptake in cultured human skeletal muscle cells, J. Lipid Res. 47 (2) (2006) 366–374.
[43] A.J. Wensaas, A.C. Rustan, M. Just, R.K. Berge, C.A. Drevon, M. Gaster, Fatty acid incubation of myotubes from humans with type 2 diabetes leads to enhanced release of beta-oxidation products because of impaired fatty acid oxidation: effects of tetradecylthioacetic acid and eicosapentaenoic acid, Diabetes 58 (3) (2009) 527–535.
[44] M.M. Bradford, A rapid and sensitive method for the quantitation of microgram quantities of protein utilizing the principle of protein-dye binding, Anal. Biochem. 72 (1976) 248–254.
[45] M. Gaster, S.R. Kristensen, H. Beck-Nielsen, H.D. Schroder, A cellular model system of differentiated human myotubes, APMIS 109 (11) (2001) 735–744.
[46] M. Gaster, A.C. Rustan, V. Aas, H. Beck-Nielsen, Reduced lipid oxidation in skeletal muscle from type 2 diabetic subjects may be of genetic origin: evidence from cultured myotubes, Diabetes 53 (3) (2004) 542–548.
[47] A.J. Wensaas, A.C. Rustan, K. Lovstedt, B. Kull, S. Wikstrom, C.A. Drevon, S. Hallen, Cell-based multiwell assays for the detection of substrate accumulation and oxidation, J. Lipid Res. 48 (4) (2007) 961–967.
[48] V. Bezaire, A. Mairal, C. Ribet, C. Lefort, A. Girousse, J. Jocken, J. Laurencikiene, R. Anesia, A.M. Rodriguez, M. Ryden, B.M. Stenson, C. Dani, G. Ailhaud, P. Arner, D. Langin, Contribution of adipose triglyceride lipase and hormone-sensitive lipase to lipolysis in hMADS adipocytes, J. Biol. Chem. 284 (27) (2009) 18282–18291.
[49] E.E. Blaak, S.L. Schiffelers, W.H. Saris, M. Mensink, M.E. Kooi, Impaired beta-adrenergically mediated lipolysis in skeletal muscle of obese subjects, Diabetologia 47 (8) (2004) 1462–1468.
[50] S. Skrede, J. Bremer, R.K. Berge, A.C. Rustan, Stimulation of fatty acid oxidation by a 3-thia fatty acid reduces triacylglycerol secretion in cultured rat hepatocytes, J. Lipid Res. 35 (8) (1994) 1395–1404.
[51] A. Subramanian, P. Tamayo, V.K. Mootha, S. Mukherjee, B.L. Ebert, M.A. Gillette, A. Paulovich, S.L. Pomeroy, T.R. Golub, E.S. Lander, J.P. Mesirov, Gene set enrichment analysis: a knowledge-based approach for interpreting genome-wide expression profiles, Proc. Natl. Acad. Sci. U. S. A. 102 (43) (2005) 15545–15550.
[52] G. Peluso, O. Petillo, S. Margarucci, P. Grippo, M.A. Melone, F. Tuccillo, M. Calvani, Differential carnitine/acylcarnitine translocase expression defines distinct metabolic signatures in skeletal muscle cells, J. Cell. Physiol. 203 (2) (2005) 439–446.
[53] R.A. Coleman, T.M. Lewin, C.G. Van Horn, M.R. Gonzalez-Baro, Do long-chain acyl-CoA synthetases regulate fatty acid entry into synthetic versus degradative pathways? J. Nutr. 132 (8) (2002) 2123–2126.
[54] R.S. Rector, R.M. Payne, J.A. Ibdah, Mitochondrial trifunctional protein defects: clinical implications and therapeutic approaches, Adv. Drug Deliv. Rev. 60 (13–14) (2008) 1488–1496.
[55] C. Roepstorff, M. Donsmark, M. Thiele, B. Vistisen, G. Stewart, K. Vissing, P. Schjerling, D.G. Hardie, H. Galbo, B. Kiens, Sex differences in hormone-sensitive lipase expression, activity, and phosphorylation in skeletal muscle at rest and during exercise, Am. J. Physiol. Endocrinol. Metab. 291 (5) (2006) E1106–E1114.
[56] A. Lass, R. Zimmermann, G. Haemmerle, M. Riederer, G. Schoiswohl, M. Schweiger, P. Kienesberger, J.G. Strauss, G. Gorkiewicz, R. Zechner, Adipose triglyceride lipase-mediated lipolysis of cellular fat stores is activated by CGI-58 and defective in Chanarin-Dorfman Syndrome, Cell Metab. 3 (5) (2006) 309–319.
[57] R.M. Bell, R.A. Coleman, Enzymes of glycerolipid synthesis in eukaryotes, Annu. Rev. Biochem. 49 (1980) 459–487.
[58] K. Thörn, P. Bergsten, Fatty acid-induced oxidation and triglyceride formation is higher in insulin-producing MIN6 cells exposed to oleate compared to palmitate, J. Cell. Biochem. 111 (2) (2010) 497–507.
[59] S. Cases, S.J. Stone, P. Zhou, E. Yen, B. Tow, K.D. Lardizabal, T. Voelker, R.V. Farese, Cloning of DGAT2, a second mammalian diacylglycerol acyltransferase, and related family members, J. Biol. Chem. 276 (42) (2001) 38870–38876.
[60] T. Kato, H. Shimano, T. Yamamoto, M. Ishikawa, S. Kumadaki, T. Matsuzaka, Y. Nakagawa, N. Yahagi, M. Nakakuki, A.H. Hasty, Y. Takeuchi, K. Kobayashi, A. Takahashi, S. Yatoh, H. Suzuki, H. Sone, N. Yamada, Palmitate impairs and eicosapentaenoate restores insulin secretion through regulation of SREBP-1c in pancreatic islets, Diabetes 57 (9) (2008) 2382–2392.
[61] M.S. Lee, I.S. Kwun, Y. Kim, Eicosapentaenoic acid increases lipolysis through up-regulation of the lipolytic gene expression and down-regulation of the adipogenic gene expression in 3T3-L1 adipocytes, Genes Nutr. 2 (4) (2008) 327–330.
[62] S. Lorente-Cebrian, M. Bustos, A. Marti, M. Fernandez-Galilea, J.A. Martinez, M.J. Moreno-Aliaga, Eicosapentaenoic acid inhibits tumour necrosis factor-alpha-induced lipolysis in murine cultured adipocytes, J. Nutr. Biochem. 23 (3) (2012) 218–227.
[63] M.J. Watt, A.J. Hoy, Lipid metabolism in skeletal muscle: generation of adaptive and maladaptive intracellular signals for cellular function, Am. J. Physiol. Endocrinol. Metab. 302 (11) (2012) E1315–E1328.
[64] T.R. Koves, J.R. Ussher, R.C. Noland, D. Slentz, M. Mosedale, O. Ilkayeva, J. Bain, R. Stevens, J.R. Dyck, C.B. Newgard, G.D. Lopaschuk, D.M. Muoio, Mitochondrial overload and incomplete fatty acid oxidation contribute to skeletal muscle insulin resistance, Cell Metab. 7 (1) (2008) 45–56.
[65] G.R. Gavino, V.C. Gavino, Rat liver outer mitochondrial carnitine palmitoyltransferase activity towards long-chain polyunsaturated fatty acids and their CoA esters, Lipids 26 (4) (1991) 266–270.
[66] M. Gaster, Mitochondrial mass is inversely correlated to complete lipid oxidation in human myotubes, Biochem. Biophys. Res. Commun. 404 (4) (2011) 1023–1028.
[67] L.L. Listenberger, X. Han, S.E. Lewis, S. Cases, R.V. Farese Jr., D.S. Ory, J.E. Schaffer, Triglyceride accumulation protects against fatty acid-induced lipotoxicity, Proc. Natl. Acad. Sci. U. S. A. 100 (6) (2003) 3077–3082.
[68] M.J. Watt, Storing up trouble: does accumulation of intramyocellular triglyceride protect skeletal muscle from insulin resistance? Clin. Exp. Pharmacol. Physiol. 36 (1) (2009) 5–11.
[69] J. Garbarino, S.L. Sturley, Saturated with fat: new perspectives on lipotoxicity, Curr. Opin. Clin. Nutr. Metab. Care 12 (2) (2009) 110–116.
[70] S.-E. Choi, I.-R. Jung, Y.-J. Lee, S.-J. Lee, J.-H. Lee, Y. Kim, H.-S. Jun, K.-W. Lee, C.B. Park, Y. Kang, Stimulation of lipogenesis as well as fatty acid oxidation protects against palmitate-induced INS-1 β-cell death, Endocrinology 152 (3) (2011) 816–827.
[71] A.K. Busch, E. Gurisik, D.V. Cordery, M. Sudlow, G.S. Denyer, D.R. Laybutt, W.E. Hughes, T.J. Biden, Increased fatty acid desaturation and enhanced expression of stearoyl coenzyme A desaturase protects pancreatic beta-cells from lipoapoptosis, Diabetes 54 (10) (2005) 2917–2924.
[72] A. Peter, C. Weigert, H. Staiger, F. Machicao, F. Schick, J. Machann, N. Stefan, C. Thamer, H.U. Haring, E. Schleicher, Individual stearoyl-CoA desaturase 1 expression modulates endoplasmic reticulum stress and inflammation in human myotubes and is associated with skeletal muscle lipid storage and insulin sensitivity in vivo, Diabetes 58 (8) (2009) 1757–1765.

Supplementary

Table S-1. Lipid distribution in PA and OA treated human myotubes. Human skeletal muscle cells were pretreated with 0.5 µCi/ml, 100 µM [^{14}C]OA and [^{14}C]PA for 24 h. Cellular lipids were extracted and separated by thin-layer chromatography, and radioactivity was quantified by liquid scintillation as described in the manuscript chapter 2.2.2. Results represent mean ratio ± SEM for n=6 donors (4 experiments). TAG: P<0.05 for OA vs PA. CE, cholesteryl ester; DAG, diacylglycerol; FFA, free fatty acid; OA, oleic acid; PA, palmitic acid; PL, phospholipid; TAG, triacylglycerol; Total lipids (sum of all above).

	OA		**PA**	
nmol/mg	***Mean***	***SEM +/-***	***Mean***	***SEM +/-***
PL	166.8	20.1	136.6	20.2
DAG	23.0	4.7	13.1	1.9
FFA	45.7	12.6	18.1	4.2
TAG	253.6	60.0	102.3	17.2
CE	8.3	2.0	6.0	0.7
Total lipids	497.4	95.9	276.1	37.1

Table S-2. Genes involved in pathways regulated by PA related to OA. Myotubes were incubated with OA or PA (100 µM) for 24 h and then harvested for RNA isolation. Gene expression was measured by Affymetrix human NuGO GeneChip arrays, and gene set enrichment analysis (GSEA) was performed to identify pathways regulated by PA compared with OA. Pathways with FDR (q-value) < 0.2 (that is, log (q) > 0.7) were considered significantly regulated. Genes included in some of these pathways are presented with their rank metric score, score used to position the gene in the ranked list. OA, oleic acid; PA, palmitic acid.

Gene	**Gene name**	**Rank metric score**
	Lipogenesis	
SCD	stearoyl-CoA desaturase (delta-9-desaturase)	7.245
FADS2	fatty acid desaturase 2	6.929
ELOVL5	elongation of very long chain fatty acids protein 5	3.225
SREBF1	sterol regulatory element binding transcription factor 1	2.879
ME1	NADP-dependent malic enzyme	1.983
MOGAT1	monoacylglycerol O-acyltransferase 1	1.878
MTTP	microsomal triglyceride transfer protein	1.443
HSD17B12	hydroxysteroid (17-beta) dehydrogenase 12	1.392
ELOVL4	elongation of very long chain fatty acids protein 4	1.237
PPARG	peroxisome proliferator-activated receptor gamma	1.198
	Fatty acid β-oxidation	
ACSS2	acyl-CoA synthetase short-chain family member 2	3.365
ACSL1	acyl-CoA synthetase long-chain family member 1	2.652
DLD	dihydrolipoamide dehydrogenase	2.267
CRAT	carnitine O-acetyltransferase	1.389
BTBD1	BTB (POZ) domain containing 1	1.301

ACSL5	acyl-CoA synthetase long-chain family member 5	1.060
LPL	lipoprotein lipase	1.024
ABCA7	ATP-binding cassette, sub-family A (ABC1), member 7	0.888
ABCA3	ATP-binding cassette, sub-family A (ABC1), member 3	0.,848
DRP2	dystrophin related protein 2	0.836
FXR1	fragile X mental retardation, autosomal homolog 1	0.812
ACADM	medium-chain(C-4 to C-12) specific acyl-CoA dehydrogenase	0.692
HADHA	mitochondrial trifunctional protein, alpha subunit	0.656
ABCA5	ATP-binding cassette, sub-family A (ABC1), member 5	0.594
DCTD	dCMP deaminase	0.591
GPD2	glycerol-3-phosphate dehydrogenase 2 (mitochondrial)	0.511
ATN1	atrophin 1	0.509
SLC25A20	solute carrier family 25 (carnitine/acylcarnitine translocase), member 20	0.454
	Cholesterol biosynthesis	
DHCR7	7-dehydrocholesterol reductase	4.803
MVD	mevalonate (diphospho) decarboxylase	3.908
IDI1	isopentenyl-diphosphate delta isomerase 1	3.468
FDPS	farnesyl diphosphate synthase	3.435
SC4MOL	sterol-C4-methyl oxidase-like	3.403
HMGCS1	3-hydroxy-3-methylglutaryl-CoA synthase 1	3.401
CYP51A1	cytochrome P450, family 51, subfamily A, polypeptide 1	2.632
FDFT1	farnesyl-diphosphate farnesyltransferase 1	2.314
LSS	lanosterol synthase (2,3-oxidosqualene-lanosterol cyclase)	2.001
SC5DL	sterol-C5-desaturase-like	1.960
SQLE	squalene epoxidase	1.906
NSDHL	NAD(P) dependent steroid dehydrogenase-like	1.637
	Oxidative Phosphorylation	
TCIRG1	T-cell, immune regulator 1, ATPase, H+ transporting, lysosomal V0 subunit A3	-3.100
COX4I2	cytochrome c oxidase subunit IV isoform 2	-2.898
NDUFA4L2	NADH dehydrogenase (ubiquinone) 1 alpha subcomplex, 4-like 2	-2.787
ATP6V1F	ATPase, H+ transporting, lysosomal, V1 subunit F	-2.768
NDUFB10	NADH dehydrogenase (ubiquinone) 1 beta subcomplex, 10	-2.065
ATP6V0C	ATPase, H+ transporting, lysosomal, V0 subunit c	-1.834
NDUFA13	NADH dehydrogenase (ubiquinone) 1 alpha subcomplex, 13	-1.833
ATP5I	ATP synthase, H+ transporting, mitochondrial Fo complex, subunit E	-1.777
ATP6V1B2	ATPase, H+ transporting, lysosomal, V1 subunit B2	-1.776
CYC1	cytochrome c-1	-1.738
NDUFA2	NADH dehydrogenase (ubiquinone) 1 alpha subcomplex, 2	-1.722
ATP6V1G3	ATPase, H+ transporting, lysosomal, V1 subunit G31	-1.713
NDUFS8	NADH dehydrogenase (ubiquinone) Fe-S protein 8 (NADH-coenzyme Q reductase)	-1.635
ATP6V0B	ATPase, H+ transporting, lysosomal, V0 subunit b	-1.612
COX5B	cytochrome c oxidase subunit Vb	-1.589

NDUFAB1	NADH dehydrogenase (ubiquinone) 1, alpha/beta subcomplex, 1	-1.526
ATP6V1H	ATPase, H+ transporting, lysosomal, V1 subunit H	-1.459
NDUFA7	NADH dehydrogenase (ubiquinone) 1 alpha subcomplex, 7	-1.446
ATP5D	ATP synthase, H+ transporting, mitochondrial F1 complex, delta subunit	-1.348
ATP6V0D1	ATPase, H+ transporting, lysosomal, V0 subunit d1	-1.332
NDUFA12	NADH dehydrogenase (ubiquinone) 1 alpha subcomplex, 12	-1.328
NDUFS7	NADH dehydrogenase (ubiquinone) Fe-S protein 7, (NADH-coenzyme Q reductase)	-1.271
UQCRQ	ubiquinol-cytochrome c reductase, complex III subunit VII	-1.243
UQCR	ubiquinol-cytochrome c reductase	-1.195
NDUFA8	NADH dehydrogenase (ubiquinone) 1 alpha subcomplex, 8	-1.187
NDUFA3	NADH dehydrogenase (ubiquinone) 1 alpha subcomplex, 3	-1.186
ATP5G1	ATP synthase, H+ transporting, mitochondrial Fo complex, subunit C1	-1.154
ATP12A	ATPase, H+/K+ transporting, nongastric, alpha polypeptide	-1.104
NDUFB8	NADH dehydrogenase (ubiquinone) 1 beta subcomplex, 8	-1.084
NDUFB7	NADH dehydrogenase (ubiquinone) 1 beta subcomplex, 7	-1.051
NDUFC2	NADH dehydrogenase (ubiquinone) 1, subcomplex unknown, 2	-0.990
COX8A	cytochrome c oxidase subunit VIIIA	-0.922
COX7A1	cytochrome c oxidase subunit VIIa polypeptide 1	-0.877
NDUFS3	NADH dehydrogenase (ubiquinone) Fe-S protein 3,(NADH-coenzyme Q reductase)	-0.868
COX6A2	cytochrome c oxidase subunit VIa polypeptide 2	-0.860
ATP6V1G1	ATPase, H+ transporting, lysosomal, V1 subunit G1	-0.735
ATP4A	ATPase, H+/K+ exchanging, alpha polypeptide	-0.709
COX4I1	cytochrome c oxidase subunit IV isoform 1	-0.708
NDUFS6	NADH dehydrogenase (ubiquinone) Fe-S protein 6,(NADH-coenzyme Q reductase)	-0.691
NDUFA11	NADH dehydrogenase (ubiquinone) 1 alpha subcomplex, 11	-0.690
ATP6V1E2	ATPase, H+ transporting, lysosomal, V1 subunit E2	-0.681
NDUFC1	NADH dehydrogenase (ubiquinone) 1, subcomplex unknown, 1	-0.649
UCRC	Ubiquinol-cytochrome c reductase complex	-0.588
NDUFV1	NADH dehydrogenase (ubiquinone) flavoprotein 1	-0.582
NDUFB5	NADH dehydrogenase (ubiquinone) 1 beta subcomplex, 5	-0.546
ATP5G2	ATP synthase, H+ transporting, mitochondrial Fo complex, subunit C2	-0.544
NDUFB9	NADH dehydrogenase (ubiquinone) 1 beta subcomplex, 9	-0.541
COX7A2L	cytochrome c oxidase subunit VIIa polypeptide 2 like	-0.535
ATP6V1G2	ATPase, H+ transporting, lysosomal, V1 subunit G2	-0.515
ATP4B	ATPase, H+/K+ exchanging, beta polypeptide	-0.489
SDHD	succinate dehydrogenase complex, subunit D	-0.481
SDHB	succinate dehydrogenase complex, subunit B	-0.465
ATP5J2	ATP synthase, H+ transporting, mitochondrial Fo complex, subunit F2	-0.460
ATP6V1A	ATPase, H+ transporting, lysosomal, V1 subunit A	-0.456
NDUFS4	NADH dehydrogenase (ubiquinone) Fe-S protein 4,(NADH-coenzyme Q reductase)	-0.434
UQCRC1	ubiquinol-cytochrome c reductase core protein I	-0.407

NDUFB4	NADH dehydrogenase (ubiquinone) 1 beta subcomplex, 4	-0.403
NDUFB11	NADH dehydrogenase (ubiquinone) 1 beta subcomplex, 11	-0.380
ATP6V0D2	ATPase, H+ transporting, lysosomal, V0 subunit d2	-0.377
NDUFA10	NADH dehydrogenase (ubiquinone) 1 alpha subcomplex, 10	-0.368
ATP6V1C2	ATPase, H+ transporting, lysosomal 42kDa, V1 subunit C2	-0.361

Table S-3. Genes involved in pathways regulated by EPA related to OA. See table text for table S-2.

Gene	Protein	Rank metric score
	Glycolysis and gluconeogenesis	
ALDOC	aldolase C, fructose-bisphosphate	4.075
GCK	glucokinase (hexokinase 4)	3.479
PFKP	phosphofructokinase	3.117
ENO1	enolase 1	2.066
ENO2	enolase 2	1.915
DLD	dihydrolipoamide dehydrogenase	1.647
PGK1	phosphoglycerate kinase 1	1.624
GOT1	glutamic-oxaloacetic transaminase 1	1.381
ALDOA	aldolase A, fructose-bisphosphate	1.306
	Fructose and Mannose metabolism	
ALDOC	aldolase C, fructose-bisphosphate	4.075
PFKP	phosphofructokinase	3.117
RDH11	retinol dehydrogenase 11	1.930
ALDOB	aldolase B, fructose-bisphosphate	1.861
PFKFB3	6-phosphofructo-2-kinase/fructose-2,6-biphosphatase 3	1.855
AKR1B10	aldo-keto reductase family 1, member B10 (aldose reductase)	1.764
PGM2	phosphoglucomutase 2	1.616
GMDS	GDP-mannose 4,6-dehydratase	1.499
ALDOA	aldolase A, fructose-bisphosphate	1.306
B4GALNT2	beta-1,4-N-acetyl-galactosaminyl transferase 2	1.279
HSD3B7	hydroxy-delta-5-steroid dehydrogenase, 3 beta- and steroid delta-isomerase 7	1.267
HK1	hexokinase 1	0.995
TPI1	triosephosphate isomerase 1	0.897
RDH12	retinol dehydrogenase 12	0.874
B4GALNT3	beta-1,4-N-acetyl-galactosaminyl transferase 3	0.847
HSD17B12	hydroxysteroid (17-beta) dehydrogenase 12	0.846
UGCGL2	UDP-glucose ceramide glucosyltransferase-like 2	0.823
MTMR2	myotubularin related protein 2	0.773
RDH13	retinol dehydrogenase 13	0.727
PFKFB2	6-phosphofructo-2-kinase/fructose-2,6-biphosphatase 2	0.712
MTMR6	myotubularin related protein 6	0.664
PFKFB4	6-phosphofructo-2-kinase/fructose-2,6-biphosphatase 4	0.645
	Cholesterol biosynthesis	
SC4MOL	sterol-C4-methyl oxidase-like	6.979
SQLE	squalene epoxidase	6.606
MVD	mevalonate (diphospho) decarboxylase	6.498
HMGCS1	3-hydroxy-3-methylglutaryl-CoA synthase 1	6.386
IDI1	isopentenyl-diphosphate delta isomerase 1	5.425
DHCR7	7-dehydrocholesterol reductase	4.600
SC5DL	sterol-C5-desaturase	4.539

FDFT1	farnesyl-diphosphate farnesyltransferase 1	3.983
HMGCR	3-hydroxy-3-methylglutaryl-CoA reductase	3.818
CYP51A1	cytochrome P450, family 51, subfamily A, polypeptide 1	3.774
FDPS	farnesyl diphosphate synthase	2.957
NSDHL	NAD(P) dependent steroid dehydrogenase-like	2.527
LSS	lanosterol synthase (2,3-oxidosqualene-lanosterol cyclase)	2.179

PUBLICATION 6: LES PEPTIDES NATRIURETIQUES AUGMENTENT LA CAPACITE OXYDATIVE DU MUSCLE SQUELETTIQUE HUMAIN

Publication 6 : Natriuretic peptides enhance the oxidative capacity of human skeletal muscle

Engeli S, Birkenfeld AL, Badin PM, Bourlier V, Louche K, Viguerie N, Thalamas C, Montastier E, Larrouy D, Harant I,de Glisezinski I, Lieske S, Reinke J, Beckmann B, Langin D, Jordan J, Moro C. *(2012) J Clin Invest. 122(12):4675-9.*

Natriuretic peptides enhance the oxidative capacity of human skeletal muscle

Stefan Engeli,[1] Andreas L. Birkenfeld,[2] Pierre-Marie Badin,[3,4] Virginie Bourlier,[3,4] Katie Louche,[3,4] Nathalie Viguerie,[3,4] Claire Thalamas,[3,4,5] Emilie Montastier,[3,4,5] Dominique Larrouy,[3,4] Isabelle Harant,[3,4] Isabelle de Glisezinski,[3,4] Stefanie Lieske,[2] Julia Reinke,[1] Bibiana Beckmann,[1] Dominique Langin,[3,4,5] Jens Jordan,[1] and Cedric Moro[3,4]

[1]Institute of Clinical Pharmacology, Hannover Medical School, Hannover, Germany. [2]Department of Endocrinology, Diabetes and Nutrition, Center for Cardiovascular Research, Charité University School of Medicine, Berlin, Germany. [3]Inserm, UMR1048, Obesity Research Laboratory, Institute of Metabolic and Cardiovascular Diseases (I2MC), Toulouse, France. [4]University of Toulouse, UMR1048, Paul Sabatier University, Toulouse, France. [5]Toulouse University Hospitals, Departments of Clinical Biochemistry and Nutrition and Clinical Pharmacology, Inserm CIC-9302, Toulouse, France.

Cardiac natriuretic peptides (NP) are major activators of human fat cell lipolysis and have recently been shown to control brown fat thermogenesis. Here, we investigated the physiological role of NP on the oxidative metabolism of human skeletal muscle. NP receptor type A (*NPRA*) gene expression was positively correlated to mRNA levels of PPARγ coactivator-1α (*PGC1A*) and several oxidative phosphorylation (OXPHOS) genes in human skeletal muscle. Further, the expression of *NPRA*, *PGC1A*, and OXPHOS genes was coordinately upregulated in response to aerobic exercise training in human skeletal muscle. In human myotubes, NP induced PGC-1α and mitochondrial OXPHOS gene expression in a cyclic GMP–dependent manner. NP treatment increased OXPHOS protein expression, fat oxidation, and maximal respiration independent of substantial changes in mitochondrial proliferation and mass. Treatment of myotubes with NP recapitulated the effect of exercise training on muscle fat oxidative capacity in vivo. Collectively, these data show that activation of NP signaling in human skeletal muscle enhances mitochondrial oxidative metabolism and fat oxidation. We propose that NP could contribute to exercise training–induced improvement in skeletal muscle fat oxidative capacity in humans.

Introduction

The cardiac hormones, atrial natriuretic peptide (ANP) and brain natriuretic peptide (BNP), play a major role in the regulation of fluid homeostasis and cardiac physiology (1). Natriuretic peptide–mediated (NP-mediated) biological responses are largely mediated through cyclic GMP (cGMP) produced by the guanylyl cyclase domain of NP receptor type A (NPRA) (2). Although classically considered as cardiovascular hormones, we have shown that NP display a potent lipolytic effect in human adipocytes (3). They promote a rapid and sustained rise of intracellular cGMP that activates a cGMP-dependent protein kinase, PRKG1, which then phosphorylates perilipin 1 and hormone-sensitive lipase, necessary steps to initiate lipolysis (4). The potent lipolytic effect of NP is restricted to primates. In contrast, murine adipocytes exhibit a predominance of the clearance receptor NP receptor type C (NPR-C) and a very low expression of the biologically active NPRA (5). Interestingly, the lipolytic effect of NP is fully rescued in adipocytes of NPR-C (also known as *Npr3*) knockout mice. Moreover, NP induce a "browning" of human white adipocytes (6). This finding may be physiologically relevant considering the presence of functional brown fat in humans (7). Together, these studies suggest that NP plays a potent metabolic role in human adipose tissue. Recent data suggest that mice overexpressing *Nppb* and *Prkg1* are protected from high-fat diet–induced obesity and insulin resistance and show increased energy expenditure (8). This phenotype could be explained by significant changes in skeletal muscle fat oxidative capacity. The physiological relevance and molecular mechanisms of this finding have yet to be addressed in humans. In this study, we first show in vivo the relevance of the relationship between *NPRA* expression and oxidative metabolism in human skeletal muscle before and after 8 weeks of exercise training. We next establish that NP, in physiologically relevant concentrations, enhanced oxidative capacity in human skeletal muscle cells and unravel the molecular mechanisms.

Results and Discussion

Exercise training upregulates NPRA and oxidative phosphorylation genes in human skeletal muscle. In human skeletal muscle, we observed a positive relationship between the expression of *NPRA* and several oxidative phosphorylation (OXPHOS) genes (Supplemental Table 1; supplemental material available online with this article; doi:10.1172/JCI64526DS1). PPARγ coactivator-1α (*PGC1A*), a master regulator of OXPHOS genes (9), was also correlated with *NPRA* expression (r = 0.58, $P = 0.01$) (Supplemental Figure 1). We next investigated the potential link between NP signaling and skeletal muscle mitochondrial oxidative metabolism during an 8-week aerobic exercise training program in obese men. Exercise training improved maximal oxygen uptake (VO_{2max}) (+10%) and resting metabolic rate (RMR) (+8.9%). A 6.6% higher RMR was observed after adjustment for fat-free mass (Table 1). The observed increase in RMR, independent of fat-free mass, reflects a state of metabolic inefficiency, in agreement with other longitudinal exercise training studies (10, 11). This physiological adaptation could partly involve mitochondrial uncoupling in skeletal muscle (12). Pathway analysis of skeletal muscle microarray data revealed pathways related to mitochondrial dysfunction and OXPHOS as top-ranking biological functions ($P_{adjusted} < 0.002$) in response to exercise training. Exercise training increased skeletal muscle OXPHOS protein expression (+32%, overall effect

Conflict of interest: The authors have declared that no conflict of interest exists.
Citation for this article: *J Clin Invest.* 2012;122(12):4675–4679. doi:10.1172/JCI64526.

Table 1
Clinical and metabolic variables at baseline and after 8 weeks of exercise training

	Baseline	After training	*P* value
Age (yr)	35.4 ± 1.5	–	–
Body weight (kg)	103.0 ± 1.9	103.3 ± 2.2	0.63
BMI (kg/m^{-2})	32.6 ± 0.7	32.7 ± 0.7	0.62
Fat mass (%)	35.4 ± 1.8	34.2 ± 1.9	0.003
FFM (kg)	62.6 ± 2.0	64.0 ± 2.2	0.04
VO_{2max} (ml/min^{-1} × kg^{-1})	27.1 ± 1.2	29.8 ± 1.7	0.003
RMR (kcal/24 hour^{-1})	2,061 ± 60	2,245 ± 49	0.002
RMR (kcal/24 hour^{-1} × kg^{-1} FFM)	33.1 ± 0.9	35.3 ± 0.8	0.009
Fasting respiratory quotient	0.80 ± 0.01	0.79 ± 0.01	0.23

Values are given as mean ± SEM (n = 10). FFM, fat-free mass.

P = 0.0018) (Figure 1, A and B) independently of substantial changes in mitochondrial DNA (mtDNA) content (Figure 1C). These data are consistent with previous findings and suggest that exercise training can improve mitochondrial function per se (13). A concomitant upregulation of *NPRA* and total *PGC1A* transcripts was shown in human skeletal muscle in response to 8 weeks of aerobic exercise training (Figure 1D). No significant change in resting plasma ANP and BNP concentrations was observed after exercise training (data not shown). These data suggest a physiological link between NP/NPRA signaling and mitochondrial oxidative capacity in human skeletal muscle.

NP/cGMP signaling activates PGC1A and OXPHOS expression in human myotubes. The functional and mechanistic link between NP and mitochondrial oxidative metabolism was explored in human primary skeletal muscle cells. The NP receptor *NPRA* was expressed in differentiated myotubes, and the expression of key NP signaling components, *PRKG1* and the cGMP-specific phosphodiesterase *PDE5A*, increased during differentiation into myotubes (Figure 1, E and F). ANP and BNP dose dependently

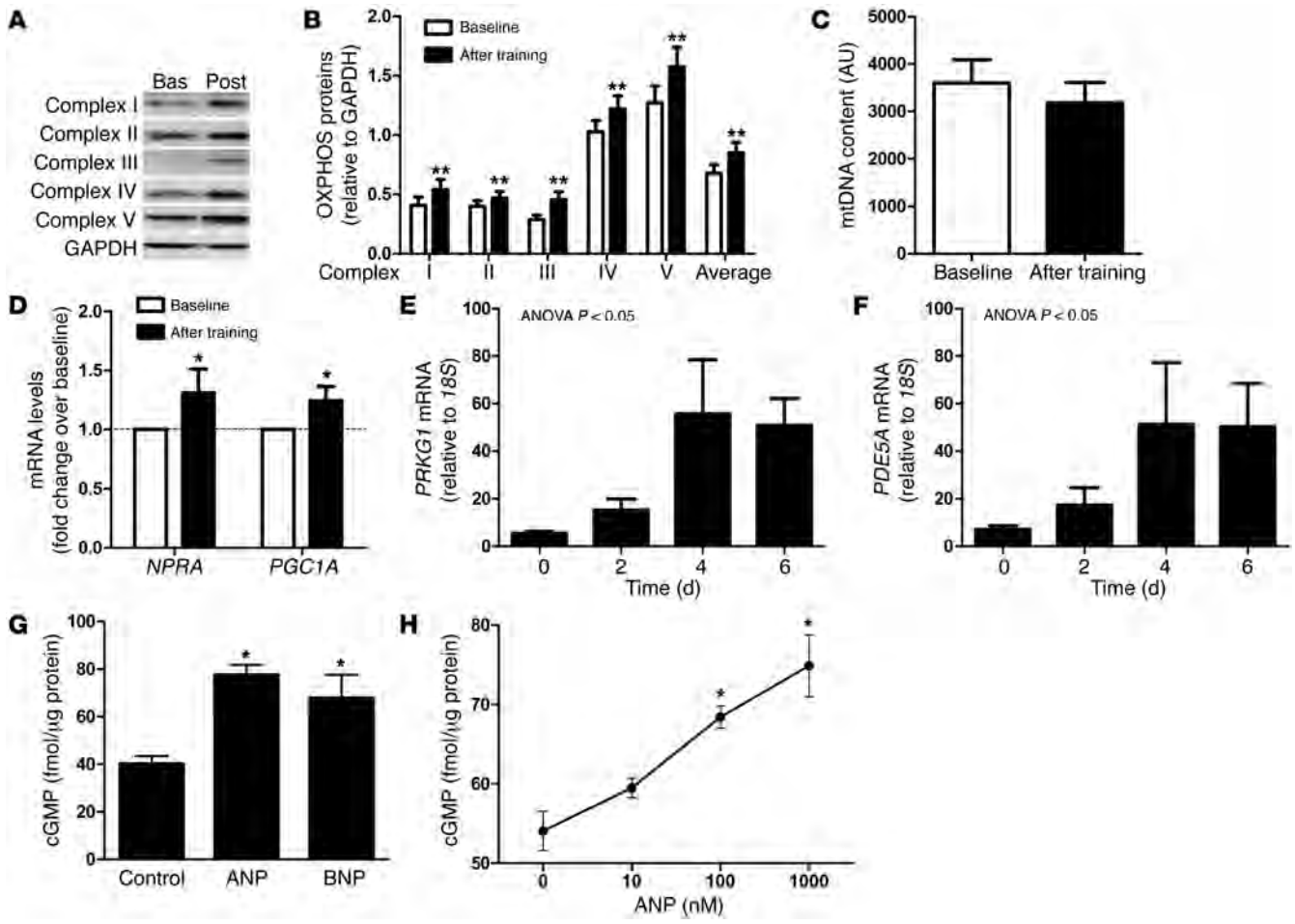

Figure 1
Functional link between NPRA expression and oxidative markers in human skeletal muscle. (**A**) Representative blot of OXPHOS proteins in skeletal muscle of one subject at baseline (Bas) and after training (Post). (**B**) OXPHOS complex protein expression, (**C**) mtDNA content, and (**D**) *NPRA* and *PGC1A* gene expression in skeletal muscle of sedentary subjects at baseline and after 8 weeks of aerobic exercise training. (**E** and **F**) Gene expression of *PRKG1* and *PDE5A* in primary human myoblasts during the time course of differentiation (n = 3–5). (**G**) Effect of acute ANP and BNP (1 μM) treatment, and (**H**) dose-response effect of ANP, on intracellular cGMP levels in differentiated human primary myotubes (n = 4–15). *P < 0.05, **P < 0.01 versus baseline.

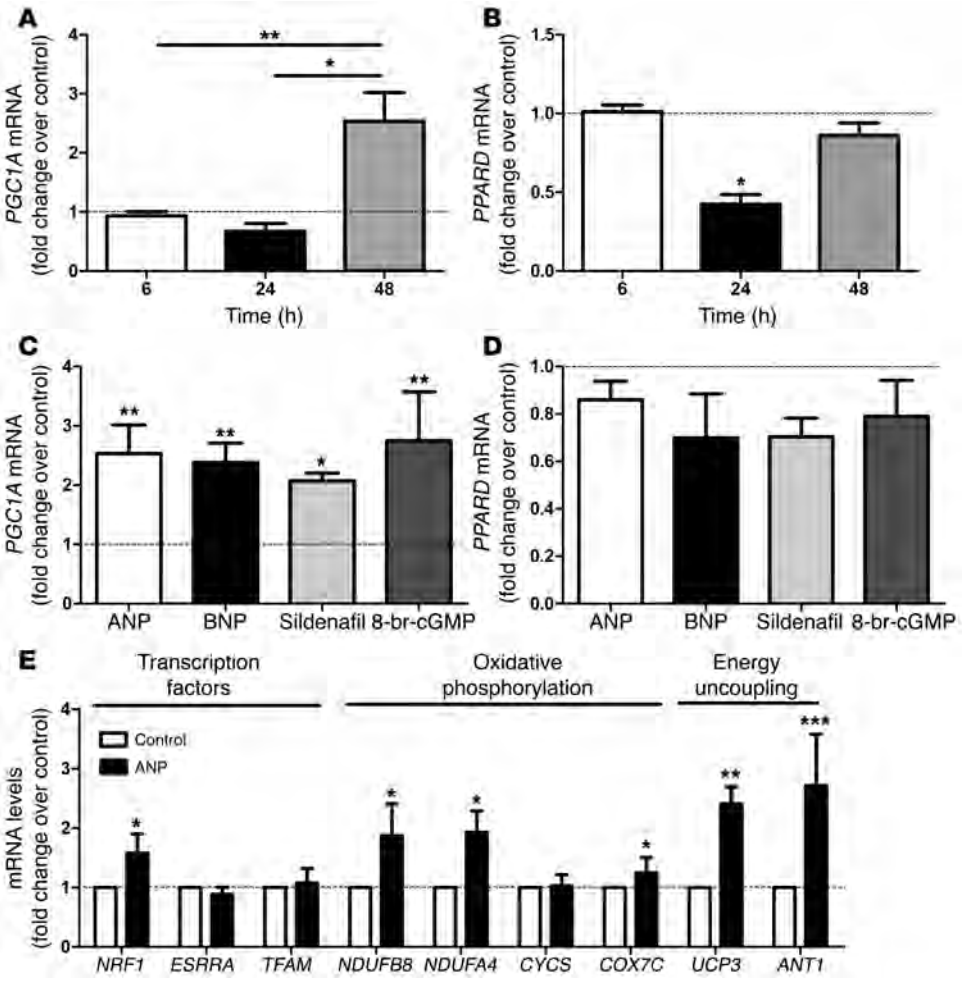

Figure 2
NP induces PGC-1α and mitochondrial oxidative genes in human primary myotubes. Time course of (**A**) *PGC1A* and (**B**) *PPARD* gene expression in response to treatment with 10 nM ANP ($n = 6$). (**C**) *PGC1A* and (**D**) *PPARD* gene expression in response to 10 nM ANP/BNP, 1 μM sildenafil, and 1 mM 8-bromo-cGMP after 48-hour treatment ($n = 6$). (**E**) Changes in transcription factors and OXPHOS and energy uncoupling genes in response to 48-hour treatment with 10 nM ANP ($n = 6$). $^*P < 0.05$, $^{**}P < 0.01$, $^{***}P < 0.001$ versus control.

increased intracellular cGMP concentrations in human myotubes (Figure 1, G and H). A physiologically relevant concentration of ANP (10 nM) induced *PGC1A* mRNA levels (2.5 fold, $P < 0.01$), while *PPARD* gene expression remained unaffected after 48 hours of treatment (Figure 2, A and B). Similar results were obtained with BNP (2.4 fold, $P < 0.01$), the stable cGMP analog 8-bromo-cGMP (2.1 fold, $P < 0.01$), and the selective PDE5 inhibitor sildenafil (2.7 fold, $P < 0.01$) (Figure 2, C and D). This finding is consistent with recent data showing a transcriptional regulation of PGC-1α by NP-mediated activation of p38 MAPK and activating transcription factor-2 (ATF2) in human adipocytes (6). The lack of transcriptional regulation of *PPARD* by the NP/cGMP signaling pathway is in agreement with previous findings using cAMP analogs in C2C12 myoblasts (14). Upregulation of *PGC1A* by NP was paralleled by a concomitant upregulation of several genes involved in OXPHOS complex I and IV, energy uncoupling, and transcriptional control of these pathways, such as nuclear respiratory factor 1 (*NRF1*) (Figure 2E). NRF1 controls the expression of nuclear genes encoding respiratory chain subunits and other proteins required for mitochondrial function (15). Similar data were obtained with BNP (Supplemental Figure 2) and sildenafil (Supplemental Figure 3). Chronic ANP treatment induced PGC-1α protein (+34%, $P = 0.06$) (Figure 3, A and B) and OXPHOS proteins from complex I (+24%, $P < 0.01$) and complex IV (+24%, $P < 0.01$) (Figure 3, A–C). These functional adaptations occurred without significant changes in the mitochondrial transcription factor A (*TFAM*) gene expression (Figure 2E), mtDNA content (Figure 3D), and mass (Figure 3E). No change in mtDNA occurred in response to 8-bromo-cGMP either (Supplemental Figure 4).

NP/cGMP signaling increases fat oxidation and maximal respiration in human myotubes. Chronic ANP treatment enhanced palmitate oxidation (+27%, $P < 0.05$) (Figure 3F). Palmitate oxidation also increased in BNP-treated myotubes (+20%, $P < 0.05$) (Supplemental Figure 5). In addition, we show that 72 hours of ANP treatment of human myotubes increased basal (+15%), uncoupled (+10% and +18% for oligomycin and rotenone, respectively), and maximal (+38% for FCCP) respiration in human myotubes (2-way ANOVA overall treatment effect $P = 0.007$) (Figure 3G and Supplemental Figure 6). In contrast, acute ANP treatment had no effect on mitochondrial respiration (data not shown). ANP-mediated fat oxidation could be related to increased fatty acid transporter expression (Figure 3H), while mRNA levels of fat oxidation genes were not significantly affected (Supplemental Figure 7). ANP-induced energy uncoupling may be partly mediated through induction of uncoupling protein-3 (*UCP3*) and ATP/ADP translocase (*ANT1*) (Figure 2E). ANT1 controls mitochondrial proton conductance, and downregulation of ANT1 in human skeletal muscle has been linked to improved OXPHOS efficiency (higher P/O ratio) (16).

Together, our data point toward a major physiological role of NP in the regulation of skeletal muscle oxidative capacity in humans. Interestingly, NP enhances mitochondrial fat oxidative capacity and respiration in skeletal muscle in vitro similarly to exercise training in vivo. It is tempting to speculate that increased NP signaling in skeletal muscle may contribute, at least in part, to exercise training–induced improvement in fat oxidative capacity. Indeed, physical exercise is a strong physiological stimulus for cardiac ANP release. We have previously reported the physiological role of ANP in the control of lipolysis during exercise in humans

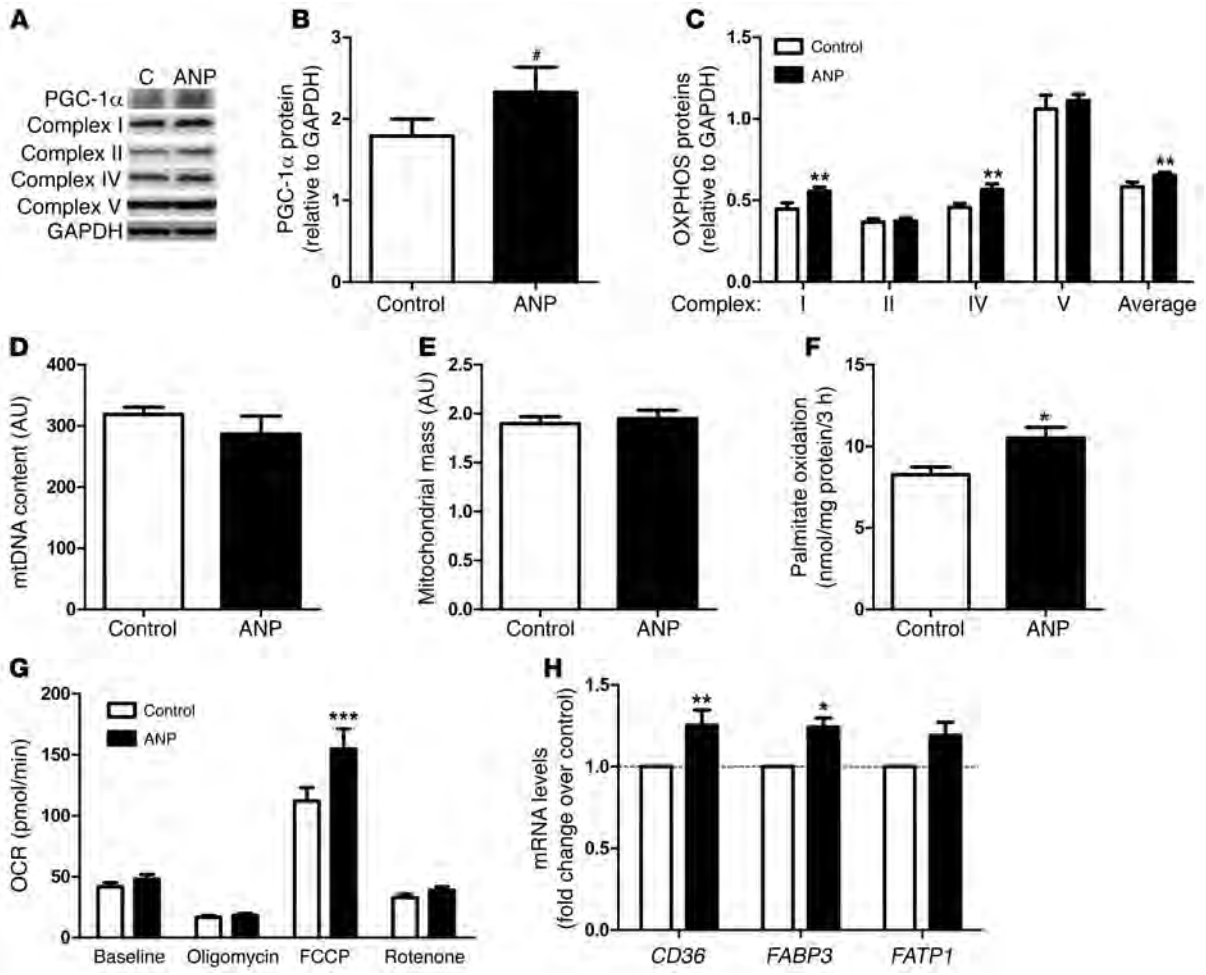

Figure 3
NP increases mitochondrial oxidative metabolism in human primary myotubes. (**A**) Representative blots of PGC-1α and OXPHOS proteins and (**B**) quantitative bar graphs of PGC-1α protein and (**C**) OXPHOS proteins after 72-hour treatment with 100 and 10 nM ANP, respectively (n = 6). C, control. (**D**) mtDNA content, (**E**) mass, and (**F**) palmitate oxidation were measured after 72-hour treatment with 10 nM ANP (n = 4–6). (**G**) Oxygen consumption rate (OCR) after 72-hour treatment with 10 nM ANP or vehicle (control) at baseline and after injection of oligomycin (ATP synthase inhibitor), FCCP (uncoupling agent), and rotenone (complex I inhibitor) plus myxothiazol (complex III inhibitor) (n = 8 experiments; control columns, mean ± SEM of 75 wells; ANP columns, mean ± SEM of 72 wells). (**H**) Changes in fatty acid transport genes in response to 72-hour treatment with 10 nM ANP (n = 6). $^{\#}P$ = 0.06, $^{*}P < 0.05$, $^{**}P < 0.01$, $^{***}P < 0.001$ versus control.

(17). Interestingly, acute infusion of ANP in lean healthy men during ingestion of a high-fat meal substantially raised postprandial energy expenditure and lipid oxidation (18). Here, we demonstrate for the first time to our knowledge that chronic NP treatment increases oxidative capacity and energy uncoupling in human skeletal muscle. The molecular mechanism involves a transcriptional activation of *PGC1A* and subsequent induction of OXPHOS genes and mitochondrial respiration.

Our data indicate that enhanced NP signaling in skeletal muscle through exercise may trigger favorable metabolic adaptations to increase fat oxidation. This is in agreement with recent data showing a protective role of NP and PRKG1 against high-fat diet–induced obesity and glucose intolerance in mice (8). Transgenic mice overexpressing *Nppb* (also known as *BNP*) and *Prkg1* display higher whole-body energy expenditure and fat oxidation, lower fat mass, and higher expression of mitochondrial oxidative genes in skeletal muscle. Interestingly, rectal temperature was significantly elevated in *Prkg1* transgenic mice, suggesting an increased metabolic rate. Similarly, high-fat diet–fed mice chronically treated with sildenafil for 12 weeks have reduced fat mass, higher energy expenditure, and insulin sensitivity (19). Our findings may be relevant for conditions associated with reduced circulating NP concentrations, such as obesity (20). The reduced NP availability in obesity may result from upregulation of NPR-C clearance receptor in adipose tissue (21). Reduced circulating NP concentrations predispose to insulin resistance and type 2 diabetes, and a genetic polymorphism in the *BNP* gene promoter region affects circulating BNP levels as well as type 2 diabetes risk (22). It is tempting to speculate that obesity-associated NP deficiency could promote metabolic disease and that physical exercise could counteract this effect.

In conclusion, exercise interventions and pharmacological treatments enhancing circulating NP levels and/or NP signaling in skeletal muscle could improve skeletal muscle fat oxidative capacity and alleviate obesity-related metabolic disorders.

Methods

Clinical study. Eighteen middle-aged healthy obese subjects were enrolled in the clinical trial (NCT01083329 and EudraCT-2009-012124-85) and ten participated in the training program (Table 1). The participants were asked to refrain from vigorous physical activity 48 hours before presenting to the clinical investigation center and ate a weight-maintaining diet consisting of 35% fat, 16% protein, and 49% carbohydrates 2 days before the experiment. Muscle biopsy of vastus lateralis, weighing 60–100 mg, was obtained using the Bergstrom technique, blotted, cleaned, and snap-frozen in liquid nitrogen (23). RMR and respiratory quotient were measured in lying position for 1 hour, while VO_{2max} was measured on a bicycle ergometer, by indirect calorimetry after a 10-hour overnight fast. The subjects were investigated at baseline and after 8 weeks of aerobic exercise training, at least 48 to 72 hours after the last acute exercise bout. Further experimental details are provided in Supplemental Methods and Supplemental Table 2.

Skeletal muscle cell culture. Satellite cells from rectus abdominis of healthy male subjects (age 34.3 ± 2.5 years, BMI 26.0 ± 1.4 kg/m^2, fasting glucose 5.0 ± 0.2 mM) were cultured as previously described (24). Differentiation of myoblasts into myotubes was initiated at approximately 80%–90% confluence by switching to α-MEM with antibiotics, 2% FBS, and fetuin. The medium was changed every other day, up to 5 to 6 days.

Cellular respiration. Human primary skeletal muscle cells were cultured on 24-well culture microplates (40,000 cells per well) (Seahorse Bioscience). Differentiated myotubes were treated for 72 hours with 1, 10, or 100 nM ANP or vehicle, and oxygen consumption was measured using the XF24-3 extracellular flux analyzer (Seahorse Bioscience). After 7 baseline measurements, cells were treated sequentially with 1 μM oligomycin to inhibit ATP synthase for 5 measurements, then with 0.25 μM FCCP to induce uncoupling of the cells for 5 measurements, and then with 1 μM rotenone plus 0.1 μM myxothiazol to inhibit complex I and III for 5 measurements.

Statistics. Statistical analyses were performed using GraphPad Prism 5.0 for Windows (GraphPad Software Inc.). Normal distribution and homogeneity of variance of the data were tested using Shapiro-Wilk and F tests, respectively. One-way ANOVA followed by Tukey's post-hoc tests and paired Student's *t* tests were performed to determine differences between treatments and the effect of exercise training (Table 1). Two-way ANOVA were applied to determine the effect of training and ANP on gene expression, OXPHOS proteins, and cellular respiration. Linear regression was performed after log transformation of nonparametric data. For pathway analysis and correlations, adjusted *P* values were calculated using the Benjamini-Hochberg method. All values in figures and tables are presented as mean ± SEM. Statistical significance was set at $P < 0.05$.

Study approval. The study was approved by the institutional review board of the Toulouse University Hospitals, and all volunteers gave written informed consent.

Acknowledgments

The authors are very grateful to François Crampes and Max Lafontan (I2MC, Toulouse) for helpful discussions, to the Toulouse Clinical Investigation Center staff, and to the study participants. The work was supported by grants from the National Research Agency ANR-09-JCJC-0019-01 (to C. Moro) and ANR-09-GENO-0018-01 (to D. Langin), European Federation for the Study of Diabetes/Novo Nordisk (to C. Moro), Inserm DHOS Recherche Translationnelle 2009 (to C. Thalamas and D. Langin), AOL-0816302 Hôpitaux de Toulouse (to C. Thalamas and D. Langin), Glaxo Smith Kline (to D. Langin), the Deutsche Forschungsgemeinschaft (Bl 1292/4-1), German Hypertension League (to A.L. Birkenfeld) and (JO 284/5-2) (to J. Jordan), and a collaborative research grant of the European Commission (SICA-HF, FP7 241558) (to S. Engeli and J. Jordan).

Received for publication April 27, 2012, and accepted in revised form September 6, 2012.

Address correspondence to: Cedric Moro, Institut des Maladies Métaboliques et Cardiovasculaires, INSERM 1048, CHU Rangueil, 1 Avenue Jean Poulhès, BP84225, 31432 Toulouse Cedex 4, France. Phone: 33561325626; Fax: 33561325623; E-mail: Cedric.Moro@inserm.fr.

1. Gardner DG. Natriuretic peptides: markers or modulators of cardiac hypertrophy? *Trends Endocrinol Metab*. 2003;14(9):411–416.
2. Kuhn M. Structure, regulation, and function of mammalian membrane guanylyl cyclase receptors, with a focus on guanylyl cyclase-A. *Circ Res*. 2003; 93(8):700–709.
3. Lafontan M, Moro C, Berlan M, Crampes F, Sengenes C, Galitzky J. Control of lipolysis by natriuretic peptides and cyclic GMP. *Trends Endocrinol Metab*. 2008;19(4):130–137.
4. Sengenès C, et al. Involvement of a cGMP-dependent pathway in the natriuretic peptide-mediated hormone-sensitive lipase phosphorylation in human adipocytes. *J Biol Chem*. 2003;278(49):48617–48626.
5. Sengenes C, et al. Natriuretic peptide-dependent lipolysis in fat cells is a primate specificity. *Am J Physiol Regul Integr Comp Physiol*. 2002;283(1):R257–R265.
6. Bordicchia M, et al. Cardiac natriuretic peptides act via p38 MAPK to induce the brown fat thermogenic program in mouse and human adipocytes. *J Clin Invest*. 2012;122(3):1022–1036.
7. Enerback S. Human brown adipose tissue. *Cell Metab*. 2010;11(4):248–252.
8. Miyashita K, et al. Natriuretic peptides/cGMP/cGMP-dependent protein kinase cascades promote muscle mitochondrial biogenesis and prevent obesity. *Diabetes*. 2009;58(12):2880–2892.
9. Handschin C, Spiegelman BM. PGC-1 coactivators and the regulation of skeletal muscle fiber-type determination. *Cell Metab*. 2011;13(4):351.
10. Potteiger JA, Kirk EP, Jacobsen DJ, Donnelly JE. Changes in resting metabolic rate and substrate oxidation after 16 months of exercise training in overweight adults. *Int J Sport Nutr Exerc Metab*. 2008; 18(1):79–95.
11. Tremblay A, Fontaine E, Poehlman ET, Mitchell D, Perron L, Bouchard C. The effect of exercise-training on resting metabolic rate in lean and moderately obese individuals. *Int J Obes*. 1986;10(6):511–517.
12. Cline GW, Vidal-Puig AJ, Dufour S, Cadman KS, Lowell BB, Shulman GI. In vivo effects of uncoupling protein-3 gene disruption on mitochondrial energy metabolism. *J Biol Chem*. 2001; 276(23):20240–20244.
13. Menshikova EV, Ritov VB, Toledo FG, Ferrell RE, Goodpaster BH, Kelley DE. Effects of weight loss and physical activity on skeletal muscle mitochondrial function in obesity. *Am J Physiol Endocrinol Metab*. 2005;288(4):E818–E825.
14. Holst D, Luquet S, Nogueira V, Kristiansen K, Leverve X, Grimaldi PA. Nutritional regulation and role of peroxisome proliferator-activated receptor delta in fatty acid catabolism in skeletal muscle. *Biochim Biophys Acta*. 2003;1633(1):43–50.
15. Finck BN, Kelly DP. PGC-1 coactivators: inducible regulators of energy metabolism in health and disease. *J Clin Invest*. 2006;116(3):615–622.
16. Larsen FJ, et al. Dietary inorganic nitrate improves mitochondrial efficiency in humans. *Cell Metab*. 2011;13(2):149–159.
17. Moro C, et al. Atrial natriuretic peptide contributes to physiological control of lipid mobilization in humans. *FASEB J*. 2004;18(7):908–910.
18. Birkenfeld AL, et al. Atrial natriuretic peptide induces postprandial lipid oxidation in humans. *Diabetes*. 2008;57(12):3199–3204.
19. Ayala JE, Bracy DP, Julien BM, Rottman JN, Fueger PT, Wasserman DH. Chronic treatment with sildenafil improves energy balance and insulin action in high fat-fed conscious mice. *Diabetes*. 2007; 56(4):1025–1033.
20. Wang TJ, et al. Impact of obesity on plasma natriuretic peptide levels. *Circulation*. 2004;109(5):594–600.
21. Sarzani R, et al. Natriuretic peptide clearance receptor alleles and susceptibility to abdominal adiposity. *Obes Res*. 2004;12(2):351–356.
22. Magnusson M, et al. Low plasma level of atrial natriuretic peptide predicts development of diabetes: the prospective malmo diet and cancer study. *J Clin Endocrinol Metab*. 2011;97(2):638–645.
23. Bergstrom J. Percutaneous needle biopsy of skeletal muscle in physiological and clinical research. *Scand J Clin Lab Invest*. 1975;35(7):609–616.
24. Badin PM, et al. Altered skeletal muscle lipase expression and activity contribute to insulin resistance in humans. *Diabetes*. 2011;60(6):1734–1742.

Supplemental Information for:

Natriuretic peptides enhance skeletal muscle oxidative capacity in humans

Stefan Engeli, Andreas L. Birkenfeld, Pierre-Marie Badin, Virginie Bourlier, Katie Louche, Nathalie Viguerie, Claire Thalamas, Emilie Montastier, Dominique Larrouy, Isabelle Harant, Isabelle de Glisezinski, Stefanie Lieske, Julia Reinke, Bibiana Beckmann, Dominique Langin, Jens Jordan and Cedric Moro

Inventory of Supplemental Information:

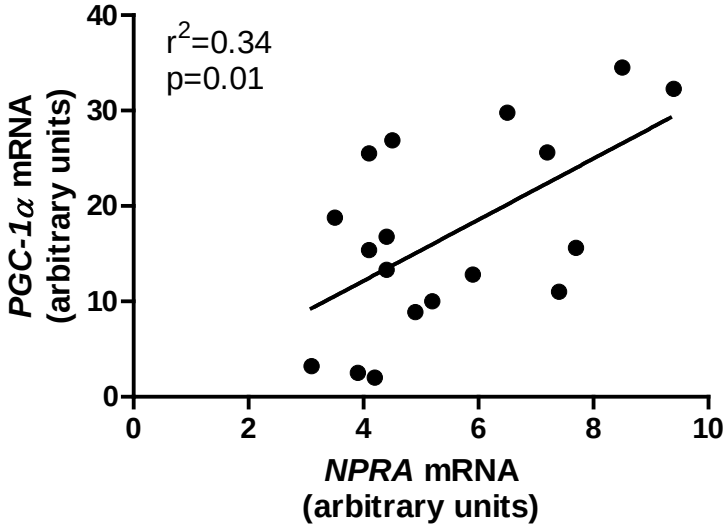

Supplemental Figure 1: Link between NPRA and PGC-1α in human skeletal muscle. Linear regression between *NPRA* and *PGC-1α* mRNA levels in human skeletal muscle of healthy obese subjects at baseline (n=18).

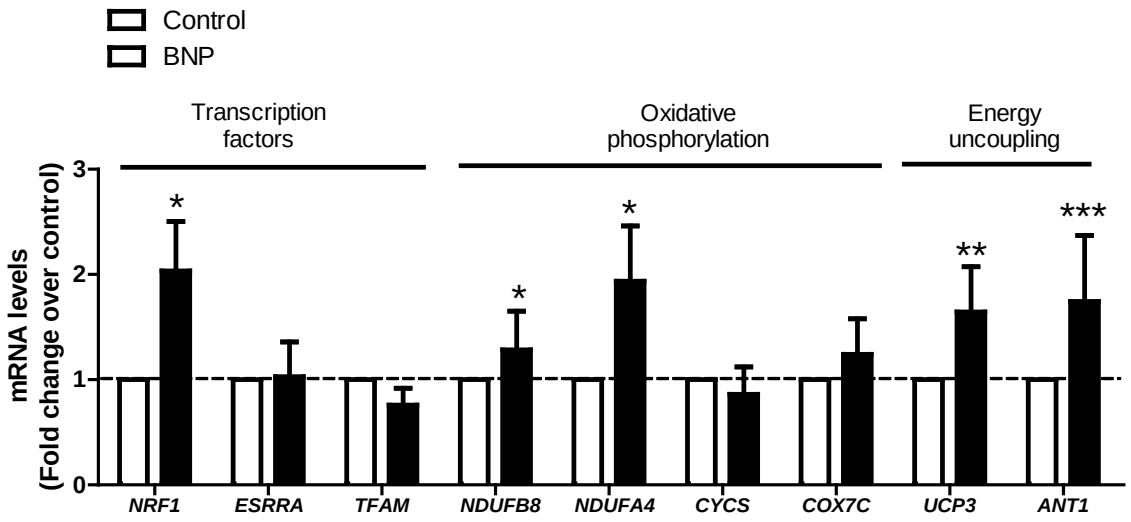

Supplemental Figure 2: BNP-induced mitochondrial genes in human myotubes. Changes in transcription factors, oxidative phosphorylation, and energy uncoupling genes in response to 48h treatment with BNP 10 nM (n=6). * p<0.05, ** p<0.01, *** p<0.001 versus control.

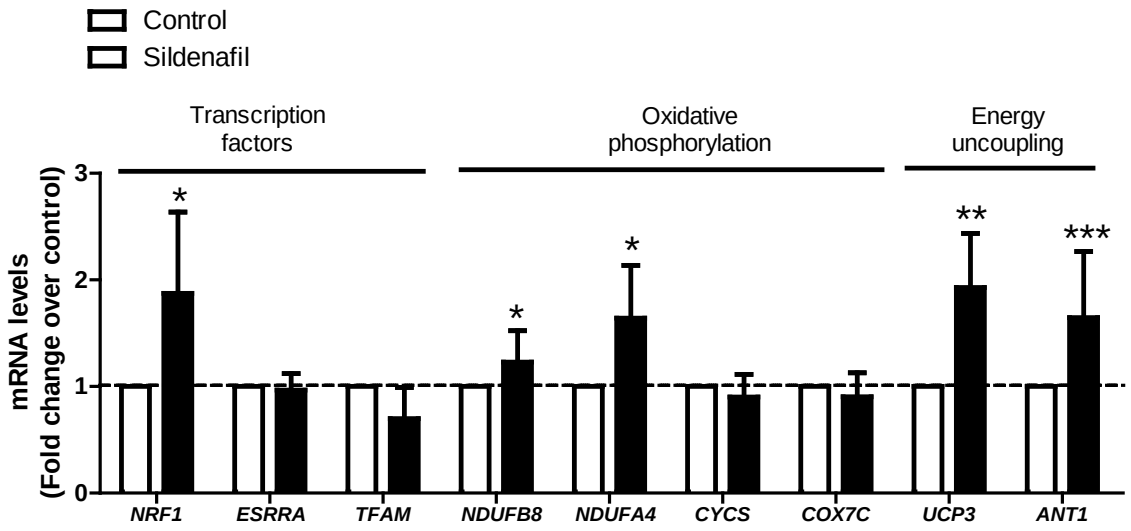

Supplemental Figure 3: Sildenafil-induced mitochondrial genes in human myotubes. Changes in transcription factors, oxidative phosphorylation, and energy uncoupling genes in response to 48h treatment with the selective phosphodiesterase-5 inhibitor, sildenafil 1 µM (n=6). * p<0.05, ** p<0.01, *** p<0.001 versus control.

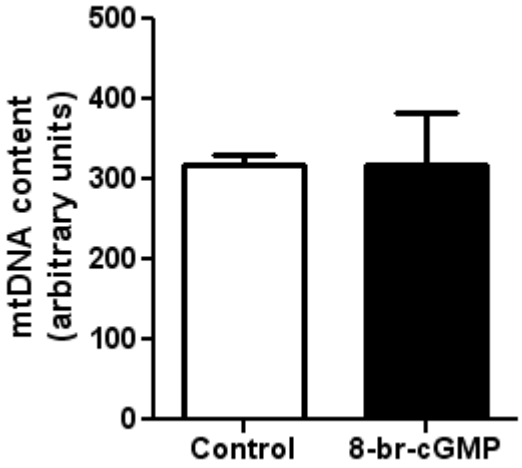

Supplemental Figure 4: cGMP does not increase mtDNA in human myotubes. Mitochondrial DNA content measured after 72h treatment with 8-bromo-cGMP 100 µM (n=3-6).

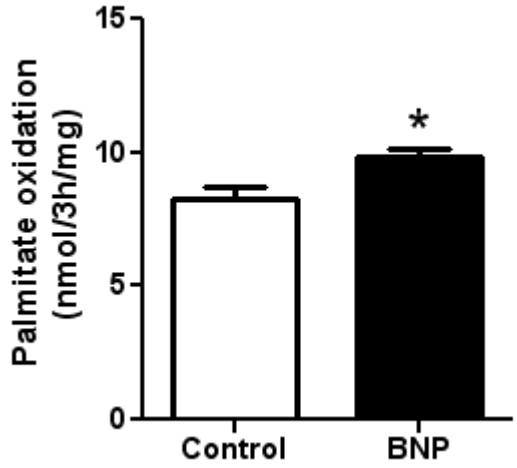

Supplemental Figure 5: BNP-induced fat oxidation in human myotubes. Palmitate oxidation measured after 72h treatment with BNP 10 nM (n=6). * $p<0.05$ versus control.

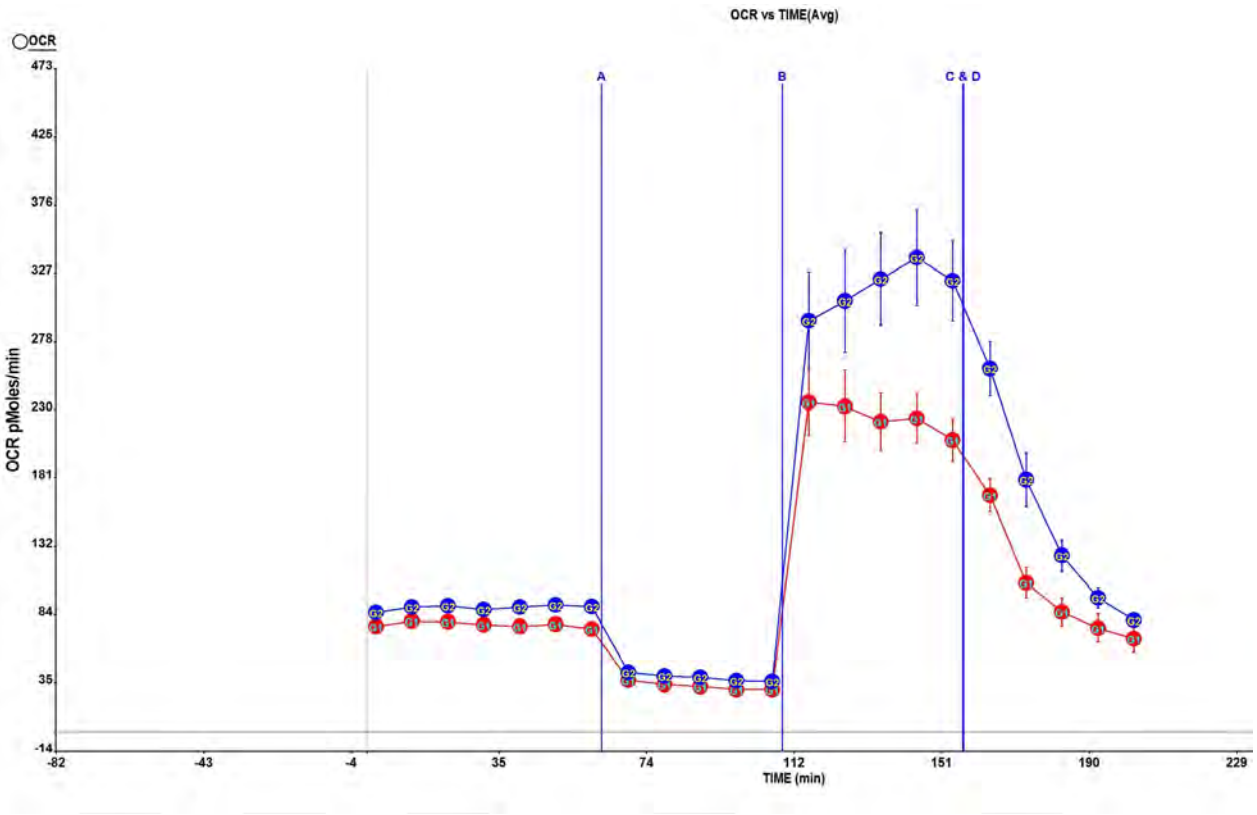

Supplemental Figure 6: ANP enhances oxygen consumption in human myotubes. Representative run of one XF24 analyzer experiment in control myotubes (red symbols) and in myotubes treated for 72h with ANP 10 nM (blue symbols) (n=9 replicates). A: injection of oligomycin (ATP synthase inhibitor); B: injection of FCCP (uncoupling agent); C & D: injection of rotenone (complex I inhibitor) and myxothiazol (complex III inhibitor). OCR: oxygen consumption rate.

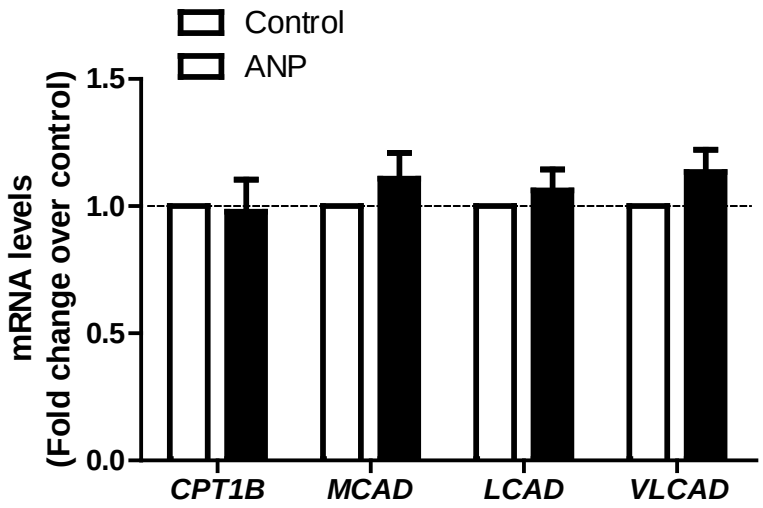

Supplemental Figure 7: ANP does not significantly change fat oxidation gene expression in human myotubes. Changes in fatty acid oxidation genes in response to 72h treatment with ANP 10 nM (n=6). * $p<0.05$, ** $p<0.01$ versus control.

Supplemental Table 1. Relationship between *NPRA* and OXPHOS mRNA levels in human skeletal muscle.

	NPRA		
Genes	r	p value	p_{adj} value
Oxidative phosphorylation			
NDUFC2	0.56	0.03	0.81
SDHA	0.69	0.005	0.15
COX15	0.81	0.0002	0.0064
ATP6AP1	0.68	0.005	0.145
ATP6V1F	0.59	0.02	0.56
Substrate oxidation			
CPT1B	0.52	0.04	1.04
PDHA1	-0.72	0.003	0.093

r: Pearson correlation coefficients from microarray data at baseline; non adjusted p value; p_{adj} value: Benjamini-Hochberg false discovery rate considered statistically significant if ≤ 15%.

Supplemental Table 2. Primers sequences used for gene expression analyses.

Gene symbol	Primers sequence
LCAD	Fwd: 5‘-AACCATGGCTCAGAAGAACAGATT-3‘ Rev: 5‘-TGTCATTGCTATTGCACCAATACA-3‘
VLCAD	Fwd: 5‘-TGGCACGGATGGTTATGCT-3‘ Rev: 5‘-CGAGCCAAAGATTTTGCTGAT-3‘
TFAM	Fwd: 5‘-GATTCCAAGAAGCTAAGGGTGATTC-3‘ Rev: 5‘-TCAGAGTCAGACAGATTTTTCCAGTT -3‘
UCP3	Fwd: 5‘-TCACCTCCAGGCCAGTACTT-3‘ Rev: 5‘-CGTTAGCTACCAGTGGCCTT-3‘
SLC25A4 (ANT1)	Fwd: 5‘-GCTGCCTGACCCCAAGAAC-3‘ Rev: 5‘-CTGCGACTGCCGTCACACT-3‘
MCAD	Fwd: 5‘-AGCTCCTGCTAATAAAGCCTTTACTG-3‘ Rev: 5‘-CATGTTTAATTCCTTTCTCCCAATC-3‘
CPT1B	Fwd: 5‘-TACAACAGGTGGTTTGACA-3‘ Rev: 5‘-CAGAGGTGCCCAATGATG-3‘

Supplemental Methods

In vivo experiments

Design of the study. Before the investigation, body composition (considering a 3-compartments model) was determined at baseline using a total body Dual-Energy X-ray Absorptiometer (Lunar-DPX). One week before the investigation, maximal oxygen uptake (VO_{2max}) was assessed using a graded exercise test conducted on an electromagnetically braked bicycle ergometer (Ergometrics 800, Ergoline, Jaeger, Germany) as previously described (1, 2). The initial workload was 50 watts and it was increased by 30 watts every 3 min until exhaustion. Heart rate was continuously monitored by telemetry using a heart rate monitor (Ergocard, Jaeger, Germany) and blood pressure was measured with an exercise-adapted monitor (Tango Stress Test BP Monitor; Suntech Medical Instruments Inc., Raleigh, North Carolina, USA). We considered that the subjects achieved their VO_2max when all the following usual and accepted criteria were achieved: maximal heart rate measured at exhaustion was higher than 90% of the age-predicted maximal heart rate, Respiratory Quotient (RQ, i.e. VCO_2/VO_2) measured at exhaustion was higher than 1.1, the subjects could not sustain a sufficient rate of cycling. On the experimental day, subjects were investigated after a 10h overnight fast. They ate standardized meals composed mainly of carbohydrate (49%), protein (16%) and fat (35%) (corresponding to their daily metabolic requirements) 48h prior to the experimental day.

Exercise training. Aerobic exercise was performed at the Centre de Ressources, d'Expertise et de Performance Sportives (CREPS) of Toulouse. Exercise sessions consisted mainly of cycling and running, 5 times per week for 8 weeks. Subjects exercised 3 times per week under supervision during the first 4 weeks and 2 times per week during the last 4 weeks. They exercised on their own during other sessions. All daily sessions consisted of at least 20 min warm-up at 35% VO_{2max} followed by progressively increasing exercise intensity (up to 85% VO_{2max}) and duration (up to 1h) throughout the training program. The subjects exercised at a target heart rate corresponding to 35–85% of their maximal oxygen uptake (VO_{2max}). Heart rate was monitored with a Suunto T3 Cardiometer (MSE, Strasbourg, France). Compliance with training was good, as checked by a training diary including day-to-day activities. The percentage of sessions completed was greater than 85%. Food and calorie intake were not modified during the training protocol.

Indirect calorimetry. At rest, gas exchanges were measured for 20 min, and values were averaged on the last 15 min. VO_2 and VCO_2 were measured and the RQ calculated as previously (2). Breath-by-breath measurements were taken at rest and throughout exercise to assess air flow and O_2 and CO_2 concentrations in expired gases by using a computerized ergospirometer (Ultima PFX, Medical Graphics, USA). Oxygen concentration was analysed by a zirconium cell and CO_2 concentration by an infrared analyser. Certified calibration gases were used to calibrate the analysers every day before the beginning of the assay. The VO_{2max} exercise trial occurred in a ventilated room to ensure a constant room temperature and hygrometry from the calibration just before the trial.

In vitro experiments

Microarrays. Briefly, target RNA was generated from 500 ng of total RNA with the Agilent low RNA input amplification kit (Agilent Technologies). Microarray experiments were performed using a reference design and whole genome 4x44k oligonucleotide arrays (Agilent Technologies). Data acquisition was performed with an InnoScan 710A scanner (Innopsys, Carbonne, France) and images were processed with Mapix software version 5.5.0 (Innopsys). Hybridization was quality checked using control spikes resulting in the analysis of microarray data from 8 subjects. Outlier replicates and spots with a signal to noise ratio less than 2 on both red and green channels were eliminated from the analyses. Mean log ratios were calculated before normalization. Raw data were normalized with a global Loess procedure and filtered with the R package LIMMA (Bioconductor). Mean spot calculation according to Gene Symbol resulted in 7859 exploitable gene IDs. Principal component analysis was used to check that all microarray experiments provided consistent data. Microarray data were analyzed using repeated measures ANOVA using Partek Genomics Suite version 6.5 (Partek Inc., St. Louis, MO, USA) resulting in 608 gene symbols. Functional analysis was done using Ingenuity Pathway Analysis (IPA) version 7.5 (3). Ingenuity's Pathways Knowledge Base was seeded with the 608 gene symbols together with the array mean fold change of the differentially expressed genes. A Benjamini-Hochberg multiple testing correction p-value was applied to the canonical pathways analysis of the 489 eligible gene symbols of the dataset. Data were considered significant for p value < 0.05. The microarray database has been deposited in Gene Expression Omnibus (GSE40551).

Real-time qPCR. Total RNA from muscle tissue and cultured myotubes was isolated in RNeasy Lysis Buffer + β-mercaptoethanol reagent (Qiagen GmbH, Hilden, Germany) as previosuly (4, 5). The quantity of the RNA was determined on a Nanodrop ND-1000 (Thermo Scientific, Rockford, IL, USA). Reverse-transcriptase PCR was performed on a GeneAmp PCR System 9700 using the Multiscribe Reverse Transcriptase method (Applied Biosystems, Foster City, CA, USA). Real-time quantitative PCR (qPCR) was performed to determine cDNA content. Sequences of SYBR primers are given in Supplemental Table 2. All other primers were bought from Applied Biosystems (Foster City, CA, USA). Primers used were: *18S* (Taqman assay ID: Hs99999901_s1), *CD36* (Hs00169627_m1), *PPARD* (Hs00602622_m1), total *PPARGC1A* transcripts (Hs00173304_m1), *FABP3* (Hs00269758_m1), *SLC27A1* (FATP1) (Hs01587917_m1), *NPR1* (Hs00181445_m1), *PRKG1* (Hs00183512_m1), *PDE5A* (Hs00153649_m1), *NRF1* (Hs00602161_m1), *ESRRA* (Hs00607062_m1), *NDUFB8* (Hs00428204_m1), *NDUFA4* (Hs00800172_s1), *CYCS* (Hs01588974_g1), *COX7C* (Hs01595220_g1), and *NPR3* (Hs00168558_m1). Quantitative PCR was then performed on a StepOnePLus real-time PCR system (Applied Biosystems, Foster City, CA, USA). For each primer, a standard curve was made prior to mRNA quantification to assess the optimal total cDNA quantity. All expression data were normalized by the $2^{(\Delta\Delta Ct)}$ method using 18S rRNA as internal control.

Western blotting. Muscle tissues and cell extracts were homogenized in a buffer containing 50 mM HEPES, pH 7.4, 2 mM EDTA, 150 mM NaCl, 30 mM NaPPO4, 10 mM NaF, 1% Triton X-100, 10 μl/ml protease inhibitor (Sigma-Aldrich), 10 μl/ml phosphatase I inhibitor (Sigma-Aldrich), 10 μl/ml phosphatase II inhibitor (Sigma-Aldrich), and 1.5 mg/ml benzamidine HCl (6). Tissue homogenates were centrifuged for 25 min at 15,000*g*, and supernatants were stored at -80°C. Solubilized proteins from muscle tissue and myotubes were run on a 4-12% SDS-PAGE (Biorad), transferred onto nitrocellulose membrane (Hybond ECL, Amersham Biosciences), and incubated with the primary antibody OXPHOS (MitoSciences) and PGC1α (Santa Cruz). Subsequently, immunoreactive proteins were determined by enhanced chemiluminescence reagent (GE Healthcare) and visualized by exposure to Hyperfilm ECL (GE Healthcare). Glyceraldehyde-3-phosphate dehydrogenase (GAPDH) (Cell Signaling Technology) served as an internal control.

cGMP measurements. Human primary myotubes were pretreated for 15 min with 0.5 µM IBMX and treated for 20 min with ANP or BNP (0.01-1.0 µM). Myotubes were then homogenized in ice cold methanol/acetonetrile. cGMP concentration was measured by ELISA (ENZO Life Sciences, cGMP complete EIA kit, Lörrach, German), and normalized by total protein content.

Determination of mitochondrial content. For quantification of mitochondrial content, we measured the mitochondrial (mt) to nuclear DNA ratio as previously described (7). The sequences for the primer sets used for determination of mtDNA for NADH dehydrogenase subunit 1 (*ND1*) were forward primer CCCTAAAACCCGCCACATCT, reverse primer GAGCGATGGTGAGAGCTAAGGT, and of nuclear DNA for lipoprotein lipase (*LPL*) were forward primer CGAGTCGTCTTTCTCCTGATGAT, reverse primer TTCTGGATTCCAATGCTTCGA. We also determined mitochondrial mass in myotubes using Mitotracker Green FM (Invitrogen, Carlsbad, CA) which stains mitochondrial matrix protein irrespective of the membrane potential and thus provides an accurate assessment of mitochondrial mass. Briefly, cells were washed with 1X PBS and incubated at 37°C for 30 minutes with 100nM of each Mitotracker. Cells were then harvested using trypsin/EDTA and re-suspended in 1X PBS. Fluorescence intensity was measured on a fluorometer and values corrected for total protein.

Palmitate oxidation assay. Myotubes were preincubated for 3-hour with [1-^{14}C]palmitate (1 µCi/ml; Perkinelmer, Boston, MA) and nonlabeled (cold) palmitate. Palmitate was coupled to a fatty acid–free BSA in a molar ratio of 5:1. Following incubation, $^{14}CO_2$ and ^{14}C-ASM was measured as previously described (4). Briefly, assayed medium is transferred into a custom–made Teflon 48-well trapping plate. The plate is clamped and sealed, and perchloric acid is injected through the perforations in the lid into the medium, which drives CO_2 through the tunnel into an adjacent well, where it is trapped in 1N NaOH. Following trapping, the media is spun twice and ^{14}C-ASM measured by scintillation counting. Aliquots of NaOH and medium are transferred into scintillation vials, and radioactivity is measured on a multipurpose scintillation counter (Tricarb 2100 TR, Packard). All assays are performed in triplicates, and data are normalized to protein content.

Supplemental References

1. Moro, C., Pillard, F., De Glisezinski, I., Harant, I., Riviere, D., Stich, V., Lafontan, M., Crampes, F., and Berlan, M. 2005. Training enhances ANP lipid-mobilizing action in adipose tissue of overweight men. *Med Sci Sports Exerc* 37:1126-1132.
2. Pillard, F., Van Wymelbeke, V., Garrigue, E., Moro, C., Crampes, F., Guilland, J.C., Berlan, M., de Glisezinski, I., Harant, I., Riviere, D., et al. 2010. Lipid oxidation in overweight men after exercise and food intake. *Metabolism* 59:267-274.
3. Calvano, S.E., Xiao, W., Richards, D.R., Felciano, R.M., Baker, H.V., Cho, R.J., Chen, R.O., Brownstein, B.H., Cobb, J.P., Tschoeke, S.K., et al. 2005. A network-based analysis of systemic inflammation in humans. *Nature* 437:1032-1037.
4. Badin, P.M., Loubiere, C., Coonen, M., Louche, K., Tavernier, G., Bourlier, V., Mairal, A., Rustan, A.C., Smith, S.R., Langin, D., et al. 2012. Regulation of skeletal muscle lipolysis and oxidative metabolism by the co-lipase CGI-58. *J Lipid Res* 53:838-848.
5. Viguerie, N., Picard, F., Hul, G., Roussel, B., Barbe, P., Iacovoni, J.S., Valle, C., Langin, D., and Saris, W.H. 2011. Multiple effects of a short-term dexamethasone treatment in human skeletal muscle and adipose tissue. *Physiol Genomics* 44:141-151.
6. Badin, P.M., Louche, K., Mairal, A., Liebisch, G., Schmitz, G., Rustan, A.C., Smith, S.R., Langin, D., and Moro, C. 2011. Altered skeletal muscle lipase expression and activity contribute to insulin resistance in humans. *Diabetes* 60:1734-1742.
7. Sparks, L.M., Moro, C., Ukropcova, B., Bajpeyi, S., Civitarese, A.E., Hulver, M.W., Thoresen, G.H., Rustan, A.C., and Smith, S.R. 2011. Remodeling lipid metabolism and improving insulin responsiveness in human primary myotubes. *PLoS One* 6:e21068.

PUBLICATION 7: L'AUGMENTATION DU METABOLISME DU GLUCOSE EST PRESERVEE AU SEIN DE MYOTUBES PRIMAIRES DE DONNEURS OBESES EN REPONSE A L'ENTRAINEMENT

Publication 7 : Enhanced glucose metabolism is preserved in cultured primary myotubes from obese donors in response to exercise training

Bourlier V, Saint-Laurent C, Louche K, Badin PM, Thalamas C, de Gliszinski I, Langin D, Sengenes C, Moro C. (2013) J Clin Endocrinol Metab. In press.

J Clin Endocrin Metab. First published ahead of print July 24, 2013 as doi:10.1210/jc.2013-1727

ORIGINAL ARTICLE

Endocrine Research

Enhanced Glucose Metabolism Is Preserved in Cultured Primary Myotubes From Obese Donors in Response to Exercise Training

Virginie Bourlier, Céline Saint-Laurent, Katie Louche, Pierre-Marie Badin, Claire Thalamas, Isabelle de Glisezinski, Dominique Langin, Coralie Sengenes, and Cedric Moro

Institut National de la Santé et de la Recherche Médicale (INSERM) (V.B., C.S.-L., K.L., P.-M.B., C.T., I.d.G., D.L., C.M.), Unité Mixte de Recherche (UMR) 1048, Obesity Research Laboratory, Institute of Metabolic and Cardiovascular Diseases, 31432 Toulouse, France; University of Toulouse (V.B., C.S.-L., K.L., P.-M.B., C.T., I.d.G., D.L., C.M.), UMR1048, Paul Sabatier University, 31062 Toulouse, France; Toulouse University Hospitals (I.d.G., D.L.), Departments of Clinical Biochemistry and Sports Medicine, 31000 Toulouse, France; Toulouse University Hospitals (C.T.), INSERM, Clinical Investigation Center 9302, 31000 Toulouse, France; and UMR5273 UPS/Centre National de la Recherche Scientifique/EFS/INSERM Unité 1031 (C.S.), STROMALab, Université de Toulouse, 31000 Toulouse, France

Context: It was suggested that human cultured primary myotubes retain the metabolic characteristics of their donor in vitro.

Objectives: The aim of the present study was to investigate whether the metabolic responses to endurance training are also conserved in culture.

Design and Volunteers: Middle-aged obese subjects completed an 8-week supervised aerobic exercise training program in which vastus lateralis muscle biopsies were collected before and after training.

Main Outcome Measures: Anthropometric and blood parameters, as well as aerobic capacity, were assessed before and after training. Muscle biopsies were either used for Western blot analysis or digested to harvest myogenic progenitors that were differentiated into myotubes. Glucose oxidation, palmitate oxidation, and glycogen synthesis assays were performed on myotubes before and after training. Gene expression was assessed by real-time quantitative PCR.

Results: Our data indicate that in parallel of in vivo improvement of whole-body aerobic capacity and glucose metabolism, biopsy-derived primary myotubes showed similar patterns in vitro. Indeed, glucose oxidation, glycogen synthesis, and inhibition of palmitate oxidation by glucose were enhanced in myotubes after training. This was associated with consistent changes in the expression of metabolism-linked genes such as *GLUT1*, *PDK4*, and *PDHA1*. Interestingly, no difference in myogenic differentiation capacity was observed before and after training.

Conclusion: Aerobic exercise training is associated with metabolic adaptations in vivo that are preserved in human cultured primary myotubes. It can be hypothesized that skeletal muscle microenvironmental changes induced by endurance training lead to metabolic imprinting on myogenic progenitor cells.

Obesity and type 2 diabetes mellitus (T2DM) are characterized by reduced insulin-stimulated glucose disposal and disturbances of lipid and oxidative metabolism (1, 2). Numerous studies have shown that skeletal muscle is an important site of glucose storage and that muscle glycogen synthesis is the principal pathway of glucose disposal in healthy humans. Thus, defects in muscle glycogen

ISSN Print 0021-972X ISSN Online 1945-7197
Printed in U.S.A.

Received March 22, 2013. Accepted July 8, 2013.
doi: 10.1210/jc.2013-1727

Abbreviations: AU, arbitrary units; DAG, diacylglycerol; FA, fatty acid; FBS, fetal bovine serum; HOMA-IR, homeostasis model of assessment for insulin resistance; qPCR, quanti-

synthesis are a dominant feature of T2DM (3). Importantly, early studies in the 1990s reported that the diabetic phenotype is conserved in primary myotubes established from patients with T2DM. These studies highlighted that insulin-stimulated glycogen synthase activation and glycogen synthesis remain blunted in cultured myotubes from T2DM donors (4, 5). Basal and insulin-stimulated glucose transports are also reduced in muscle cells cultured from T2DM subjects compared to nondiabetic control subjects (6). Interestingly, insulin-stimulated glucose uptake measured in vitro correlated with insulin-stimulated glucose disposal measured in vivo during a euglycemic hyperinsulinemic clamp. Besides defects in glucose metabolism, other studies reported that disturbances in lipid oxidation are also retained in primary myotubes established from obese T2DM donors (7). More generally, Ukropcova et al (8) reported that the preference for fat or glucose as fuel, ie, metabolic flexibility, measured in vitro in primary myotubes reflected the metabolic characteristics of their donor. Metabolic flexibility has been linked to ectopic fat deposition and insulin resistance (9, 10), and can be improved by diet-induced weight loss and exercise training (11, 12). Aerobic exercise training is effective in improving whole-body insulin sensitivity and muscle glucose disposal depending on the type of exercise, training volume, and duration (13, 14). Although several mechanisms have been proposed to explain this physiological adaptation to training, it is still unclear whether this response is mediated by external factors from the neuroendocrine milieu, or intrinsic factors within skeletal muscle, or a combination of both (15). Because skeletal muscle cell primary culture is a valuable model to study muscle substrate metabolism in a controlled environment and in the absence of external factors, we tested the hypothesis that metabolic adaptations to exercise training would be preserved in vitro in cultured primary myotubes from middle-aged obese subjects. For this purpose, we established primary culture of vastus lateralis from these donors before and after an 8-week aerobic exercise training intervention. We studied glucose and lipid metabolism, metabolic flexibility, as well as morphological and gene expression changes in paired skeletal muscle cell cultures.

Subjects and Methods

Clinical study

Middle-aged obese male subjects were enrolled in the clinical trial (no. NCT01083329) and EudraCT-2009–012124–85. The protocol was approved by the Ethics Committee of Toulouse University Hospitals, and all subjects gave written informed consent. They participated in an 8-week aerobic exercise training program in which paired biopsies were performed at rest before and after training. The participants were asked to refrain from vigorous physical activity 48 hours before presenting to the clinical investigation center, and they ate a weight-maintaining diet consisting of 35% fat, 16% protein, and 49% carbohydrates 2 days before the experiment. Anthropometric and blood parameters were measured, and maximal oxygen uptake (VO_{2max}) was investigated on a bicycle ergometer by indirect calorimetry before and after the exercise training intervention. Body composition (considering a 3-compartment model) was determined using a total body dual-energy x-ray absorptiometer (Lunar-DPX). Muscle biopsies of vastus lateralis weighing 60–100 mg each were obtained using the Bergstrom technique. Pieces of muscle were blotted, cleaned, and snap-frozen in liquid nitrogen. In a subgroup of 5 subjects, muscle tissue was collected in DMEM low glucose-Glutamax/penicillin-streptomycin 2%/fungizone 0.2% for primary cell culture before and after training intervention.

Exercise training

Aerobic exercise was performed at the Centre de Ressources, d'Expertise et de Performance Sportives of Toulouse. Exercise sessions consisted mainly of cycling and running 5 times per week for 8 weeks. Subjects exercised 3 times per week under supervision during the first 4 weeks and 2 times per week during the last 4 weeks. They exercised on their own during other sessions. All daily sessions consisted of at least a 20-minute warm-up at 35% VO_{2max} followed by progressively increasing exercise intensity (up to 85% VO_{2max}) and duration (up to 1 h) throughout the training program. The subjects exercised at a target heart rate corresponding to 35–85% of their VO_{2max}. Heart rate was monitored with a Suunto T3 Cardiometer (MSE, Strasbourg, France). Compliance with training was good, as checked by a training diary including day-to-day activities. The percentage of sessions completed was greater than 85%. Self-reported food intake remained unchanged throughout the training protocol (2165 ± 366 vs 2146 ± 230 kcal/d for pre- and post-training periods, respectively).

Primary cell culture

Chemicals and culture media were from Sigma-Aldrich (Saint-Quentin Fallavier, France) or Life Technologies (Saint-Aubin, France). Pieces of 40–60 mg of total muscle biopsies were digested in a trypsin 0.25%/collagenase type IV 0.068%/EDTA 0.05%/BSA 0.1% solution for 30 minutes (37°C, mild agitation) to isolate the stroma vascular fraction (SVF). Cells from the SVF were amplified in DMEM low glucose-Glutamax containing fetal bovine serum (FBS) 16%, human epithelial growth factor 10 ng/mL, dexamethasone 0.39 μg/mL, BSA 0.05%, fetuin 0.5 mg/mL, gentamycin 50 ng/mL, and fungizone 50 ng/mL to reach confluence. Cells were then trypsinized (0.05% trypsin-EDTA) and frozen in a cryopreservation medium (DMEM, FBS 16%, dimethylsulfoxide 10%) until used.

Skeletal muscle cell sorting

Satellite cells (ie, quiescent mononuclear muscle cell progenitors) were immunopurified from thawing cells of the SVF, after

tative PCR; SVF, stroma vascular fraction; TAG, triacylglycerol; T2DM, type 2 diabetes mellitus; VO_{2max}, maximal oxygen uptake.

a period of amplification in DMEM supplemented with 10% FBS and growth factors (human epithelial growth factor, BSA, dexamethasone, gentamycin, fungizone, fetuin), using the mouse monoclonal 5.1H11 anti-CD56 (also known as neural cell adhesion molecule 1) antibody (Developmental Studies Hybridoma Bank, Iowa City, Iowa) and MACS cell technology (Miltenyi Biotech SAS, Paris, France) (16). The satellite cell fraction purity was checked by flow cytometry (FACSCanto flow cytometer and FACSDiva software; BD Biosciences, Le Pont de Claix, France) using PE-Cy7 mouse antihuman CD56 or isotype antibodies (BD Biosciences). Differentiation of myoblasts (ie, activated satellite cells) into myotubes was initiated at approximately 80% confluence, by switching to α-MEM (minimum essential medium Eagle) low glucose-Glutamax with penicillin-streptomycin, 2% FBS, and fetuin. To study myogenic differentiation, myoblasts were lysed in RLT/DTT (2.5 mM) lysis buffer and stored at −20°C for mRNA extraction (d 0). The medium was changed every 2 d, and cells were grown typically up to 5 d (d 0 to d 4). Differentiated myotubes (d 4) were either lysed in RLT/DTT lysis buffer and stored at −20°C for mRNA extraction or used for lipid and glucose metabolism assays.

Palmitate oxidation assay

Myotubes were preincubated for 3 hours with [1-^{14}C]palmitate (1 μCi/mL; PerkinElmer, Boston, Massachusetts) and nonlabeled (cold) palmitate with or without glucose. Palmitate was coupled to a fatty acid (FA)–free BSA in a molar ratio of 5:1. To determine the relationship between FA oxidation and palmitate concentration (ie, adaptability assay), cells were incubated with a mixture of cold and radiolabeled palmitate at final concentrations of 20, 100, and 200 μM palmitate. To determine the relationship between FA oxidation and glucose concentration (ie, suppressibility assay), cells were incubated with labeled palmitate, 100 μM final concentration, and increasing concentrations of glucose (0, 0.1, 0.5, and 5 mM). After incubation, $^{14}CO_2$ and ^{14}C-ASM were measured as previously described (17). All assays were performed in duplicate, and data were normalized to cell protein content.

Neutral lipid molecular species analysis

Myotubes from palmitate oxidation assay were harvested in 0.2 mL SDS 0.1% to determine palmitate incorporation into triacylglycerols (TAGs), diacylglycerols (DAGs), and FA as previously described (18). The lipid extract was separated by thin-layer chromatography using heptane-isopropylether-acetic acid (60:40:4, vol/vol/vol) as the developing solvent. All assays were performed in duplicate, and data were normalized to cell protein content.

Glucose oxidation assay

Myotubes were preincubated with a glucose- and serum-free medium for 90 minutes. This incubation was followed by a 3-hour incubation with D[U-^{14}C]glucose (1 μCi/mL) and 5.5 mM of nonlabeled (cold) glucose in the presence or absence of 100 nM of insulin. After incubation, $^{14}CO_2$ was measured as previously described (17). All assays were performed in triplicate, and data were normalized to protein content.

Glycogen synthesis assay

After 90-minute incubation in serum- and glucose-free medium, myotubes were exposed to DMEM supplemented with D[U-^{14}C]glucose (1 μCi/mL; PerkinElmer) in the presence or absence of 100 nM of insulin (Umulin; Eli Lilly, Indianapolis, Indiana) for 3 hours to study basal and insulin-mediated glycogen synthesis as previously described (19). All assays were performed in triplicate, and data were normalized to protein content.

TAG and glycogen content determination

Pre- and post-training differentiated myotubes were scrapped in PBS/0.2% Tween, sonicated, and used for total TAG content determination using free glycerol and triglyceride reagents from Sigma-Aldrich, and scrapped in cold acetate/acetic acid buffer 0.2 M (pH 4.8) for total glycogen content. Cells were then sonicated and centrifuged for 10 minutes at 10 000 × *g* to collect supernatants that were incubated 1 hour with amyloglucosidase (Sigma-Aldrich; 1000 mU/sample final concentration) at 55°C under mild agitation. Glucose was measured with Glucose GOD FS (DiaSys France, Condom, France). Controls were performed without added enzyme and subtracted to the free glucose concentration obtained in amyloglucosidase samples. All data were normalized to cell protein content.

Reverse transcription and real-time quantitative PCR (qPCR)

Total RNA from cultured myotubes was isolated in QIAGEN RNeasy mini kit (QIAGEN GmbH, Hilden, Germany) according to the manufacturer's instructions. The quantity of the RNA was determined on a Nanodrop ND-1000 (Thermo Scientific, Rockford, Illinois). Reverse-transcriptase PCR was performed on a GeneAmp PCR System 9700 using the Multiscribe Reverse Transcriptase method (Applied Biosystems, Foster City, California). Real-time qPCR was performed to determine cDNA content. Primers bought from Applied Biosystems are listed in Supplemental Table 1 (published on The Endocrine Society's Journals Online web site at http://jcem.endojournals.org). *CPT1B* (carnitine palmitoyltransferase I, muscle) primer (sense, TACAACAGGTGGTTTGACA; antisense, CAGAGGTGCCCAATGATG) was provided by Eurogentech (Angers, France). The amplification reaction was performed in duplicate on 10 ng of the cDNA samples in a final volume of 20 μL in 96-well reaction plates on a StepOnePLus real-time PCR system (Applied Biosystems) with the appropriate program. All expression data were normalized by the $2^{(\Delta Ct)}$ method using 18S rRNA as internal control.

Determination of mitochondrial content

Mitochondrial DNA content was performed in duplicate on 10 ng of DNA isolated from cultured myotubes in QIAGEN DNeasy mini kit according to the manufacturer's instructions. *LPL* (lipoprotein lipase) primer (sense, CGAGTCGTCTTTCTCCTGATGAT; antisense, TTCTGGATTCCAATGCTTCG) and ND1 (NAD deshydrogenase 1) primer (sense, CCCTAAAACCCGCCACACATCT; antisense, GAGCGATGGTGAGAGCTAAGGT) were provided by Eurogentech and used at 300 nM in a final volume of 10 μL in 96-well reaction plates on a StepOnePLus real-time PCR system (Applied Biosystems) with the appropriate program.

Western blot analysis

Muscle tissue pieces (25 to 30 mg) were homogenized in a buffer containing 50 mM HEPES (pH 7.4), 2 mM EDTA, 150 mM NaCl, 30 mM $NaPO_4$, 10 mM NaF, 1% Triton X-100, 10 μl/mL protease inhibitor (Sigma-Aldrich), 10 μl/mL phosphatase I inhibitor (Sigma-Aldrich), 10 μl/mL phosphatase II inhibitor (Sigma-Aldrich), and 1.5 mg/mL benzamidine HCl. Tissue homogenates were centrifuged for 25 minutes at 15 000 $\times$ *g*, and supernatants were stored at −80°C. Solubilized proteins (25 μg) from muscle tissue were run on a 4–12% SDS-PAGE (Bio-Rad Laboratories, Hercules, California), transferred onto nitrocellulose membrane (Hybond ECL; Amersham Bioscience, Piscataway, New Jersey), and incubated with the primary antibodies (1/1000) OXPHOS (MitoSciences, Eugene, Oregon), then secondary antibodies (1/10 000). Subsequently, immunoreactive proteins were visualized using the ChemiDoc MP Imaging System, and data were analyzed using the Image Lab 4.1 version software (Bio-Rad Laboratories). Glyceraldehyde-3-phosphate dehydrogenase (Cell Signaling Technology, Danvers, Massachusetts) served as an internal control.

Statistical analyses

Statistical analyses were performed using GraphPad Prism version 5.0 for Windows (GraphPad Software Inc., San Diego, California). Normal distribution and homogeneity of variance of the data were tested using Shapiro-Wilk and F tests, respectively. Paired Student's *t*-tests were performed to determine the effect of training on anthropometric and clinical variables (Table 1). Two-way ANOVA was applied to determine the effect of 2 variables (ie, training and another variable [palmitate, glucose, insulin]) on various groups. Bonferroni's post hoc tests were applied when interactions were found. All values in Figures 1–5 and Table 1 are presented as mean ± SEM. Statistical significance was set at $P < .05$.

Table 1. Clinical and Biochemical Variables in Obese Subjects at Baseline (Pre-Training) and After 8 Weeks of Aerobic Exercise Training (Post-Training)

	Pre-Training	Post-Training	*P* Value
Anthropometric and blood parameters			
Age, y	34.8 ± 1.5	-	-
Body weight, kg	102.4 ± 2.6	103.0 ± 3.3	NS
Body mass index, kg/m^2	32.8 ± 1.1	33.0 ± 1.2	NS
Fat mass, %	35.5 ± 1.6	35.1 ± 2.0	NS
Fat-free mass, kg	62.1 ± 1.9	63.0 ± 2.8	NS
VO_{2max}, mL/min/kg	26.9 ± 0.7	29.4 ± 1.7	.037
HOMA-IR	4.7 ± 0.8	3.5 ± 0.4	.049
Fasting insulin, μU/mL	20.3 ± 3.3	15.1 ± 1.7	.05
Fasting glucose, g/L	0.93 ± 0.06	0.93 ± 0.02	NS
Plasma leptin, ng/mL	33.1 ± 7.4	32.3 ± 8.6	NS
Plasma adiponectin, μg/mL	11.6 ± 0.9	10.9 ± 0.9	NS
Skeletal muscle parameters, AU			
OXPHOS complex I	0.33 ± 0.05	0.49 ± 0.10	.05
OXPHOS complex II	0.38 ± 0.07	0.41 ± 0.07	NS
OXPHOS complex III	0.26 ± 0.05	0.40 ± 0.07	.006
OXPHOS complex IV	1.00 ± 0.09	1.13 ± 0.17	NS
OXPHOS complex V	1.15 ± 0.14	1.47 ± 0.19	.008

Abbreviation: NS, not significant. Values are given as mean ± SEM (n = 5).

Results

Aerobic exercise training increases skeletal muscle oxidative capacity and improves glucose homeostasis in vivo

As expected, the 8-week training intervention increased VO_{2max} and improved whole-body glucose homeostasis as observed by the reduction in fasting plasma insulin level and homeostasis model of assessment for insulin resistance (HOMA-IR) (Table 1). No significant changes in body composition and plasma adiponectin and leptin levels were observed after training. Western blot experiments on vastus lateralis biopsy-derived proteins indicated that mitochondrial respiratory chain complexes were increased after training (Table 1 and Supplemental Figure 1).

Aerobic exercise training enhances glucose oxidation and glycogen synthesis in vitro

Satellite cells (ie, muscle cell progenitors) were immunopurified from vastus lateralis-derived SVF and differentiated into myotubes. Cell purity was checked by flow cytometry and reached 97.7 ± 1.2% and 93.4 ± 3.8% of $CD56^+$ cells before and after training, respectively (Supplemental Figure 2). Glucose oxidation and glycogen synthesis were assessed on paired biopsy-derived myotubes. Insulin induced glucose oxidation by 24% (Figure 1A) and glycogen synthesis by 188% (Figure 1B) in this cell model ($P < .01$ and $P < .001$, respectively). Importantly, exercise training improvements in glucose metabolism were retained in vitro. Exercise training improved basal glucose oxidation, as well as basal and insulin-stimulated glycogen synthesis in primary myotubes (Figure 1, A and B). This occurred independently of significant changes in total

cell glycogen content (95.8 ± 7.3 vs 80.9 ± 7.7 μg/mg proteins).

Effect of aerobic exercise training on lipid metabolism in vitro

We determined metabolic switching in vitro by measuring FA oxidation to increased concentrations of palmitate (ie, adaptability) and glucose inhibition of FA oxidation (ie, suppressibility). We first observed a nonlinear concentration-dependent increase of palmitate oxidation before exercise training (Figure 2A; $P < .001$). This pattern of response remained unchanged after exercise training. Of interest, palmitate oxidation as measured ex vivo in biopsy samples was not significantly modified in response to exercise training (1075 ± 271 vs 1110 ± 404 nmol/2 h/mg protein; nonsignificant). We also show that palmitate incorporation into neutral lipids (TAG, DAG, and FA) remained unchanged in response to exercise training (Figure 2B). Also, no significant change in total TAG content was noted (19.78 ± 4.97 vs 19.06 ± 2.85 nmol/mg proteins).

Effect of aerobic exercise training on metabolic flexibility in vitro

We measured, as previously described (8), glucose suppressibility of FA oxidation in paired culture of primary myotubes. Increasing concentrations of glucose from 0 to 5 mM reduced palmitate oxidation rates in a concentration-dependent manner (Figure 3A; $P < .001$). Maximal glucose suppressibility increased by 53% ($P < .05$) in response to aerobic exercise training (Figure 3B).

Aerobic exercise training modulates metabolic gene expression in cultured primary myotubes

To understand how aerobic exercise training modulates metabolic responses in myotubes, we measured the mRNA level of several genes involved in glucose and FA metabolism. Of interest, we observed an up-regulation of *GLUT1*, *PDHA1*, and *GYS1* (statistical trend) gene expression in response to exercise training (Figure 4A). In contrast, *PDK4* gene expression, known to inhibit glucose oxidation, was down-regulated in myotubes after training (Figure 4A). No difference was found with exercise training in GLUT4 mRNA level (0.16 ± 0.03 vs 0.11 ± 0.02 arbitrary units [AU]). In agreement with functional data, the expression of FA oxidation gene set was not significantly modified before and after training (Figure 4B). No change in mitochondrial DNA content was observed in myotubes cultured after training (380.70 ± 90.70 vs 371.76 ± 66.51 AU). This was consistent with the lack of change in *TFAM* and *PPARGC1α* gene expression after training during the time-course of myotube differentiation (data not shown).

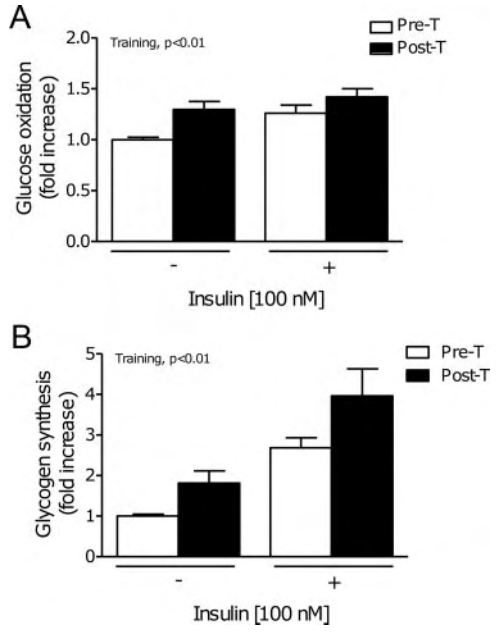

Figure 1. Aerobic exercise training increases glucose oxidation and glycogen synthesis in cultured primary myotubes. Glucose oxidation (A) and glycogen synthesis (B) were measured in myotubes derived from paired (ie, pre- and post-training) vastus lateralis muscle biopsies in the absence or presence of 100 nM insulin. Data were normalized as fold change compared to basal pretraining values (n = 5). Two-way ANOVA analysis revealed a significant effect of training ($P < .01$) and insulin ($P < .01$ and $P < .001$, respectively) on both parameters without interactions.

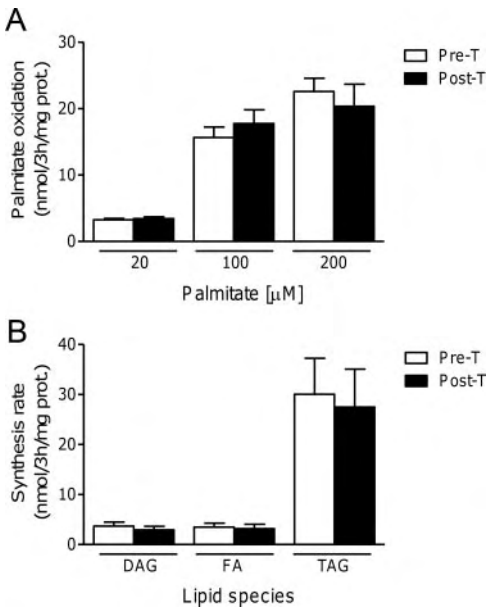

Figure 2. Aerobic exercise training does not alter palmitate oxidation and storage in cultured primary myotubes. A, Dose-response of palmitate oxidation (20, 100, and 200 μM) measured in primary myotubes derived from paired (ie, pre- and post-training) vastus lateralis muscle biopsies (n = 5). Two-way ANOVA analysis revealed a significant effect of palmitate concentration ($P < .001$) but no effect of training. B, Neutral lipid contents (TAG, DAG, FA) determined by thin-layer chromatography.

Aerobic exercise training does not affect myogenic differentiation in vitro

Because exercise training could affect myogenic differentiation, we assessed myogenic differentiation capacity on paired biopsy-derived myotubes. No significant difference in morphology and gene expression patterns of satellite cells commitment *PAX7* and of myosin heavy chain 7 (*MYH7*) expressions was observed in response to training (Figure 5, A–C). Similar results were obtained with *MHY1* and *MHY2* gene levels that were increased with differentiation ($P < .01$ and $P < .001$, respectively; Supplemental Figure 3) but were not differently expressed in pre- and post-training cultures.

Discussion

Regular physical exercise has repeatedly been shown to improve metabolic health. However, it is still unclear whether exercise training-mediated improvements in skeletal muscle function are stable when examined outside their native environment in vivo. In this study, we show that skeletal muscle cells retain an "exercise-trained phenotype" in vitro. Specifically, we demonstrate an enhanced basal and insulin-stimulated glucose metabolism in vitro in cultured myotubes obtained at baseline and after 8 weeks of aerobic exercise training, a classical metabolic response of aerobic exercise. Our data also suggest that environmental factors such as regular physical exercise induce a metabolic imprinting of skeletal muscle cell progenitor, ie, satellite cells. The metabolic imprinting may be permitted by signals exchanged between satellite cells and their related myofibers and/or by exposure to similar systemic signals (hormones, peptides, or metabolites). This finding is consistent with a recent study demonstrating that acute exercise induces epigenomic changes in human skeletal muscle (20). The authors reported a state of promoter hypomethylation of key genes involved in the regulation of oxidative metabolism in response to an acute exercise bout.

In the current study, we first observed that our exercise training intervention was effective to increase VO_{2max} and whole-body glucose homeostasis as reflected by HOMA-IR index. This is in line with numerous studies (14, 21, 22). In the same line, the expression of mitochondrial respiratory chain complexes increased after training, suggesting an overall improvement of the maximal oxidative capacity of skeletal muscle. Besides enhancing muscle glucose uptake, endurance exercise training has been shown to stimulate glycogen synthesis (23). An increase in glycogen storage is a well-known physiological adaptation of exercise training to increase endurance capacity during submaximal exercise (24). Elevated glycogen con-

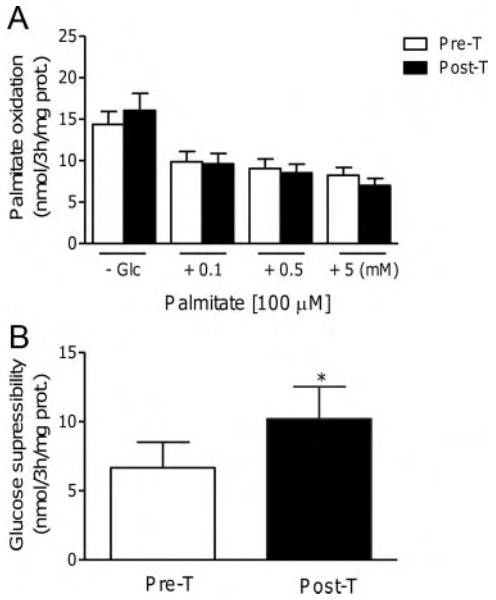

Figure 3. Aerobic exercise training increases glucose suppressibility in cultured primary myotubes. A, Dose-response inhibition of palmitate oxidation by glucose (Glc; 0.1, 0.5, and 5 mM) assessed in vitro in primary myotubes pre- and post-exercise training (n = 5). Two-way ANOVA analysis revealed a significant effect of glucose concentration ($P < .001$) but no effect of training. B, Bar graph representing glucose suppressibility (ie, absolute difference between basal and 5 mM glucose condition) of palmitate oxidation. *, $P < .05$ vs pretraining.

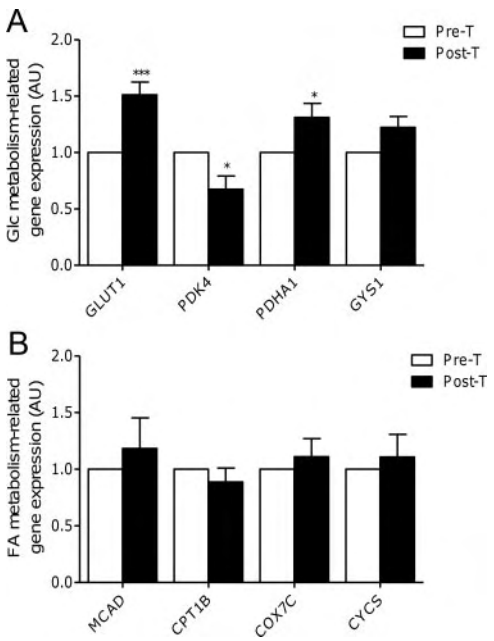

Figure 4. Aerobic exercise training changes metabolic gene expression in cultured primary myotubes. A, Expression of genes involved in glucose (Glc) metabolism was analyzed by qPCR in myotubes derived from paired (ie, pre- and post-training) vastus lateralis muscle biopsies. Two-way ANOVA analysis revealed a significant effect of training ($P < .01$) and genes ($P < .0001$) with interactions ($P < .0001$). *, $P < .05$; ***, $P < .001$ vs pretraining (post hoc test). B, Expression of genes involved in FA metabolism was analyzed in the same myotubes. Data were expressed as fold change compared to pretraining condition (n = 5).

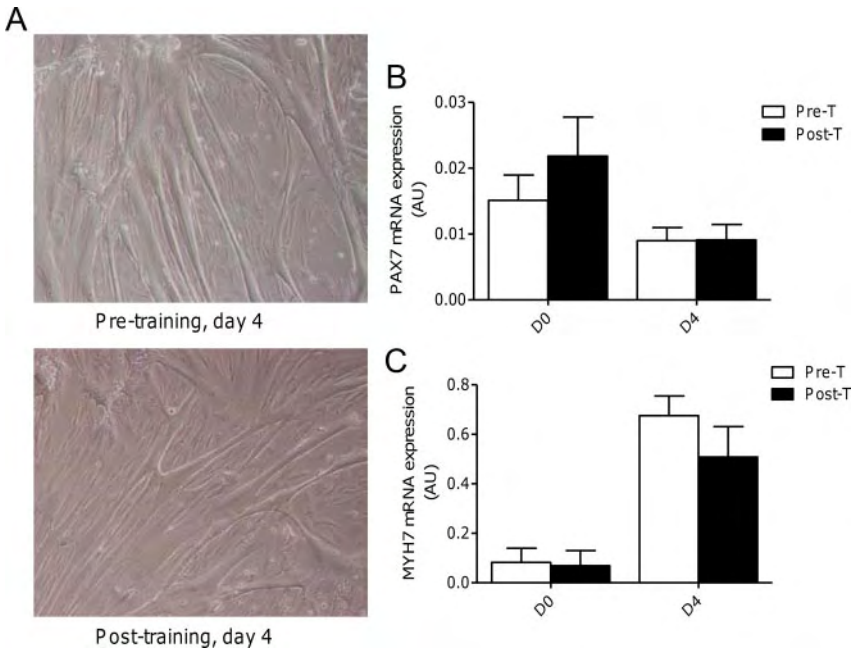

Figure 5. Aerobic exercise training does not modify myogenic differentiation capacity. A, Representative photomicrographs of myotubes derived from paired (ie, pre- and post-training) vastus lateralis muscle biopsies after 4 days of differentiation. B and C, Expression of the myogenic progenitor cell marker PAX7 (B) and of the myotube maturation marker myosin heavy chain 7 (MYH7) (C) were assessed by qPCR at day 0 (D0) and day 4 (D4) of differentiation (n = 5). Two-way ANOVA analysis revealed a significant effect of differentiation ($P < .05$ and $P < .001$, respectively) but no effect of training.

tent is also a consequence of improved insulin action in skeletal muscle. Very interestingly, we show for the first time that both basal and insulin-stimulated glycogen synthesis are increased in primary myotubes cultured from biopsy samples obtained after exercise training. We also observed a higher basal glucose oxidation rate in myotubes cultured after exercise training. This was associated with a consistent up-regulation of *GLUT1* and *PDHA1* mRNA levels and a down-regulation of *PDK4*. GLUT1 is a high-affinity glucose transporter mostly involved in basal glucose transport in human primary skeletal muscle cells (25). Our data are in agreement with at least 1 cross-sectional study reporting a higher basal glucose uptake and trend for increased *GLUT1* mRNA in cultured myotubes from trained- vs sedentary-matched healthy men (26). PDHA1 is a protein of the pyruvate dehydrogenase complex, which is a rate-limiting step in glucose oxidation by controlling pyruvate influx into the mitochondria. In contrast, PDK4 is the predominant pyruvate dehydrogenase kinase in skeletal muscle that inhibits the pyruvate dehydrogenase complex by phosphorylation (27, 28). PDK4 is induced by high FA availability as observed during fasting. Thus, down-regulation of PDK4 promotes glucose oxidation. This also suggests that exercise training induced epigenetic changes to alter the transcription of metabolic genes. Lifestyle factors such as exercise and nutrition could influence epigenetic metabolic programming of muscle cells and predisposition to obesity and T2DM, as recently discussed (29).

Because endurance exercise training has been shown to improve metabolic flexibility (11, 12), we assessed 2 parameters of fuel switching in vitro previously characterized, ie, adaptability and suppressibility. Our data are in agreement with a previous study showing a dose-dependent increase in palmitate oxidation in response to increasing doses of palmitate (8). However, no significant changes of in vitro adaptability to increasing concentrations of palmitate were observed in response to exercise training. No change in key β-oxidation gene (*MCAD*, *CPT1B*) expression was noted as well. We did not find significant changes in palmitate oxidation rates measured ex vivo on biopsy samples after exercise training either. The lack of effect of exercise training on in vitro fat oxidation rates is unclear at this stage. One hypothesis could be that exercise training volume and/or duration were insufficient to raise skeletal muscle fat oxidation significantly. In fact, whereas subtle changes in fat oxidation were observed in response to short-term training (10 d) in some studies (30), significant changes in maximal fat oxidation rates of skeletal muscle are often observed with longer duration of exercise training up to 9 months (31). Thus, up-regulation of muscle fat oxidation is mostly observed during submaximal exercise but not in the resting state after exercise training (32, 33). Additionally, the exercise training intervention did not affect palmitate storage rates in vitro. This excludes the possibility that higher storage of palmitate into TAG pools channels FA away from mitochondrial β-oxidation. Combined, these results highlight that the exercise training intervention did not impact significantly on lipid metabolism of skeletal muscle cells in vitro. However, in agreement with the higher basal glucose uptake observed in vitro after training, we found a greater glucose suppressibility of palmitate oxidation. A physiological concentration of glucose (5 mM) suppressed by about half the palmitate oxidation as predicted by the reverse Randle cycle (34). Increased glucose oxidation can lead to production of malonyl-coenzyme A and inhibition of carnitine palmitoyl-transferase I, the rate-limiting step of fatty acyl-coenzyme A entry into mitochondria.

It is noteworthy that the improvement of glucose metabolism observed in response to exercise training in vitro was independent of noticeable changes in satellite cells differentiation. Both satellite cells and differentiated myotubes had comparable morphological aspect before and after exercise training intervention. Moreover, no statistical changes in the expression of the quiescence factor *PAX7* and of the structural protein *MYH7* were observed in response to training in the early and late stages of the differentiation process toward myotube maturation.

Collectively, our data show that aerobic exercise training-induced changes in glucose metabolism are retained in vitro in primary culture of skeletal muscle cells from obese donors. This fascinating observation suggests that skeletal muscle microenvironmental changes induced by endurance training lead to metabolic imprinting on myogenic progenitor cells. The myogenic progenitor cells, ie, satellite cells, are then reprogrammed to form new myofibers with a higher capacity for glycogen storage. These functional changes are likely mediated by epigenetic molecular events modulating metabolic gene expression. It will be interesting in future studies to examine whether changes in promoter methylation are associated with changes in metabolic gene expression in this setting. It will be interesting as well to investigate whether longer exercise training interventions and/or interventions using different types of exercise (high intensity, sprint interval, etc.) can also lead to functional changes in lipid metabolism that are retained in primary culture of skeletal muscle cells.

Acknowledgments

The authors are very grateful to Dr François Crampes for critical reading of the manuscript and helpful discussions. We are also grateful to the study participants.

Address all correspondence and requests for reprints to: Cedric Moro, PhD, Institut National de la Santé et de la Recherche Médicale, Unité Mixte de Recherche 1048, Institut des Maladies Métaboliques et Cardiovasculaires, Centre Hospitalier Universitaire Rangueil, BP 84225, 1 Avenue Jean Poulhès, 31432 Toulouse Cedex 4, France. E-mail: Cedric.Moro@inserm.fr.

This work was supported by grants from the National Research Agency ANR-12-JSV1–0010–01, the European Federation for the Study of Diabetes/Novo Nordisk and Société Francophone du Diabète (to C.M.), Inserm DHOS Recherche Translationnelle, and AOL0816302 Hôpitaux de Toulouse (to D.L.).

Clinical Trial Registration no. NCT01083329.

Disclosure Summary: The authors have no conflict of interest to disclose.

References

1. **Defronzo RA.** Banting Lecture. From the triumvirate to the ominous octet: a new paradigm for the treatment of type 2 diabetes mellitus. *Diabetes*. 2009;58:773–795.
2. **Samuel VT, Shulman GI.** Mechanisms for insulin resistance: common threads and missing links. *Cell*. 2012;148:852–871.
3. **Shulman GI, Rothman DL, Jue T, Stein P, DeFronzo RA, Shulman RG.** Quantitation of muscle glycogen synthesis in normal subjects and subjects with non-insulin-dependent diabetes by 13C nuclear magnetic resonance spectroscopy. *N Engl J Med*. 1990;322:223–228.
4. **Henry RR, Ciaraldi TP, Abrams-Carter L, Mudaliar S, Park KS, Nikoulina SE.** Glycogen synthase activity is reduced in cultured skeletal muscle cells of non-insulin-dependent diabetes mellitus subjects. Biochemical and molecular mechanisms. *J Clin Invest*. 1996;98:1231–1236.
5. **Gaster M, Petersen I, Hojlund K, Poulsen P, Beck-Nielsen H.** The diabetic phenotype is conserved in myotubes established from diabetic subjects: evidence for primary defects in glucose transport and glycogen synthase activity. *Diabetes*. 2002;51:921–927.
6. **Henry RR, Abrams L, Nikoulina S, Ciaraldi TP.** Insulin action and glucose metabolism in nondiabetic control and NIDDM subjects. Comparison using human skeletal muscle cell cultures. *Diabetes*. 1995;44:936–946.
7. **Gaster M, Rustan AC, Aas V, Beck-Nielsen H.** Reduced lipid oxidation in skeletal muscle from type 2 diabetic subjects may be of genetic origin: evidence from cultured myotubes. *Diabetes*. 2004;53:542–548.
8. **Ukropcova B, McNeil M, Sereda O, et al.** Dynamic changes in fat oxidation in human primary myocytes mirror metabolic characteristics of the donor. *J Clin Invest*. 2005;115:1934–1941.
9. **Kelley DE, Mandarino LJ.** Fuel selection in human skeletal muscle in insulin resistance: a reexamination. *Diabetes*. 2000;49:677–683.
10. **Galgani JE, Moro C, Ravussin E.** Metabolic flexibility and insulin resistance. *Am J Physiol Endocrinol Metab*. 2008;295:E1009–E1017.
11. **Corpeleijn E, Mensink M, Kooi ME, Roekaerts PM, Saris WH, Blaak EE.** Impaired skeletal muscle substrate oxidation in glucose-intolerant men improves after weight loss. *Obesity (Silver Spring)*. 2008;16:1025–1032.
12. **Meex RC, Schrauwen-Hinderling VB, Moonen-Kornips E, et al.** Restoration of muscle mitochondrial function and metabolic flexibility in type 2 diabetes by exercise training is paralleled by increased myocellular fat storage and improved insulin sensitivity. *Diabetes*. 2010;59:572–579.
13. **Dube JJ, Allison KF, Rousson V, Goodpaster BH, Amati F.** Exercise dose and insulin sensitivity: relevance for diabetes prevention. *Med Sci Sports Exerc*. 2012;44:793–799.
14. **Klimcakova E, Polak J, Moro C, et al.** Dynamic strength training improves insulin sensitivity without altering plasma levels and gene expression of adipokines in subcutaneous adipose tissue in obese men. *J Clin Endocrinol Metab*. 2006;91:5107–5112.
15. **Egan B, Zierath JR.** Exercise metabolism and the molecular regulation of skeletal muscle adaptation. *Cell Metab*. 2013;17:162–184.
16. **Blau HM, Webster C.** Isolation and characterization of human muscle cells. *Proc Natl Acad Sci USA*. 1981;78:5623–5627.
17. **Hulver MW, Berggren JR, Carper MJ, et al.** Elevated stearoyl-CoA desaturase-1 expression in skeletal muscle contributes to abnormal fatty acid partitioning in obese humans. *Cell Metab*. 2005;2:251–261.
18. **Badin PM, Loubiere C, Coonen M, et al.** Regulation of skeletal muscle lipolysis and oxidative metabolism by the co-lipase CGI-58. *J Lipid Res*. 2012;53:839–848.
19. **Badin PM, Louche K, Mairal A, et al.** Altered skeletal muscle lipase expression and activity contribute to insulin resistance in humans. *Diabetes*. 2011;60:1734–1742.
20. **Barres R, Yan J, Egan B, et al.** Acute exercise remodels promoter

methylation in human skeletal muscle. *Cell Metab*. 2012;15:405–411.
21. **Schenk S, Harber MP, Shrivastava CR, Burant CF, Horowitz JF.** Improved insulin sensitivity after weight loss and exercise training is mediated by a reduction in plasma fatty acid mobilization, not enhanced oxidative capacity. *J Physiol*. 2009;587:4949–4961.
22. **Dube JJ, Amati F, Stefanovic-Racic M, Toledo FG, Sauers SE, Goodpaster BH.** Exercise-induced alterations in intramyocellular lipids and insulin resistance: the athlete's paradox revisited. *Am J Physiol Endocrinol Metab*. 2008;294:E882–E888.
23. **Saitoh S, Shimomura Y, Tasaki Y, Suzuki M.** Effect of short-term exercise training on muscle glycogen in resting conditions in rats fed a high fat diet. *Eur J Appl Physiol Occup Physiol*. 1992;64:62–67.
24. **Perseghin G, Price TB, Petersen KF, et al.** Increased glucose transport-phosphorylation and muscle glycogen synthesis after exercise training in insulin-resistant subjects. *N Engl J Med*. 1996;335:1357–1362.
25. **Al-Khalili L, Cartee GD, Krook A.** RNA interference-mediated reduction in GLUT1 inhibits serum-induced glucose transport in primary human skeletal muscle cells. *Biochem Biophys Res Commun*. 2003;307:127–132.
26. **Berggren JR, Tanner CJ, Koves TR, Muoio DM, Houmard JA.** Glucose uptake in muscle cell cultures from endurance-trained men. *Med Sci Sports Exerc*. 2005;37:579–584.
27. **Peters SJ, Harris RA, Wu P, Pehleman TL, Heigenhauser GJ, Spriet LL.** Human skeletal muscle PDH kinase activity and isoform expression during a 3-day high-fat/low-carbohydrate diet. *Am J Physiol Endocrinol Metab*. 2001;281:E1151–E1158.
28. **Pilegaard H, Neufer PD.** Transcriptional regulation of pyruvate dehydrogenase kinase 4 in skeletal muscle during and after exercise. *Proc Nutr Soc*. 2004;63:221–226.
29. **Kirchner H, Osler ME, Krook A, Zierath JR.** Epigenetic flexibility in metabolic regulation: disease cause and prevention? *Trends Cell Biol*. 2013;23:203–209.
30. **Berggren JR, Boyle KE, Chapman WH, Houmard JA.** Skeletal muscle lipid oxidation and obesity: influence of weight loss and exercise. *Am J Physiol Endocrinol Metab*. 2008;294:E726–E732.
31. **Sparks LM, Johannsen NM, Church TS, et al.** Nine months of combined training improves ex vivo skeletal muscle metabolism in individuals with type 2 diabetes. *J Clin Endocrinol Metab*. 2013;98:1694–1702.
32. **Kiens B, Essen-Gustavsson B, Christensen NJ, Saltin B.** Skeletal muscle substrate utilization during submaximal exercise in man: effect of endurance training. *J Physiol*. 1993;469:459–478.
33. **Tarnopolsky MA, Rennie CD, Robertshaw HA, Fedak-Tarnopolsky SN, Devries MC, Hamadeh MJ.** Influence of endurance exercise training and sex on intramyocellular lipid and mitochondrial ultrastructure, substrate use, and mitochondrial enzyme activity. *Am J Physiol Regul Integr Comp Physiol*. 2007;292:R1271–R1278.
34. **Randle PJ, Garland PB, Hales CN, Newsholme EA.** The glucose fatty-acid cycle. Its role in insulin sensitivity and the metabolic disturbances of diabetes mellitus. *Lancet*. 1963;1:785–789.

Supplemental Table 1. Taqman PCR probes used for gene expression analyses

Gene symbol	Probe ID
18S	Hs99999901_s1
GLUT1 (glucose transporter 1)	Hs00892681_m1
GLUT4 (glucose transporter 4)	Hs00168966_m1
PDK4 (pyruvate dehydrogenase kinase, isozyme 4)	Hs01037712_m1
PDHA1 (pyruvate dehydrogenase (lipoamide) alpha 1)	Hs00264851_m1
GYS1 (glycogen synthase 1)	Hs00157863_m1
ACADM (MCAD, medium-chain acyl-CoA dehydrogenase)	Hs00163494_m1
COX7C (cytochrome c oxidase, subunit VIIc)	Hs01595220_g1
CYCS (cytochrome c, somatic)	Hs00428600_m1
MYH2 (myosin heavy chain 2)	Hs00430042_m1
MYH7 (myosin heavy chain 7)	Hs01110632_m1

Figure 1. Representative Western blot experiments performed on paired *vastus lateralis* biopsy-derived proteins for mitochondrial complexes.

Figure. 2 Representative dot blots of flow cytometry cellular staining profiles of both *vastus lateralis* biopsy-derived subcultured SVF (A,B) or $CD56^{+}$ cell-sorted population (C,D) with anti-CD31 (marker of endothelial cells), anti-CD45 (marker of leukocytes) and anti-CD56 (marker of satellite cells) antibodies.

Figure. 3. Expression of myotube maturation markers myosin heavy chain (MYH) 1 (A) and MYH2 (B) assessed by qPCR at day0 (D0) and day4 (D4) of differentiation in primary cultures derived from paired (i.e, pre and post-training) *vastus lateralis* muscle biopsies (n=5).

Supplemental Figure 1

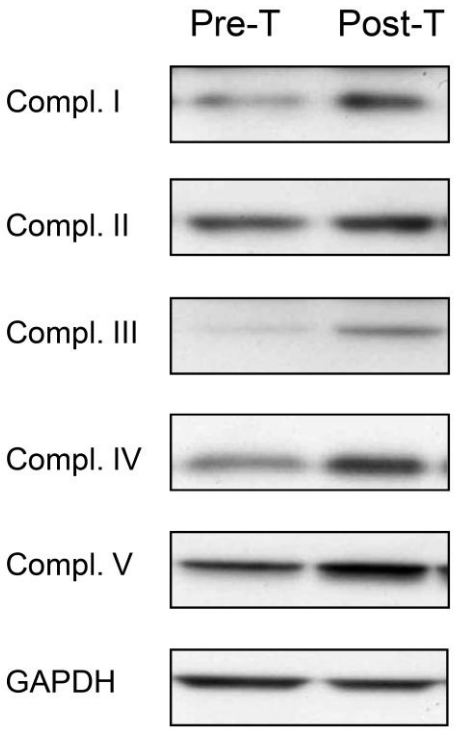

Supplemental Figure 2

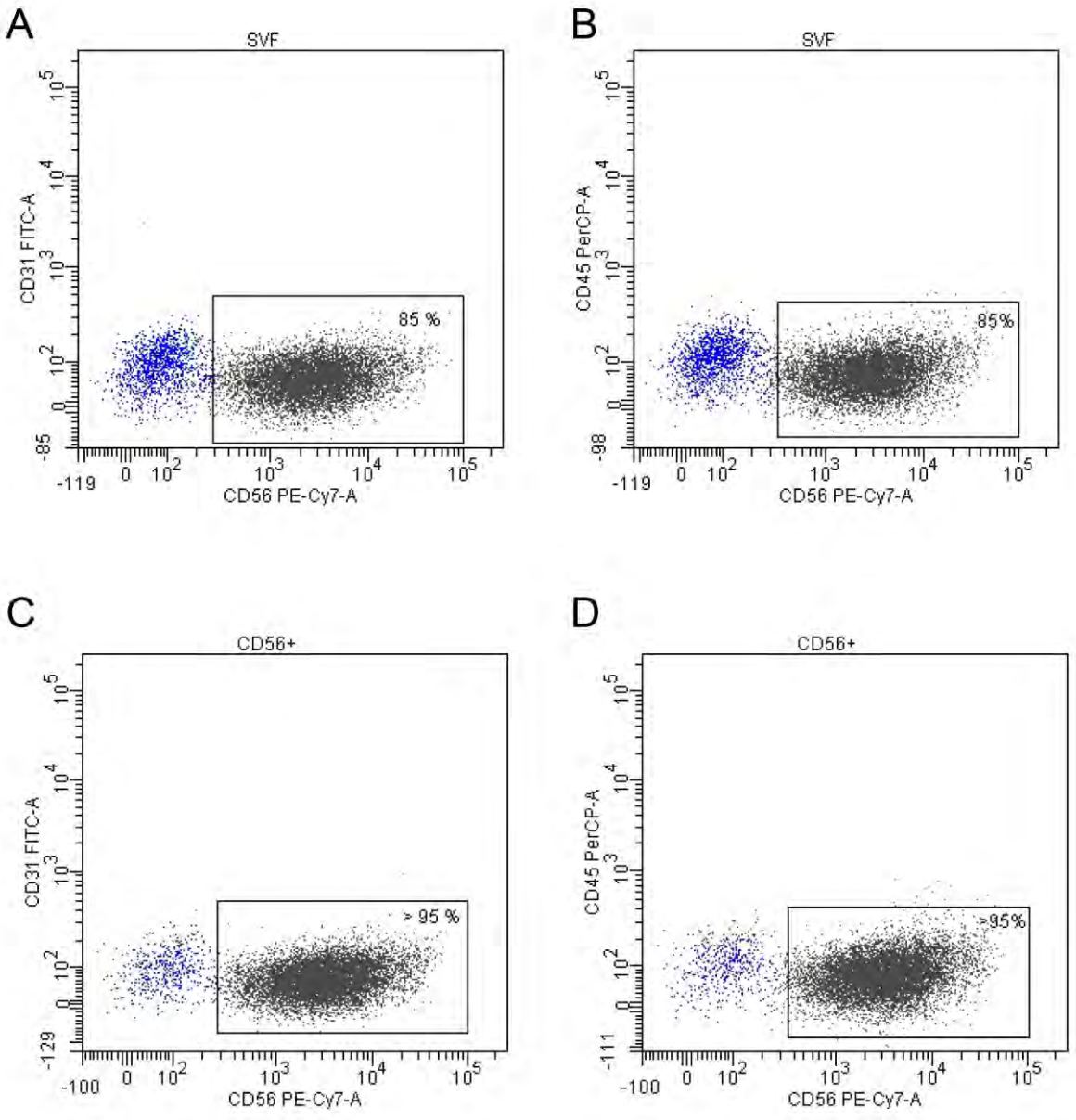

Supplemental Figure 3

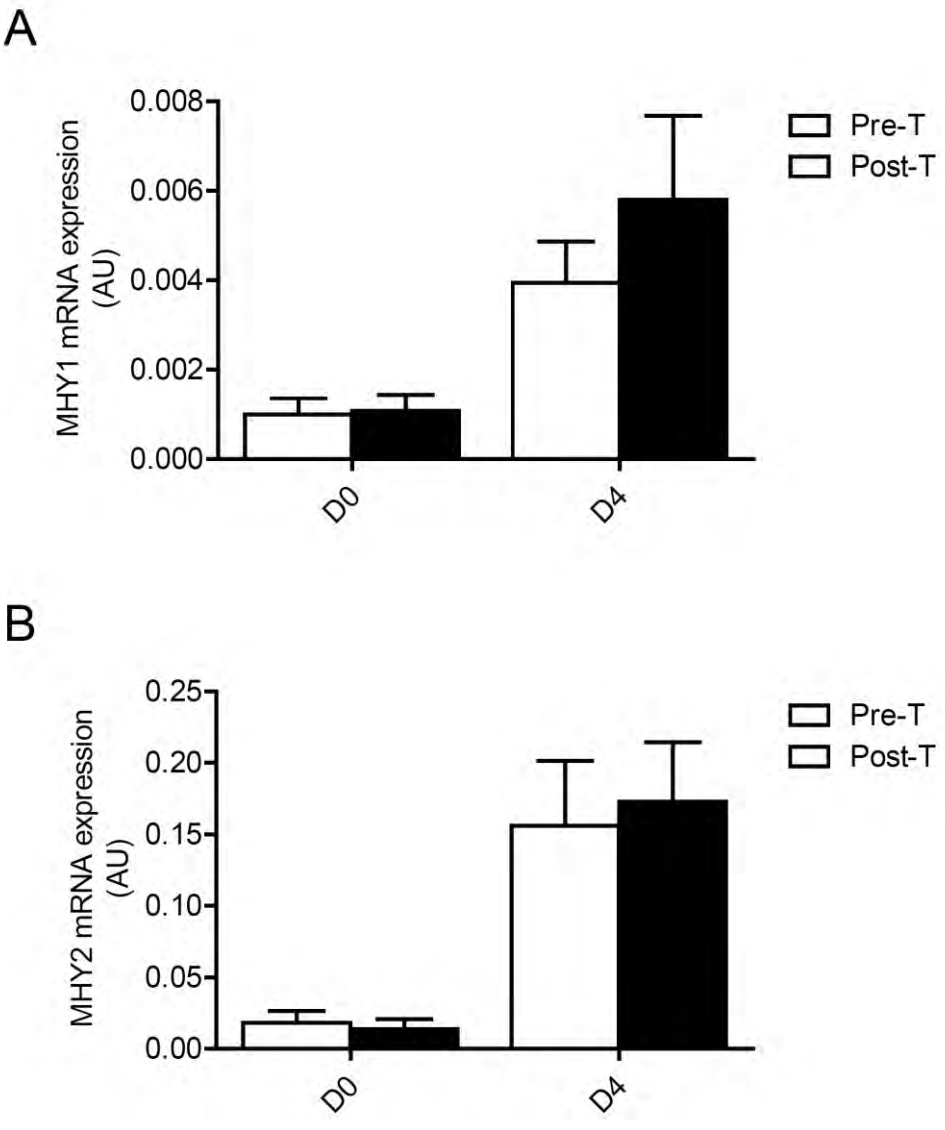

Author : Pierre-Marie Badin

Title : Study of muscular lipase function on lipid metabolism and insulin sensitivity

Supervisor(s) : Dr Cédric Moro, Pr Dominique Langin

Place and date of defense : Toulouse, 12 July 2013

Study of muscular lipase function on lipid metabolism and insulin sensitivity

Under supervision of Dr C.Moro, INSERM I2MC/UMR 1048 Team of Pr D.Langin

During my PhD thesis, we studied the pathophysiological link between skeletal muscle lipolysis and insulin-resistance. We also evaluated the role of skeletal muscle lipolysis in the regulation of lipid and oxidative metabolism.

We have shown that the expression of *adipose triglyceride lipase* (ATGL) in skeletal muscle, a limiting enzyme of lipolysis, was negatively correlated with insulin sensitivity in a cohort of lean, obese and type 2 diabetic subjects. To study the effect of ATGL up-regulation on insulin sensitivity, we next over-expressed ATGL in human primary myocytes. Insulin-sensitivity and signaling were both reduced. We also showed that these effects were dependant on diacylglycerol (DAG) production and *protein kinase C* (PKC) activation. PKC are known to inhibit *insulin receptor substrate 1* by serine phosphorylation. We next studied, in a murine mouse model, the effect of high fat feeding on insulin resistance and skeletal muscle lipase expression. We have shown an increase of *comparative gene identification 58* (CGI-58) expression (a co-activator of ATGL) and a decrease of hormone sensitive lipase phosphorylation on its activating residue at serine 660. This deregulation of lipolysis was associated with a strong increase of total DAG concentration and PKC θ and ε membrane translocationin skeletal muscle.

In parallel to this work, we studied the metabolic role of CGI-58 in skeletal muscle through overexpression and knockdown studies in primary human myocytes. We have shown that CGI-58 is a co-activator of ATGL in skeletal muscle. Moreover we observed during the knockdown of CGI-58 a decrease of lipid oxidation and an increase of glucose oxidation. These effects were partly explained by the down-regulation of *pyruvate dehydrogenase kinase 4* expression. These effects were mostly mediated by a decrease of *peroxysome proliferator-activated receptor β/δ* activation by fatty acid from lipolysis.

Finally our work shows for the first time a pathophysiological link between lipases deregulation and insulin-resistance in skeletal muscle. These data also significantly contribute to a better understanding of the molecular and physiological regulation of skeletal muscle lipolysis.

Auteur : Pierre-Marie Badin

Titre : Étude du rôle des lipases musculaires dans la régulation du métabolisme des lipides et de la sensibilité à l'insuline

Directeur(s) de thèse : Dr Cédric Moro, Pr Dominique Langin

Lieu et date de soutenance : Toulouse, le 12 Juillet 2013

Mon travail de thèse a été axé sur l'étude le la lipolyse musculaire. Nous avons notamment étudié son impact sur la sensibilité à l'insuline ainsi que sur la régulation du métabolisme lipidique et oxydatif.

Nous avons pu montrer que l'expression musculaire de l'*adipose triglycéride lipase* (ATGL), enzyme limitante de la lipolyse, était corrélée négativement avec la sensibilité à l'insuline dans une cohorte de personnes de poids normal, obèses et diabétiques. Afin d'identifier l'impact de cette augmentation d'expression de l'ATGL musculaire nous avons surexprimé la protéine dans des myocytes primaires humains. La signalisation ainsi que la sensibilité à l'insuline étaient diminuées dans ces cellules. Nous avons pu établir que ceci passait par une augmentation de la production de diacylglycérols (DAG) et l'activation de protéines kinases C (PKC) connus pour phosphoryler négativement l'*insulin receptor substrate 1*. Pour compléter ce travail nous avons étudié dans un modèle murin soumis à un régime riche en graisse, s'il existait une détérioration de l'expression des lipases associée à la perte de sensibilité à l'insuline. Nous avons ainsi pu montrer que le régime hyper lipidique entrainait un déséquilibre de la lipolyse musculaire avec une augmentation de l'expression de *comparative gene identification 58* (CGI-58) (co-activateur de l'ATGL) et une baisse de la phosphorylation activatrice de la *lipase hormono-sensible* en sérine 660. Ceci était associé à une augmentation de l'activation des PKC-θ et -ε et à une accumulation de DAG.

En parallèle, nous avons étudié la fonction de CGI-58 dans le muscle squelettique. Pour cela nous avons réalisé des expériences de surexpression ou d'extinction de CGI-58 dans des myocytes. Nous avons montré que, comme dans l'adipocyte, CGI-58 était un co-activateur de l'ATGL dans le muscle squelettique. De façon intéressante, nous avons également observé que la diminution de la lipolyse, résultant de l'extinction de CGI-58, passait par une diminution de l'oxydation des lipides et une hausse de celle des glucides. Ces effets pourraient s'expliquer par la baisse de l'expression de la *pyruvate dehydrogenase kinase 4*. Cette baisse d'expression est du dans notre modèle à une diminution de l'activation de *peroxysome proliferator-activated receptor β/δ* par les acides gras de la lipolyse.

Ces travaux ont montré pour la première fois un lien causal entre une dérégulation de la lipolyse musculaire et l'insulino-résistance. Nos données participent également à l'élargissement des connaissances existantes sur le contrôle physiologique et moléculaire de la lipolyse musculaire.